Geotechnical Performance of Group of Stone Columns

Mohammad Etezad-Borojerdi

A thesis

in

The Department

of

Building, Civil and Environmental Engineering

Presented in Partial Fulfillment of the Requirements

For the Degree of Doctor of Philosophy at

Concordia University

Montreal, Quebec, Canada

August 2007

Your file Votre référence
ISBN: 978-0-494-31136-3
Our file Notre référence
ISBN: 978-0-494-31136-3

ABSTRACT

Geotechnical Performance of Group of Stone Columns

Mohammad Etezad Borojerdi, Ph.D.
Concordia University, 2007

Stone columns are known to be a cost effective and environmental friendly ground improvement technique, which is widely used to enhance the performance of shallow foundations built on soft ground. Stone columns increase bearing capacity, reduce settlement, reduce significantly the consolidation period and minimize the liquefaction potential of the ground.

The current design of these columns is generally based on theories developed for single columns, ignoring the group interaction and accordingly the group efficiency. In the literature, reports can be found to confirm that the failure of single stone column is mostly due to bulging, meantime for a group of stone columns, the failure mechanism takes place by massive shear failure of the group and the surrounding soils.

The objective of this thesis is to develop a numerical model, based on a two dimensional finite element technique. The model is capable to identify the different mode of failures of single and group of stone columns for a given columns/soil/loading condition. In these cases, group interactions were examined and evaluated. Parametric study was conducted on the parameters believed to govern this behavior. The results produced in this study showed that ground reinforced by group of stone columns may fail by general, local or punching shear failure, depending on geometry of the group and properties of the surrounding soils.

Analytical models were developed for the ultimate bearing capacity of single and groups of stone columns. The models take into consideration the column interaction among the group and the strength of the surrounding soils and accordingly depict the appropriate mode of failure. Furthermore, analytical model was developed for the prediction of settlement of foundations under single or widely spaced stone columns. The design theories are provided with design procedures and charts for practical use.

ACKNOWLEDGEMENTS

I am deeply grateful to my supervisor and mentor Professor Adel Hanna. Working with him has been both scientifically and personally exceptional experience. His assistance, unparallel wisdom, patience and invaluable support are greatly appreciated.

I would like to thank my former supervisor Professor Hormoz Poorooshasb for his assistance, encouragements and advices at the early stage of this research.

I would like to extend my gratitude to Dr. Tahar Ayadat for his valuable discussions and comment over the years. I gratefully appreciate his support, his precious time and experience.

I greatly acknowledge the financial support from the Natural Science and Engineering Research Council of Canada (NSERC) and Concordia University.

Last but not least I wish to express my sincere gratitude to my parents and my sister for their support and encouragement throughout this study. I could not have made it without their unconditional love and patience.

To My Family:

My parents and my sister

TABLE OF CONTENTS

LIST OF FIGURES

LIST OF TABLES

LIST OF SYMBOLS

a	=Column radius in single column model
A_s	=Area replacement ratio of reinforced ground
b	=Unit cell radius in single column model
B	=Width of the foundation
E	=Young's modulus
c_c	=Cohesion of soft soil
c_{comp}	=Cohesion of composite soil
d	=Stone column diameter
D_f	=Height of the soil over foundation bottom
K_o	=Coefficient of earth pressure at rest
K_p	=Coefficient of passive earth pressure
l	=Stone columns length
n	=Stress ratio of reinforced ground
n	=Settlement ratio in single column model
N_γ, N_q, N_c	=Bearing capacity factors
p	=Vertical soft soil stress in single column model
P_1	=Load applied on the reinforced soil at a given displacement
P_2	=Load applied on the unreinforced soil at a given displacement
q	=Soil surcharge
q_u	=Ultimate bearing capacity of reinforced ground
R	=Frictional resisting force along failure surface

r_o & r_1 =radius of log spiral

s =Spacing between the neighboring stone columns

S_t =Settlement of treated soil

S_u =Settlement of untreated soil

W =Wright of soil

β = Slop of the ground free surface regarding to the horizontal surface

γ_c =Unit weight of soft soil

γ_{comp} =Unit weight of composite soil

γ_s =Unit weight of stones

ϵ_1 =Axial strain of soil under the foundation

ϵ_f =Axial strain at failure point

θ =Angle of center of logspiral

λ = Angle between the soil section and vertical line

ν =Poisson's ratio of soil

σ_1 =Vertical column stress in single column model

σ_3 =Horizontal column stress in single column model

σ_c =Vertical stress in surrounding soil

σ_s =Vertical stress in stone column

ϕ_c =Angle of shearing resistance of soft soil

ϕ_{comp} =Angle of shearing resistance of composite soil

ϕ_f =Angle of shearing resistance at the state of failure

ϕ_s =Angle of shearing resistance of stones

ψ =Cone angle under the foundation

CHAPTER 1

INTRODUCTION

1.1 General

In recent years, increasing value of land and the limited availability of sites were greatly encouraging geotechnical engineers to develop techniques to improve ground made of soft and compressible soils. Stone columns, preloading, densification, chemical treatments and vertical drains are to name a few.

Stone column technique is considered as an efficient, cost effective and environmentally friendly for improving soft cohesive and cohesionless soils to sustain foundations of light to moderately loaded buildings; such as low-rise buildings, storage tanks, embankment dams, warehouses, highways and bridge approaches are to name a few. Stone columns were used to provide higher bearing capacity, reduce settlements, speed-up the settlement, and reduce liquefaction potential of cohessionless material under seismic loading and to enhance the stability of natural and man-made slop.

In the literature, reports showed that stone columns were used to replace about 10 to 35 percent of the weak soil. These columns are usually made of granular compacted material and approximately carry about 20 to 50 tons. Furthermore, evidences were presented to support that the stone columns are superior as compared to other ground improvement techniques, with respect to costs and durability, besides being known as environmentally friendly and easy to install.

1.2 Research Objectives

Although stone columns have been widely used in practice, research in this field is lagging behind due to the complexity of modeling the composite media of soils and columns, and accordingly, the current design practice is based on experimental methods or theories, which were developed for single isolated columns based on the concept of unit cell; ignoring the columns interaction and further the group efficiency; therefore, the ultimate capacity of a group of stone columns is taken as the total load of the individual columns. Furthermore, for the unit cell theory, the column fails by bulging; nevertheless, it has been observed that a column in a group fails by massive shear of the entire group and the surrounding soils.

The objectives of the research are:

1. To develop a numerical model to simulate the cases of single and group of stone columns below a raft foundation. The model is a two dimensional finite element, which is capable to determine the mode of failure of a group under geometry/soil/loading conditions, as general, local, punching or bulging form.
2. To perform a parametric study to establish the effect of the governing parameters believed to affect the performance of a group of stone columns.
3. To develop analytical models, design procedures and design charts to be used in practice for the case of bearing capacity of the reinforced ground under the modes of failure mentioned above.
4. To develop an analytical model for the case of settlements of single stone column.
5. To validate these models with available experimental and numerical data in the literature.

6. To develop a procedure to identify the mode of failure for a given condition and accordingly, utilize the appropriate design theory to predict the capacity of the group.

1.3 Organization of Thesis

The historical development of the subject is presented in chapter 2. In chapter 3, numerical models for single and group of stone column are presented. In this chapter, group interaction of columns and the associated modes of failure are presented. Furthermore, parametric study on the parameters governing this behavior is also presented. Chapter 4 presents analytical models for general, local, punching shear failure and bulging failures. Conclusions drawn from the present study and recommendation for future study are presented in chapter 5.

CHAPTER 2

Literature Review

2.1 General

Stone columns technique is considered as an effective ground improvement method for foundation on soft ground. Stone columns were first used by Moreau et al in 1830 (Hughes and Withers, 1974). They used 0.2m diameter and two meters in length columns to support the foundations of ironworks for the military purpose in Bayonne, France. Moreau reported a significant reduction of settlement and large increase in the capacity of soil/column system. In 1939, Steuermann proposed the vibro-compaction technique to treat ground using water injection and vibration into the soil simultaneously. The combination of jetting and vibration enables the device to sink by its own weight to the required depth. In 1940s the development of vibroflot was continued in USA and Germany. By the end of 1950's the depth of treatment increased to about 20m. Stone column technique has been used widely in Japan since 1955. Later this method has been used in China, India and many other countries.

During last 40 years many researches were conducted to estimate the amount of bearing capacity and settlement of the ground reinforced by stone columns. Due to the analytical complexity of modeling the problem, simplified assumptions were used to develop design theories. However, these assumptions have lead to an unrealistic modeling of the composite system and accordingly misleading results.

2.2 Failure Mechanism

Prior to 1974 most of the research on stone columns was limited to field experimental work. In 1974, Hughes and Withers reported that bulging took place at the upper part of the column, roughly about four-diameter length from the top of the column (Figure 2.1). They also reported that stone columns in a group fail by bulging following the unit cell concept (Figure 2.2). According to the unit cell concept, each column in the group of stone columns will act independently from the neighboring columns and accordingly, there will be no interaction effects between the columns in the group. (Figure 2.3) Therefore, the capacity of the group can be determined as the total capacity of columns in the group. Accordingly, the unit cell theory stipulates that:

1. Lateral deformation does not occur across the boundaries of the unit cell.
2. Shear stresses on the outside boundaries of the unit cell must be zero.

In 1984 Bachus and Barksdale conducted series of laboratory tests to investigate the interaction effect between two adjacent columns. Based on the results obtained from a group of 2x3 (Figure 2.4), it was noted that the presence of adjacent columns provides some confinement for the column in question, furthermore, bulging was restrained in the interior side of the columns. This characterization was later defined as group interaction. This study shed some doubt on the assumptions of the unit cell technique.

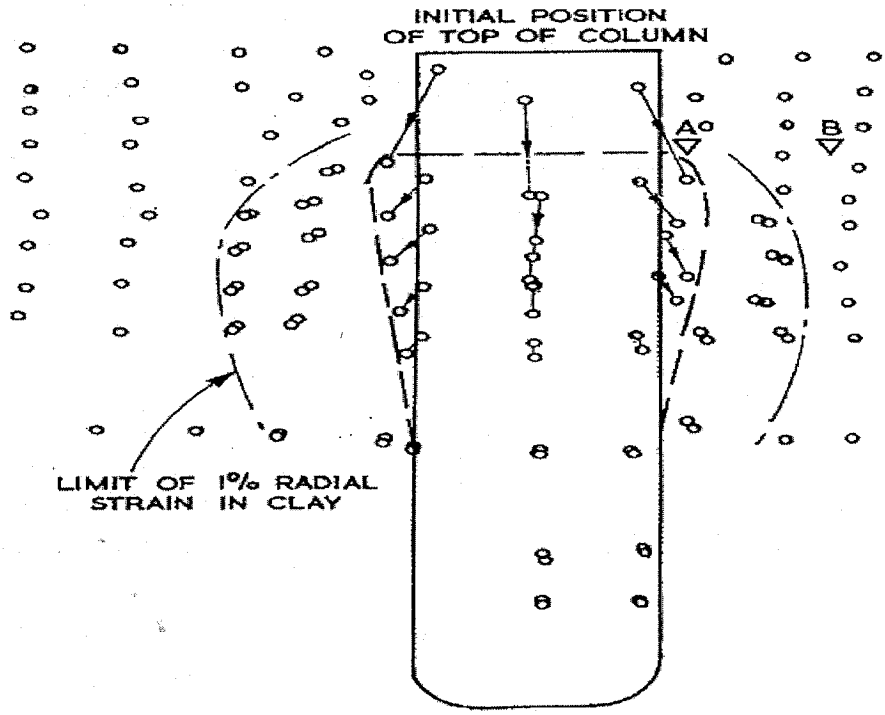

Figure 2.1 Failure shape of a single stone column, after Hughes and Withers (1974).

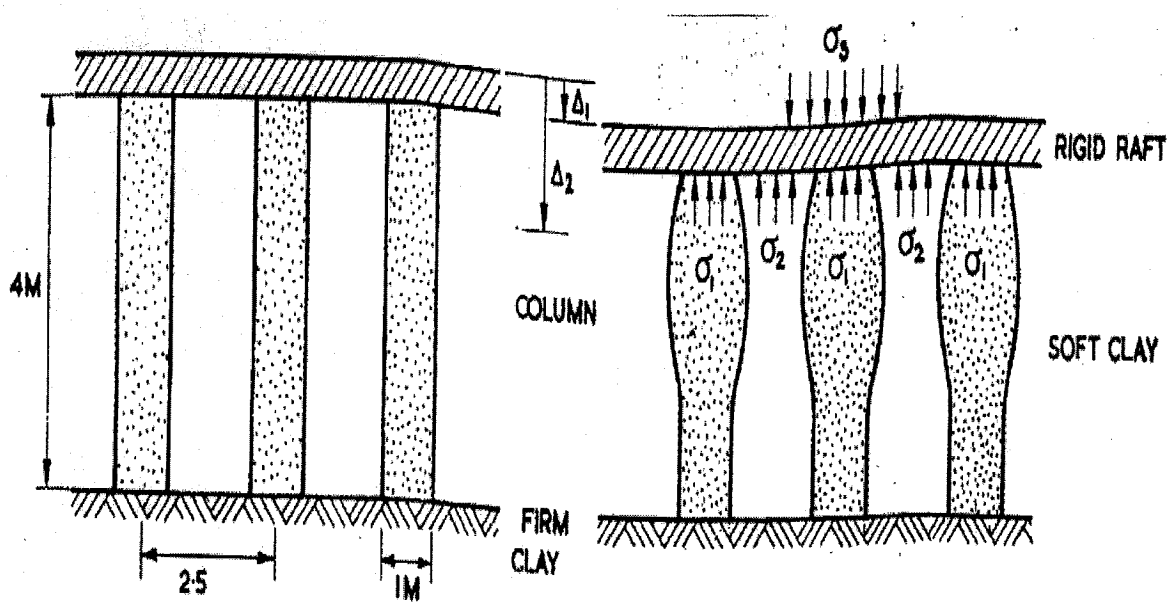

(a) Before failure (b) After failure

Figure 2.2 Group of stone columns under a large raft, after Hughes and Withers (1974).

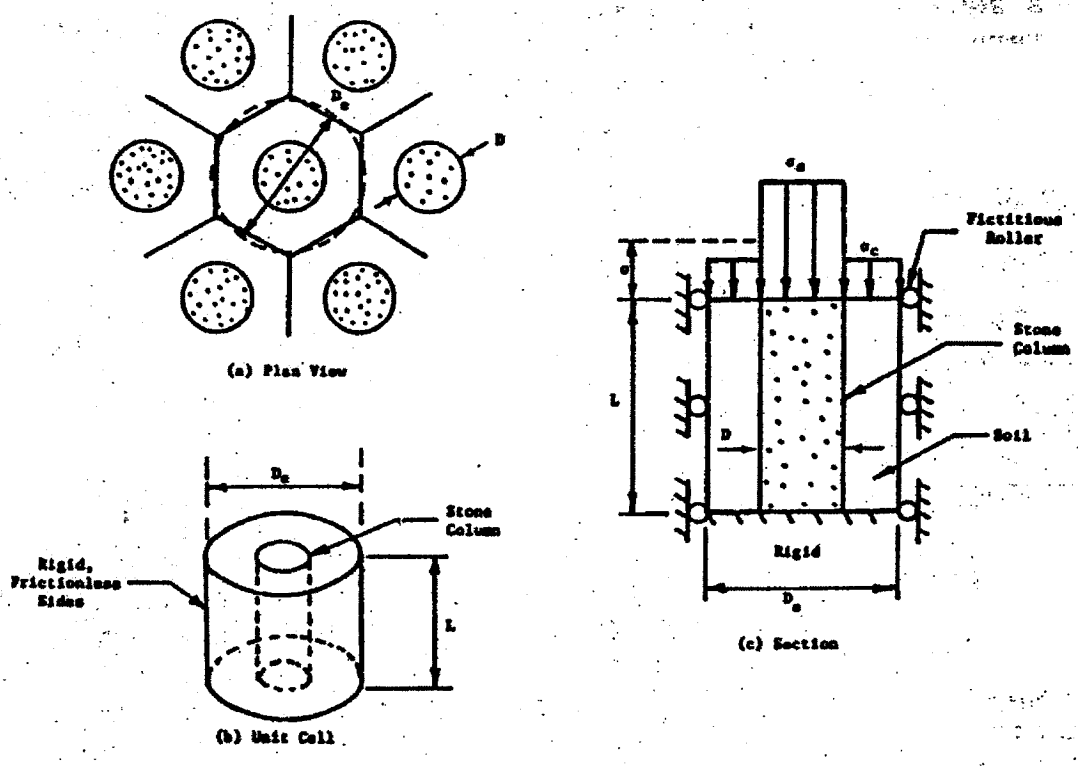

Figure 2.3 Idealization of unit cell, after Barksdale and Bachus (1983).

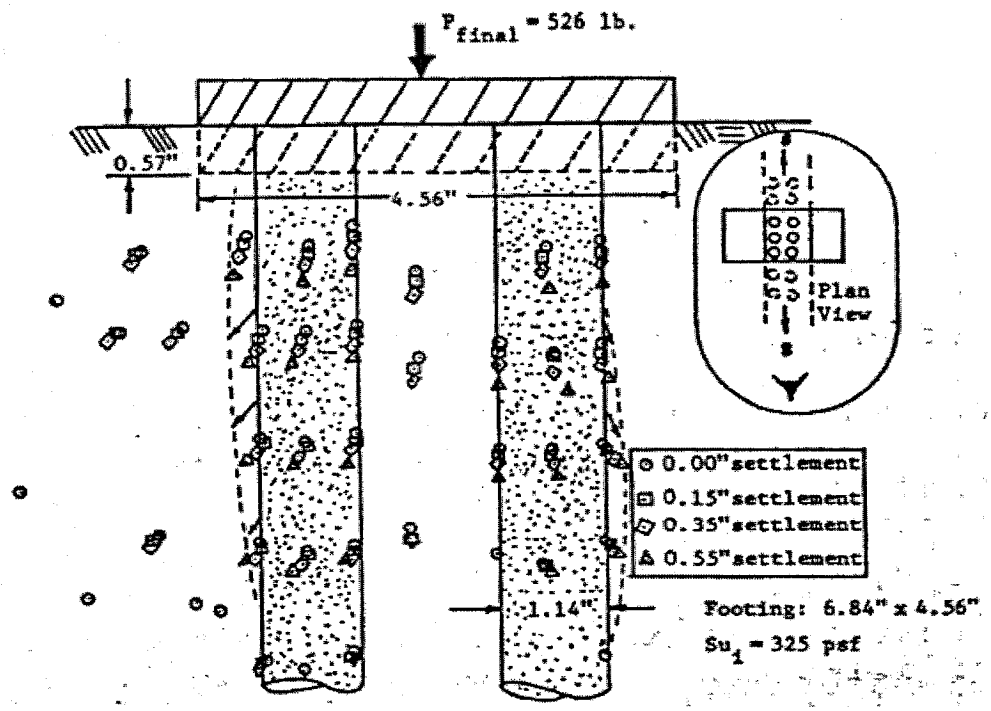

Figure 2.4 Displacements of stone columns, after Bachus and Barksdale (1984).

Terashi et al. (1991) was the first to report on the group interaction and accordingly efficiency. Based on the results of the laboratory tests they conducted on a centrifuge set-up, they reported different failure mechanism than those described by the unit cell theory (Figures 2.5 and 2.6), where group interaction of columns can be noted. Terashi et al (1991) also reported a full-scale test, which was carried out at Kyoto, Japan (Figure 2.7). In this test stone columns were not equally distributed inside the ground. The test was completed over three year period (1986 to 1988). Figure 2.8 shows the failure of the structure and the surrounding soils.

In 1995 Hu performed laboratory tests on group of stone columns. He concluded that group interaction plays a major rule in understating the behavior of group of stone columns. He reported that columns deform by bulging, punching, shearing and bending; furthermore, during loading, interaction between neighboring columns prevent bulging to occur in the upper part of individual columns. Accordingly, to column interaction, bulging will to take place in the lower portion of the interior column, while exterior columns bulging remains in the upper part of the column (Figure 2.9). Figure 2.10 presents the deformed shape of a group of stone columns. He further suggested that general shear failure is the mode of failure for a group of stone columns.

In 1997 Rao et al. conducted laboratory tests on single and group of stone columns. They reported that spacing between columns significantly influences the behavior of stone columns. They suggested that considering the group efficiency factor, the spacing of 3 times of the column's diameter can be used for practical purposes. They declared that when the spacing of columns is close the bulging zones of adjacent columns are overlapped, and accordingly, the group capacity increases due to confinements.

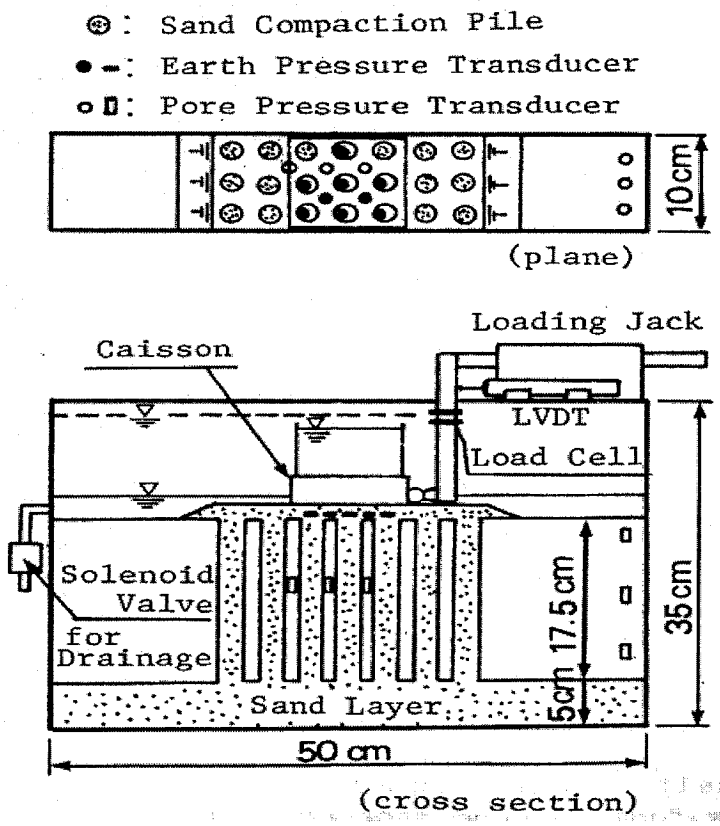

Figure 2.5 Setup of model test, after Terashi et al. (1991).

Figure 2.6 Failure mode of a group of sand columns, after Terashi et al. (1991).

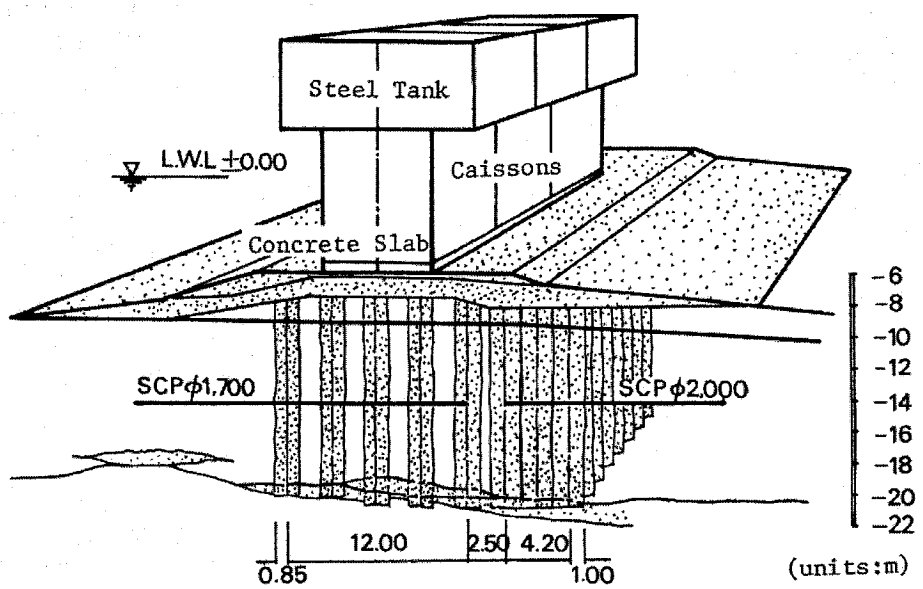

Figure 2.7 Set-up of full-scale load test of a group of stone columns, after Terashi et al. (1991).

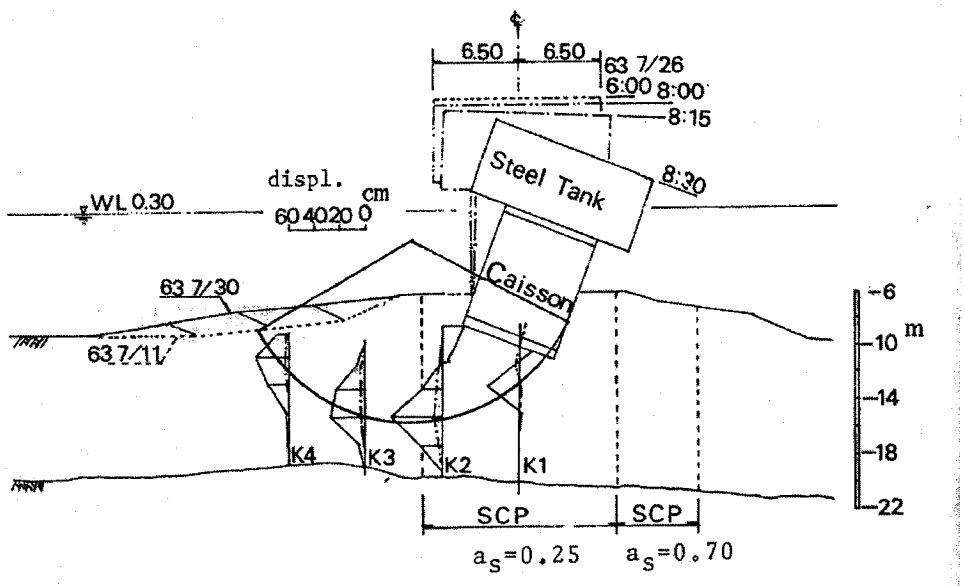

Figure 2.8 Displacement of the structure and deformation of the ground, after Terashi et al. (1991).

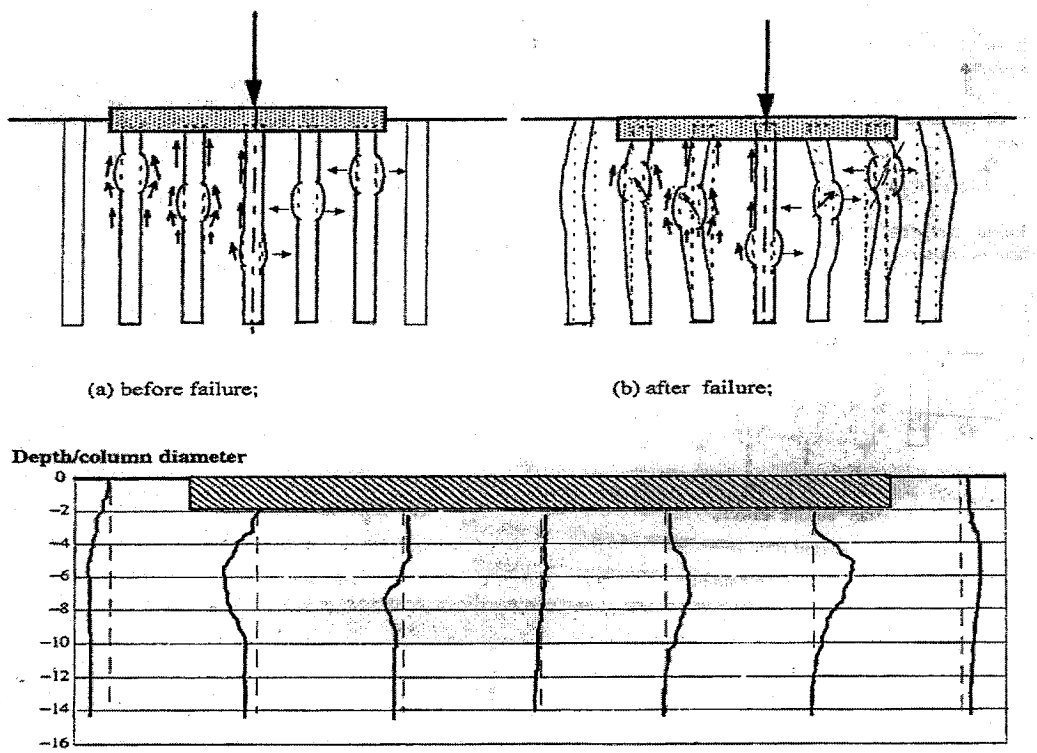

Figure 2.9 Suggested mode of failure for long columns, after Hu et al. (1997).

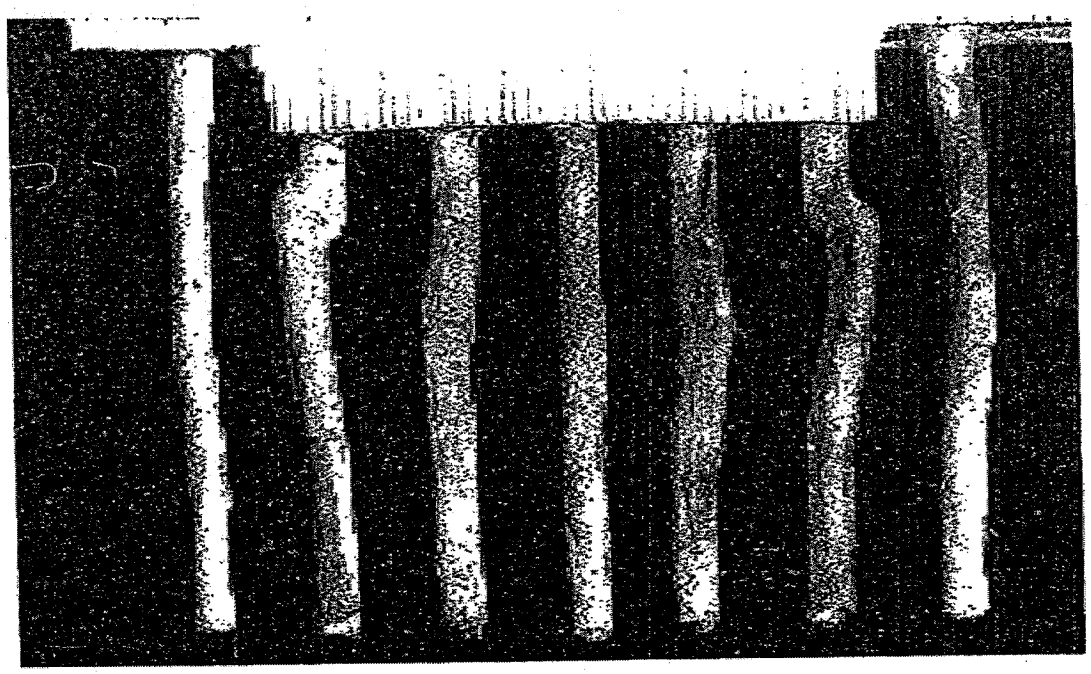

Figure 2.10 Deform shapes of the model test TS17 stone columns after Applying load, after Hu (1995).

Wehr (1999) investigated the group effect using finite element analysis on three-dimensional model. He used the constitutive law of elasto-plastic to model the soil/column system. He confirmed same conclusion of Hu (1995). Figure 2.11 shows the deformed shape as produced by the numerical model, due to 10mm surface displacement.

Christoulas et al. (2000) performed laboratory model tests on stone columns in clay. They used pressure cells and electronic piezometers to monitor lateral stresses and the pore water pressure in the soil mass. They observed the bulging failure and confirmed the results of Hughes and Withers (1974). Furthermore, they reported that the length of bulging was about 2.5 to 3 times the column diameter. However, in their study columns were considered too close to the boundaries and accordingly, boundary effect was expected.

In 2002 McKelvey examined experimentally the performance of small group of stone columns, partially penetrating a rigid foundation. She preformed two series of tests. In the first series transparent material was utilized to replace the clay layer. For the second series of tests kaolin clay was used. Group interaction was observed in both tests, as shown in Figure 2.12.

Bae et al (2002) preformed model test on a group of stone columns. They compared their result with results produced by a numerical model utilizing finite element technique, where agreement was noted and that the group will fail in general shear having a conical shape.

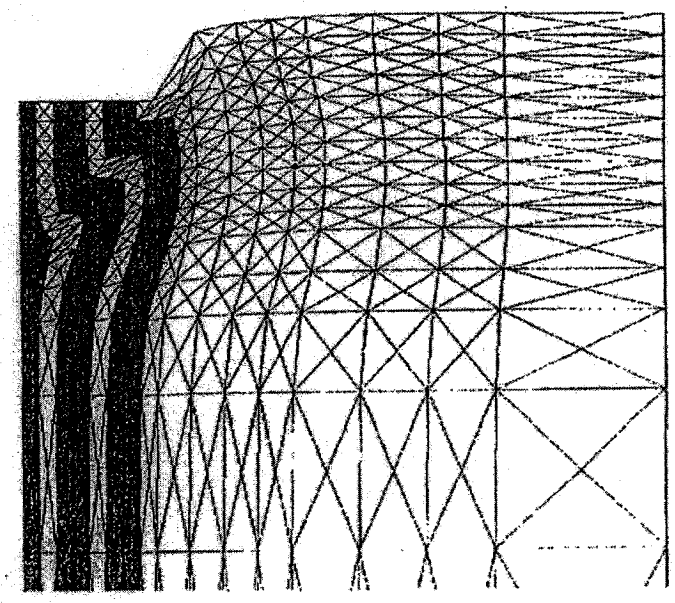

Figure 2.11 Failure shape for group of stone columns, after Wehr (1999).

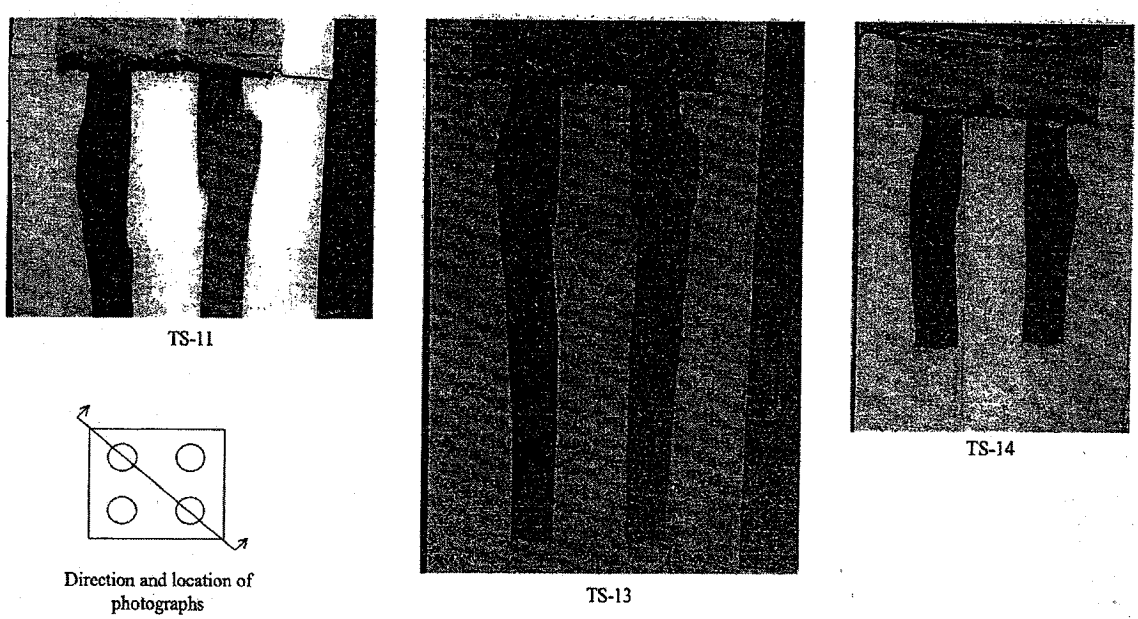

Figure 2.12 Deformed columns TS-11(L/d=10), TS-13 (L/d=10) and TS-14 (L/d=6), after McKelvey (2002).

In 2007, Ambily and Gandhi conducted experimental and numerical analysis on singles and groups of stone columns. They reported that bulging does not occur in reinforced soil with stone columns. By comparing the load displacement curve of single and group of columns for area replacement ratio of 10%, they observed close agreement between the two models. Reduction of replacement area, leads to reducing the effect of group interaction and hence for very low area replacement ratios, bulging failure may take place. However, area replacement ratio of 10% and less are not normally used in practice as there is no noticeable improvement on performance of the reinforced system.

2.3 Theoretical and Numerical Analysis

Based on field data, Glasgow, Thorburn and MacVicar (1968) suggested that the shearing force resisted by the soil can be completely ignored; furthermore, the number of columns can be determined by dividing the working load of a single column over the total load on the foundation. Considering that the surrounding soil will support a large portion of the total load, this approach gives approximate estimation of the capacity of the group.

Greenwood (1970) presented an empirical method to determine the settlement of a ground reinforced by stone columns, based his experimental data. He reported that the method is valid for the given rage of column spacing and the strength of the clay. McKelvey and Sivakumar (2000) reported that Greenwood method comparers well with many recent theoretical methods.

Vesic (1972) developed cylindrical cavity expansion theory, which is applicable to both cohesive and frictional soils. Considering the unit cell concept, this method can be used to predict the capacity for group of stone columns. Bachus and Barksdale, (1983) suggested the ultimate lateral resistance of soil can be given by the following equation.

$$\sigma_3 = cF_c' + qF_q' \tag{2.1}$$

where c and q represent the cohesion and the stress at the failure depth respectively. F_c' and F_q' are the cavity expansion factors as given by Vesic. The ultimate bearing capacity of the column is expressed as.

$$q_{ult} = (cF_c' + qF_q')K_p \tag{2.2}$$

Based on the laboratory test results for single stone column, Hughes and Withers (1974), considered bulging as the failure mode of group of stone columns. Utilizing the elastic plastic theory developed by Gibson and Anderson (1961), the maximum lateral pressure on single stone column was estimated as follows.

$$\sigma_{rL} = \sigma_{ro} + (1 + \log_e \frac{E}{2c(1+\mu)}) \tag{2.3}$$

where σ_{ro}, E, μ and c are total in-situ lateral pressure, modulus of elasticity, Poisson's ratio and the undrained cohesion of the soil respectively. They stated that Equation 2.4 can be used as an approximation of Equation 2.3

$$\sigma_{rL} = \sigma_{ro}' + 4c + u \tag{2.4}$$

Therefore the ultimate load which a stone column can support is given as.

$$\sigma_v' = \frac{(1+\sin\varphi')}{(1-\sin\varphi')}(\sigma_{ro} + 4c - u) \tag{2.5}$$

where φ' is the angle of friction of the material of the stone column and u is the pore water pressure. For frictionless soil Vesic's equation agreed well with the results of given by Gibson and Anderson. It should be reported herein that this method compared well with the data obtained for single columns, McKelvey and Sivakumar (2000).

Priebe (1976) assumed stone column as a cylindrical made within the compressible soil. The surrounding soil was idealized as an elastic media. Furthermore, he assumed that the column ends on a rigid layer. He introduced an improvement factor as the ratio of the settlement of the untreated ground to the improved ground.

$$\frac{s}{s_t} = 1 + A_s \frac{.5 + 2\nu \frac{1 - A_s}{\nu + A_s}}{K_{ac} 2\nu \frac{1 - A_s}{\nu + A_s}} \tag{2.6}$$

K_{ac} is the active earth pressure of the granular material and the value of 1/3 is assumed for ν. In this analysis, the effect of overburden pressure was neglected. In 1995 Priebe incorporated the effect of compressibility of the column material and the overburden. He developed design charts to calculate the settlement of single and strip footings reinforced by a limit number of stone columns.

Dhouib (2004) declared that Priebe's method is widely used for the design of stone columns. Based on comparison of equilibrium method and limited field results, Barksdale and Bachus (1983) reported that this method overestimate the effect of stone columns in settlement reduction.

Balaam (1977) modeled a ground reinforced with stone columns supporting a flexible raft foundation, using finite element method. Both soil and column material were elasto-plastic and Mohr-Coulomb failing criterion was applied. Surprisingly, it was observed that the calculated settlement using the elastic analysis has only 6% difference comparing to the plastic analysis. Greenwood and Kirsch (1984) criticized this report, stating that the result should be checked with an alternative approach. Balaam observed significant reduction on settlement when the area replacement ratio was near 25%. He

noted that the effect of increasing the column length and decreasing columns spacing on the increasing the rate of settlement.

In 1981 Balaam and Booker proposed an analytical solution based on theory of elasticity to estimate foundation settlement. Both soil and column were assumed to be in elastic condition. Balaam and Booker (1985) stated that this method can grossly overestimate the effect of stone columns in reducing settlement. Rigid raft was considered and equal settlement of column and soil was assumed (Figures 2.13, 2.14 and 2.15). In these figures subscript 1 and 2 represents the properties and column material and soft soil respectively. Furthermore, they reported that when load is initially applied to the unit cell, soil carries larger portion than the column. This is due to the fact that clay initially is in undrained condition and behaves as an incompressible material. However, as the excessive pore water pressure dissipates column carries more vertical stress rather than the surrounding soil.

In 1985 Balaam and Booker developed another method to analyze the load settlement response of ground. The problem was idealized assuming that the stone column is in triaxial state. Unlike previous method, they assumed that yielding takes place in the column while soil remains elastic. They reported good agreement between the methods and the experimental data.

Brauns (1978) developed a theory assuming that the upper portion of the stone column yields like a cylindrical sample of cohesionless soil and fails by shear having an angle of $45+\frac{\varphi_s}{2}$ (Figure 2.16). Using Equation 2.7 and by calculating the cone angle, δ, using a charts, which he developed the ultimate load for single column will be estimated as follows.

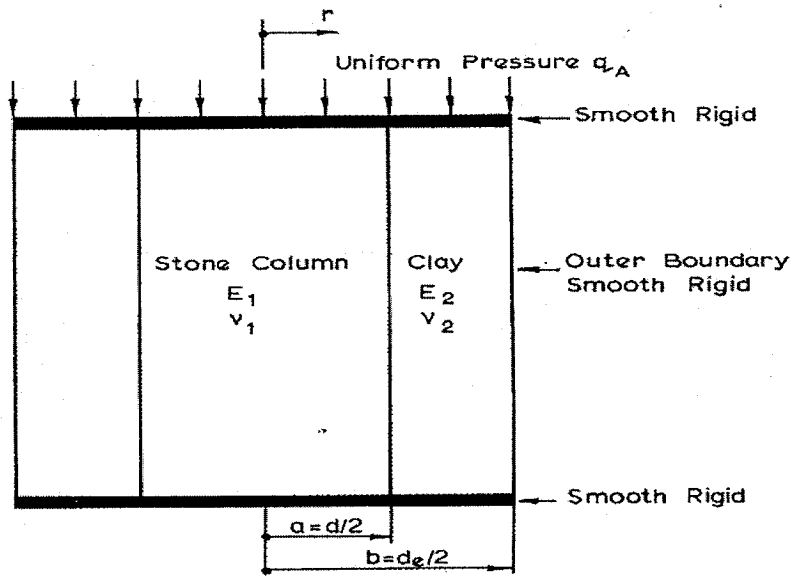

Figure 2.13 Numerical model, after Balaam and Booker (1981).

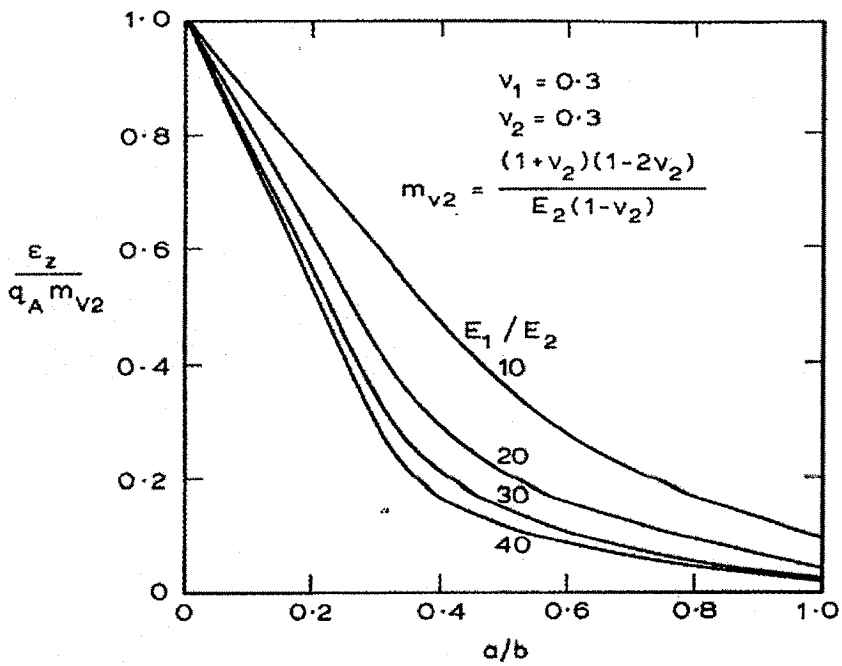

Figure 2.14 Vertical strain of column-soil unit with varying spacing, after Balaam and Booker (1981).

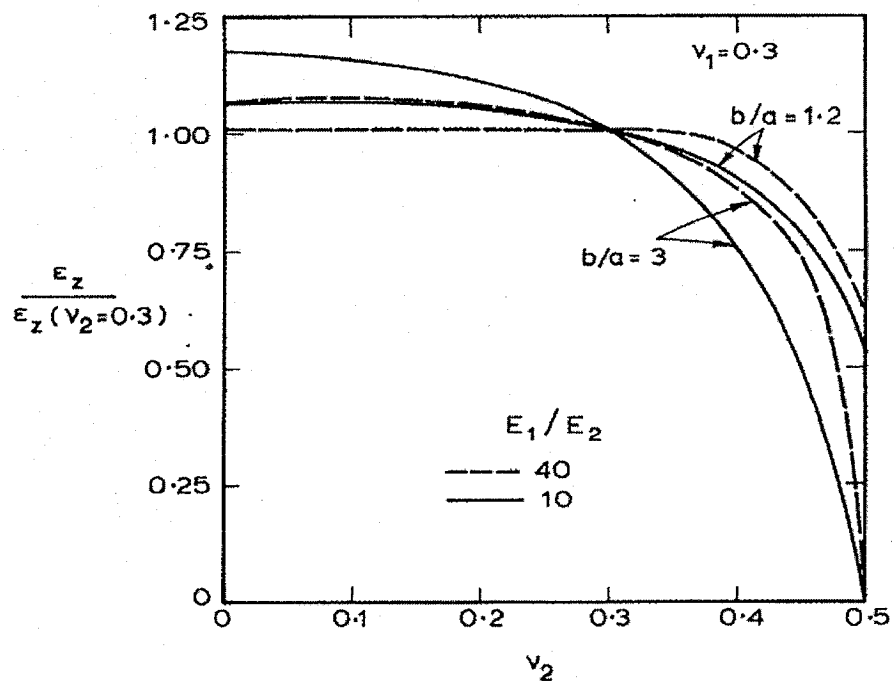

Figure 2.15 Ratio of strain for calculating settlements for different Poisson ratio of soil, after Balaam and Booker (1981).

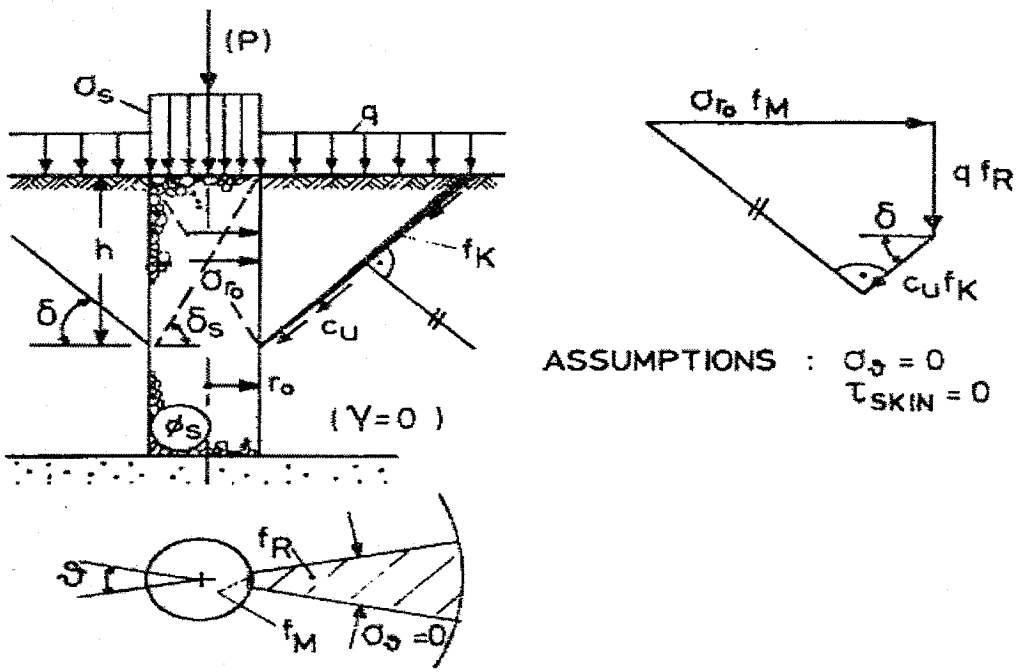

Figure 2.16 Simplified analysis of the bearing capacity of stone columns, after Brauns (1978).

$$\frac{\sigma_s}{c_u} = (\frac{q}{c_u} + \frac{2}{\sin 2\delta})(1 + \frac{\tan \delta_s}{\tan \delta})K_p \tag{2.7}$$

Madhav and Vitkar (1978) presented a method to calculate the bearing capacity of a trench or single pile based on general shear failure (Figure 2.17). They developed a formula similar to the general bearing capacity formula for shallow foundations.

$$q_{ult} = C_c N_c + \frac{\gamma_c B}{2} N_\gamma + D_f \gamma_c N_q \tag{2.8}$$

The factors N_c, N_q and N_γ are dependent on the ratio $\frac{A}{B}$ and the properties of trench and soil material.

Aboshi et al. (1979) introduced simple yet realistic method to calculate settlement of the reinforced ground based on stress concentration factor and one dimensional consolidation theory. Stress concentration in soil and column can be written as follows:

$$\sigma = \sigma_s A_s + \sigma_c (1 - A_s) \tag{2.9}$$

$$\sigma_c = \frac{\sigma}{1 + (n-1)A_s} = \mu_c \sigma \tag{2.10}$$

$$\sigma_s = \frac{n\sigma}{1 + (n-1)A_s} = \mu_s \sigma \tag{2.11}$$

where n is the stress concentration factor and μ_c and μ_s are the ratio of stresses in clay and stone respectively. The settlement of the reinforced ground is then expressed as

$$S_t = m_v \sigma_c H = m_v (\mu_c \sigma) H \tag{2.12}$$

where m_v is the volume compressibility and H is the thickness of the clay layer.

μ_c is the settlement reduction ratio; where

$$\frac{s}{s_t} = \frac{m_v \sigma H}{m_v \sigma_c H} = \frac{1}{1 + (n-1)A_s} = \mu_c \tag{2.13}$$

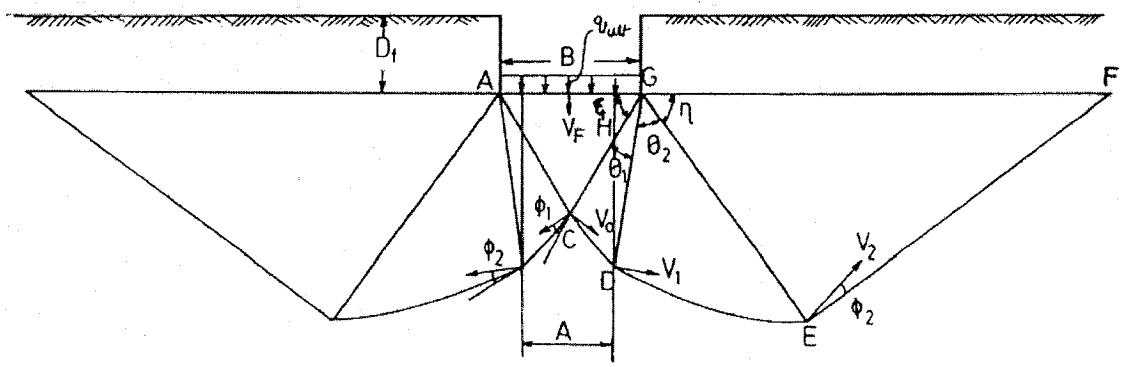

(a) Failure mechanism for A/B ≤1

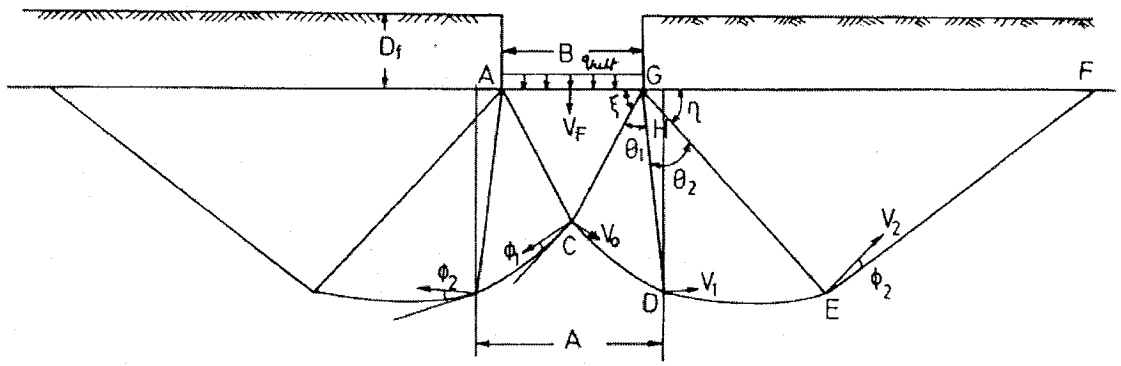

(b) Failure mechanism for A/B ≥1

Figure 2.17 Failure mechanism of a trench, after Madhav and Vitkar (1978).

Abashi et al. indicated that Equation 2.13 should only be used when the ratio of area replacement, A_s, is less than 30%, otherwise the method will overestimate the settlement. This is due to the fact that beyond this ratio, the replacement effect of stone columns can no longer be neglected. Barksdale and Goughnour (1983) reported that method is overestimating the measured settlements for all replacement ratios.

Goughnour and Bayuk (1979a) assumed that column material is incompressible, both the column and soil will equally settle and neglect the shear stress between them. Goughnour and Bayuk (1979b) concluded that the magnitude of this stress is always less than 9.6 KPa. The analysis considers both elastic and plastic behavior of stone and clay. The value of K starts from K_o line for the initial condition and is bilinear with the increase of stress. Furthermore, the value of K was found to be in between K_o and $1/K_o$.

Barksdale and Bachus (1983) proposed an approximate approach, which can be used for preliminary analysis of individual stone column within a group. They proposed that the ultimate load of the stone column can be calculated as

$$q_{ult} = c_u N_c \tag{2.14}$$

c_u is the undrain shear strength of the surrounding soil and N_c is bearing capacity factor of the material of the stone columns. N_c is dependent on the compressibility of surrounding soil and has the limit of 18 to 22 for low to high initial stiffness respectively. Mitchell (1981) recommended the value of 25 for vibro-replacement stone column. Datye et al. (1982) recommended the value of 25 to 30 for vibro- replacement stone columns, 45 to 50 for cased, rammed stone columns and 40 for uncased, rammed stone columns.

For the group of stone column, Barksdale and Bachus considered the failure shape given in Figure 2.18 and assumed that the foundation is loaded quickly so that undrained

shear strength is developed in the cohesive soil. A composite ground were assumed and based on shear failure in soil and stone the following equations were obtained.

$$(\tan\varphi)_{avg} = \mu_s A_s \tan\varphi_s \tag{2.15}$$

$$c_{avg} = (1 - A_s)c \tag{2.16}$$

$$\beta = 45 + \frac{\varphi_{avg}}{2} \tag{2.17}$$

$$\sigma_3 = \frac{\gamma_c B \tan\beta}{2} + 2c \tag{2.18}$$

where $tan\phi_{avg}$ and c_{avg} are the tangent of the composite angle of friction and the cohesion respectively. μ_s is the stress concentration factor of stone, γ_c is the unit weight of the soil and B is width of the foundation. The total bearing capacity of the reinforced ground is then defined as

$$q_{ult} = \sigma_3 \tan^2\beta + 2c_{avg} \tan\beta \tag{2.19}$$

However except in slopes, this mode of failure is rarely occur in reality.

For the case of settlement of stone columns, Barksdale and Bachus assumed the following two conditions:

1. Low compressibility soils

For $E_s/E_c \leq 10$ curves developed base on linear elastic theory. (Figure 2.19)

2. Compressible cohesive soils

For $E_s/E_c > 10$ design chart are presented based on elasto-plastic condition. The effect of slipping between the column and the soil was examined and was found that it has a negligible influence on the calculated settlement. When the lateral bulging is taking place and the interaction effect between the neighboring columns is created, they

concluded that a rigid unit cell method could not be representative for this condition. Accordingly, flexible boundaries were assumed (Figure 2.20). Nevertheless, as it will be presented in this thesis, none of these models can represent a true deformed shape of a group of stone columns for the majority of ground conditions and soil properties.

Gerrard et al. (1984) were one of the first to employ homogenization approximation method for group of stone columns. Homogenization technique is based on the assumption that column granular materials are scattered homogenously throughout the soil. They then utilized Tresca yield criterion for clay soil and adopted Mohr- Column yield criteria for stone material. Furthermore, they assumed that the total vertical strain in the clay and the stone are equal. The analysis of settlement was conducted for the cases of linear elastic and elasto-plastic conditions for both materials. They reported that the maximum stress occurs at depth of 0.25 to 1 times of the width of the foundation.

Mitchell and Huber (1985) presented an approximate solution to consider a three-dimensional stone columns model as axisymmetric cylindrical rings. The surface dimensions of the stone column rings were calculated in a way that the relationship between columns' surface area to the total surface area remained constant. (Figure 2.21) Utilizing axisymmetric finite element model developed by Duncan, they were able to compare the results of field load test conducted in Santa Barbara, California with their homogenization technique. While, the predicted values were greater all the time, a reasonable agreement was noted.

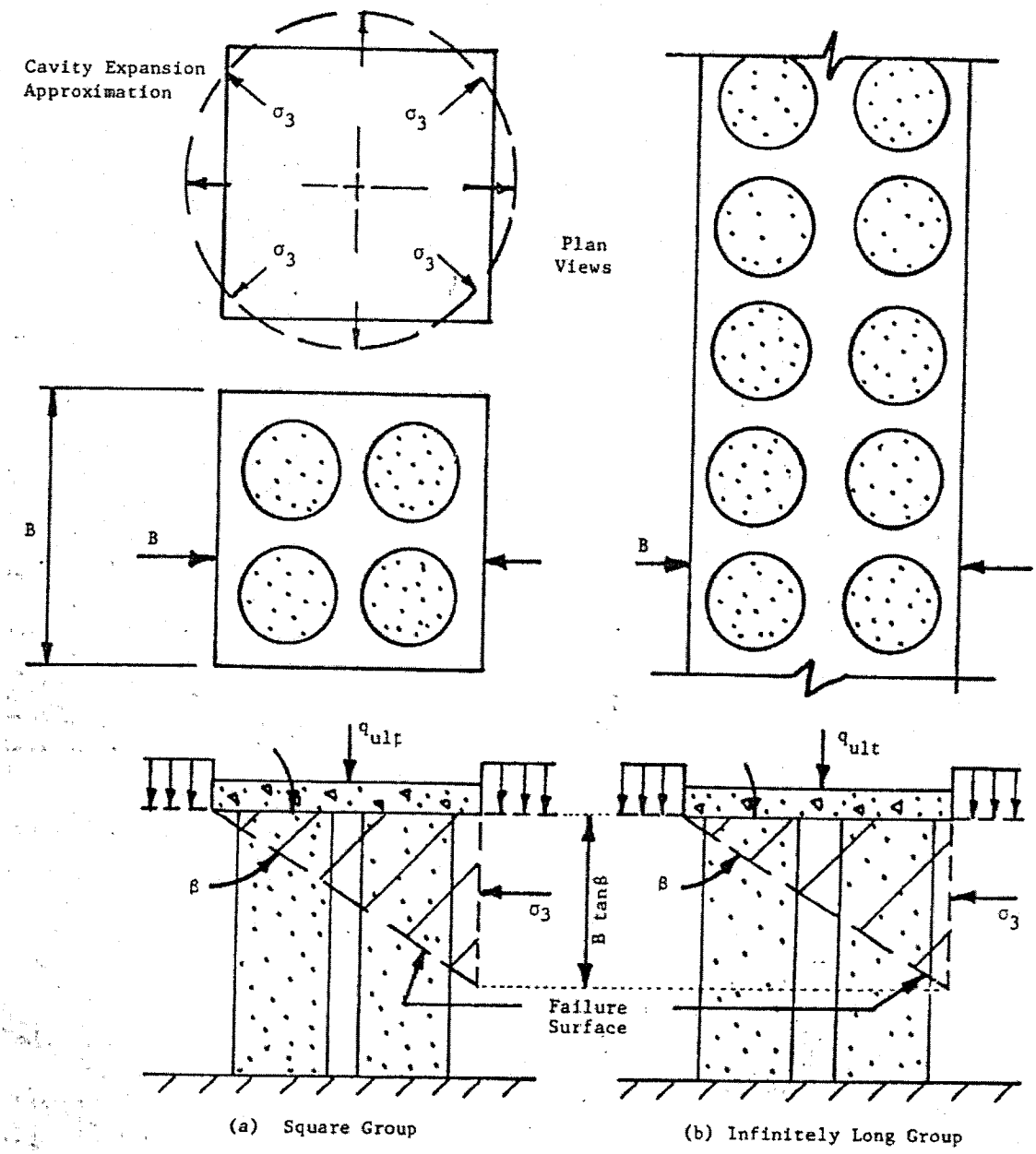

Figure 2.18 Shear failure shape for group of stone columns, after Barksdale and Bachus (1983).

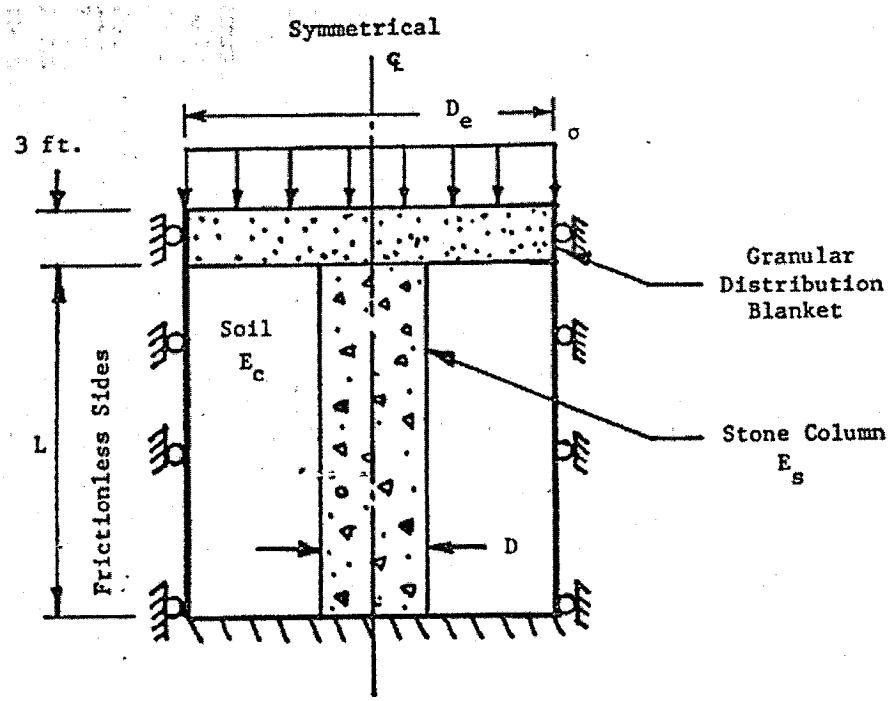

Figure 2.19 Elastic unit cell solution, after Barksdale and Bachus (1983).

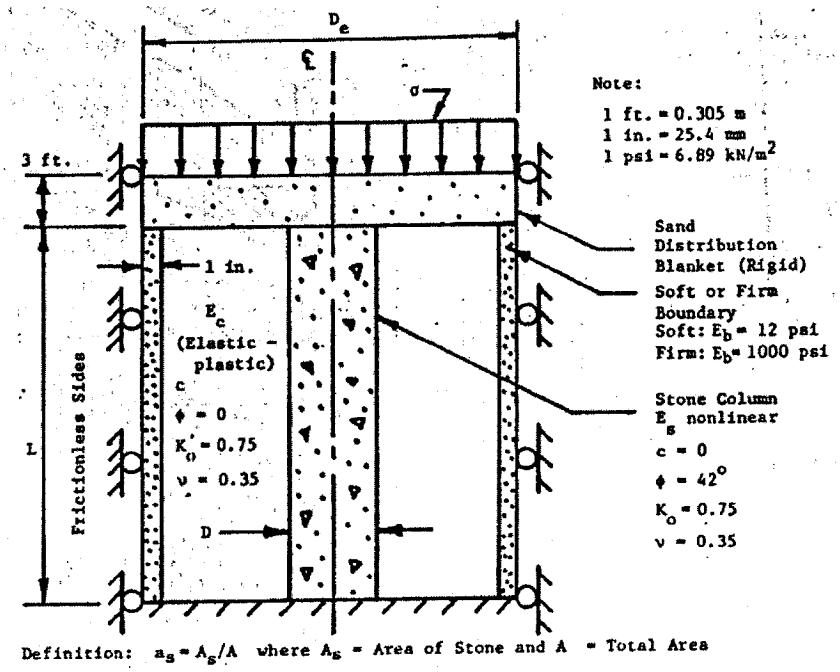

Figure 2.20 Nonlinear unit cell solution, after Barksdale and Bachus (1983).

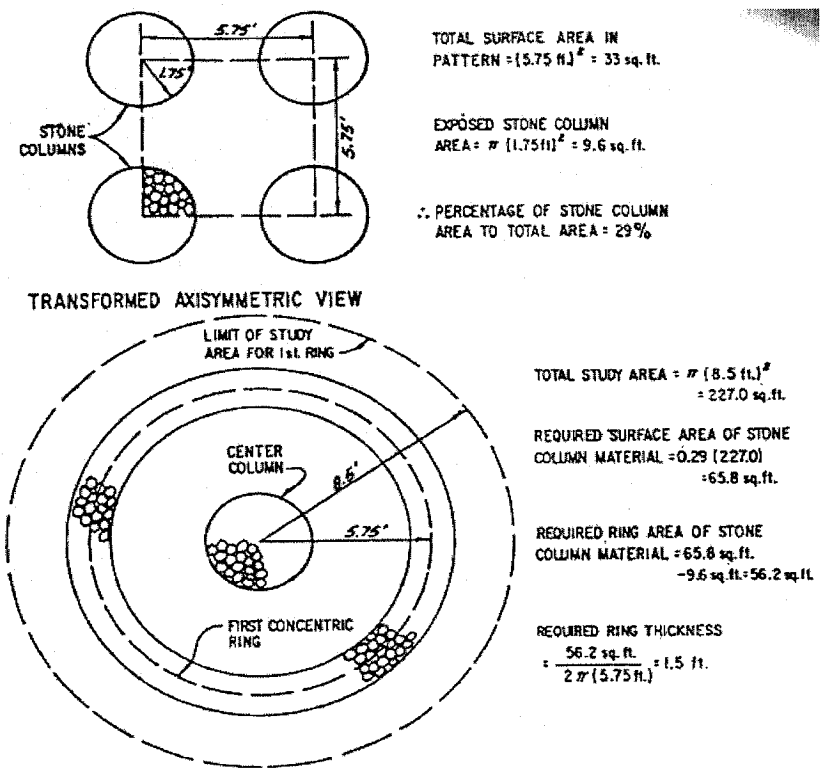

Figure 2.21 Analysis of stone column, after Mitchell and Huber (1985).

The homogenization technique was further advanced by Schweiger and Pande (1986). In 1988 Schweiger and Pande utilized their method to model a road embankment constructed on soft clay reinforced by stone column. They declared that homogenization technique was used to illustrate a realistic behavior of stone columns.

Priebe (1991) assumed that general shear failure occurs in the reinforced ground with stone columns. He developed two methods based on equivalent soil assumption. In the first model, the average cohesion and angle of shearing resistance of the equivalent and surrounding soft soil were considered and the ultimate load on the foundation was calculated using the theoretical methods for unreinforced soil. In the second model the average width of the foundation was assumed and the capacity was then calculated using the material characteristics of the untreated ground (Figure 2.22).

Lee and Pande (1994) developed another homogenization model using Mohr-Coulomb yield criterion for stone and the modified critical state model for in-situ soil, and further the non-associate flow rule was employed for the stone material. The model was incorporated on an axisymmetric finite element code. Figure 2.23 shows the comparison of the test results of Stewart & Wu (1993) with the theoretical method.

Hu (1995) compared the results of physical modeling of stone columns based on laboratory work with the results of Lee and Pande's homogenization technique and declared that the homogenization method over predicts the total bearing capacity by about 20%. The stiffness of the reinforced ground was also overestimated by a large proportion. Furthermore the non-liner stress dependent hardening behavior observed in all the physical model tests was not shown in the numerical solution.

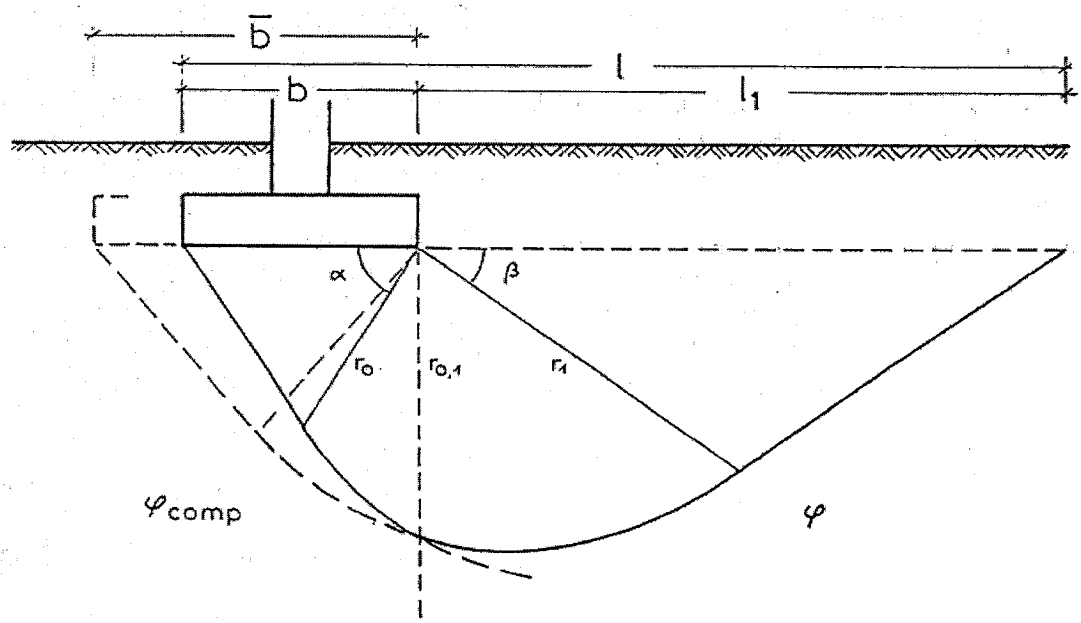

Figure 2.22 Approximate ground failure line, after Priebe (1991).

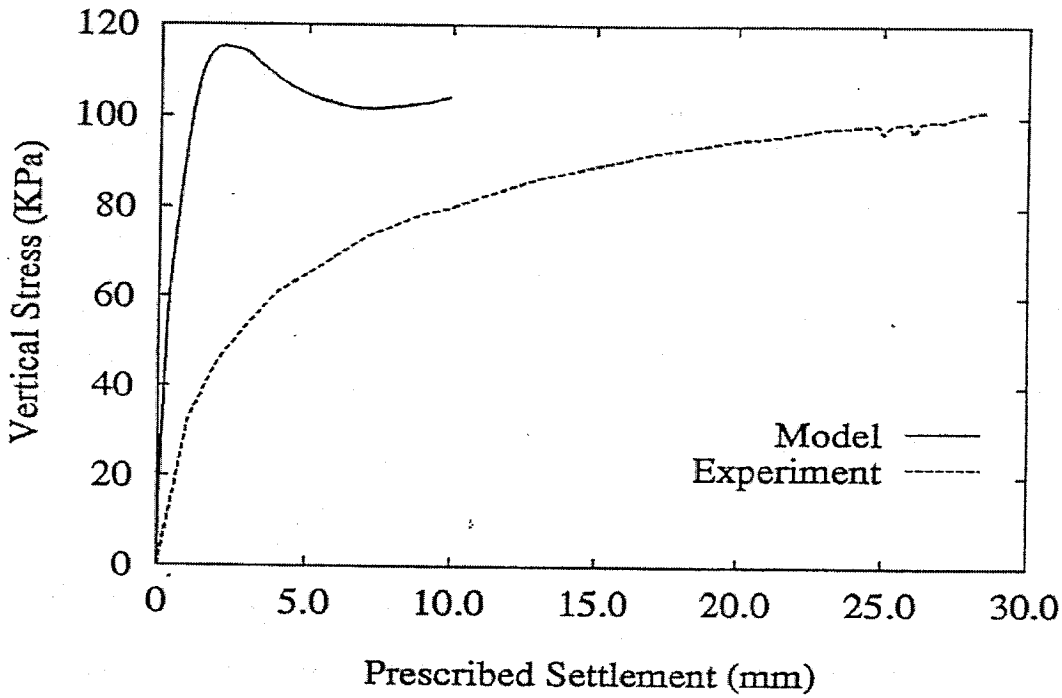

Figure 2.23 Prescribed settlement and vertical stress relationship, after Lee and Pande (1994).

Lee and Pande investigated the effect of reduction length of the central column. Figure 2.24 shows that this reduction in length does not make any significant changes on the behavior of a group of stone columns. This reduce of length may lead to an economical design. However, Hu (1995) criticized this concept in reducing cost of the construction and questioned the applicability of this change of length in terms of construction practice.

Lee and Pande (1998) have refined their model developed in 1994. Figure 2.25 presents a comparison of their results and those of Hu, where good agreement was noted. Nevertheless, the results were only validated for single experimental test.

Based on thick cylindrical problem, elastic properties for soil and plastic condition for column material Poorooshasb and Meyerhof (1997) have developed a method to calculate the settlement of ground reinforced with stone columns. It was assumed that both soil and column materials undergo the same displacement. This assumption is proven by Vautrain (1977). Furthermore, Poorooshasb et al. (1997) employed the Canasand model proposed by Poorooshasb et al. (1966, 1967). In this method the unit cell was divided into a number of equal sections and settlements were developed for each section. The settlement of the whole system was the sum of the settlement of all sections.

Shahu et al. (2000) developed a theoretical model which analyzes soft soil with stiff crust overlain by granular mat and treated with granular piles. Equal strain condition and the distribution of shear stresses between column and the crust-soil system were considered.

Ayadat and Hanna (2005) conducted experimental study on encapsulated stone columns in geofabric installed in collapsible soil. Bearing capacity and settlement of the columns were investigated. Columns made of sand were tested with different lengths and strengths of geofabric. They reported that un-reinforced stone columns did not improve significantly the characteristics of the soft soil. Nevertheless, bearing capacity of reinforced stone columns was increased considerably.

2.4 Discussion and Scope of Present Research

Vibroflotation Group Co., one of the world's leading ground improvement companies, have reported large scatter between the results of different stone column theoretical methods to calculate the settlement of reinforced ground (Figure 2.26), which may lead to the conclusion that in the literature, there is no viable theory to predict settlement of stone columns. This was explained due lack of well-documented full-scale load tests for stone columns or the varieties in installation techniques and vibratory equipments.

In 2004 during the International Symposium on Ground Improvement (ASEP-GI 2004) settlement prediction exercise had been organized where 17 participants calculated settlement of an embankment constructed on soft soil improved with stone column using different available methods (Mestat et al, 2006). The estimated results were compared with the available field measurements where poor agreement between the measured and predicted results was observed, with a large scattering of the calculated results.

Furthermore, Ambily and Gandhi (2007) reported that: "In spite of the wide use of stone columns and development in construction methods/equipments, present design methods remained empirical and only limited information is available on the design of stone columns in codes/textbooks."

All these statements and recent researches imply that there is lack of proper understanding of actual behavior of stone columns and accordingly lack of reliable theoretical for this ground reinforcement technique. In the next chapter a through study related to behavior of single and a group of stone columns will be conducted.

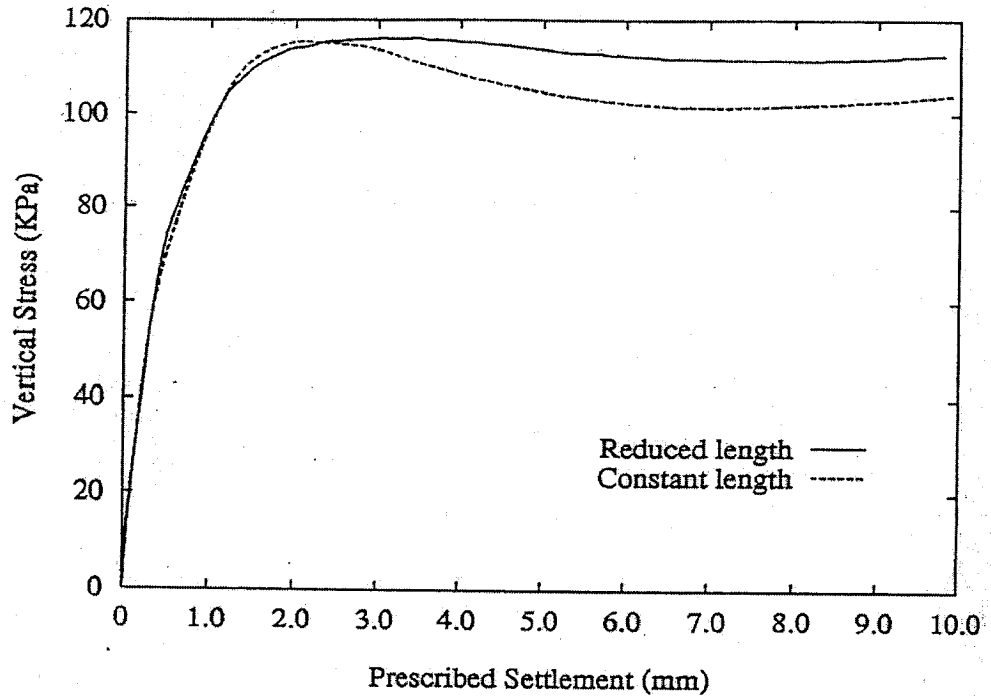

Figure 2.24 Analysis of foundation with reduced column length near the center-prescribed settlement and vertical stress relationship, after Lee and Pande (1994).

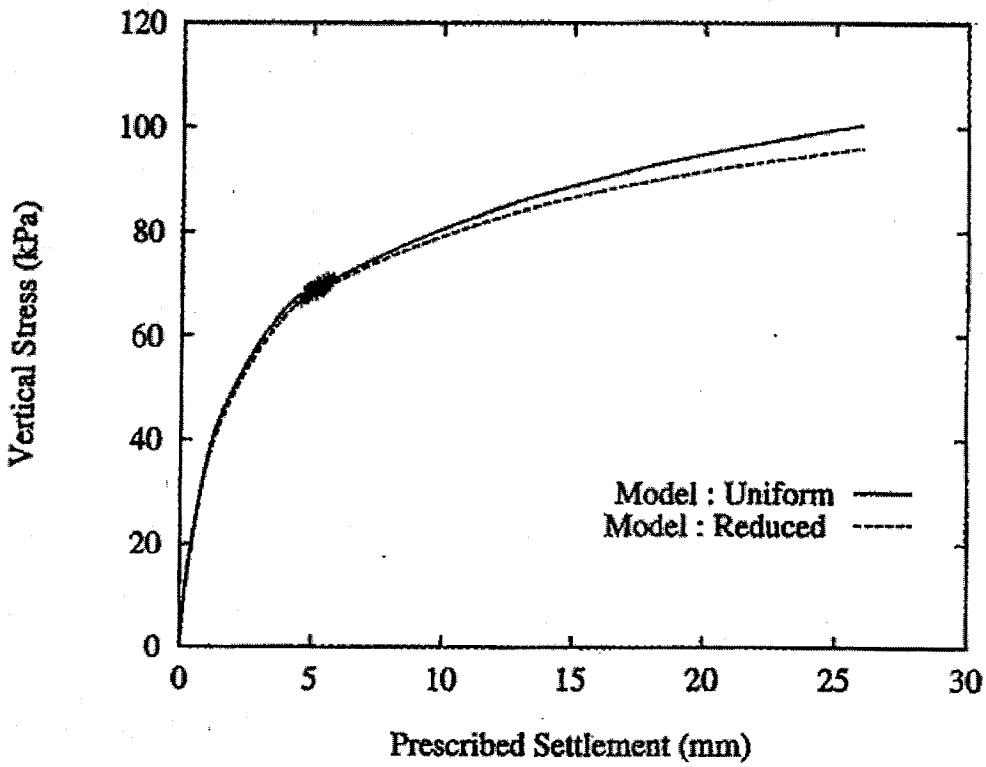

Figure 2.25 Settlement and stress relationship, after Lee and Pande (1998).

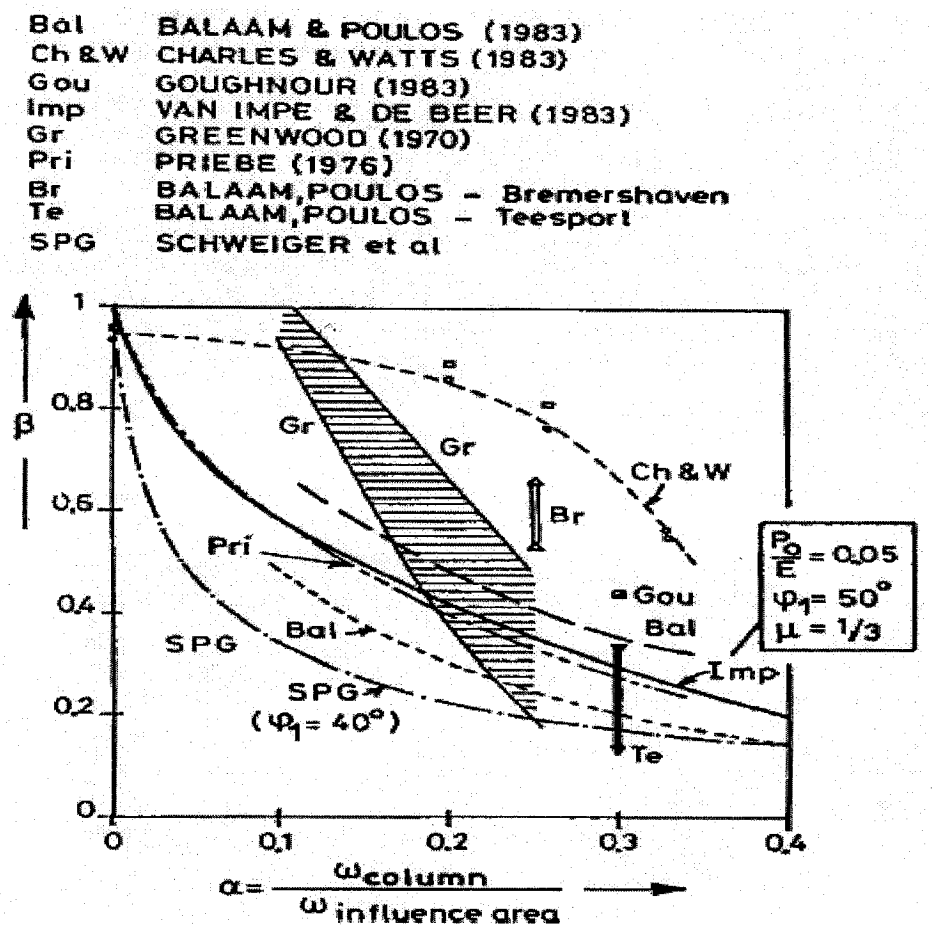

Figure 2.26 Comparison of settlement estimation methods, after Vibroflotation Group Co. (Vibratory Ground Improvement Manual).

CHAPTER 3

Numerical Model

3.1 General

Several reports can be found in the literature dealing with the prediction of bearing capacity and settlement of group of stone column based on the performance of single column. This assumption led researchers to ignore the possibility of group interaction; consequently, bulging was considered as the only mode of failure. Accordingly, the theories developed have produced wide discrepancies. In this chapter a numerical model will be developed to investigate single and group of stone columns. The objective is to predict the capacity and settlement of these columns under given soil/load/geometry conditions. Parametric study will be then performed on the parameters believed to govern this performance. Furthermore, the model is capable to identify the mode of failure under given loading/soil/columns conditions.

3.2 Numerical Model

The numerical model developed in the present investigation utilizing the nonlinear elasto-plastic finite element technique. Two-dimensional finite element model was developed to simulate the case of strip foundation on stone columns. 15 triangular node elements were used to develop the mesh. The mesh was medium generation, utilized as the global coarseness of the model; whereas, it was refined in the area of reinforced ground, where higher stresses and displacements are expected. In this investigation, it was assumed that

the raft is rigid, and accordingly, both the stone columns and the surrounding soil undergo the same amount of settlement. Fixed support was considered at the bottom of the mesh and roller supports were on the vertical boundaries. This arrangement represented a realistic case in the field. Figures 3.1 and 3.2 present the general layout of the numerical model.

In this investigation, the constitutive laws of Mohr Coulomb, Cam Clay and Soil Hardening to model the soil were examined. After several trials, it was concluded to implement Mohr Coulomb constitutive law for both the stone columns and the soft soil. Axisymmetrical condition was assumed for the case of single columns; whereas, plane-strain condition was considered for groups in a continious pattern. Boundaries of the numerical model were set after several trials in order to avoid horizontal and vertical stress confinements at the boundaries. No slip elements were installed at the interface between the column and the surrounding soil. This can be explained by the fact that the vertical displacement of both the rigid raft and the soil will take place together under the applied load, and accordingly, no differential settlement will be allowed (Goughnour and Bayuk (1979b)). Mitchell and Huber (1985), Saha et al (2000) and Ambily and Gandhi (2007) have implemented similar procedure in developing their numerical models.

Numerical model was developed using PLAXIS V8 program. PLAXIS is developed in 1986 at Delf University of Technology in cooperation with Dutch Ministry of Public Works and is widely used in soil mechanic analysis. Number of soil models is in the program available in order to model the non-linear analysis and the software is also capable to perform elastic and dynamic analysis.

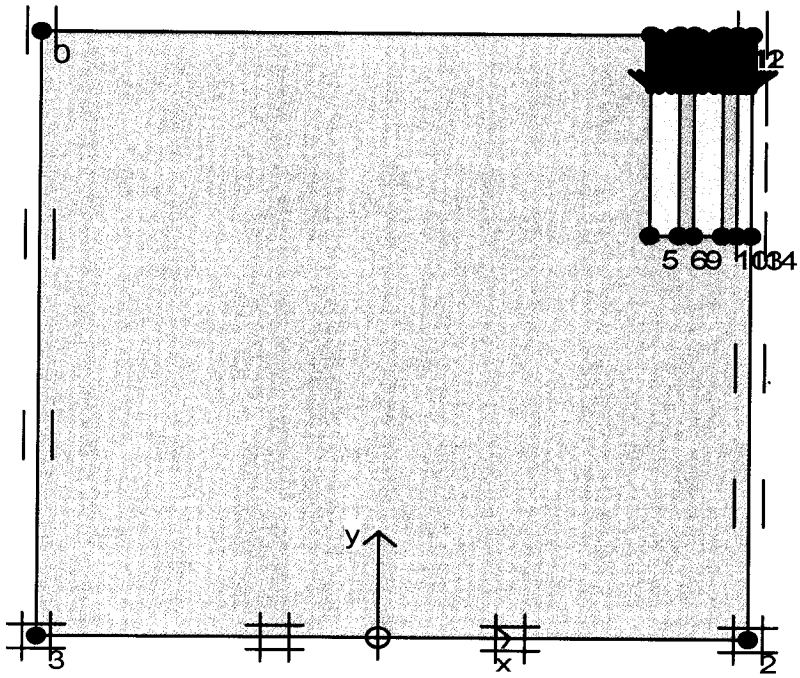

Figure 3.1 Layout of the numerical model.

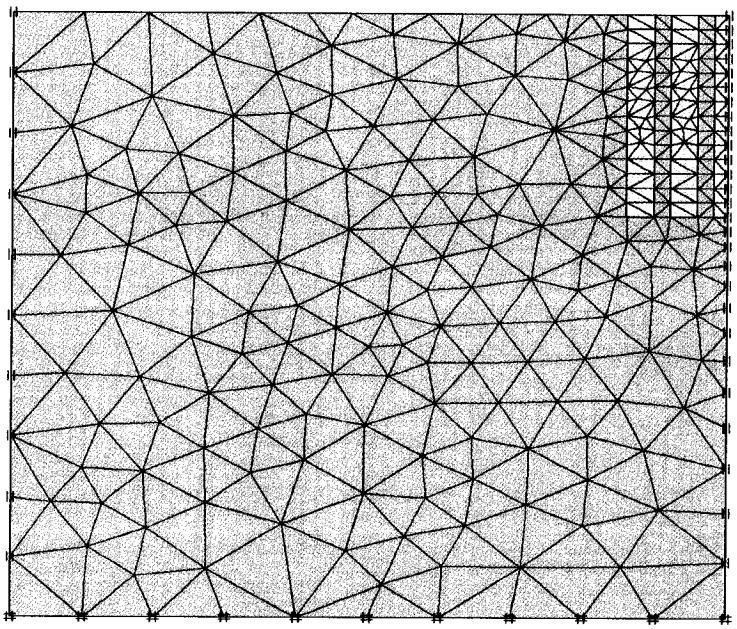

Figure 3.2 Mesh generation of the model.

3.2.1 Material Properties and Geometry Condition

Appropriate choices of material properties are necessary in order to have an accurate simulation of the reinforcement system in the numerical modeling. The properties of stone column, soft soil material and the geometry condition can be found in the literature. These characteristics are presented in tables 3.1 and 3.2 and were used in the numerical modeling.

The area replacement ratio, total area of stone columns over the area of unreinforced soil, which is normally used for a group of stone columns, is considered to be between 10% to 35%. For the amount of less than 10% no significant improvement in the ground properties would be achieved (Hu et al, 1997); whereas, there would be installation difficulties for A_s more than 35%. The columns diameter varies between 0.6 to 1.2 meter. One of the factors which are believed to have significant effect on the performance of reinforcement ground is the ratio of modulus of elasticity of stone over soft soil. Datye et al. (1982) indicated the lower limit of 100 for this ratio; however, Barksdale and Bachus (1983) suggested the upper limit of 100. Costet and Sanglerate (1983) recommended usage of modulus elasticity of column material about 10 times of the soil when $E_{column} \leq 100$ kN/m^2. This ratio is considered to have the lower limit of 10 and upper limit of 40 by Balaam et al (1981, 1985). Mestat and Riou (2004) stated the ratio has the range of 10 to 300 with the average of 40.

Table 3.1 Typical values for stone columns granular material.

Soil property	Range of values		Source
ϕ°	38 to 42 recommended		Barksdale and Bachus (1983)
υ	0.2 to 0.4 (dense sand) 0.3 0.2 to 0.25 0.3 0.25 to 0.35 (dense sand) 0.3 to 0.45 (dense sand) 0.35		Bowles (1982) Balaam (1985) Kolar and Nemec (1989) Lee and Pande (1998) Budhu (2000) Das (2000) Wright and Touquet (2004)
γ (kN/m^3)	Dry	14.4 to 17.1 (16.5 recommended) 19 to 21 15 to17 (gravel) 13 to16 (sand) 18 (dense sand) 18 (sand)	Barksdale and Bachus (1983) Kolar and Nemec (1989) Budhu (2000) Budhu (2000) Das (2000) Wright and Touquet (2004)
	Sat.	20.2 (for γ_d = 16.5) 20 to 22 (gravel) 18 to 20 (sand)	Barksdale and Bachus (1983) Budhu (2000) Budhu (2000)
E (kN/m^2)	58′000 48′000 96′000 to 192′000 48′000 to 81′000 (dense sand) 80′000 to 500′000 40′000 to 80′000 (dense sand)		Englehart and Kirsh (Balaam, 1978) Datye et al (1982) Bowles (1982) Bowles (1982) Kolar and Nemec (1989) Budhu (2000)
ψ°	30-ϕ		Bolton (1986)

Table 3.2 Typical values for unreinforced soft soil (clay).

Soil property	Range of values		Source
ϕ°	15 to 30		Budhu (2000)
υ	0.1 to 0.3 0.35 to 0.45 (very soft to soft) 0.3 and also 0.4 0.3 0.35 to 0.4 (soft) 0.3 to 0.35 (medium) 0.15 to 0.25 (soft) 0.2 to 0.5 (medium)		Bowles (1982) Barksdale and Bachus (1983) Balaam (1985) Lee and Pande (1998) Budhu (2000) Budhu (2000) Das(2000) Das(2000)
γ (kN/m^3)	Dry	14 to 21 11.5 to 14.5 (soft) 16	Budhu (2000) Das (2000) Wright and Touquet (2004)
	Sat.	16 to 22	Budhu (2000)
E (kN/m^2)	2′000 to 15′000 (very soft) 1′500 to 3′000 (soft) 1′000 to 15′000 (soft) 15′000 to 30′000 (medium)		Bowles (1982) Kolar and Nemec (1989) Budhu (2000) Budhu (2000)

3.2.2 Model Validation

The proposed model was validated using the laboratory test results of single stone column and a group of columns reported by Hu (1995). In this analysis, the geometry, boundary conditions and soil properties were duplicated in the present numerical model. Table 3.3 presents comparison between the results produced by the present numerical model and the data of Hu, where good agreement can be noted.

Figures 3.3 and 3.4 present the deform columns of the test number TS-17 of Hu's experimental work together with the one deduced from the present investigation, where interaction between columns within the group can be noted.

3.2.3 Deformed Shape of Single Stone Column

Based on field and laboratory experiments, it is well-known that single stone column deforms and fails as the result of bulging which forms in the upper portion of the column (Hughes and Withers (1974)). Numerical modeling was conducted in order to investigate the deformed shape of an isolated column. Table 3.4 presents material properties corresponding to a typical model developed for this purpose. Figures 3.5 to 3.8 show deformed mesh of the model for 0.05, 0.1, 0.2 meter uniform vertical displacement and at the failure respectively. These figures illustrate development of bulging with respect to the increasing load. Bulging gradually develops with load increments and failure eventually occurs. Figure 3.9 presents soil total displacement as the result of the foundation load. Large amount of soil movement in the bulging area is clearly seen. Horizontal soil displacement in the bulging area is observed in Figures 3.10 and 3.11. These figures show expansion of the stone columns in that area. Figure 3.12 presents relative shear shading which the area of red color represents failure of the reinforced area.

Table 3.3 Comparison between experimental test results of Hu's and the present numerical model.

Test Number	A_s (%)	Cu (kPa)	Spacing (mm)	Column Length (mm)	Test results (Hu et al) (kPa)	Present study (kPa)
Ts11	0	14			54	60
TS05	30	10.5	17.6	100	79	72
TS17	24	14	19.8	160	71	64
TS04	24	16.5	19.8	150	77	72
TS10	30	11.5	28	100	75	69

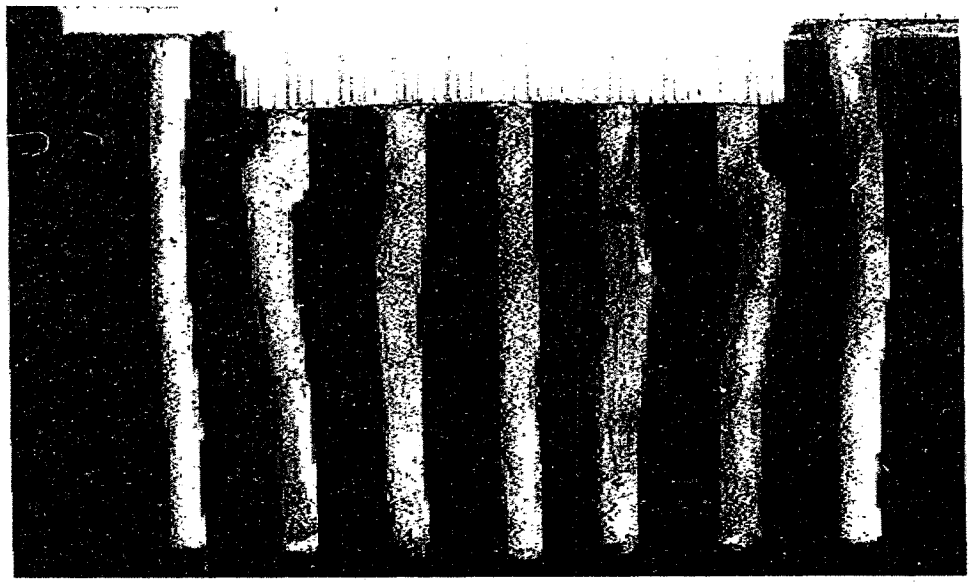

Figure 3.3 Deformed shape of the model test TS-17 after applying load, after Hu (1995).

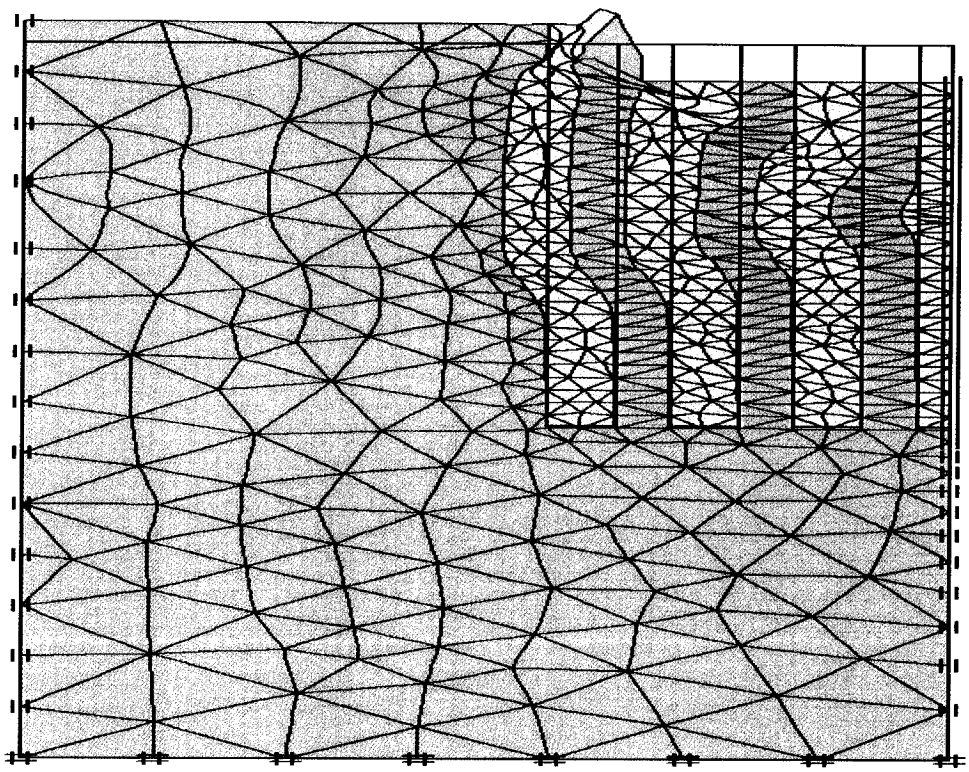

Figure 3.4 Test results of the Numerical model (Hu's test TS-17).

Table 3.4 Properties of soft soil and granular material for single stone column.

	E (kN/m^2)	υ	φ (^{o})	c (kN/m^2)	ψ (^{o})	Length (m)	Diameter (m)
Sand	100000	0.3	40	0	10	14	1
Clay	2000	0.3	10	5			

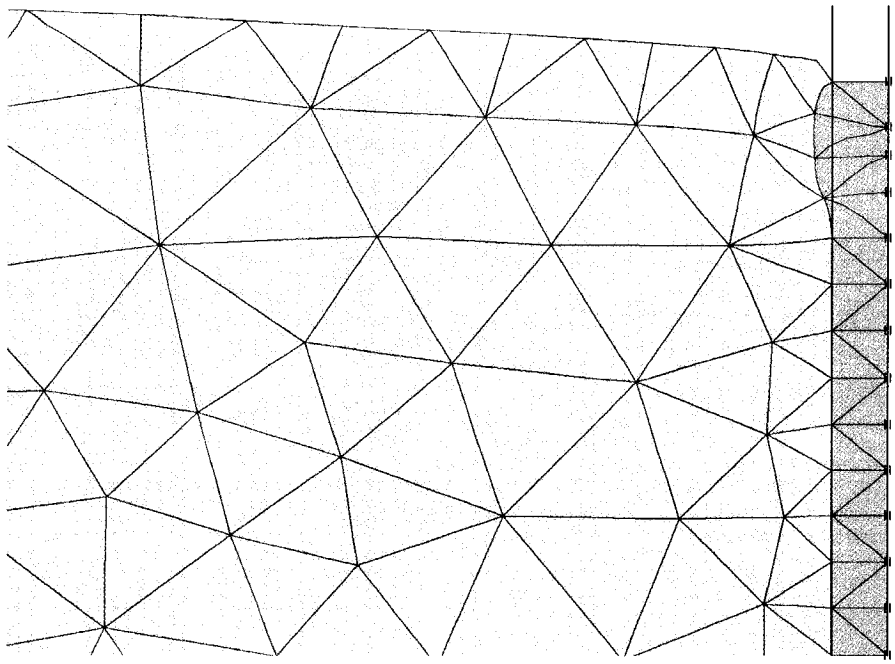

Figure 3.5 Deformed shape of single stone column due to 0.05 m displacement.

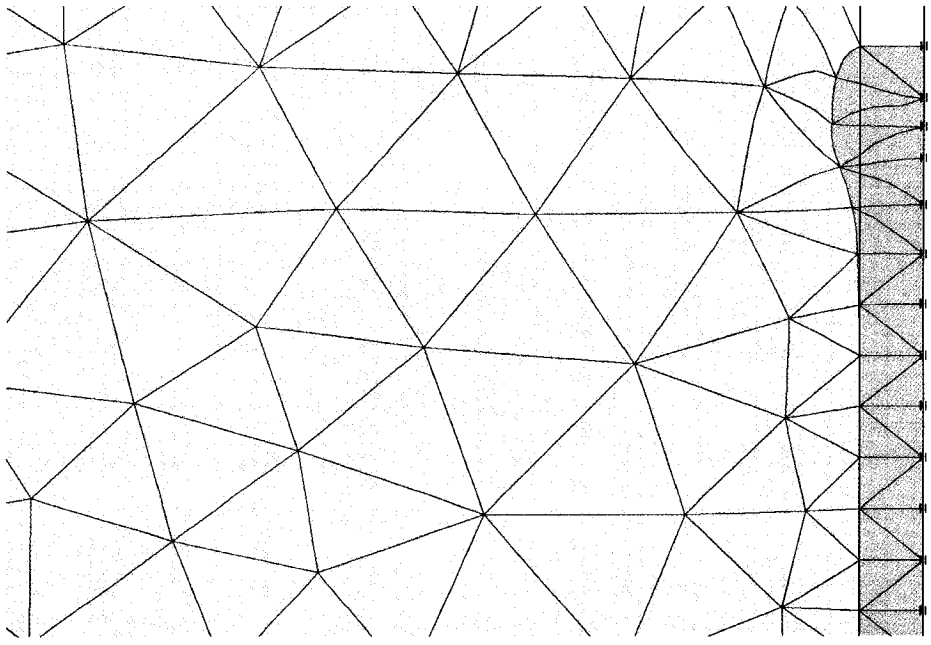

Figure 3.6 Deformed shape of single stone column due to 0.1 m displacement.

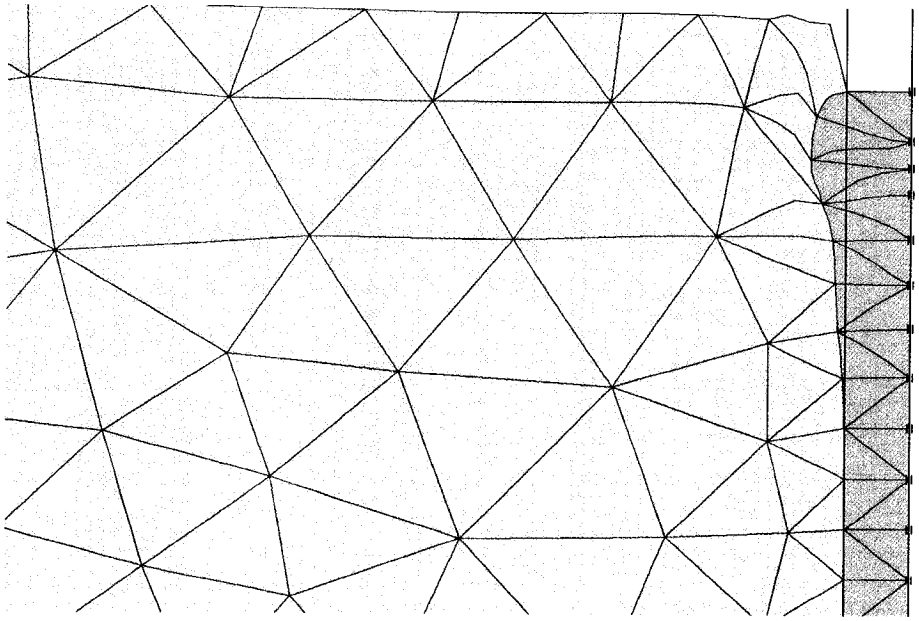

Figure 3.7 Deformed shape of single stone column due to 0.2 m displacement.

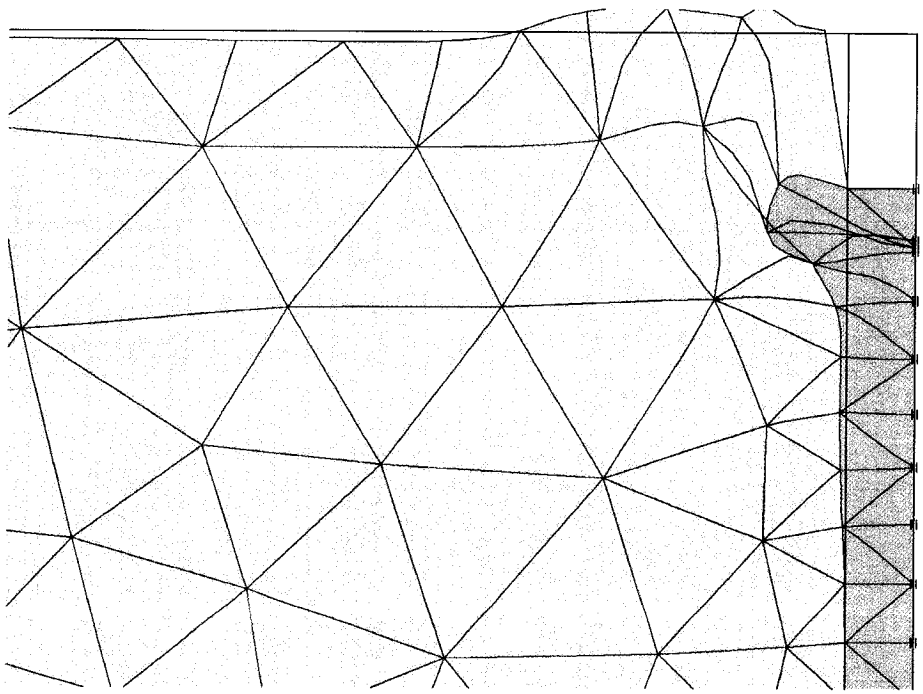

Figure 3.8 Deformed shape of single stone column at failure.

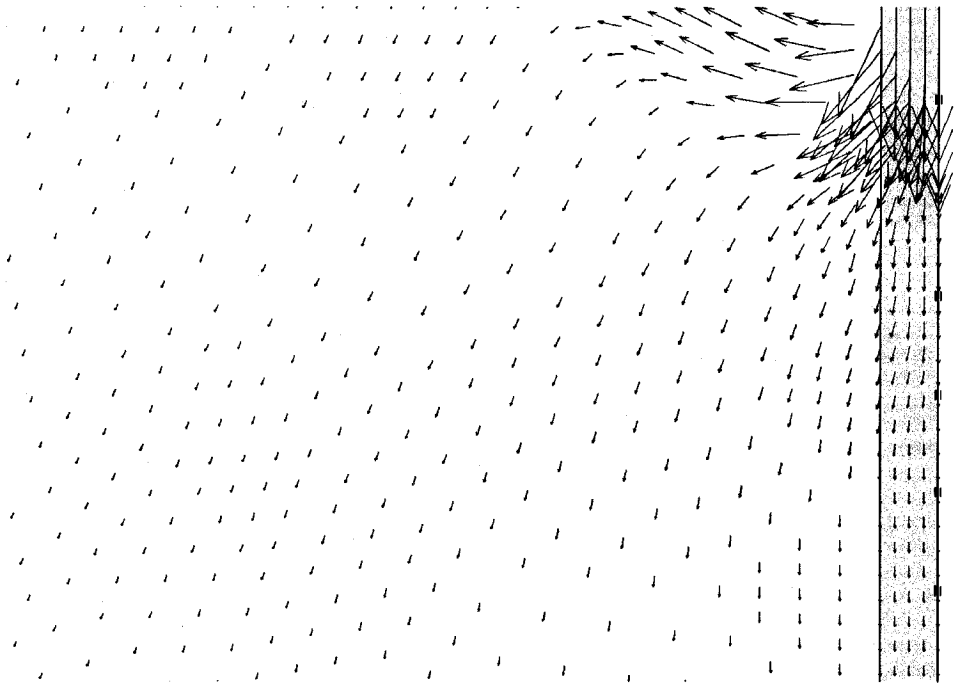

Figure 3.9 Total displacement of single stone column at failure.

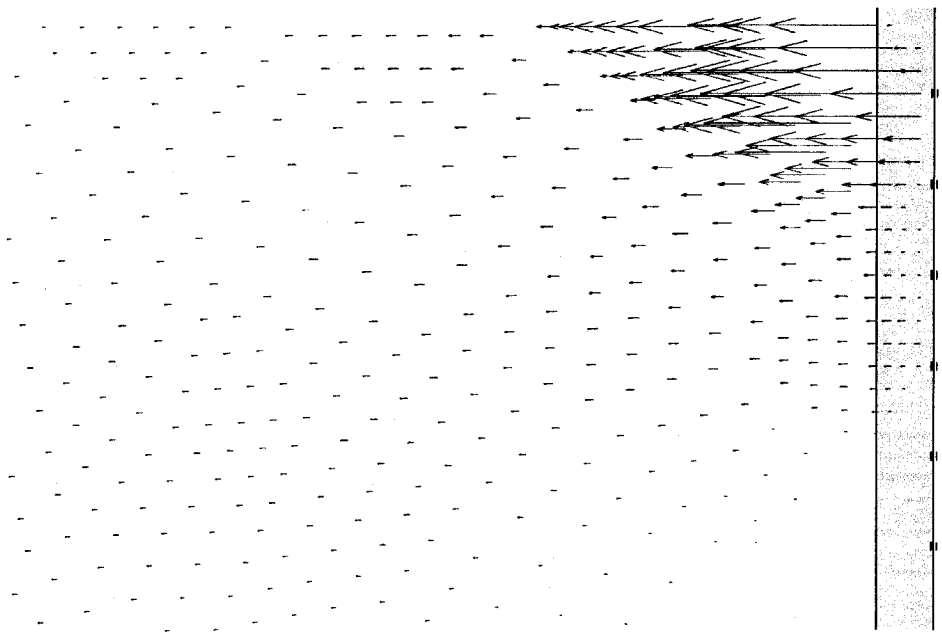

Figure 3.10 Direction of horizontal displacement of single stone column at failure.

Figure 3.11 Shading illustration of horizontal displacement of single stone column at failure.

Figure 3.12 Relative shear shading illustration for single stone column at failure.

All these observations clearly confirm that single stone column bulges as the result of applying load and it fails consequently as bulging develops. The developed finite element approach results similar deformed shape as was reported in the previous experiments. Hughes and Withers (1974) indicated that bulging happens within a depth equivalent to 4 times of the column diameter in the upper part of the column. Using the numerical model same depth was observed.

3.2.4 Deformed Shape of Group of Stone Columns

In order to extrapolate the limit experimental finding of group of stone columns to the other soil conditions large number of numerical modeling tests for different soil properties and reinforced ground geometries was conducted. Results of these tests would give a clear knowledge about the deform shape and mode of failure for group of columns.

All of the parameters which were believed to have influence on the performance of the system were considered in the development of the numerical model. The parameters considered in the model were chosen in order to cover all the possible cases for the reinforcement of stone columns. These parameters are listed in Table 3.5. Both cases of floating and rigid base stone columns were studied in this research and tests were conducted for long stone columns. In all the tests group interaction was observed. It should be mentioned that in these tests the lower limit of A_s was considered as 10%. By reduction of A_s and increment of the spacing among the columns, effect of column interaction reduces which may imply that for A_s less that 10% bulging failure might be possible for group of stone columns. This suggestion might be true which further investigations should verify it. However, area replacement ratio less that 10% is not normally used in the real case as there will be no significant improvement for the

reinforcement system (Hu at al. (1997)). Therefore, the lower limit of A_s is considered as 10% in this research.

Deformed shape for group of columns is presented here with a representative test. Table 3.6 illustrates the material properties and ground geometry of the test. Figures 3.13 to 3.15 show deform shape of stone columns as the result of vertical displacement of 0.1 m, half time of the failure and at failure.

Figure 3.13 demonstrates that even for low foundation load, bulging does not take place for the group of columns. Figures 3.16 and 3.17 represent the total and horizontal soil incremental displacement as the result of applying load respectively. Due to the group interaction and accordingly the soil movement which is seen in Figures 3.16 and 3.17 middle and outside columns deform laterally and are pushed outward. The direction of soil displacement and concentration of stresses does not allow bulging, which takes place for single stone column, to occur in the group of stone columns reinforcement system. This happens as the result of horizontal pressure of the neighboring columns on each other. Due to the direction of the soil movement, depending to the length of the columns, short or long, they move or partially bend to the outer direction of the reinforcement area. Only the center column, which is in the center of symmetry of the system, bulges. However, this bugling happens at much deeper depth comparing to single column. This is due to the column interaction effect which the horizontal pressure of the neighboring columns pushes bulging to occur in the lower depth where the effect of the horizontal stress becomes lower.

Table 3.5 Range of parameters used in the numerical model.

No.	Site conditions	Range of values
1	Clay module of elasticity	1500 to 14000 kN/m^2
2	Sand module of elasticity	35000 to 175000 kN/m^2
3	Clay Poisson's ratio	0.15 to 0.45
4	Sand Poisson's ratio	0.2 to 0.45
5	Sand friction angle	38° to 45°
6	Area ratio	10%, 20%, 30% and 40%
7	Stone column diameter	0.6; 0.8; 1 and 1.2 m
8	Stone column length	14 to 20 m
9	Type of loading	Uniform rigid loading

Table 3.6 Properties of soil and stone columns used in the numerical model.

	E (kN/m^2)	υ	φ (°)	C (kN/m^2)	ψ (°)	Length (m)	Diameter (m)
Sand	80000	0.3	38	0	8	20	1
Clay	3000	0.3	15	5	0		

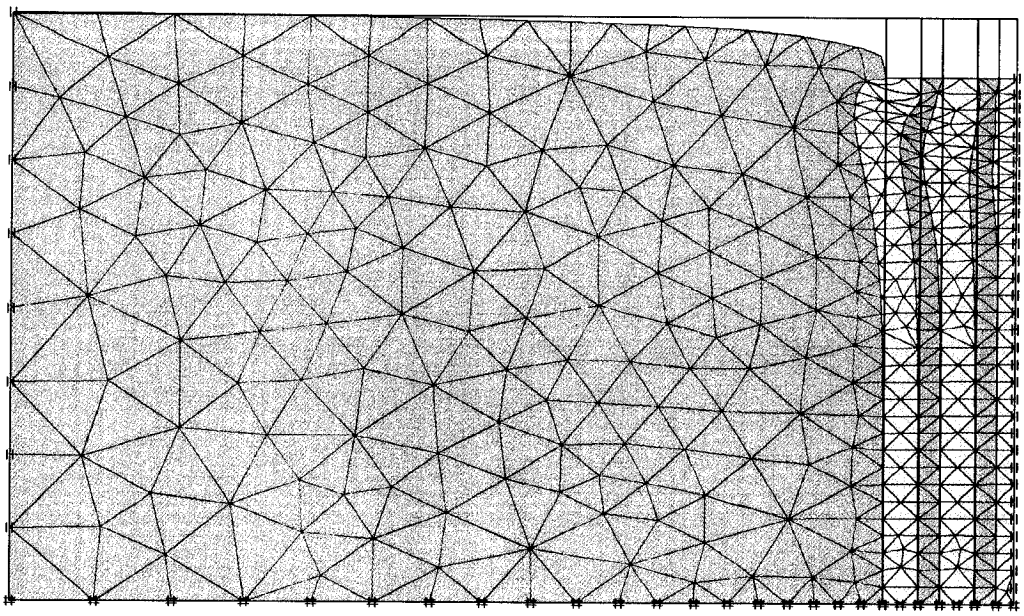

Figure 3.13 Deformed shape of group of stone columns due to 0.1 m displacement.

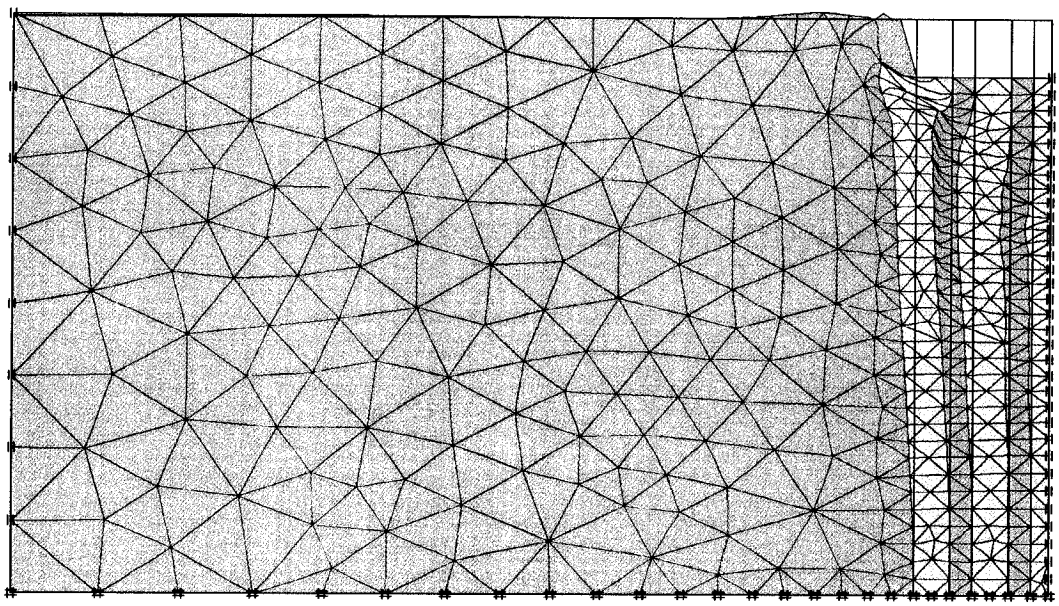

Figure 3.14 Deformed shape of group of stone columns at 0.5 time of failure.

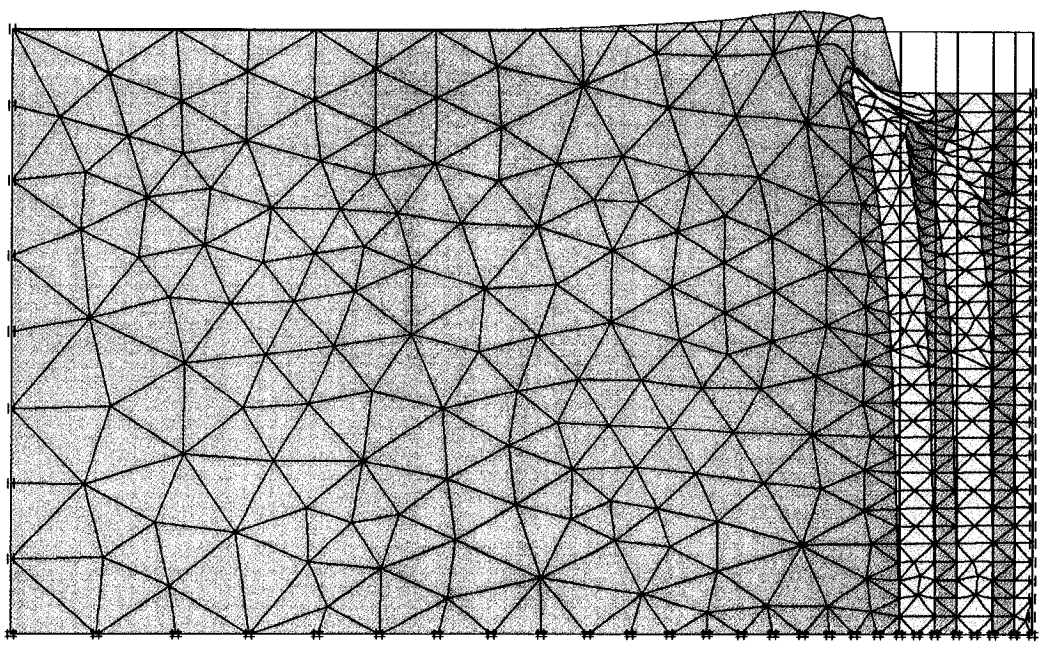

Figure 3.15 Deformed shape of group of stone columns at failure.

Considering Hu's (1995) experimental result, he reported shear failure and group interaction. However, he suggested that though failure happens due the shear, bulging shifts down for all the columns in the group as is presented in Figure 3.18. This suggestion is not observed in the numerical modeling where bulging occurs only in the center column as the foundation load is applied. By closely examining the results deduced from Hu's experimental work and also the laboratory experimental results of McKelvey (2002) no indication of Hu's suggestion can be accomplished.

Figure 3.3 illustrates test results of Hu's. It can be noted from this figure that the effect of pressure of neighboring columns on each other shows group interactions between columns. The neighboring column horizontal pressure and movement of the soil outside of the reinforcement area only let bulging to happen in the outer part of the column but not in the inner part (Figures 3.13 to 3.15).

The findings of this research show that group interaction takes place for all the model tests. These finding creates doubts of using unit cell concept and the theories which are developed based on this approach that may use unrealistic failure shape for group of columns (Figure 3.19).

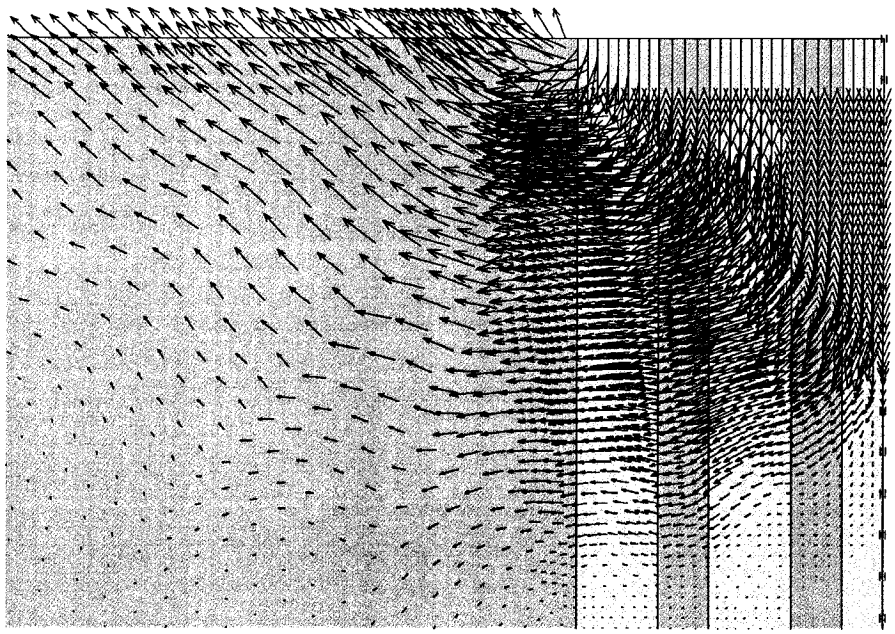

Figure 3.16 Total increamental displacement of group of stone column at failure.

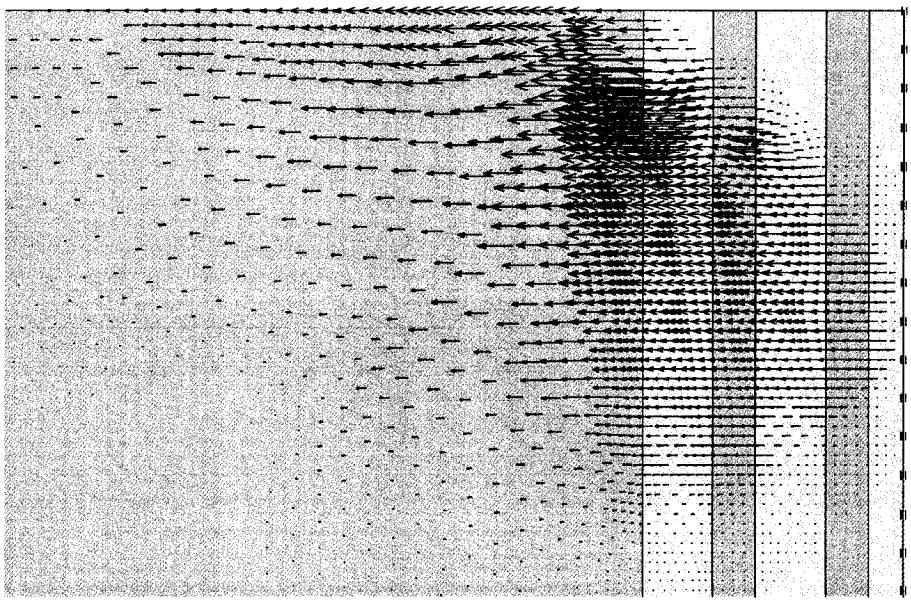

Figure 3.17 Horizontal increamental displacement of group stone column at failure.

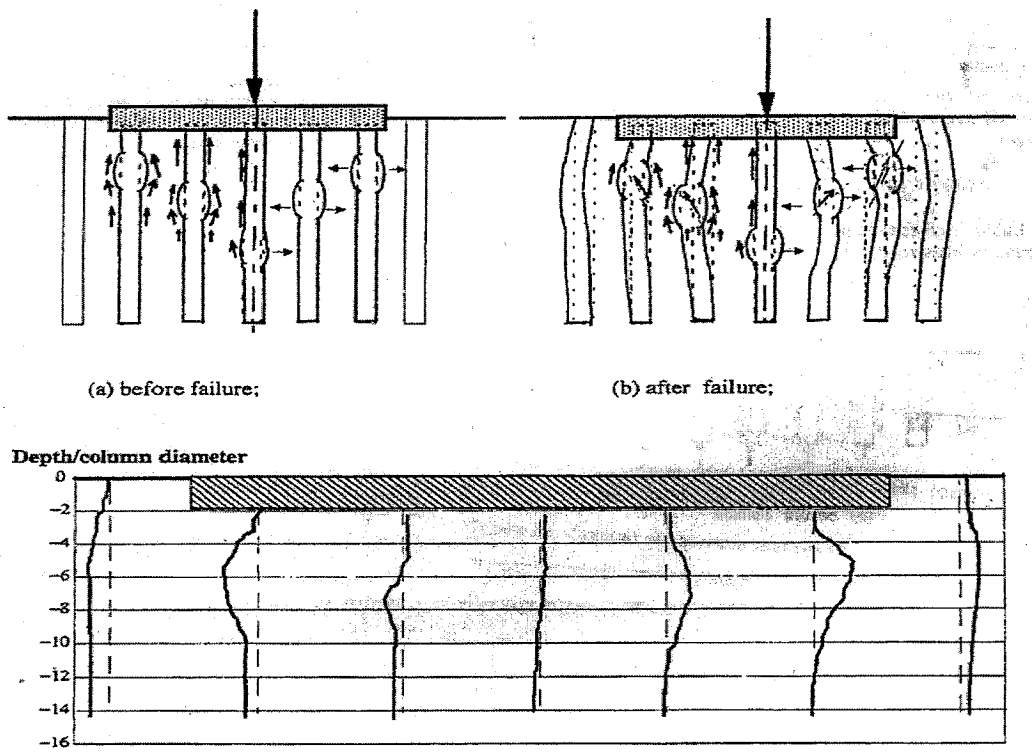

Figure 3.18 Suggested mode of failure for long columns, after Hu et al (1997).

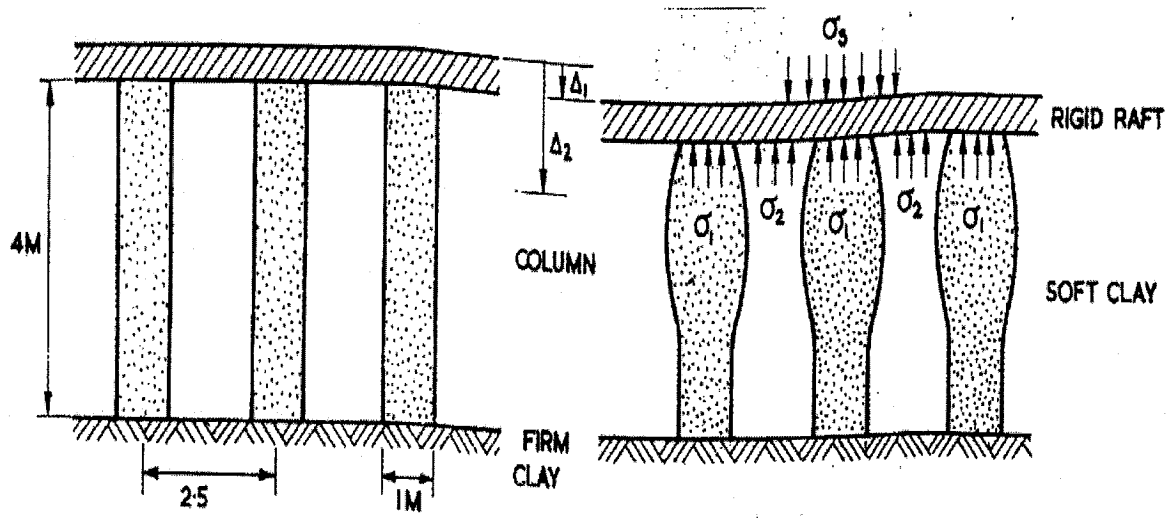

Figure 3.19 Behavior of columns under a large raft, after Hughes and Withers (1974).

3.2.5 Parametric Study

The influence of various material properties can affect the behavior of reinforced ground. Understanding the degree of influence of each property can be important in designing and enhancing knowledge about this reinforcement technique mechanism. Investigation on the effect of these parameters when the group of columns is considered has not been studied yet. Considering results from previous section, which confirms the difference between performance of single and group of columns, utilizing the results of single column for group may lead to unrealistic judgments. The effect of Poisson's ratio on the system is presented herein to demonistrate the negative effects of using unit cell to model group of stone column.

Numerical model was used to study the effect of each of these factors on group of columns and finite element technique was utilized. Large number of tests was carried out and the effect of properties, which mostly influence the bearing capacity and settlement of reinforced ground were investigated. The range of parameters used for these tests is illustrated in Table 3.5.

Both cases of floating and rigid base stone columns were modeled which are represented herein as test series 1 and 2 respectively. Different test were preformed with changing properties of the materials. In order to apply rigid foundation condition to the model, relative vertical axial displacements (ε_a) of 2% and 7% for test series 1, and 1.5% and 5% for test series 2 were applied. Uniform load corresponding to the relative displacement was calculated and eventually the ratio of the load applied in case of reinforced soil over the load in the case of unreinforced soil at a given displacement was

estimated. This ratio is introduced as load ratio and is presented as $\frac{P_2}{P_1}$. The horizontal axis is presented as the sum of the stone column diameters in the vertical plane over the width of the foundation. This represents the area replacement ratio for group of stone columns in plain-strain condition.

In Figure 3.20 (a) and (b) the effect of Poisson's ratio of natural soil (clay) and stone (or sand) with changing of the area replacement ratio for ϵ_a=2% and ϵ_a=7% are illustrated for floating stone columns. The Poisson's ratio is changes from 0.15 to 0.45 for clay and from 0.2 to 0.45 for stone. Stone Poisson's ratio is presented by dash lines in figures; whereas, full lines are used for clay illustration. It can be seen that with increasing the Poisson's ratio of clay the load ratio decreases. In higher Poisson's ratios, clay becomes more incompressible so when stone columns deform clay shifts the all the horizontal displacement by column to the neighboring column; i.e. magnifies the horizontal stress, helps columns deformation and therefore reduces the load ratio. Opposite result is seen for stone where with increasing of υ load ratio increases. This is due to incompressibility of stone columns. When a stone column becomes incompressible, while they wants to bulge the incompressibility and bulging effect of the neighboring column resists against the free deformation of the first column. This phenomenon eventually reduces the deform shape of the stone columns and increases the load ratio. Comparison between Figures 3.20 (a) and (b) reveals that for floating stone columns, load ratio reduces with increasing the vertical relative displacement. When foundation load is low increment of stresses due to the load is only occurred in the upper part of the stone columns. By increasing the vertical relative displacement, foundation load increases and the stresses inside the soil shifts to the lower part of the stone columns.

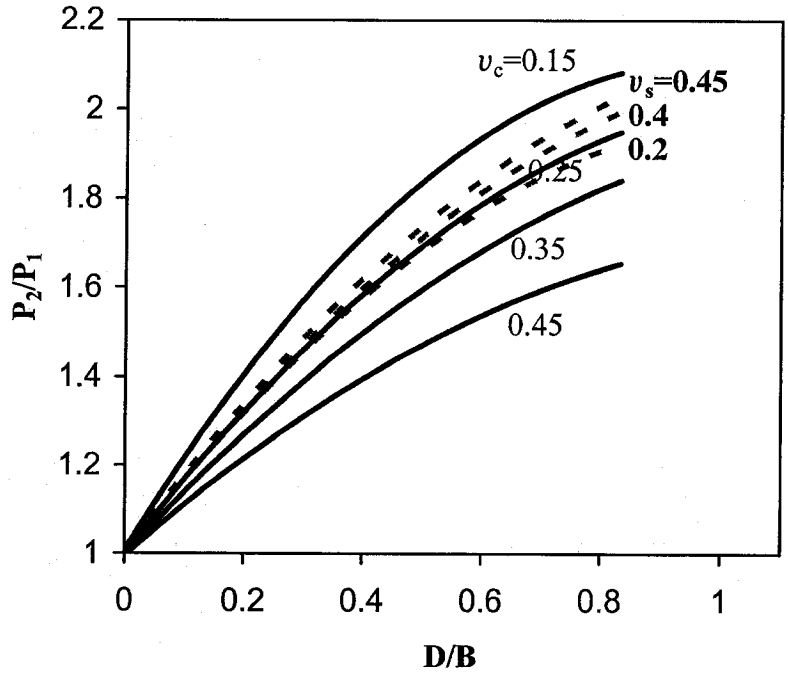

(a)

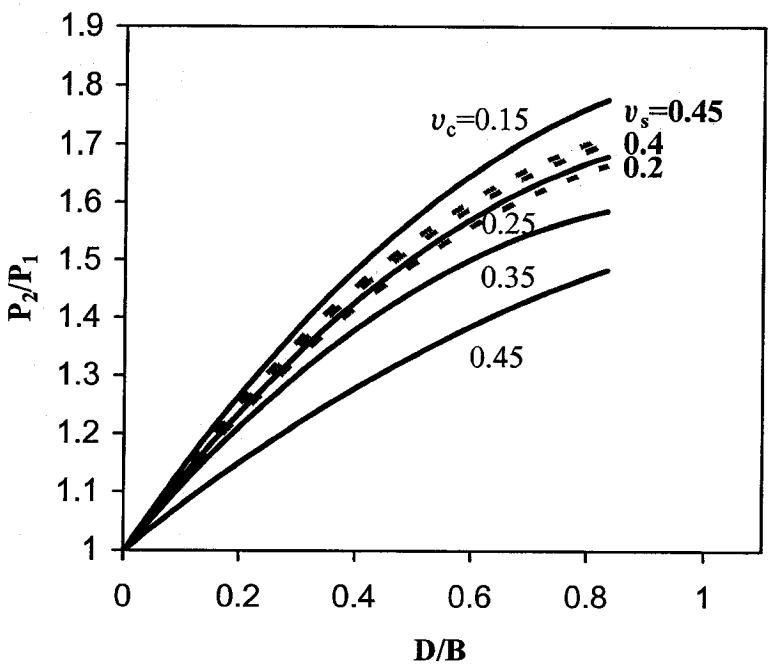

(b)

Figure 3.20 Load ratio versus $\frac{D}{B}$ for different sand and clay Poisson's ratio for floating stone columns (a) ϵ_a=2% (b) ϵ_a=7%.

This shifting of stress increases so that it reaches the end of the floating stone column where there is not much resistance to the load. In this condition the stone columns settle more in the soil and therefore load ratio decreases for higher vertical relative displacements. This trend can be better seen in Figure 3.21.

Figures 3.22 (a) and (b) represents the effect of Poisson's ratio for ϵ_a=1.5% and ϵ_a=5% where rigid base stone columns is considered. Same trend is observed as the case of floating columns. The only difference with the previous case is that now there is no more reduction in load ratio with increment of relative displacement. This is expected as in this case stone columns are placed on the rigid substratum for both conditions.

Figure 3.23 shows the setup of parametric study which is conducted by Balaam and Booker (1981). They did their study based on unit cell assumption and used finite elements technique. Figure 3.24 presents changes of the Poisson's ratio of soft soil versus the ratio of settlement of the raft on the stabilized site to that on unstabilized site of their study. It can be seen that with increment of Poisson's ratio the settlement ratio decreases which means that stone columns reinforcement system is more efficient when the factor υ is increased. This is opposite of what is observed in Figures 3.20 and 3.22. The reason of this observation is due to the nature of unit cell assumption. When the boundaries are rigid and stone column is placed under the rigid foundation (Figure 3.23) soft soil material is trapped inside the system. Therefore when soft soil is becoming incompressible it resists against occurrence of bulging of stone column and reduces the settlement. It may be concluded that unit cell assumption and theories based on it can not be a good representation for the problems dealing with group of stone columns.

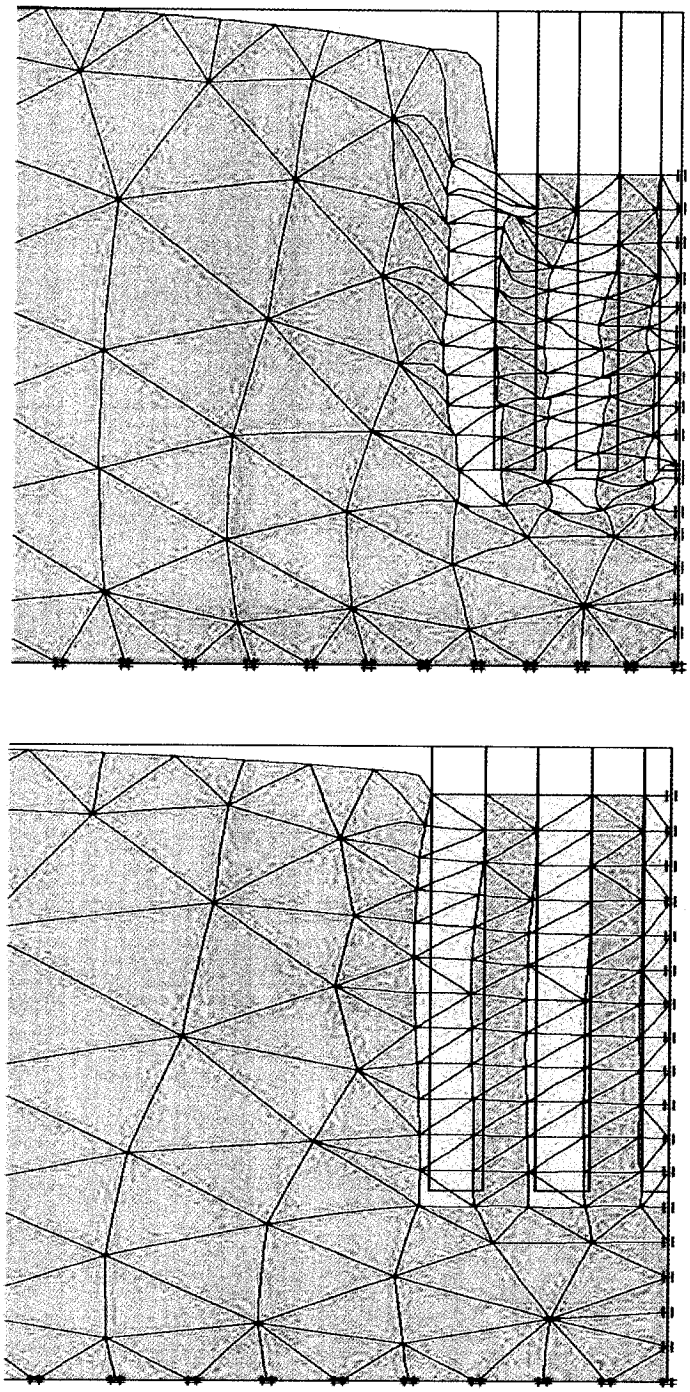

Figure 3.21 Settlement and deform shape of stone columns due to increment of relative vertical displacement.

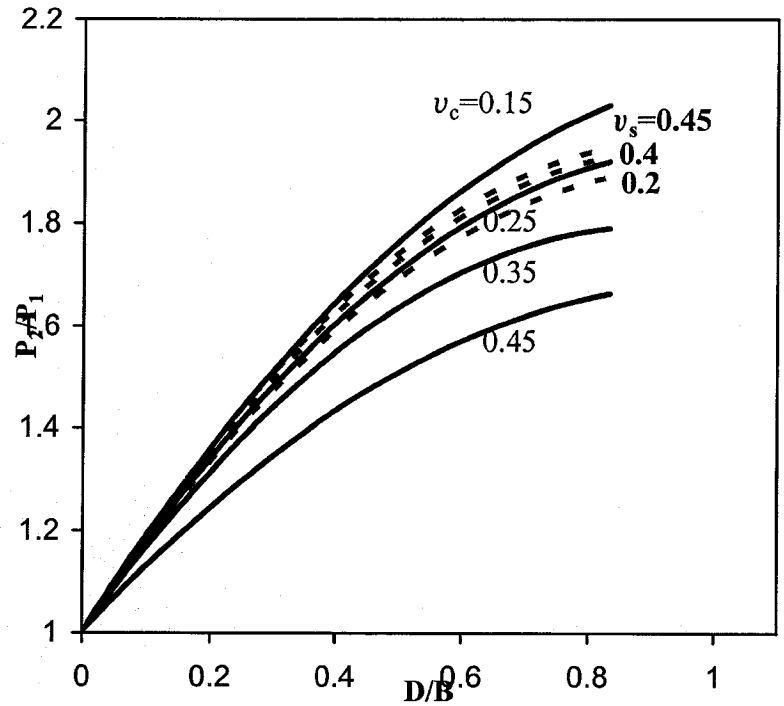

(a)

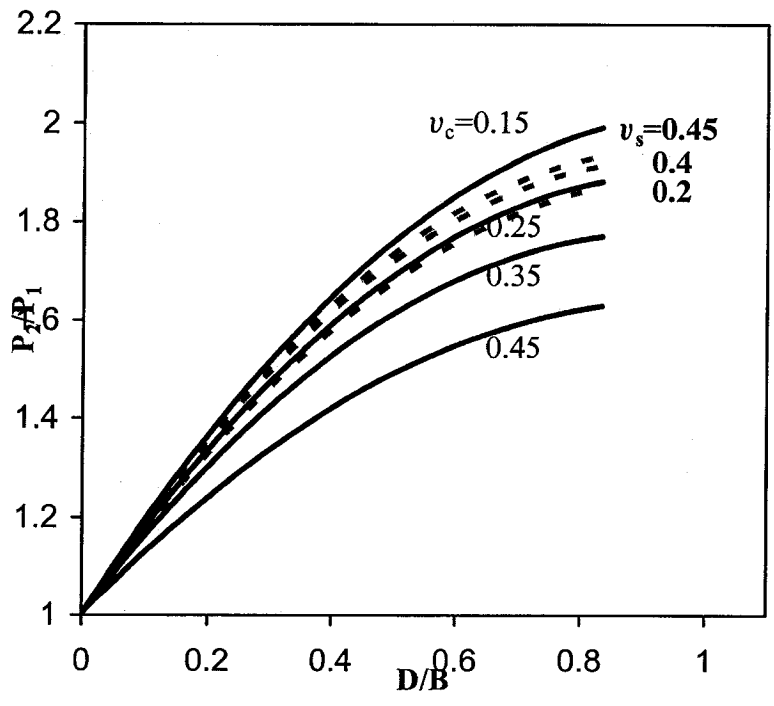

(b)

Figure 3.22 Load ratio versus $\frac{D}{B}$ for different sand and clay Poisson's ratio for rigid base stone columns (a) ϵ_a=1.5% (b) ϵ_a=5%.

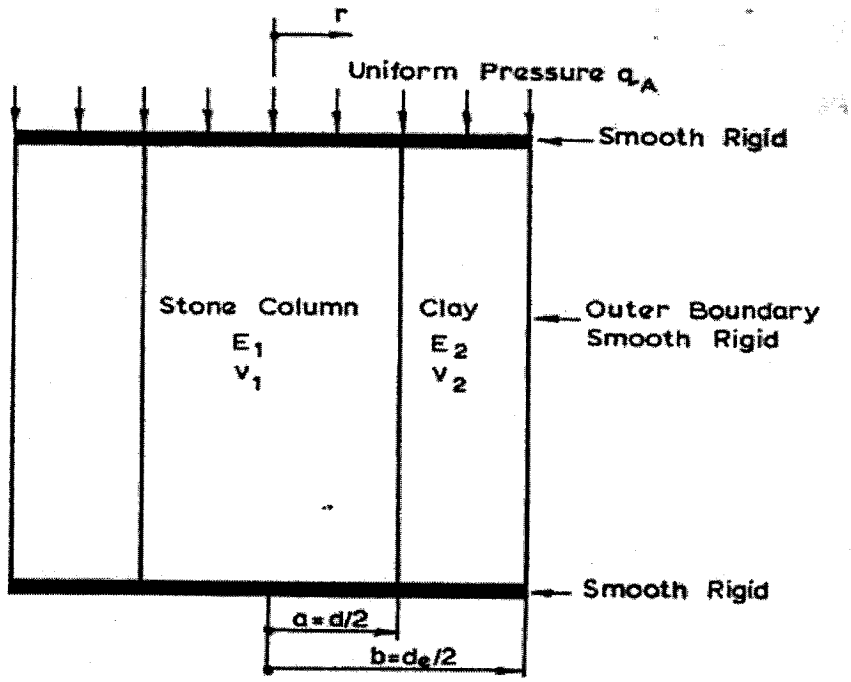

Figure 3.23 Setup of the parametric numerical tests, after Balaam and Booker (1981).

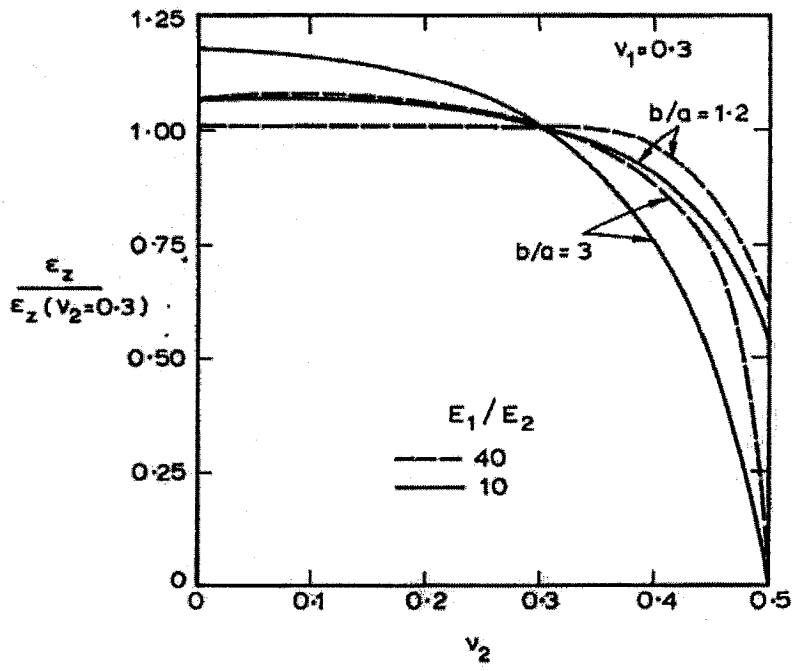

Figure 3.24 Ratio of strains for calculating settlements for the range of clay Poisson's ratio, after Balaam and Booker (1981).

Figures 3.25 and 3.26 show the column diameter changes with respect to load ratio for floating and rigid base stone columns respectively. The column diameter varies from 0.6 to 1.2 meters, which corresponds to the minimum and maximum values that are normally used in construction of stone columns. As before it is seen that for floating stone columns increment of vertical relative displacement results in the reduction of load ratio.

The increase of shearing resistance angle of sand, ϕ_s is expected to have a great influence in load ratio values. In practice the friction angle of stone columns changes normally between 38 to 45 degrees. Figures 3.27 and 3.28 show the results for shearing resistance angle for floating and rigid base stone columns respectively. As expected the great influence of this parameter is observed.

The influence of ratio of modulus of elasticity of sand over clay is also investigated. With increment of this ratio, stone columns carry more of the foundation load and less load would be carried out by clay therefore the effectiveness of the reinforcement system is improved. Figure 3.29 (a) and (b) illustrates load ratio versus module of elasticity ratio of stone over clay for floating stone columns with ϵ_a=2% and rigid base stone columns with ϵ_a=1.5% respectively. Increment of this parameter results settlement reduction of the ground reinforcement system.

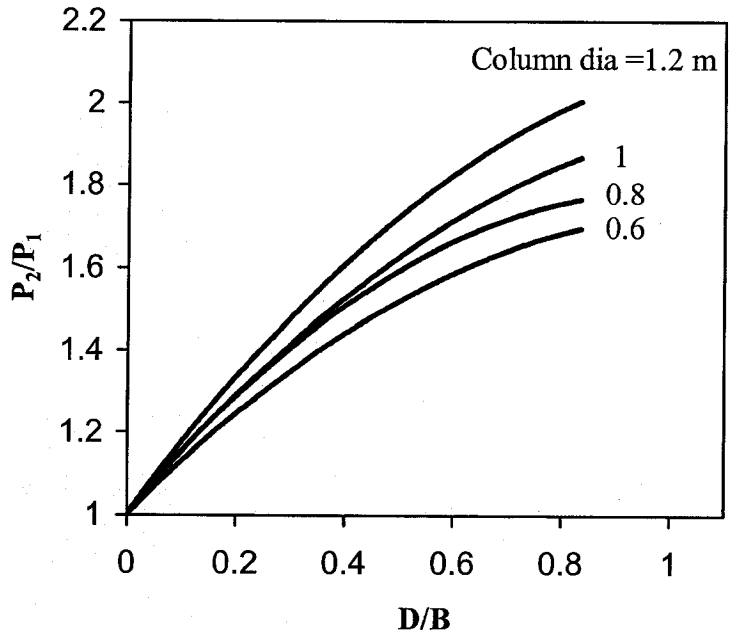

(a)

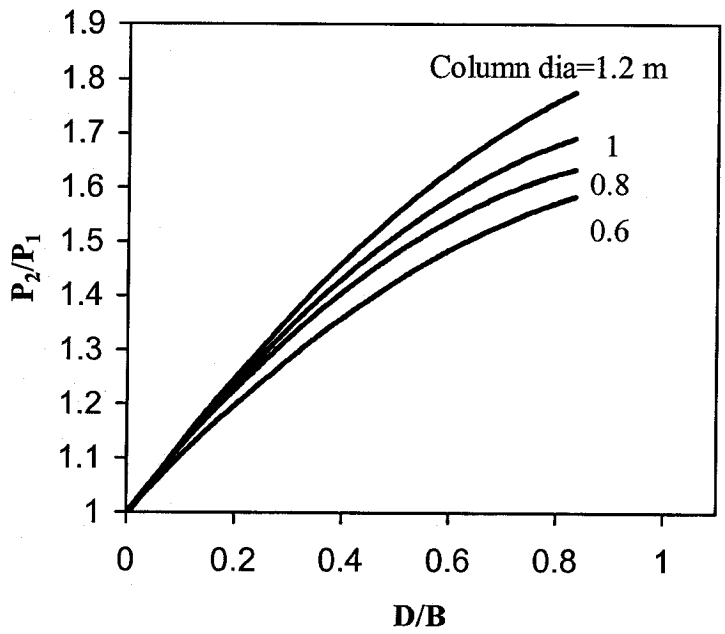

(b)

Figure 3.25 Load ratio versus $\frac{D}{B}$ for different column diameter for floating stone columns (a) ϵ_a=2% (b) ϵ_a=7%.

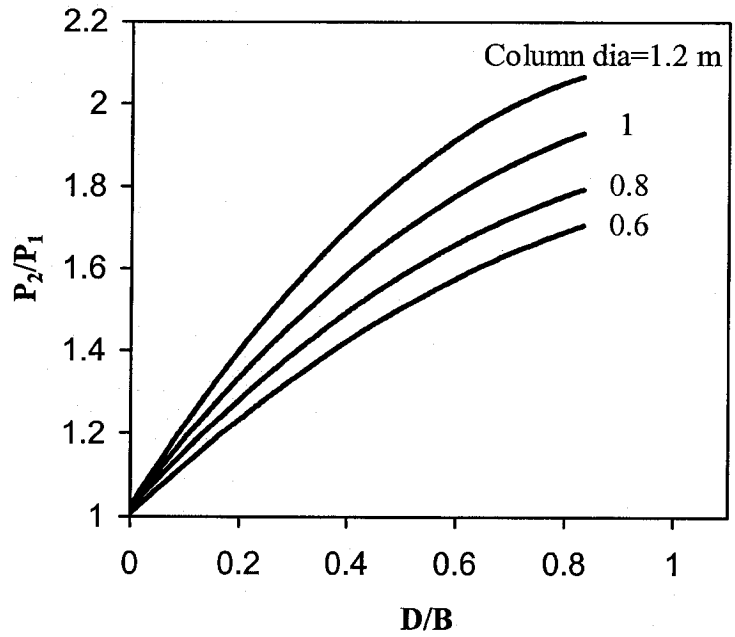

(a)

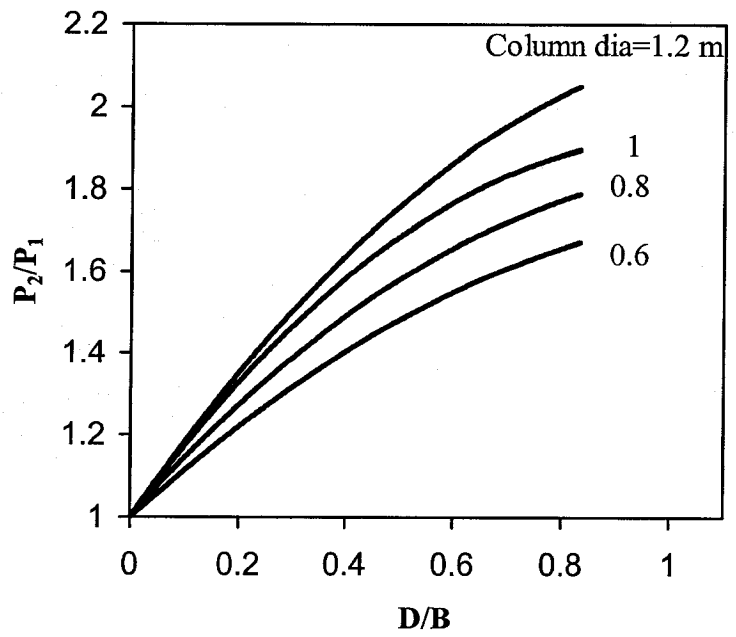

(b)

Figure 3.26 Load ratio versus $\frac{D}{B}$ for different column diameter for rigid base stone columns (a) ϵ_a=1.5% (b) ϵ_a=5%.

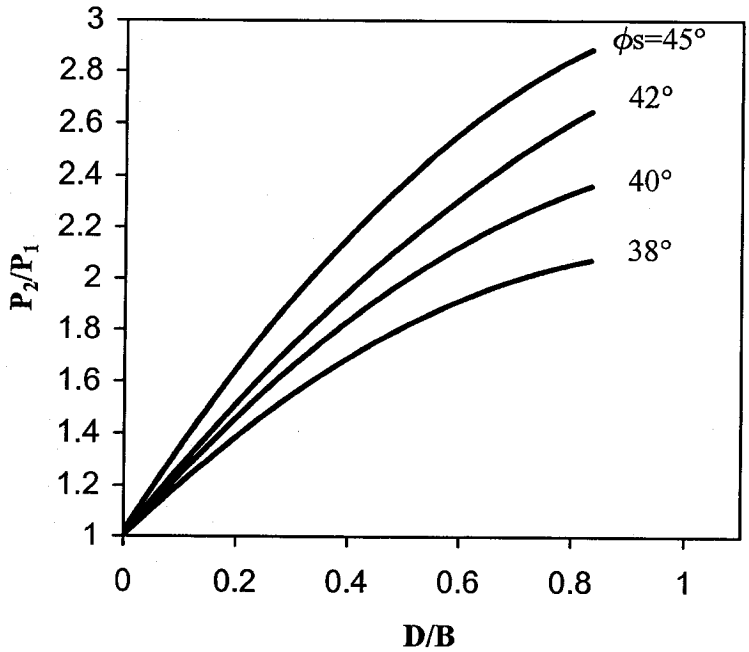

(a)

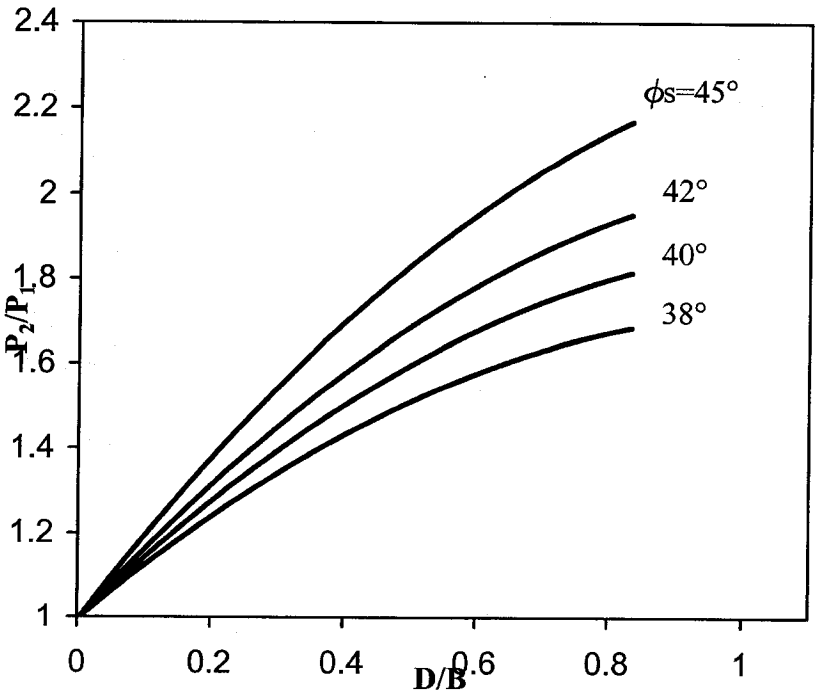

(b)

Figure 3.27 Load factor versus $\frac{D}{B}$ for different shearing resistance angle for floating stone columns (a) ϵ_a=2% (b) ϵ_a=7%.

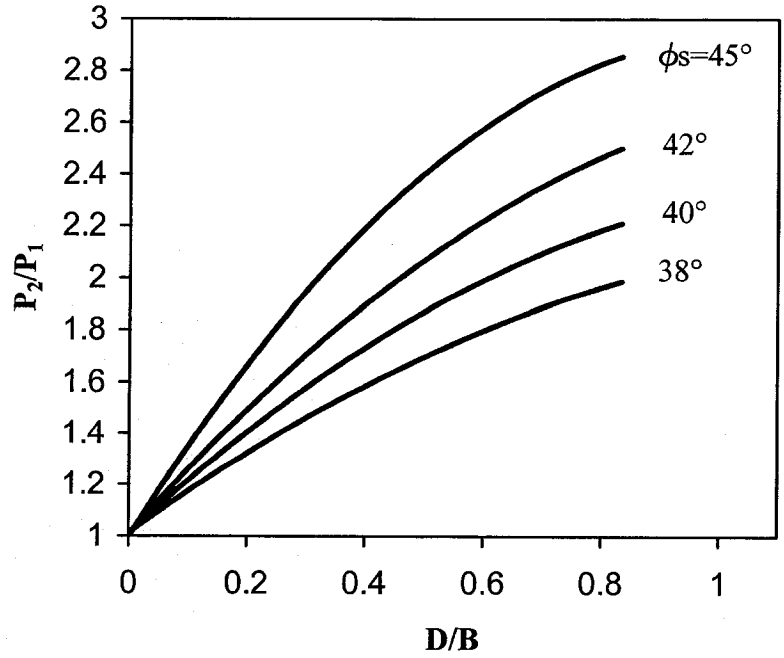

(a)

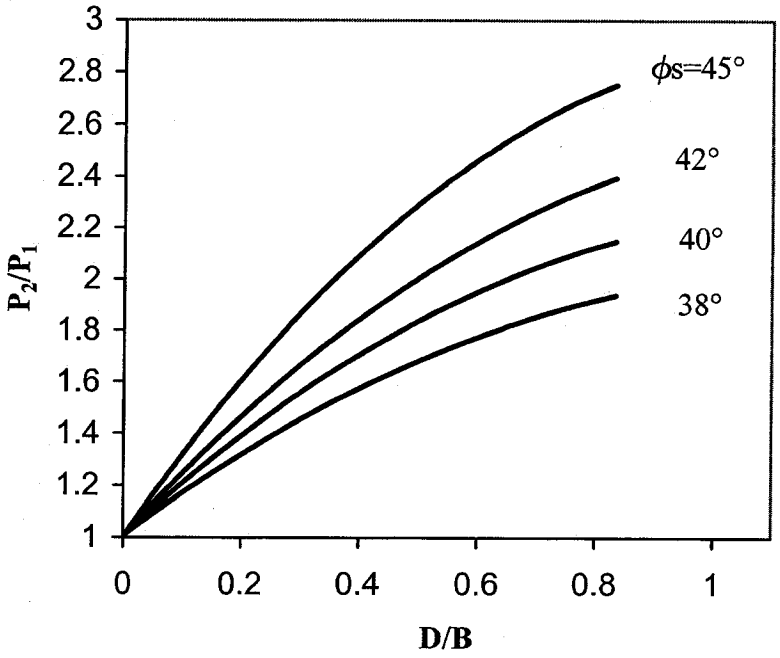

(b)

Figure 3.28 Load factor versus $\frac{D}{B}$ for different shearing resistance angle diameter for rigid base stone columns (a) ϵ_a=1.5% (b) ϵ_a=5%.

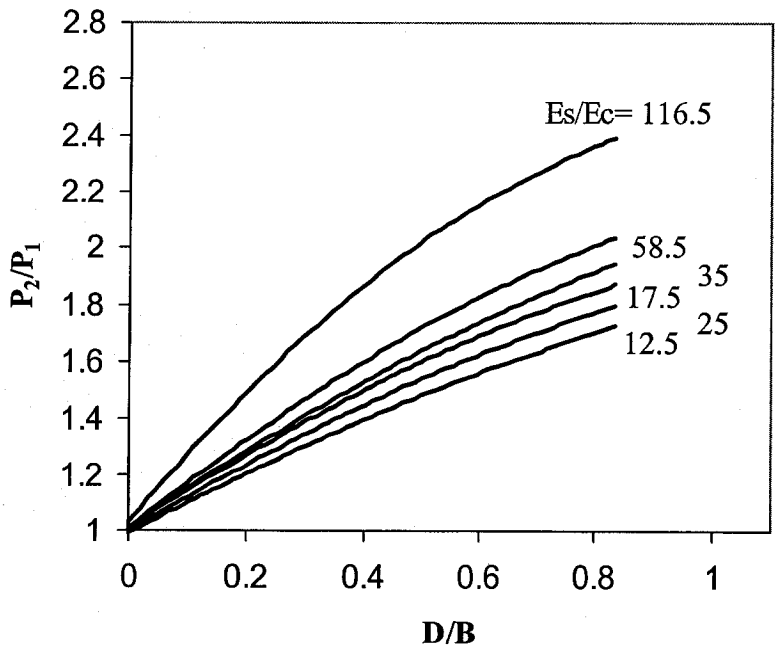

(a)

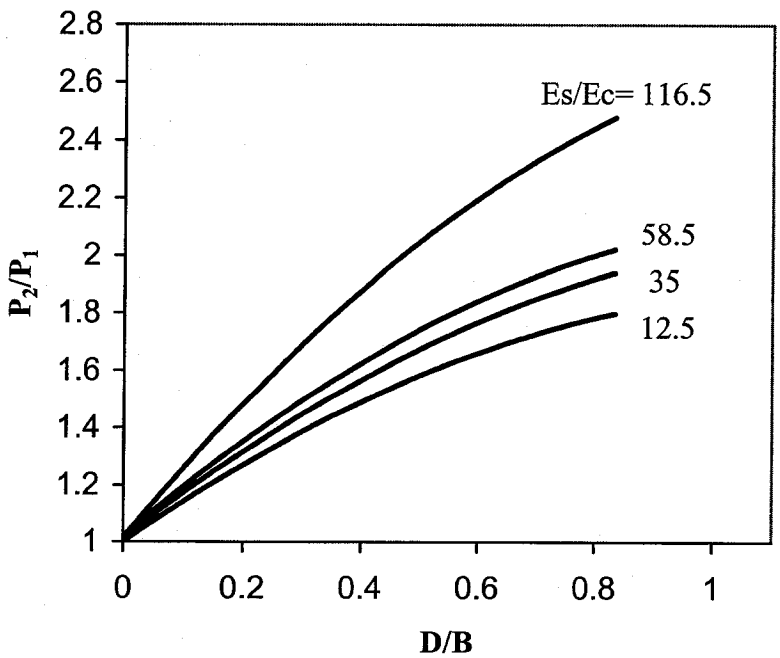

(b)

Figure 3.29 Load ratio versus $\frac{D}{B}$ for different module of elasticity ratio of stone/clay (a) floating stone columns ϵ_a=2% (b) rigid base stone columns ϵ_a=1.5%.

3.2.6 Modes of Failure of Group of Stone Columns

As described in chapter 2, failure shape for group of stone columns reinforced soil is assumed as either bulging (Hughes and Withers (1974), Barksdale and Bachus (1983)) or general shear failure (Madhav and Vitkar, (1978), Priebe (1995)). Large observed scatter in different available theoretical methods as described in previous chapter might be due to the inappropriate selection of failure mechanism related to the theoretical models. The research was extended to examine the mode of failure of a group of stone columns for a given soil/loading/geometry conditions. Knowing the possible failure mechanism which might take place (general, local or punching), designers will be able to estimate the bearing capacity of the system realistically and accordingly accurately.

Table 3.7 presents the range of parameters, which were examined in this investigation. The range of these parameters was considered to cover all the possible cases encountered in practice for stone column reinforcement system.

All the parameters which were believed to have effect on the failure mechanism namely; soft soil and granular material properties (angle of friction, unit weight, modulus of elasticity and cohesion), foundation width and depth, stone column diameter and area replacement ratio were considered in the model. Cohesion of column material (granular) was taken to be zero. In the numerical tests, uniform load was applied to the foundation till ultimate bearing capacity of the system was achieved. Bearing capacity of foundations was determined from the load-displacement curves obtained from the present analysis at the point of maximum curvature on the curve. Failure mechanism of the model was evaluated by observing the failure shape of the system at that point.

Table 3.7 Range of the input data used in this investigation.

	Site conditions	Range of values
Clay	Angle of shearing resistance	5°-25°
	Cohesion	2-15 kN/m^2
	Modulus of elasticity	1000 – 15'000 kN/m^2
Granular material	Angle of shearing resistance	35° to 45°
	Modulus of elasticity	60'000 – 300'000 kN/m^2
	Angle of dilatancy	$\psi = \phi$-30°
Geometry condition	Area replacement ratio (A_s)	10%, 20% , 30% and 35%
	Diameter of stone columns	0.6 - 1.2 m
	Depth of the foundation	0-5 m

The trials were repeated to cover all the different soil/loading/geometry conditions. The description of the tests is presented in Appendix 1. The observed failure shapes were categorized as general, local and punching shear failures depending on the observed forms. In this study, the general and punching failure mechanisms were defined similar to Vesic (1973). Local shear failure is defined herein when the log-spiral curve of the failure plane ends at outsider edges of columns' system. This assumption is based on the fact that due to the high level of compaction at the boundary columns, the failure plan ends at that area. Figure 3.30 illustrates different forms of shear failure due to soil displacement which were observed in the present investigation. The case that failure was between general and local conditions was considered as local failure and between local and punching as punching failure condition. This assumption was considered however to be on the safe side.

Siveral trials were carried out in order to obtain the best presentation covering all possible governing parameters. For a given ratio $\frac{d}{B}$ and A_s, all the deduced values of the different parameters for an observed failure shape were plotted in a representative graph. The different points obtained were grouped in different zones depending on failure form. Furthermore, best fitting curves were drawn between the boundaries of theses zones (Figure 3.31). Some tests which showed error were eliminated in the final plots. The charts were developed for area replacement ratio, A_s of 10, 20, 30 and 35%. The parameters used in the charts were ϕ_c, ϕ_s, γ_c, c, d, B and D_f representing respectively the angle of shearing resistance of soft soil, angle of shearing resistance of granular column material, unit weight of soft soil, cohesion of soft soil, column diameter, width and depth of the foundation.

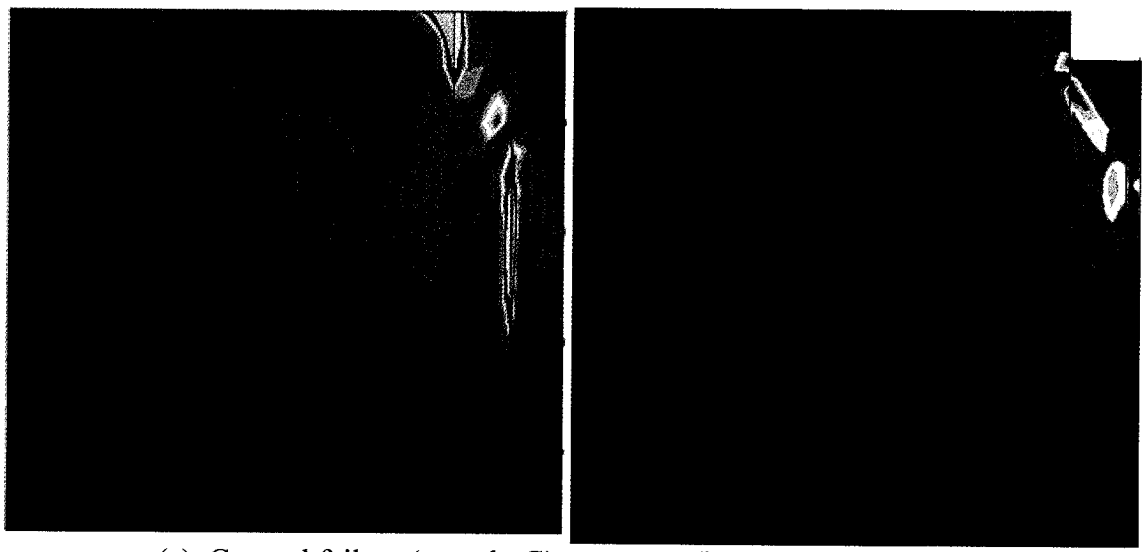

(a) General failure (namely G) (b) Local failure (namely L)

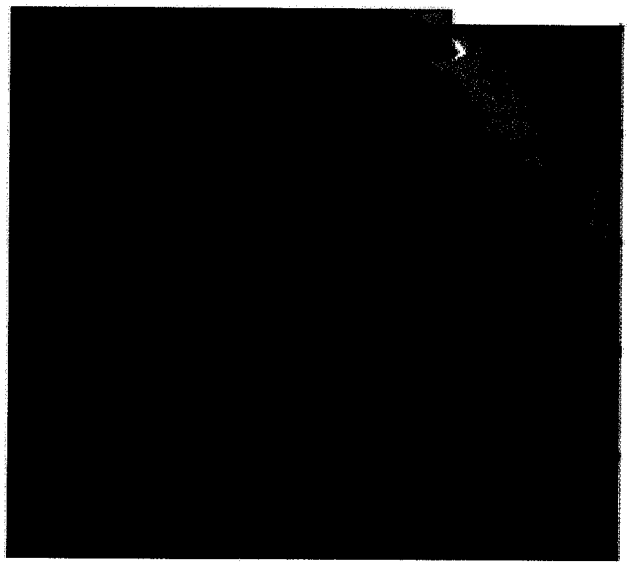

(c) Punching shear (namely P)

Figure 3.30 Failure mechanisms of group of stone columns.

Figure 3.32 represents the final plots developed for practical purpose. It should be mentioned that these charts should be used only for the ranges of parameters presented in Table 3.7. However these ranges were selected to cover all possible cases encountered in the field for stone columns reinforced system.

In this investigation, shear failure (general, local and punching failure) was observed during loading of a group of stone columns in soft soil. Bulging failure was not observed which confirm the indication that bulging failure may not take place for A_s more than 10%. By reducing A_s for less than 10% the effect of column interaction reduces, and accordingly individual failure may took place. However, as described before area replacement ratio less than 10% has no significant improvement on reinforced ground reinforcement subjected to uniform loading (Hu et al., 1997).

General shear failure was observed for higher area replacement ratios, stiffer soil and stone columns, and for low foundation width and depth. Furthermore, with the increase of A_s and $\frac{d}{B}$, the failure mechanism gradually change from general to local shear failure and from local to punching shear failure. For example, for A_s=20% and 10% only local and punching failure was observed. The effect of the foundation width and stiffness of the ground on the failure mechanism reported by Vesic (1973) and Clark (1997) agreed well with the results of this investigation. Interpolation is required for intermediate values of $\frac{d}{B}$.

Using the result of the present numerical model will reveal the actual mode of failure of the composit reinforced ground. In the next chapter, design theoreties will be developed and presented for practical use.

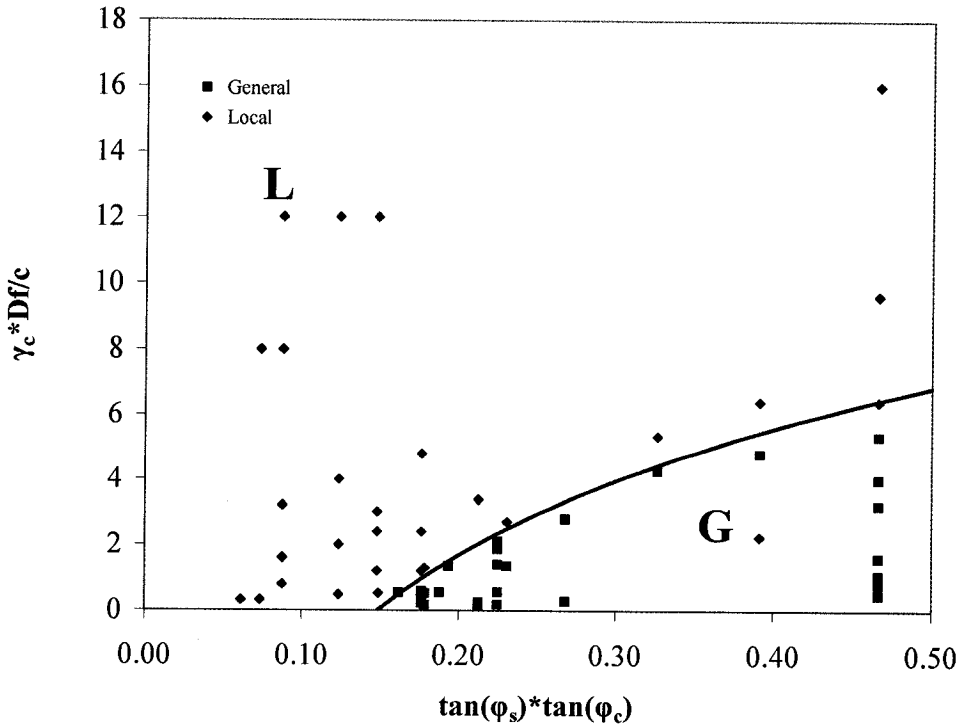

(a) A_s=35%, d/B=0.4

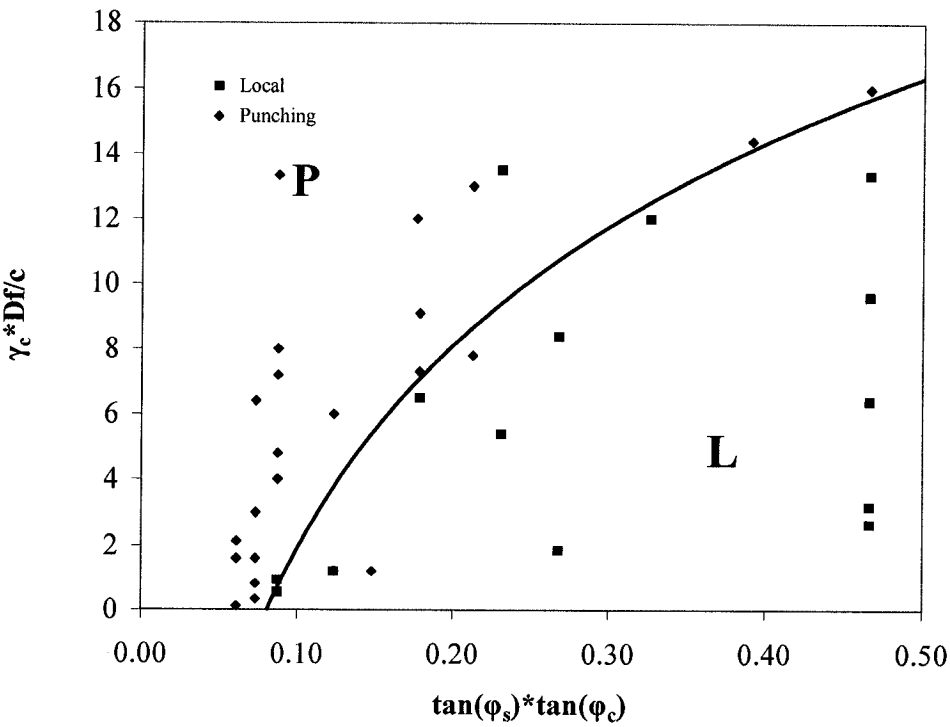

(b) A_s=35%, d/B=0.25

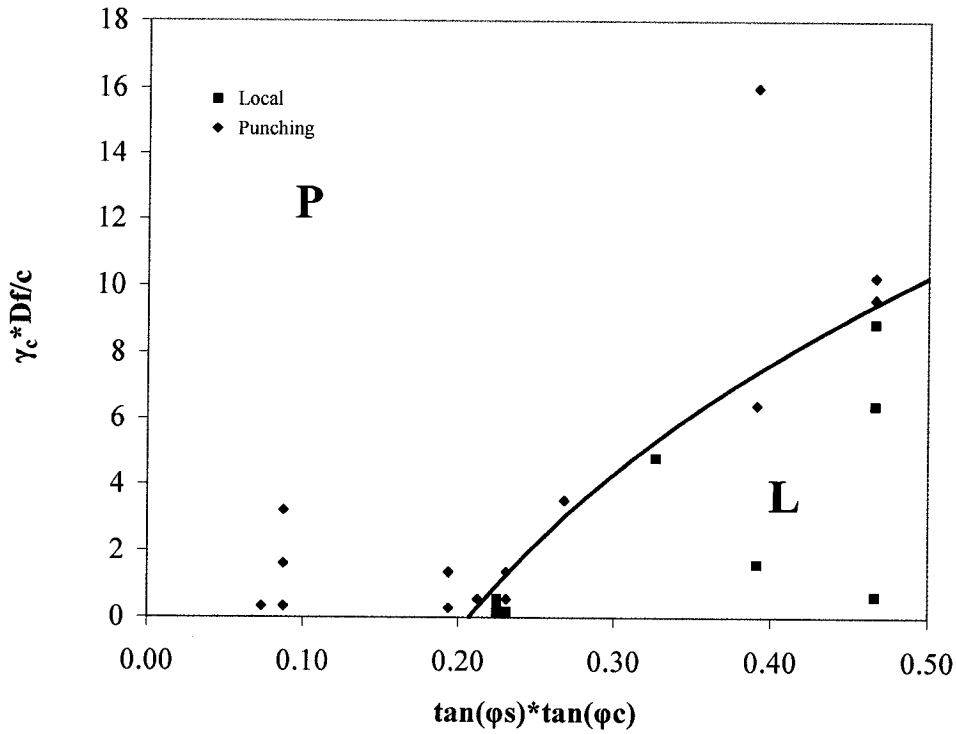

(c) *As*=35%, *d/B*=0.18

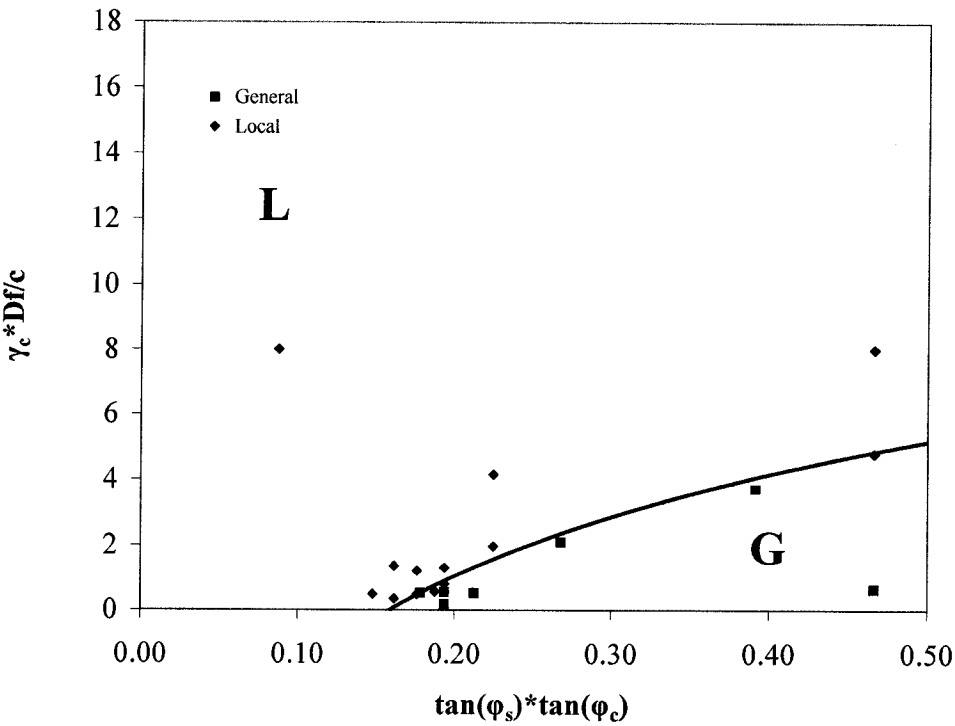

(d) A_s=30%, *d/B*=0.38

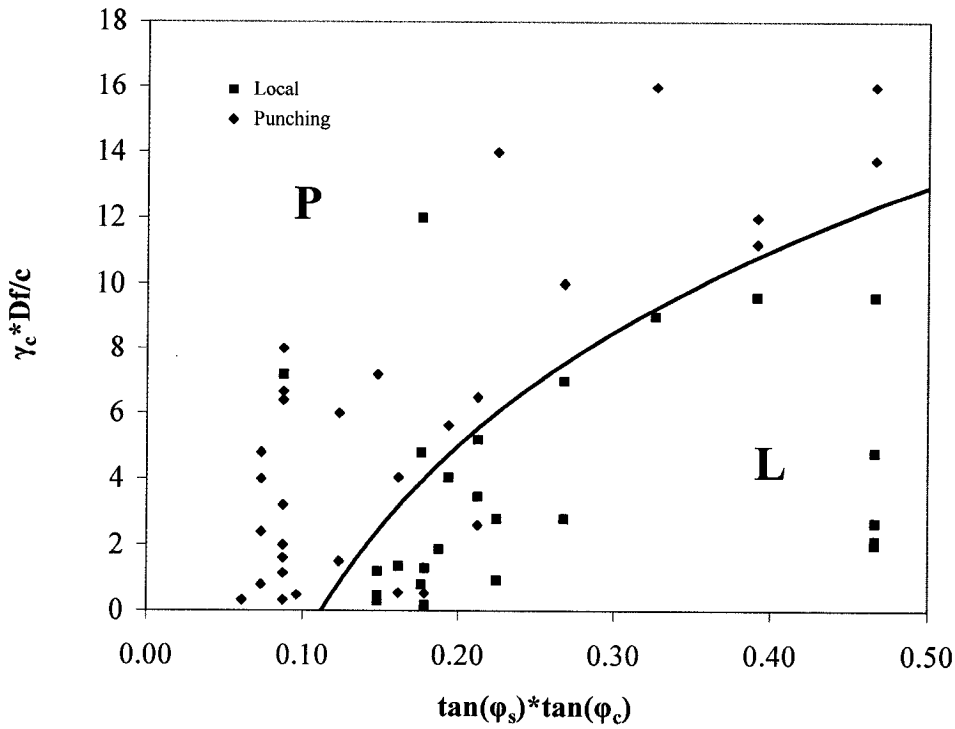

(e) A_s=30%, d/B=0.24

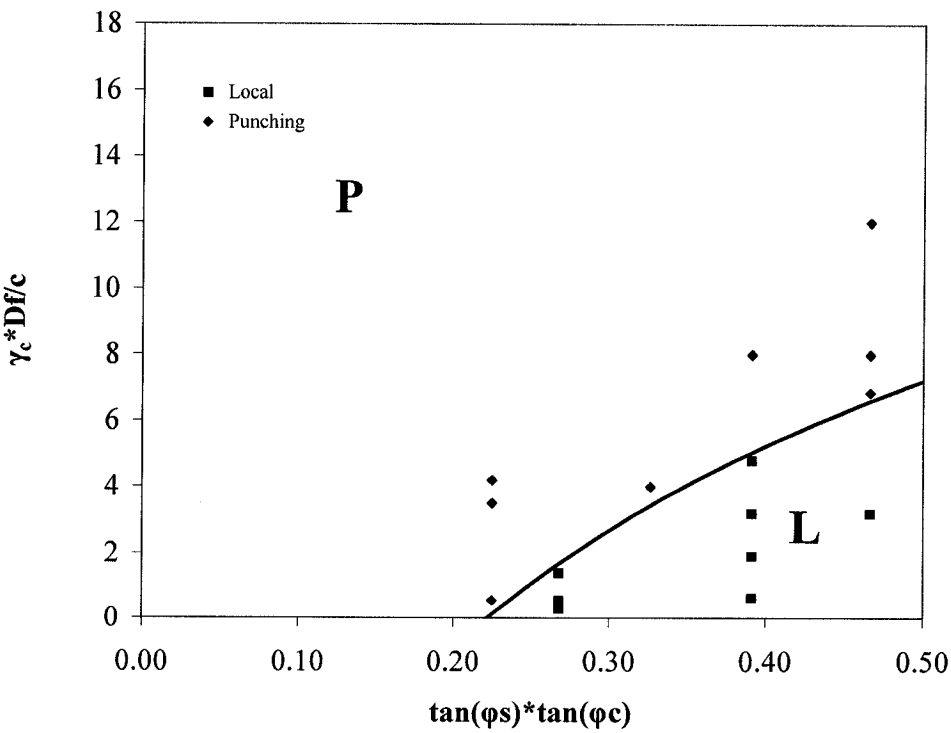

(f) A_s=30%, d/B=0.17

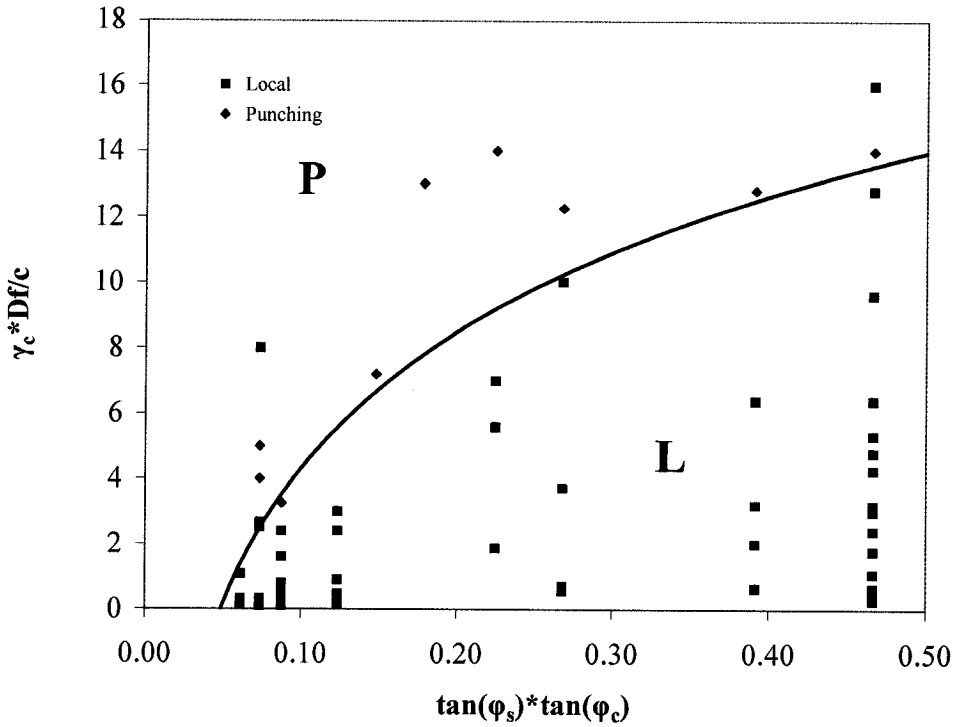

(g) A_s=20%, d/B=0.34

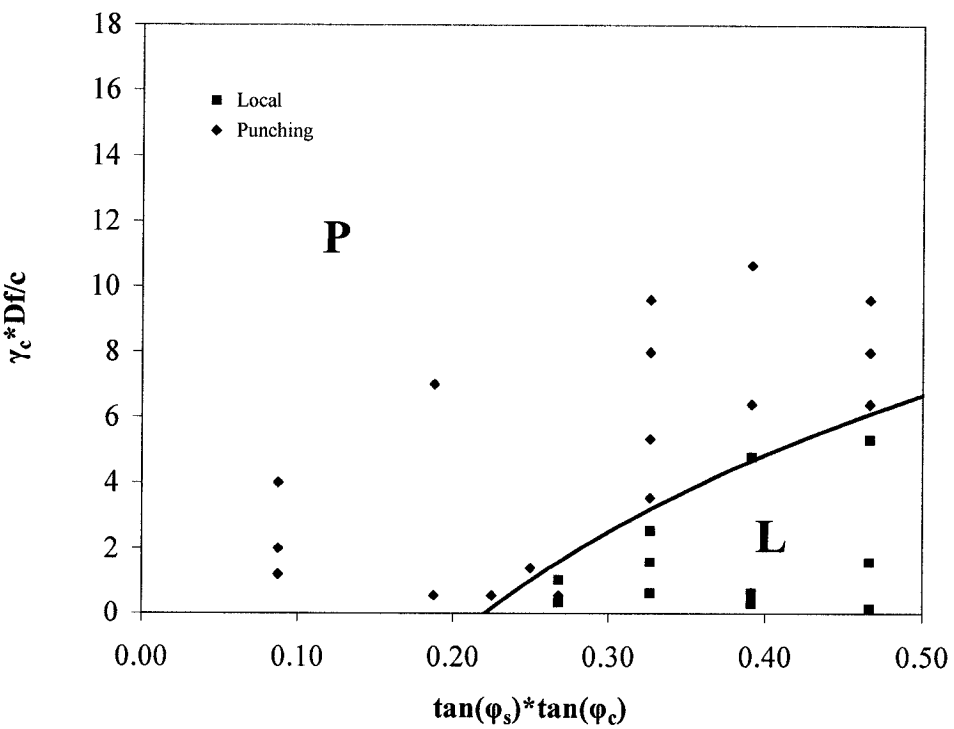

(h) A_s=20%, d/B=0.2

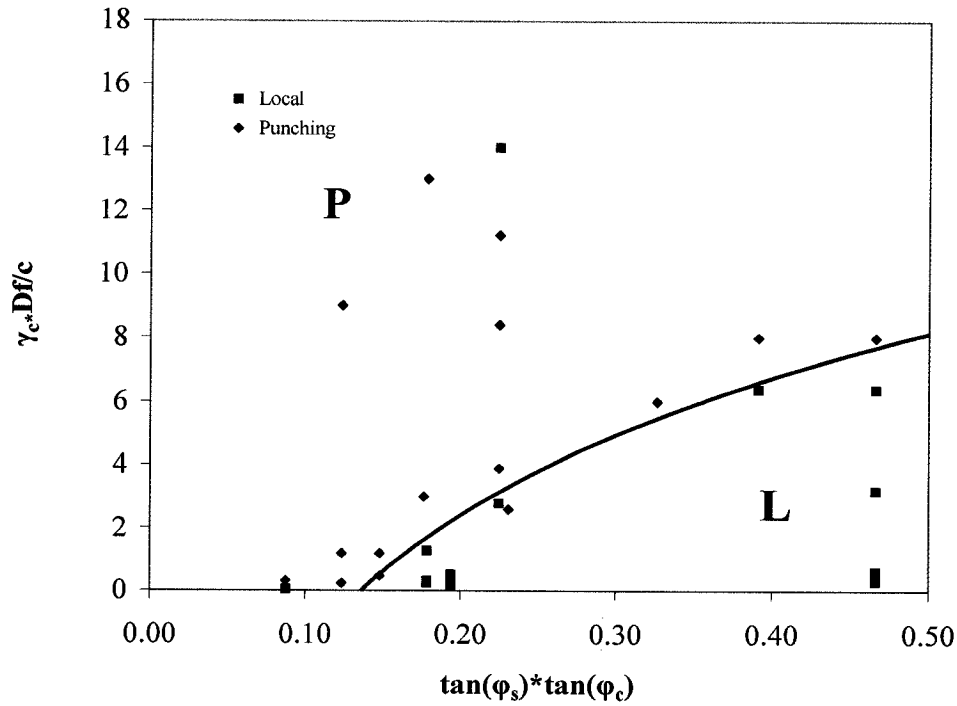

(i) A_s=10%, d/B=0.26

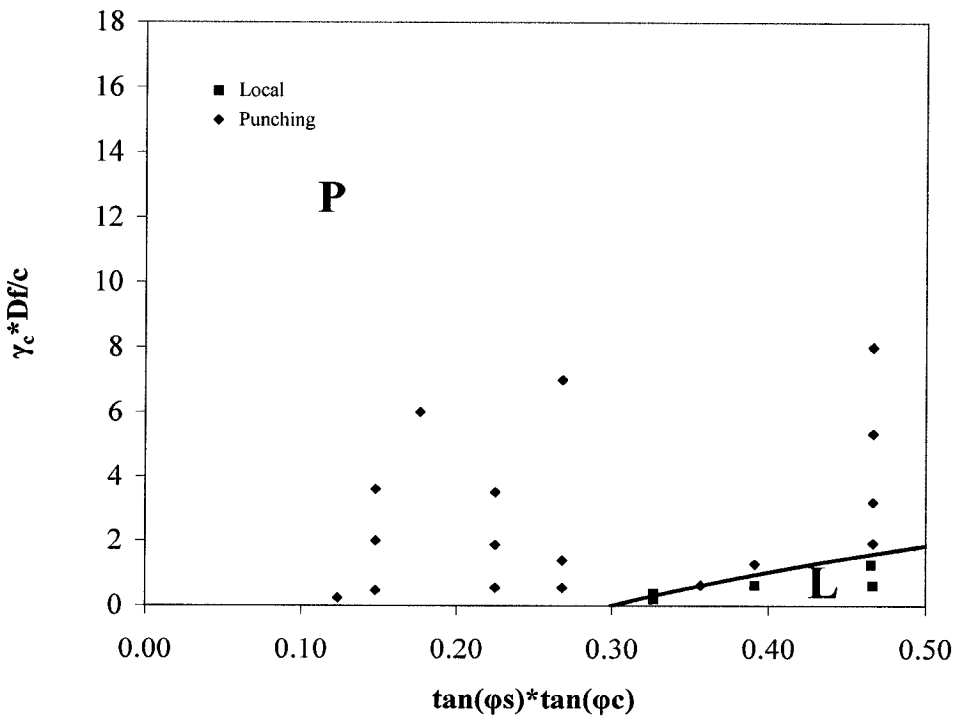

(j) A_s=10%, d/B=0.15

Figure 3.31 Test results and failure mode of reinforced ground for different $\frac{d}{B}$ and A_s.

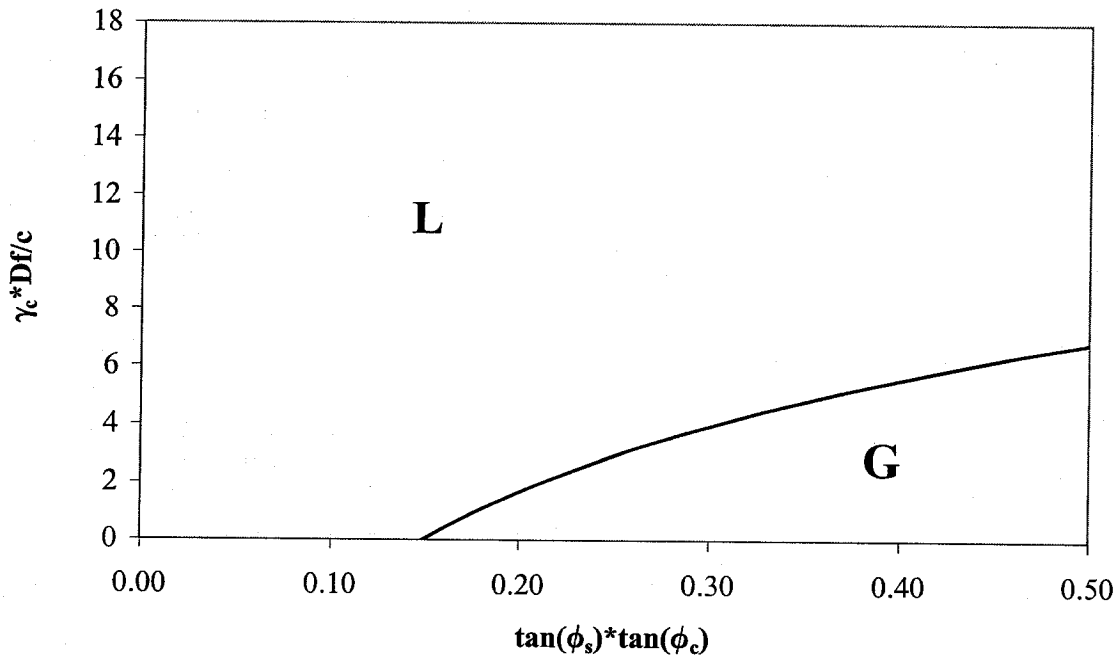

(a) A_s=35%, d/B=0.4

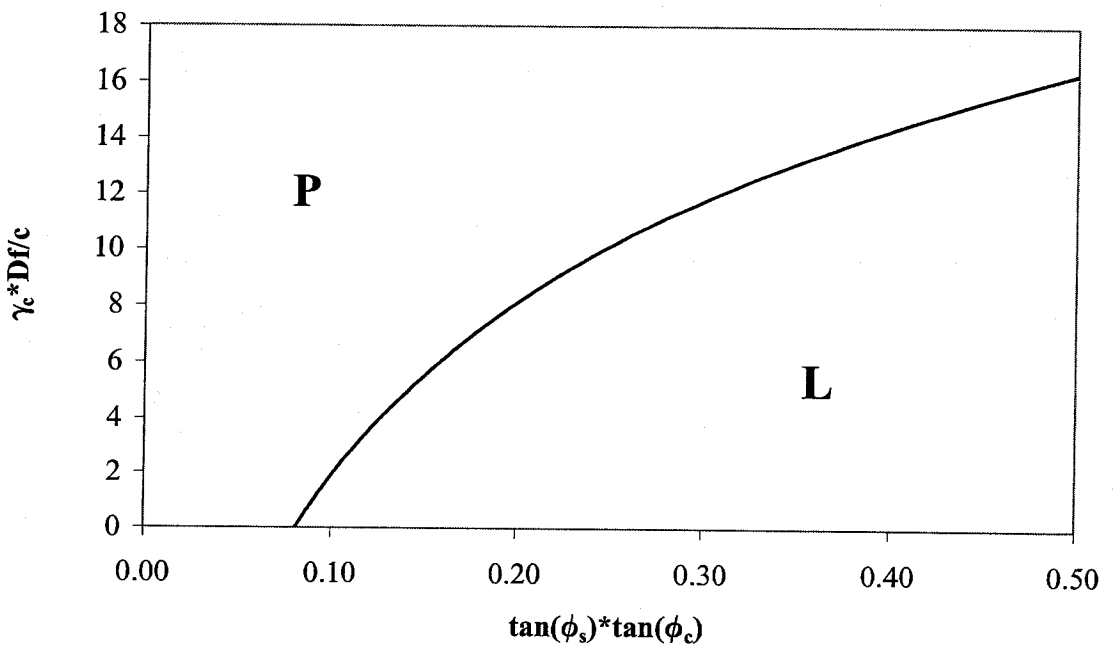

(b) A_s=35%, d/B=0.25

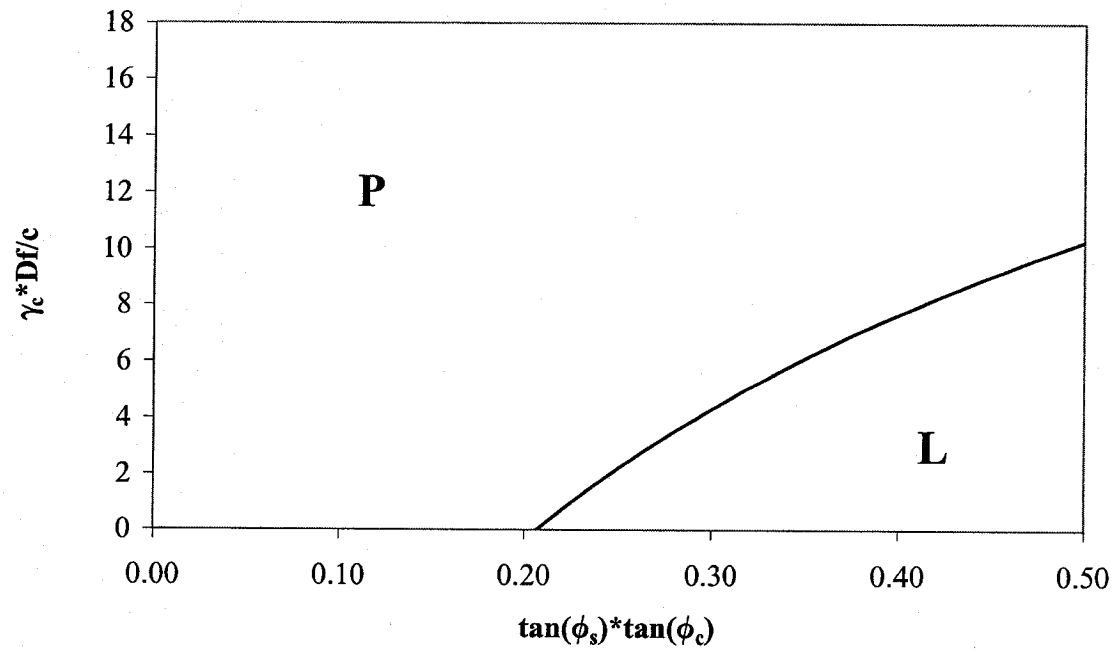

(c) A_s=35%, d/B=0.18

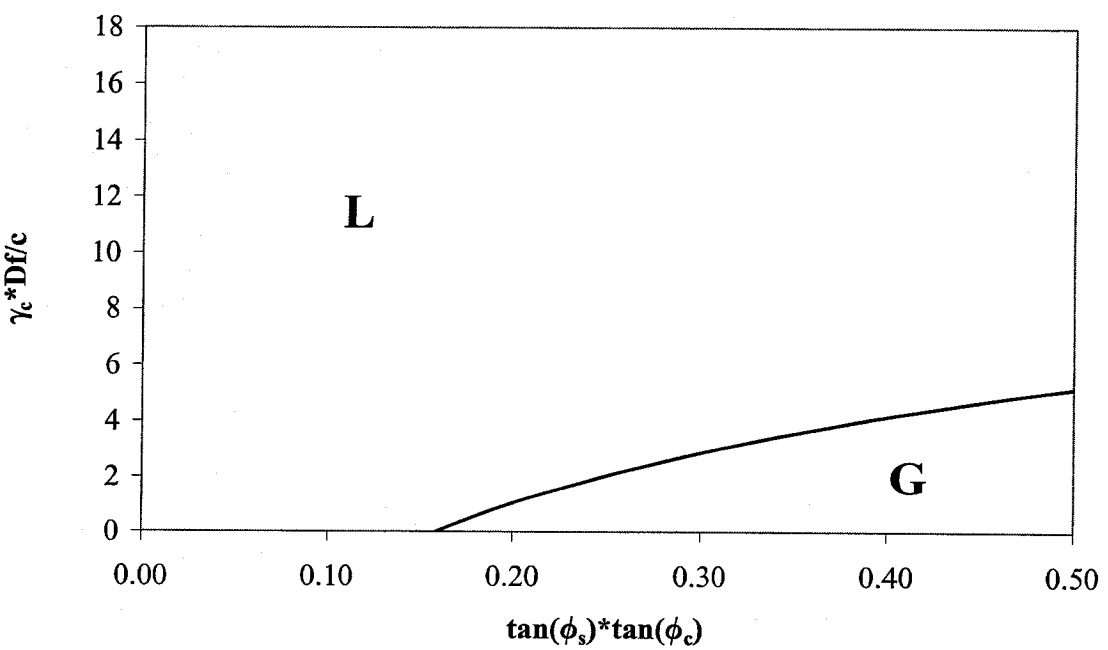

(d) A_s=30%, d/B=0.38

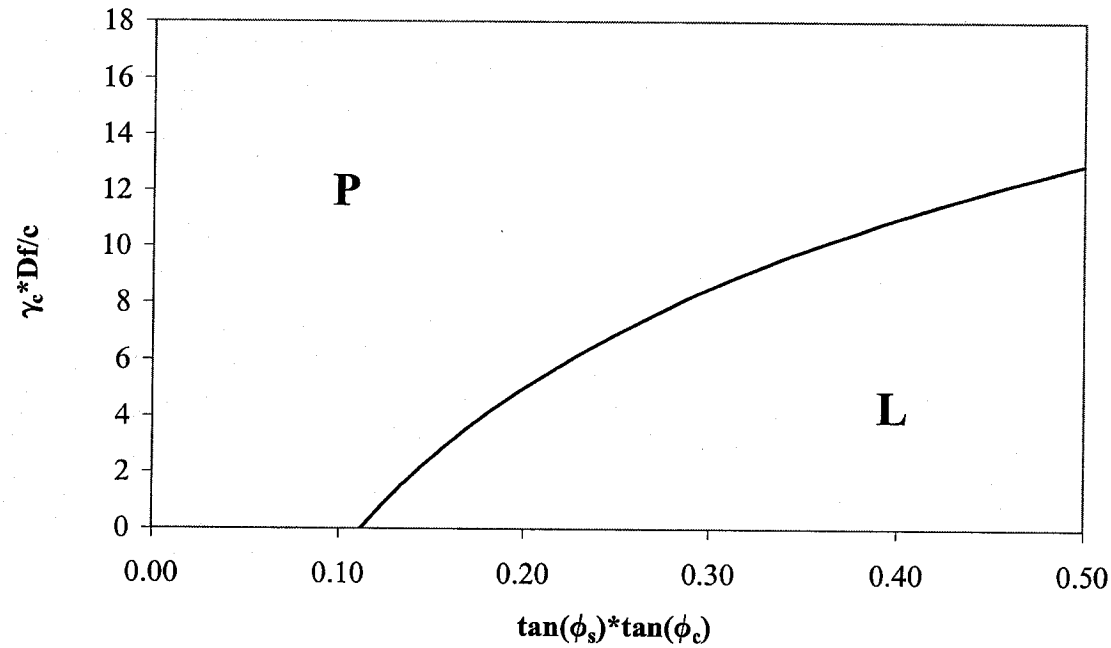

(e) A_s=30%, d/B=0.24

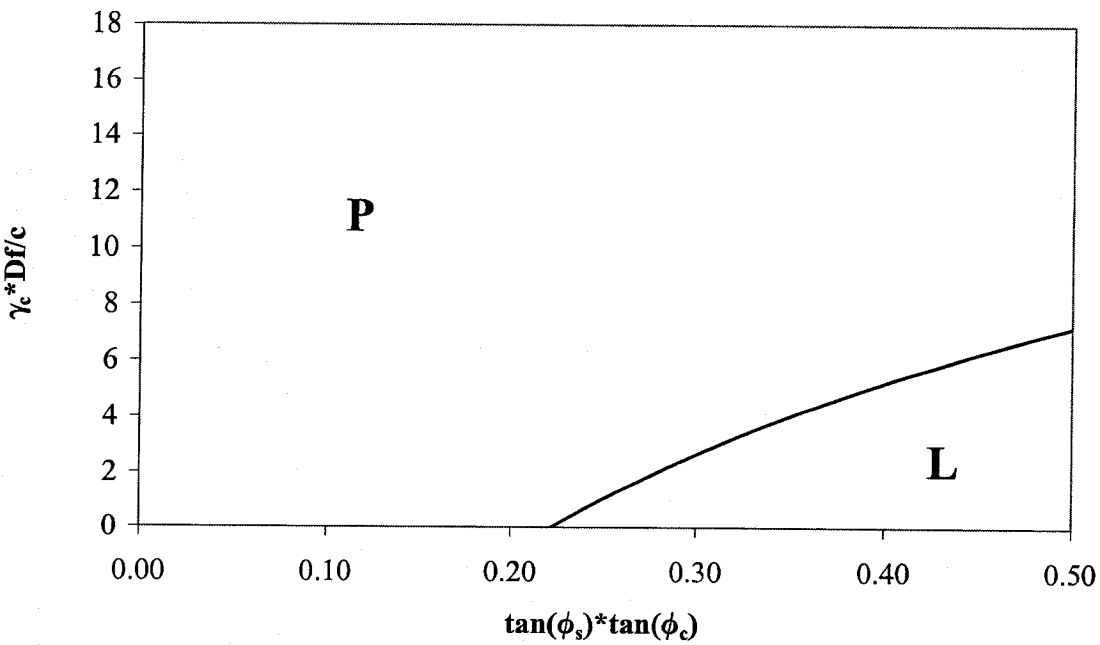

(f) A_s=30%, d/B=0.17

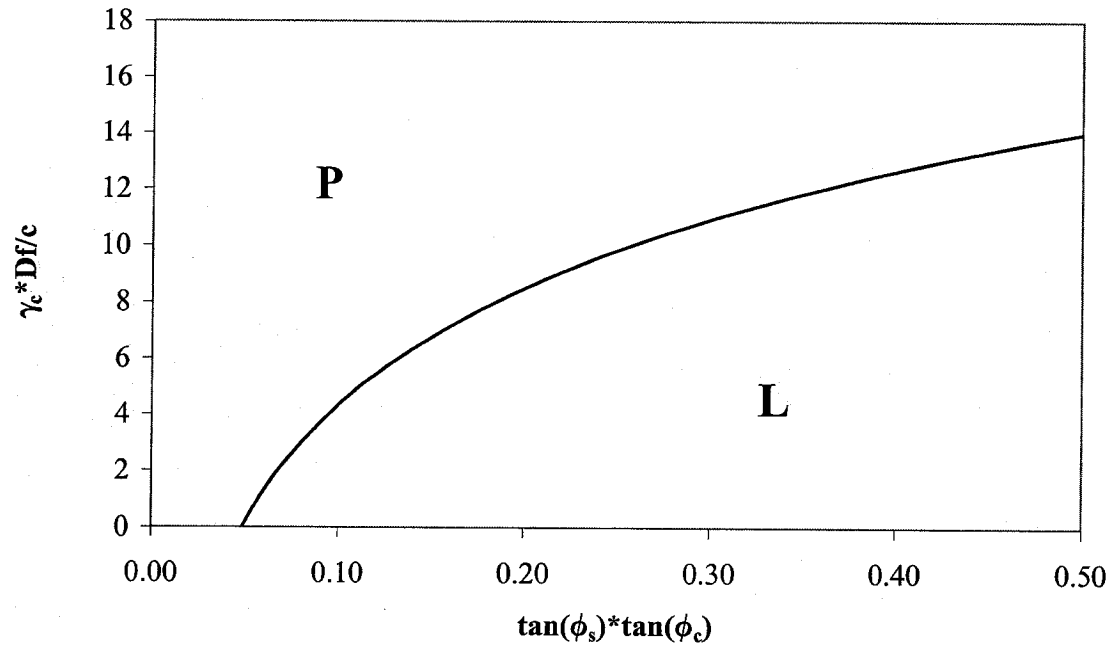

(g) A_s=20%, d/B=0.34

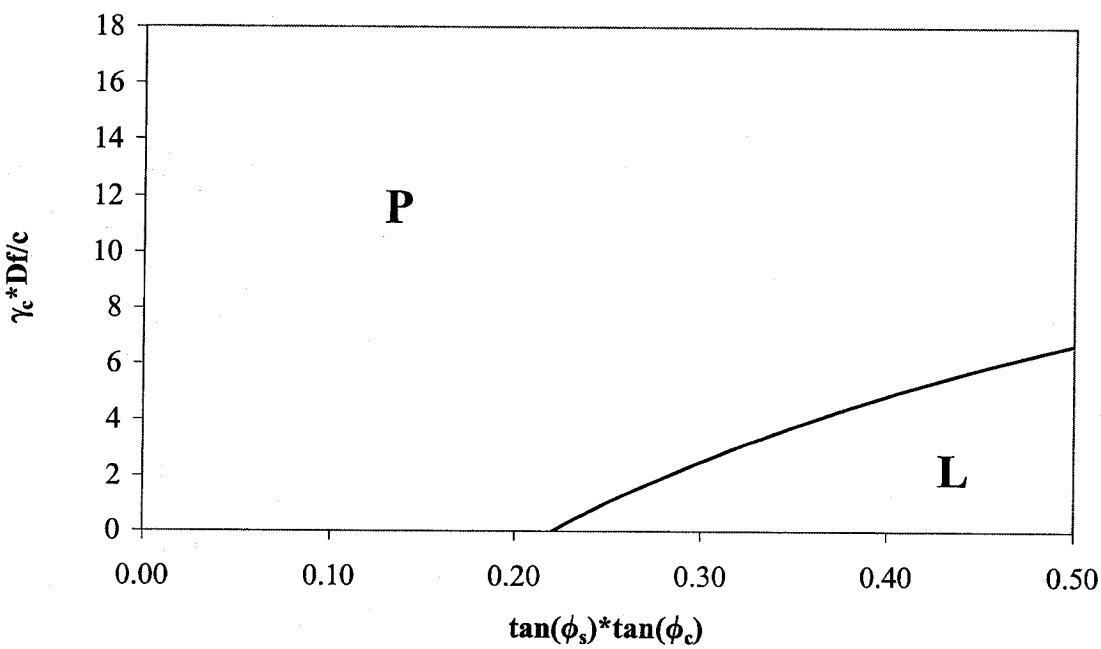

(h) A_s=20%, d/B=0.2

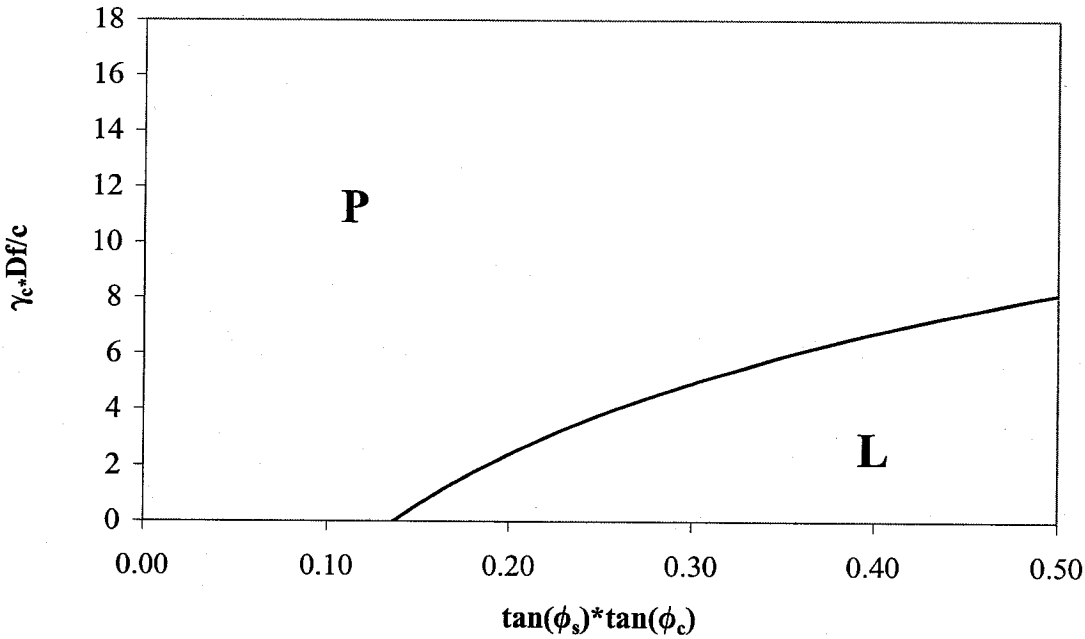

(i) A_s=10%, d/B=0.26

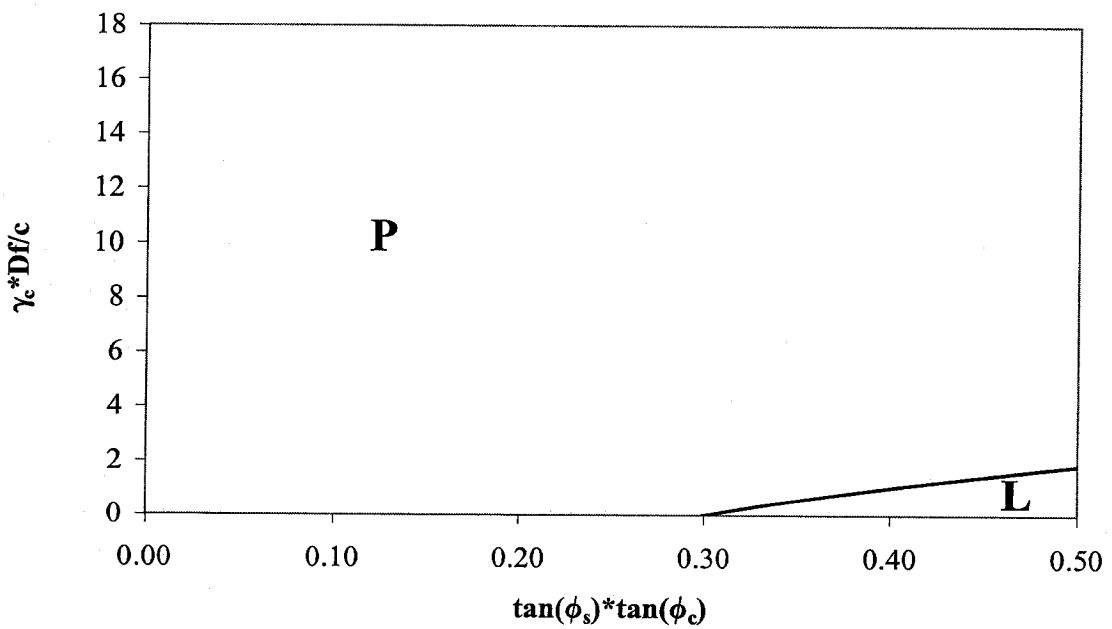

(j) A_s=10%, d/B=0.15

Figure 3.32 Mode of failure of reinforced ground for different $\frac{d}{B}$ and A_s.

CHAPTER 4

ANALYTICAL MODELS

4.1 General

Based on the results of the numerical model presented in chapter 3 of this thesis, and the reports published by (Vesic, 1973, Clark, 1997 and Hu, 1995), analytical models and design theories are developed and presented in this chapter for group of stone columns subjected to general, local or punching shear failure modes. Furthermore, for the case of single stone column analytical model will be developed for estimating the settlement and the ultimate bearing capacity based on bulging mode of failure.

4.2 Analytical Model for Bulging Failure

Many previous studies assumed this mode of failure for group of stone columns. However, utilizing results from this research, it has been observed that for ground improvement cases that are normally used in practice, group of columns usually fails by shear and not by bulging failure. This study covers the area replacement ratio between 10% to 35% which is normally used in field. Considering that this ratio represents spacing between the neighboring columns, as discussed before for A_s less that 10% or for ground supported by single stone column bulging failure might take place. For the case of single stone column results of this study agrees with previous researches that bulging failure happens. The failure pattern of A_s less than 10% was not studied in this research as it is known that this low area ratio does not have sufficient improvement on the reinforced ground. Despite of this statement there might be cases in the field that large

spacing of columns may be used. A theory is presented herein for single stone column and for these minority cases. The model is capable to calculate settlement and bearing capacity of stone columns based on bulging mode of failure.

4.2.1 Governing Equations

In the model it is assumed that the tributary soil surrounding a stone column in the reinforced ground can be approximated by a cylinder which is restricted from movement at its bottom and exterior surroundings. (Figure 4.1) By applying load on the reinforced area the interior column expands laterally till failure occurs. The stress and displacement equations were written for both the stone column and soft soil. The solution of problem was obtained when both stress and displacement of soft soil and column materials became equal to each other. In the following equations the subscript 1 and 3 represents the major (vertical direction) and minor (horizontal direction) of stress or strain respectively.

For the granular material, having the yield function

$$\eta = \frac{\sigma_1}{\sigma_3} \tag{4.1}$$

Poorooshasb and Meyerhof (1997) showed that

$$\eta = \eta(\varepsilon_1) \tag{4.2}$$

Using curve fitting technique for axial strain ϵ_1 and yield function η Poorooshasb et al. (1997) developed equations for the compact standard gravel. In the following equations ϵ_f is the axial strain at failure point.

$$\text{for } \varepsilon_1 \le \varepsilon_f \quad \eta = A + B\varepsilon_1 + C\varepsilon_1^2 \tag{4.3}$$

where

$$A = 1$$

$$C = \frac{1-\eta_f}{\varepsilon_f^2}$$

$$B = -2C\varepsilon_f$$

and

$$\text{for } \varepsilon_1 \geq \varepsilon_f \quad \eta = A + B\varepsilon_1^{-1} + C\varepsilon_1^{-2} \tag{4.4}$$

where

$$A_f = \eta_c$$

$$C_f = (\eta_c - \eta_f)\varepsilon_f^2$$

$$B_f = -\frac{2C_f}{\varepsilon_f}$$

η_f and η_c are determined as

$$\eta_f = \frac{1+\sin\varphi_f}{1-\sin\varphi_f} \tag{4.5}$$

$$\eta_c = \frac{1+\sin\varphi_c}{1-\sin\varphi_c} \tag{4.6}$$

ϕ_f and ϕ_c are frictional angle at failure and critical state.

The results of Equations 4.3 and 4.4 were validated by the authors with tests conducted by Lee (1965) where good agreement between the two was observed. The axial strain ϵ_1 in these two equations is the sum of initial strain due to the self weight of soil and strain related to foundation load.

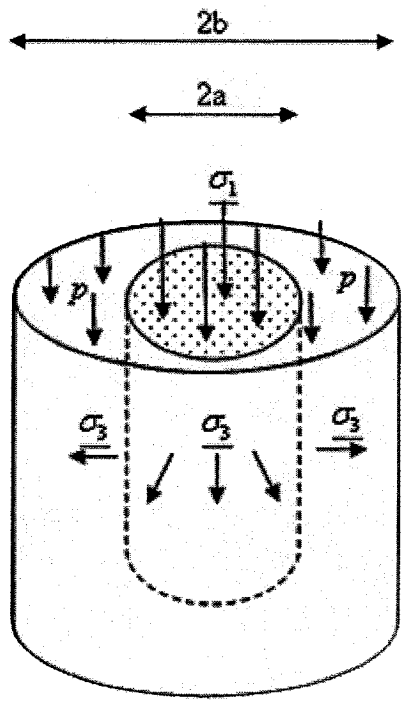

Figure 4.1 Scheme and pressure distribution of the theoretical model.

$$\varepsilon_1 = \varepsilon_o + \Delta\varepsilon_1 \tag{4.7}$$

The amount of $\Delta\varepsilon_1$ was determined using relationship between volumetric and axial strain developed by Poorooshasb et al. (1997).

$$\Delta\varepsilon_1 = m\Delta\varepsilon_3 \tag{4.8}$$

The value of m was determined using Table 4.1.

So

$$\varepsilon_1 = \varepsilon_o + m\Delta\varepsilon_3 \tag{4.9}$$

The axial stress on the column is sum of weight of soil and the load intensity carried by column so

$$\underline{\sigma_1} = \sigma_1 + \sigma_{1o} \tag{4.10}$$

The all round pressure of column consist of initial stress and pressure developed due to the foundation load

$$\underline{\sigma_3} = \sigma_3 + \sigma_{3o} \tag{4.11}$$

σ_{1o} and σ_{3o} represent the initial vertical and horizontal stress respectively where

$$\sigma_{1o} = \gamma' l \tag{4.12}$$

and

$$\sigma_{3o} = k_o \gamma' l \tag{4.13}$$

Therefore the value of η equals to

$$\eta = \frac{\underline{\sigma_1}}{\underline{\sigma_3}} = \frac{\sigma_1 + \gamma' l}{\sigma_3 + k_o \gamma' l} \tag{4.14}$$

The relationship between lateral stress and strain is determined by (Poorooshasb et al. (1997))

Table 4.1 Determination of the factor m.

Stone type	ϕ_f	ϕ_c	ϵ_f	M
Very dense	44°	30°	.04	.61
Dense	41°	30°	.05	.44
Medium dense	38°	30°	.07	.32

$$\sigma_3 = c_1 p - c_2 \Delta\varepsilon_3 \tag{4.15}$$

where

$$c_1 = \frac{\nu}{1-\nu}$$

and

$$c_2 = E' \frac{(1+\nu)a^2 + (1-\nu)b^2}{(1-\nu^2)(b^2 - a^2)}$$

Combining Equations 4.3, 4.9, 4.14 and 4.15 gives

$$\text{for } \varepsilon_1 \le \varepsilon_f \quad \sigma_1 = (k_o \gamma' l + c_1 p - c_2 \Delta\varepsilon_3)[A + B(\varepsilon_o + m\Delta\varepsilon_3) + C(\varepsilon_o + m\Delta\varepsilon_3)^2] - \gamma' l \tag{4.16}$$

Similarly combining Equations 4.4, 4.9, 4.14 and 4.15 gives

$$\text{for } \varepsilon_1 \ge \varepsilon_f \quad \sigma_1 = (k_o \gamma' l + c_1 p - c_2 \Delta\varepsilon_3)[A_f + B_f(\varepsilon_o + m\Delta\varepsilon_3)^{-1} + C_f(\varepsilon_o + m\Delta\varepsilon_3)^{-2}] - \gamma' l \tag{4.17}$$

The value of ϵ_o should be determined in above equations. Substituting Equations 4.12 and 4.13 into Equation 4.1 yields

$$\eta = \frac{\sigma_{1o}}{\sigma_{3o}} = \frac{1}{k_o} \tag{4.18}$$

By substituting Equation 4.18 into Equation 4.3 ϵ_o was calculated.

Vertical strain of soil section due to foundation load is given as (Poorooshasb and Meyerhof (1997))

$$\Delta\varepsilon_1 = \frac{(1-2\nu^2-\nu)p}{(1-\nu)E'} + \frac{2\nu a^2}{(1-\nu)(b^2-a^2)}\Delta\varepsilon_3 \tag{4.19}$$

where

$$E' = \frac{1-\nu}{1-\nu-2\nu^2}E$$

Considering that improved ground is under a raft foundation, settlement of soft soil and column should be equal to each other. Combining Equations 4.8 and 4.19 gives

$$\Delta\varepsilon_3 = \frac{(1-2\nu^2-\nu)p}{E'(m(1-\nu)-\frac{2\nu a^2}{(b^2-a^2)})} \tag{4.20}$$

If q represents the uniform pressure of foundation, load pressure of soil section can be determined as (Figure 4.1)

$$p = \frac{b^2q - a^2\sigma_1}{b^2-a^2} \tag{4.21}$$

4.2.2 Calculation Methodology and Computer Program

In order to calculate the settlement of reinforced soil an arbitrary value for σ_1 was be assumed. The amount of vertical pressure in soil was estimated using Equation 4.21. Next, the initial strain ϵ_o was calculated. The lateral strain was calculated using Equation 4.20 following by calculation of vertical strain ϵ_1. (Equation 4.19) Using estimated values of ϵ_o, ϵ_1 and ϵ_3 vertical pressure of stone column was determined by Equations 4.16 or 4.17. Eventually, the calculated σ_1 was compared with the initial assumed value. If the difference between the two is less than 0.001 then σ_1 is the exact value and the settlement was calculated using $S_i = \epsilon_1.l$ otherwise procedure started again till this condition was satisfied. The value of ground improvement was calculated as

$$n = \frac{S_u}{S_t} \tag{4.22}$$

where S_u and S_t and settlement of untreated and treated ground.

Computer program B-STColumn was written Utilizing Visual Basic V8 in order to perform the above procedure. B-STColumn stands for Bulging Failure of Stone Column. The parameters should be used as input of the program are foundation load, height of the reinforced ground, radius of column and soft soil (Figure 4.1), angle of shearing resistance of granular material and soft soil, Poisson's ratio, failure strain of stone, modulus of elasticity of soft soil and unit weight of stone material. The code calculates and presents the vertical pressure of soft soil and stone column, lateral strain of column and settlement of treated ground.

In order to develop design chart, effect of mentioned input values was investigated for settlement radio of the system. For the representative tables below area replacement ratio of 10%, ϕ_s =38° and foundation uniform load of 200 kPa were used. Table 4.2 illustrates the effect of Poisson's ratio on settlement ratio. This influence was observed to be small; therefore, the ν value of 0.1 was used in the tests which give the conservative value.

Table 4.3 represents effect of column length. Again small influence of this parameter was detected. Tables 4.4, 4.5 and 4.6 show the influence of modulus of elasticity of soft soil, failure strain and unit weight of stone. As before small effect of these factors were observed. Therefore the values that gave the most conservative results were used in the design charts. The values of parameters illustrated in the tables are those that are in use for practical purposes.

Influence of the ultimate angle of shearing resistance of stone was investigated in Figures 4.2, 4.3 and 4.4 for different A_s and different stone compactions. No significant effect of ϕ_c was seen.

Design chart is presented in Figure 4.5 where having the area ratio and angle of shearing resistance of stone column, settlement ratio of treated ground is estimated. By determination of settlement of unimproved soil, settlement of reinforced system can be evaluated using Equation 4.22.

Bearing capacity of reinforced ground can be estimated as the load corresponding to settlement equal to 10% of stone column diameter. (Rao et al. (1997)) Settlement of unreinforced soft soil equals to

$$S_u = \frac{C_s H}{1+e_o} \log\left(\frac{\sigma_o + \Delta\sigma'}{\sigma_o}\right) \tag{4.23}$$

where σ_o, e_o and H are the initial average overburden pressure of the soil layer, initial void ratio and thickness of soil layer respectively.

Combining Equations 4.22 and 4.23 yields

$$\Delta\sigma' = \sigma_o \left(10^{\frac{S_t \cdot n(1+e_o)}{C_s H}} - 1\right) \tag{4.24}$$

Therefore assuming S_t 10% of column diameter, using Figure 4.5 and Equation 4.24 ultimate load of the reinforced soil can be evaluated.

Table 4.2 Influence of Poisson's ratio on settlement ratio.

υ	**0.1**	**0.2**	**0.3**
n	1.23	1.27	1.31

Table 4.3 Settlement ratio for various column lengths.

l (m)	**5**	**10**	**15**
n	1.32	1.35	1.39

Table 4.4 Effect of modulus of elasticity on settlement ratio.

E	**1000**	**3000**	**5000**
n	1.39	1.44	1.43

Table 4.5 Influence of failure strain of stone on settlement ratio.

ϵ_f (%)	3	5	8
n	1.36	1.39	1.41

Table 4.6 Settlement ratio for various column unit weights.

$\gamma_s (\frac{kN}{m^3})$	14	18	22
n	1.37	1.38	1.39

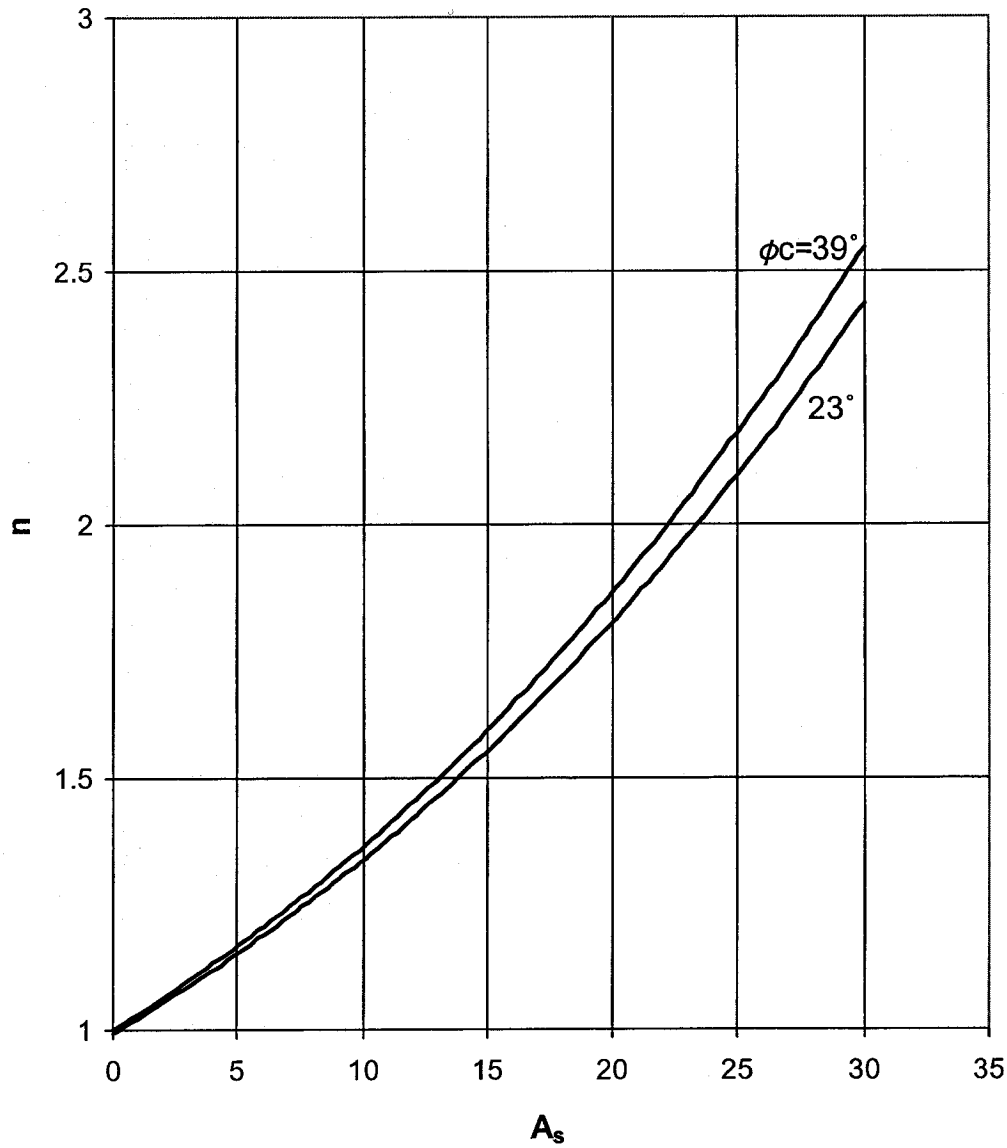

Figure 4.2 Settlement ratio vs. A_s for medium dense stones ϕ_f=38°.

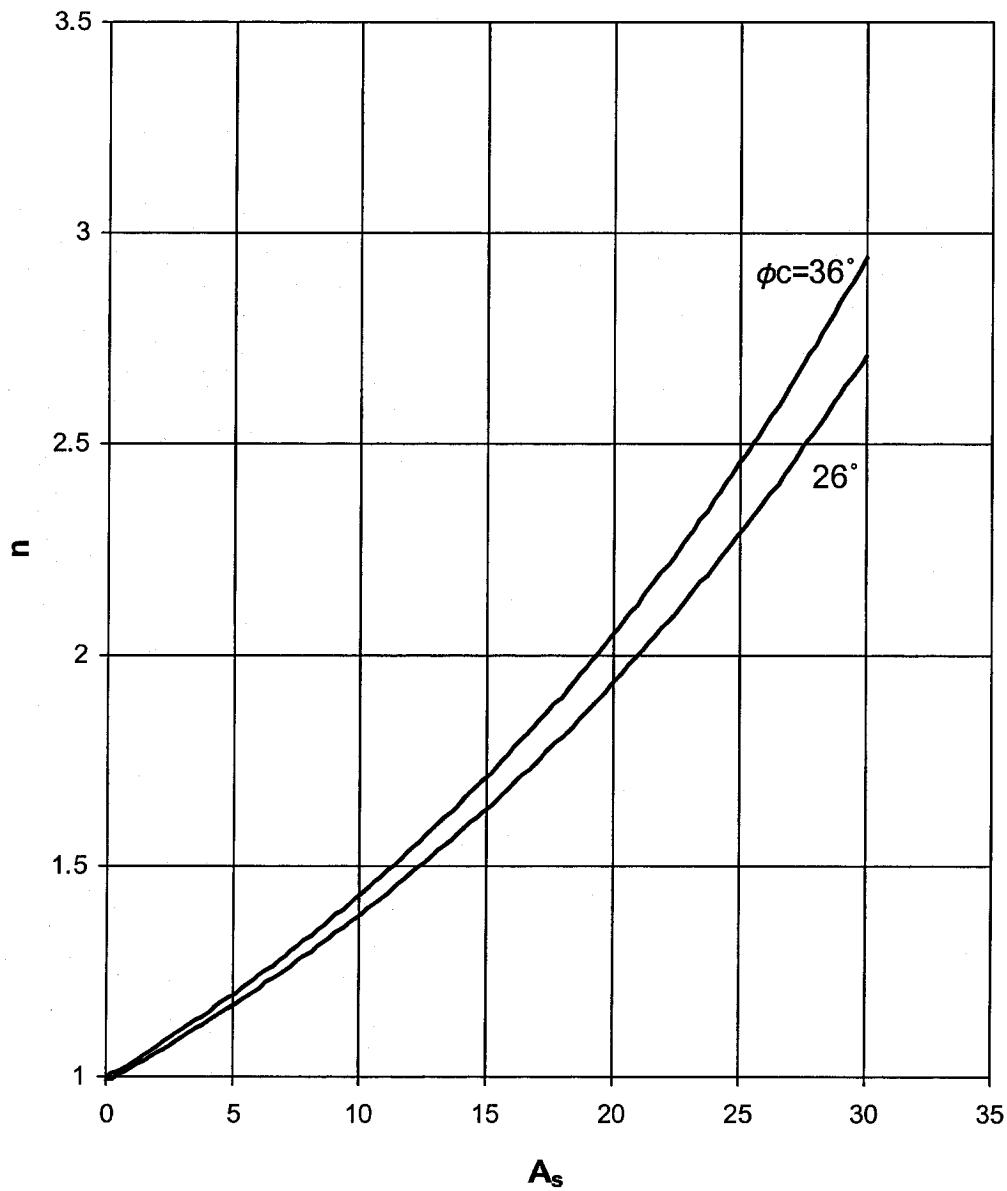

Figure 4.3 Settlement ratio vs. A_s for dense stones ϕ_f=41°.

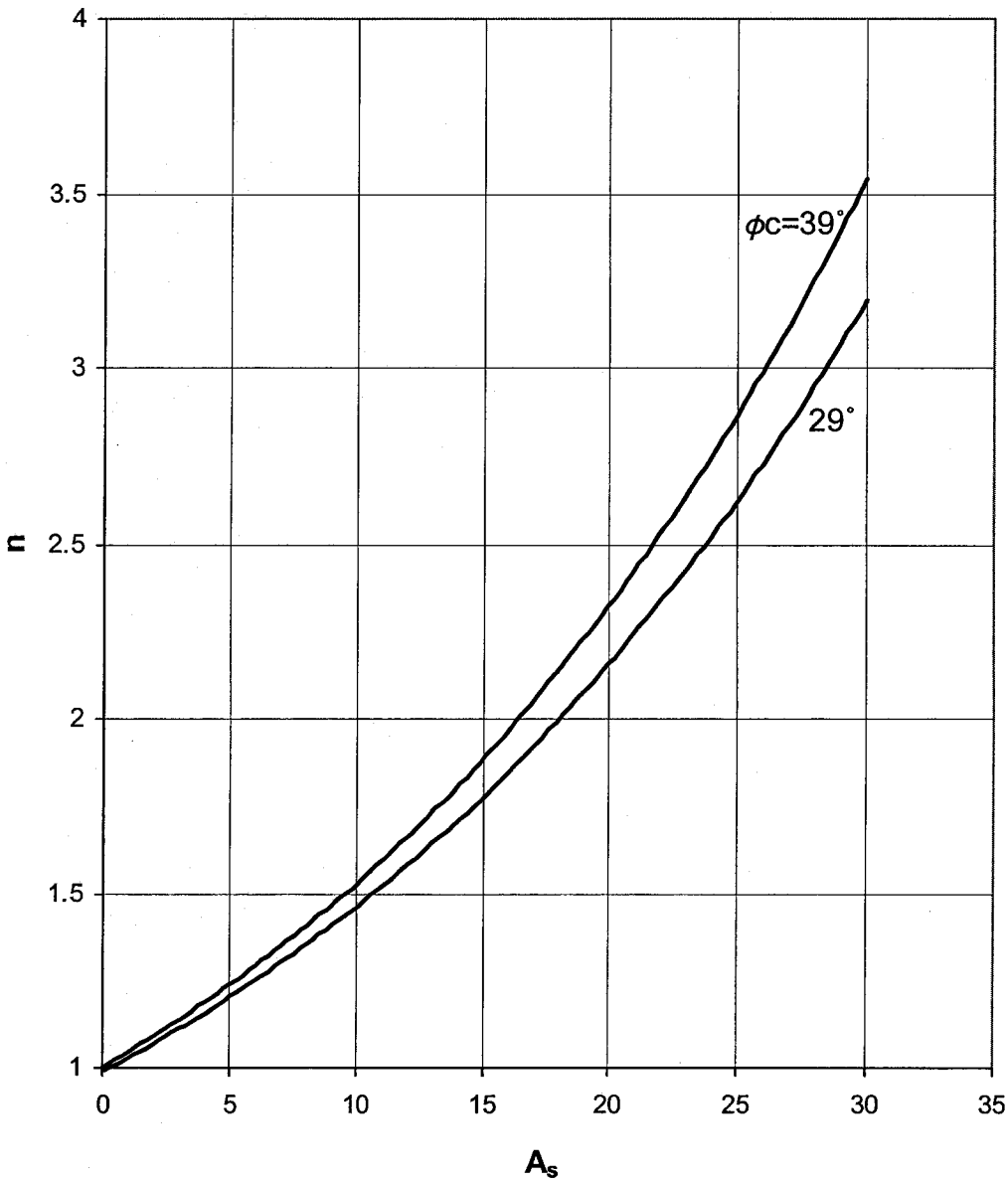

Figure 4.4 Settlement ratio vs. A_s for very dense stones ϕ_f=44°.

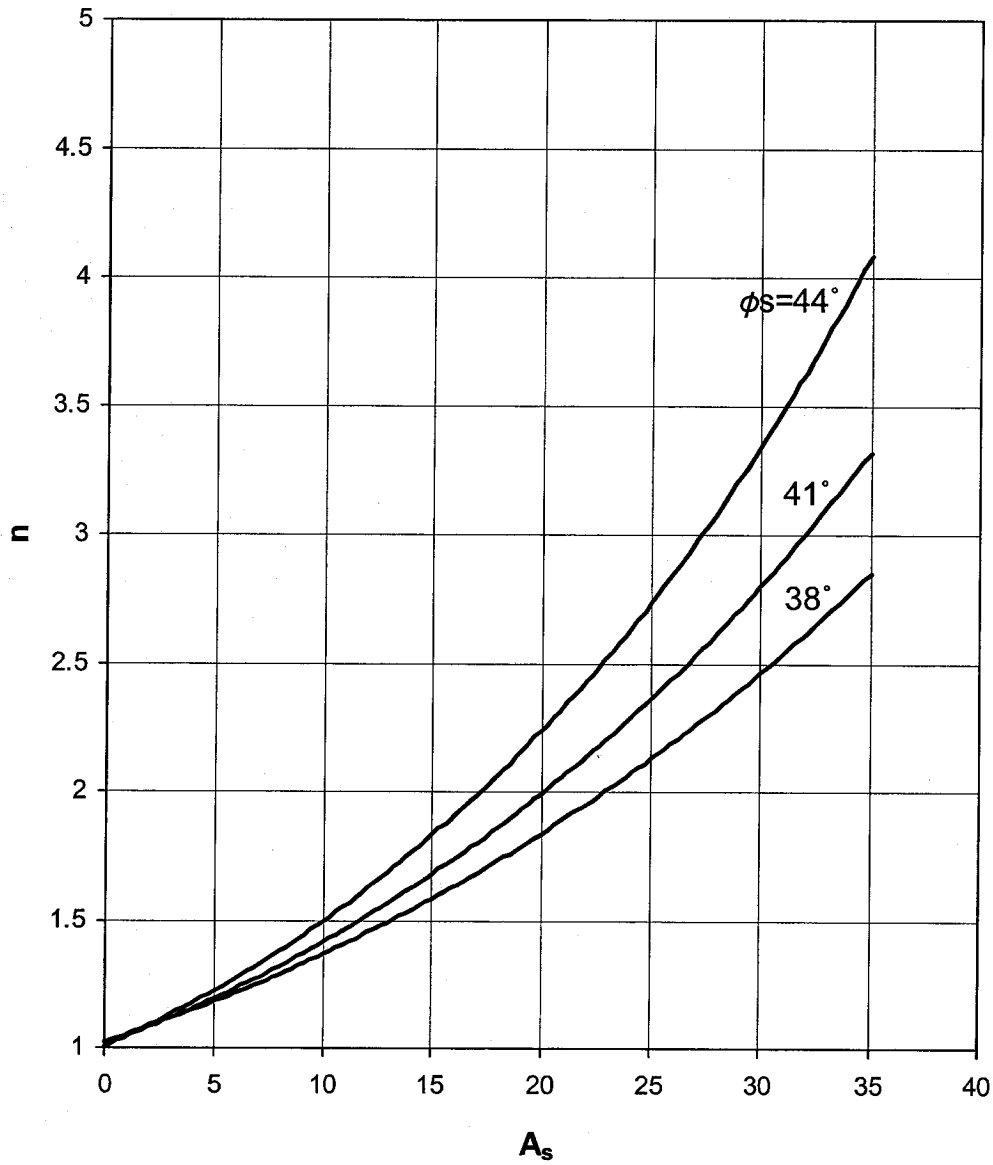

Figure 4.5 Design chart for bulging theoretical model.

4.2.3 Model Validation

Results obtained from the theoretical model were compared with other methods reported in the literature. Figures 4.6 to 4.8 show the comparison of the model with Priebe (1976), Aboshi et al. (1979), Poorooshasb and Meyerhof (1997) and Poorooshasb et al. (1997). The theory of Aboshi is also known as Equilibrium method. Value of n was assumed 5 for this method which gives closer values to the other theories. Results of Equilibrium method is far from the other ones. The present theory gives values in the middle of other theories for all medium dense, dense and very dense stones.

The present model was validated using the experimental tests conducted by Ambily and Gandhi (2007). (Table 4.7) The experiments were done for single column. Good agreement between the two models was observed. The experimental study was also compared with the other available theoretical models where the present theory resulted in better agreement with the laboratory tests comparing to the others.

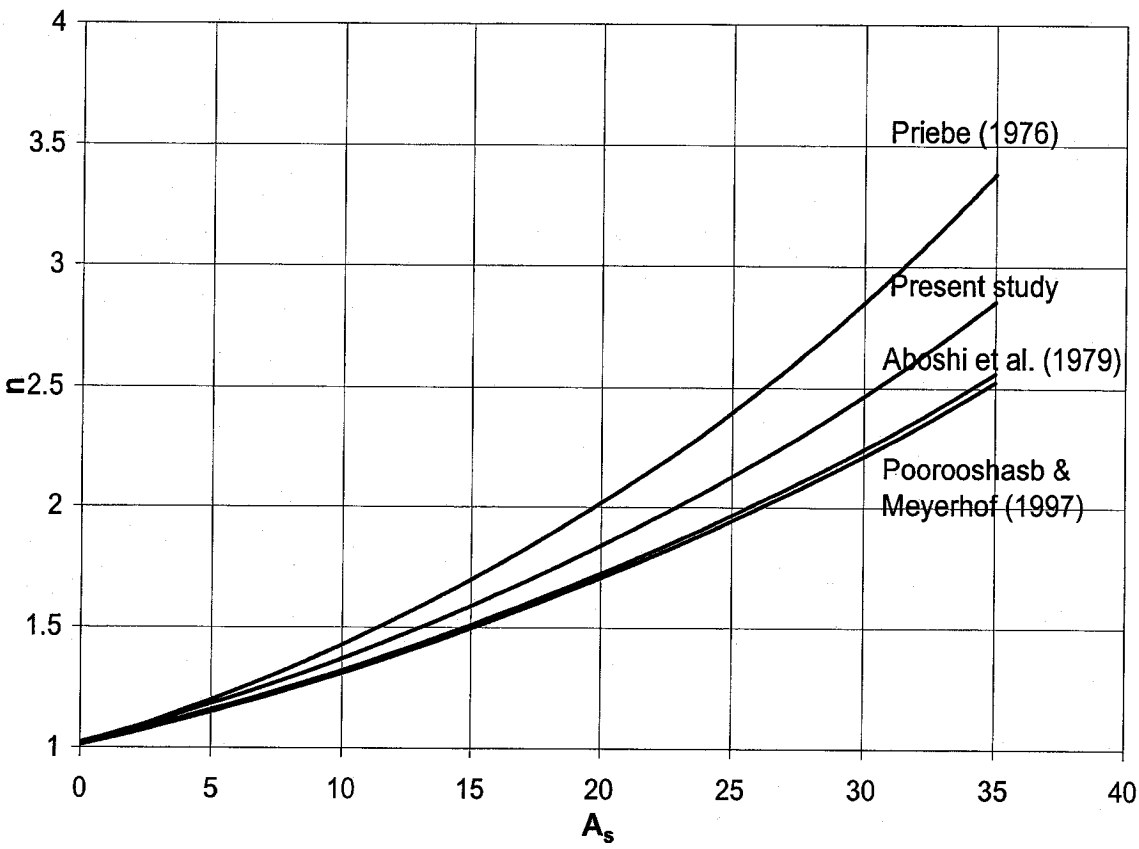

Figure 4.6 Comparison between test results of the analytical model and the available theories, for medium dense stones, ϕ_s =38°.

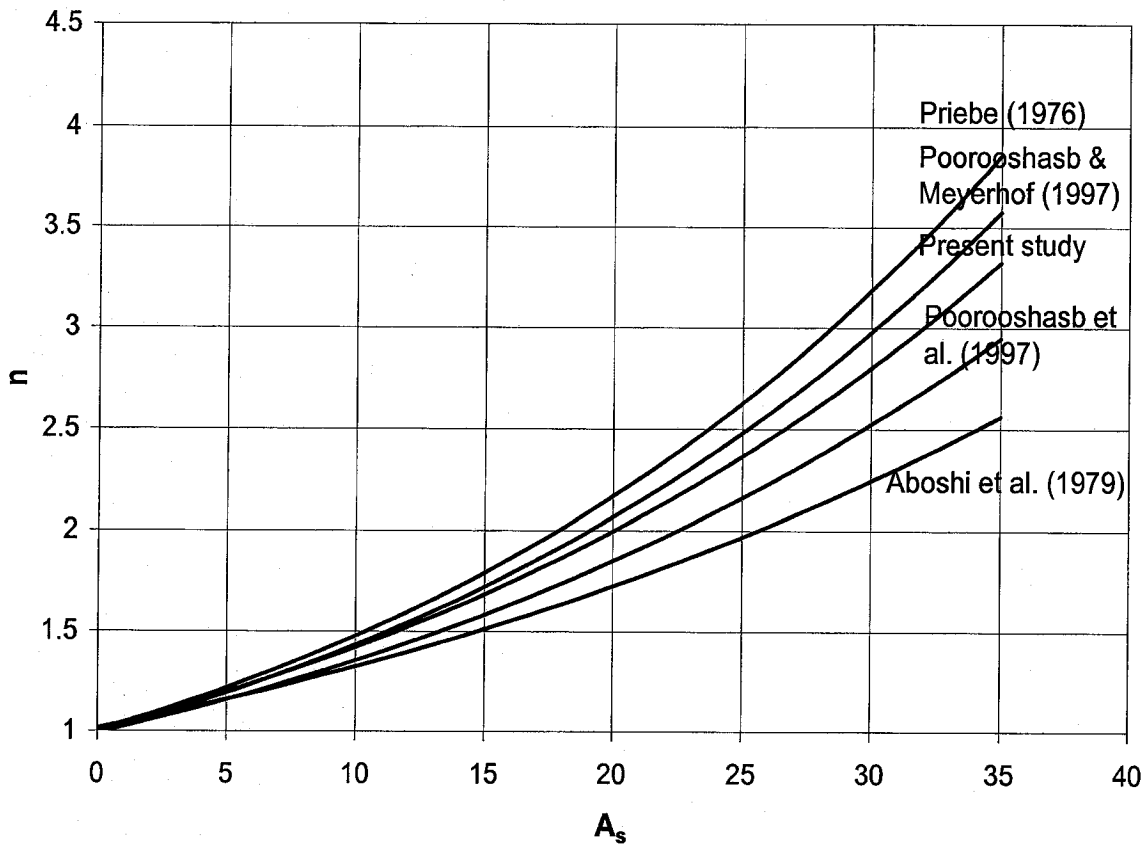

Figure 4.7 Comparison between test results of the analytical model and the available theories, for dense stones, ϕ_s =41°.

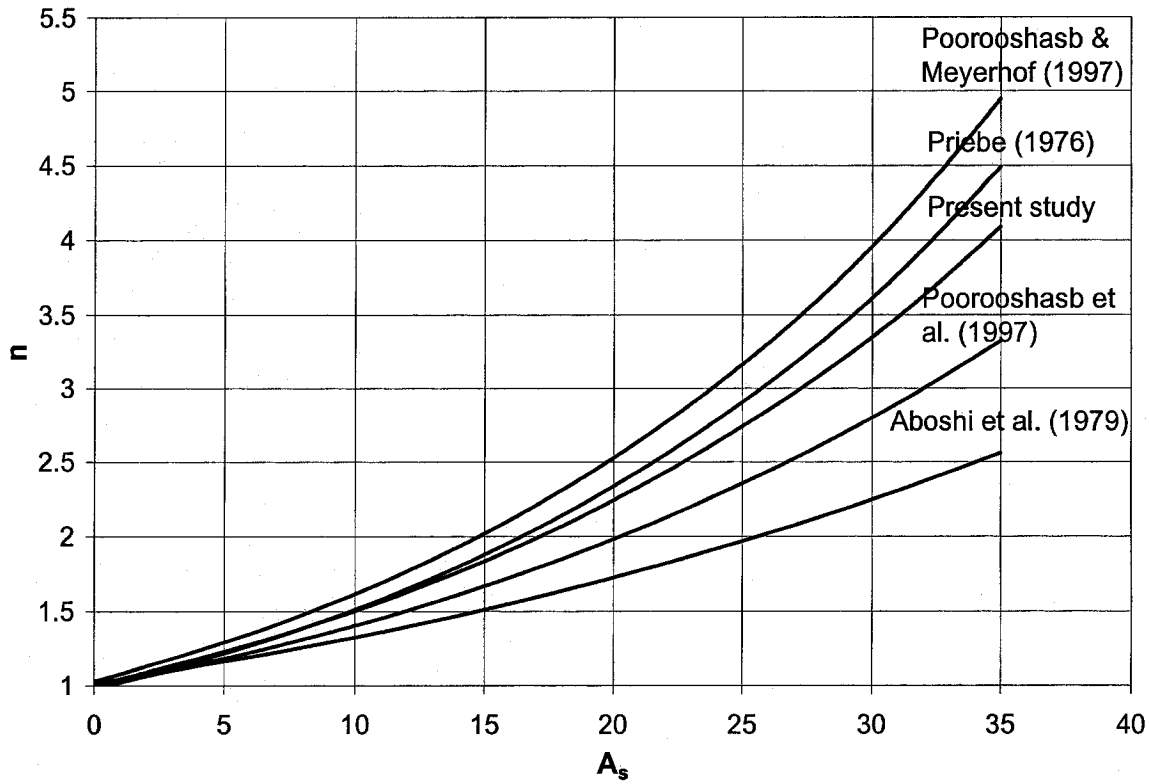

Figure 4.8 Comparison between test results of the present analytical model and the available theories (ϕ_s =44°).

Table 4.7 Validation of the theoretical model.

No.	c_u kPa	ϕ_s °	A_s %	q kPa	S_t M	S_t (m) present theory	error %	S_t (m) Priebe (1976)	error %	S_t (m) Poorooshasb & Meyerhof (1997)	error %
1	7	43	25	100	7.71E-03	7.91E-03	7.7	8.67E-03	12.5	7.23E-03	6.3
2	14	43	25	100	5.36E-03	5.48E-03	2.1	6.01E-03	12.2	5.01E-03	6.4
3	30	43	25	100	3.10E-03	3.09E-03	4.1	3.39E-03	9.3	2.82E-03	8.9
4	30	43	11	100	5.43E-03	5.59E-03	5.2	5.36E-03	1.2	4.76E-03	12.2
5	30	43	6	100	6.43E-03	6.71E-03	3.5	6.44E-03	0.1	6.05E-03	6.0

4.3 Analytical Model for General Shear Failure

In developing this model, the concept of the equivalent of soil/columns system was used. This concept was used by researches such as Priebe (1995), Lee and Pande (1998) to introduce soil properties to replace the soil/columns system. Limit equilibrium technique was used to perform the analysis. The objective of the proposed model is to determine the bearing capacity coefficients (N_γ, N_q and N_c) of the composite ground and consequently to estimate the ultimate bearing capacity of the reinforced ground.

In order to comply with the basic of mechanism of soils, the system should be both kinematically (upper bond) and statically (lower bond) admissible. A system is considered kinematically admissible when displacement of soil elements along the failure surface is feasible whereas for statically admissible condition, the 3 equilibrium equations (forces and moment) must be satisfied. In the real cases, it is difficult rather impossible to satisfy both conditions, however limit equilibrium technique, though exact solution can not be obtained, is widely acceptable in the geotechnical engineering in solving bearing capacity problems.

In this analysis, A_s is defined as ratio of the area of stone columns over total area of ground under the foundation. The composite cohesion and unit weight of the reinforced soil is taken as

$$\gamma_{comp} = A_s\gamma_s + (1 - A_s)\gamma_c \tag{4.25}$$

$$c_{comp} = A_s c_s + (1 - A_s)c_c \tag{4.26}$$

where c_s, c_c, γ_s and γ_c are cohesion and unit weight of the column material and soil respectively. The cohesion c_s is assumed to be zero for the sand material. Christoulas et

al. (1997), Cooper and Rose (1999) and Mestat and Riou (2004) consider the composite angle of friction as

$$\varphi_{comp} = A_s\varphi_s + (1 - A_s)\varphi_c \tag{4.27}$$

However by replacement of c_{comp} and ϕ_{comp} in Mohr-Coulomb failure criterion it can be observed that this criterion is not satisfied in their model. In order that this criterion becomes valid instead of Equation 4.27 the following equation was derived and used in this study.

$$\tau_{comp} = A_s\tau_s + (1 - A_s)\tau_c \tag{4.28}$$

and

$$\tau = \sigma \tan\varphi + c \tag{4.29}$$

where τ_{comp},τ_s and τ_c are the shear stress of the composite soil, stone column and soft soil. ϕ_s and ϕ_c represent the angle of friction of the stone column material and the soft soil respectively.

Substituting Equation 4.26 and 4.29 into Equation 4.28 results

$$\tan\varphi_{comp} = A_s\frac{\sigma_s}{\sigma}\tan\varphi_s + (1 - A_s)\frac{\sigma_c}{\sigma}\tan\varphi_c \tag{4.30}$$

The distribution of vertical stress in the reinforced area can be expressed by the stress ratio n as

$$n = \frac{\sigma_s}{\sigma_c} \tag{4.31}$$

where

σ_s= stress in stone column

σ_c= stress in surrounding soil

In order that equilibrium condition is satisfied at the vertical direction, the following equation should be valid.

$$\sigma_{comp} = A_s\sigma_s + (1 - A_s)\sigma_c \tag{4.32}$$

Combining equations 4.31 and 4.32 yields

$$\mu_s = \frac{\sigma_s}{\sigma} = \frac{n}{1 + (n-1)A_s} \tag{4.33}$$

$$\mu_c = \frac{\sigma_c}{\sigma} = \frac{1}{1 + (n-1)A_s} \tag{4.34}$$

Substituting equations 4.33 and 4.34 into Equation 4.32, friction angle of equivalent soil calculates as

$$\varphi_{comp} = \tan^{-1}[A_s\mu_s \tan\varphi_s + (1 - A_s)\mu_c \tan\varphi_c] \tag{4.35}$$

γ_{comp}, c_{comp} and ϕ_{comp} in Equations 4.25, 4.26 and 4.35 were used as the composite unit weight, cohesion and friction angle of the reinforced ground in the theoretical model. The stress ratio in Equations 4.33 and 4.34 is suggested between 2.5 to 5 by Barksdale and Bachus (1983). Mckelvey et al. (2004) declared that this ratio takes place at the beginning of loading. However, at failure, the value of n approaches approximately the value of 3. The stress ratio of 3 was used in this study.

Figures 4.9 and 4.10 show the observed failure shape deduced from the present numerical model together with the proposed failure pattern. It can be noted From Figure 4.10 that the observed failure pattern consists of 3 zones:

1. Zone 1, represents the elastic cone shape which is immediately under the foundation and has an angle ψ with the horizontal axis. This wedge (block ABC) moves together with the footing during loading.

2. Zone 2, is logspiral section (curve *CD* and *CF*) which is originated from the intersection of the foundation axis of symmetry and the wedge. Discontinuity of the material in the boundary of reinforced area and soft soil (Figure 4.10) results divergence of the logspiral failure extension in the soft area. In other words, failure pattern changes its shape at this point due to the change of the soil properties. Consequently collapse shape consists of two logspiral surfaces; one is within the equivalent soil part and the other is in the surrounding soil section.
3. Zone 3, is known as passive Rankine section where the failure surface has from of the straight line (*DE* and *FG*). This zone connects the logspiral part to the ground surface.

4.3.1 Equilibrium Analysis

To carry out the equilibrium analysis, due to symmetry it is sufficient to consider only the half side of the proposed model. Figure 4.11 presents the forces acting on the logspiral sections. These sections were divided into two separate parts; composite soil and soft soil. Equilibrium equations were written separately for each part. The passive force due to the unit weight, cohesion and surcharge was considered separately.

For the case that passive force due to unit weight is concerned, the free body of the composite section (Figure 4.12) is subjected of the following forces:

1. Weight W_1 which is equal to the weight of a sector of the logspiral block O_1CH given as

$$W_1 = \gamma_{comp} \frac{r_1^2 - r_0^2}{4 \tan \varphi_{comp}} \tag{4.36}$$

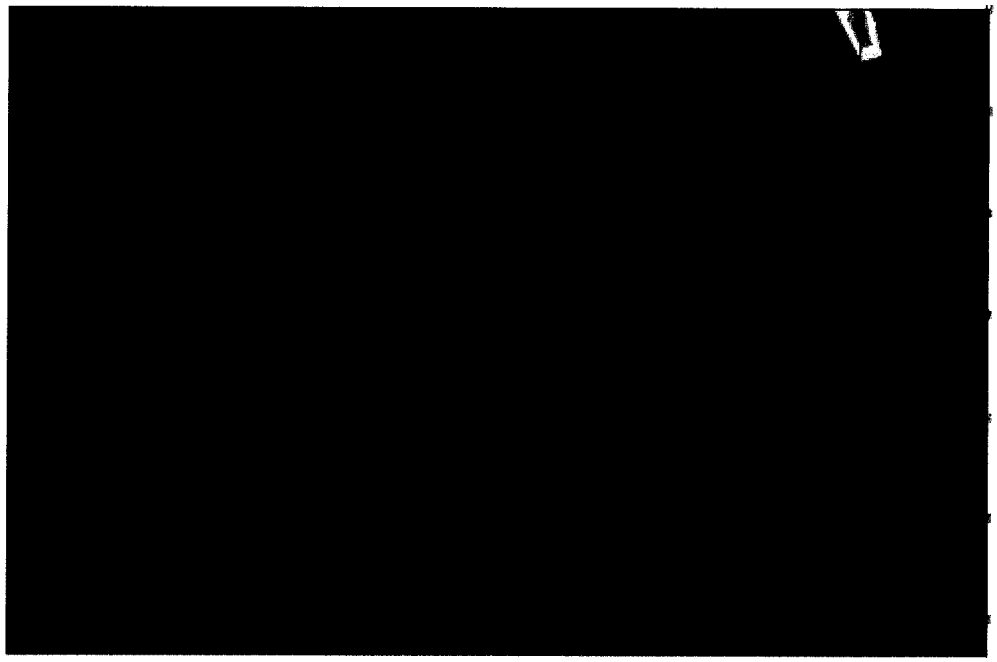

Figure 4.9 Rupture surface deduced from numerical model.

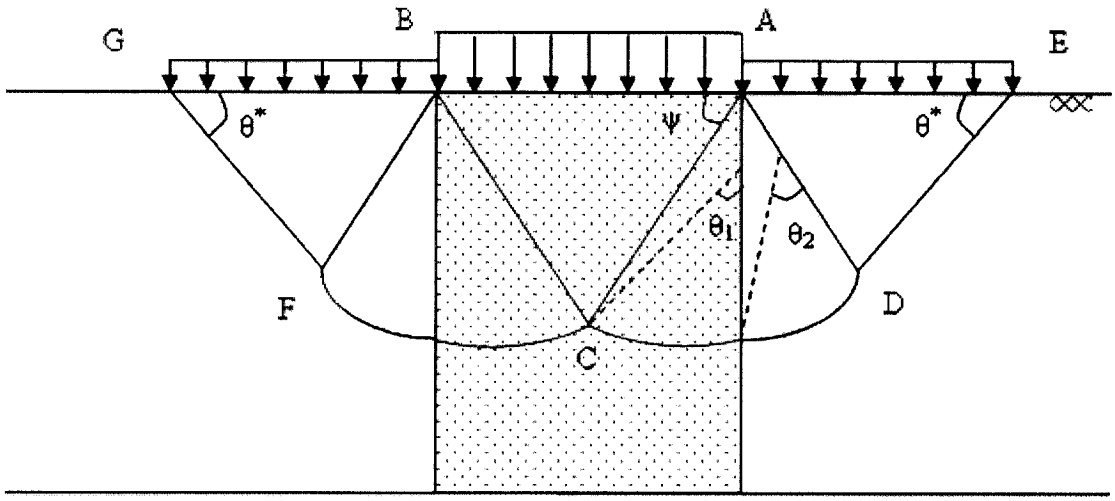

Figure 4.10 Proposed failure Mechanism.

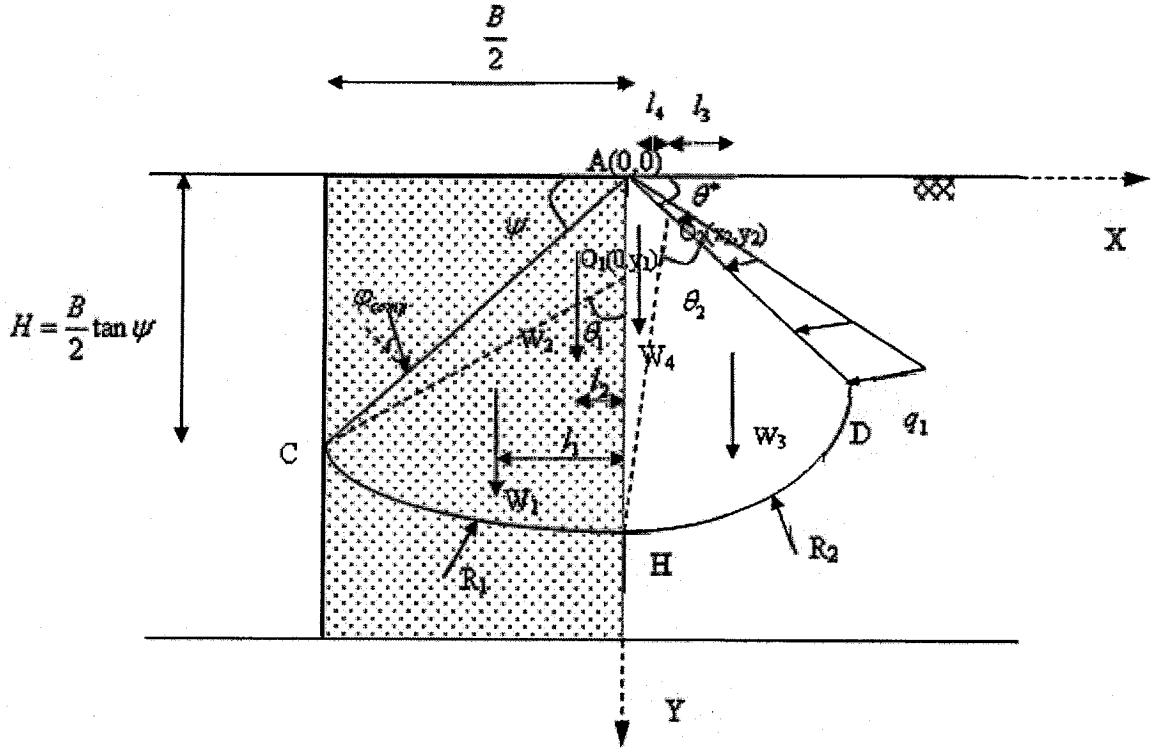

Figure 4.11 Acting forces on the logspiral sections.

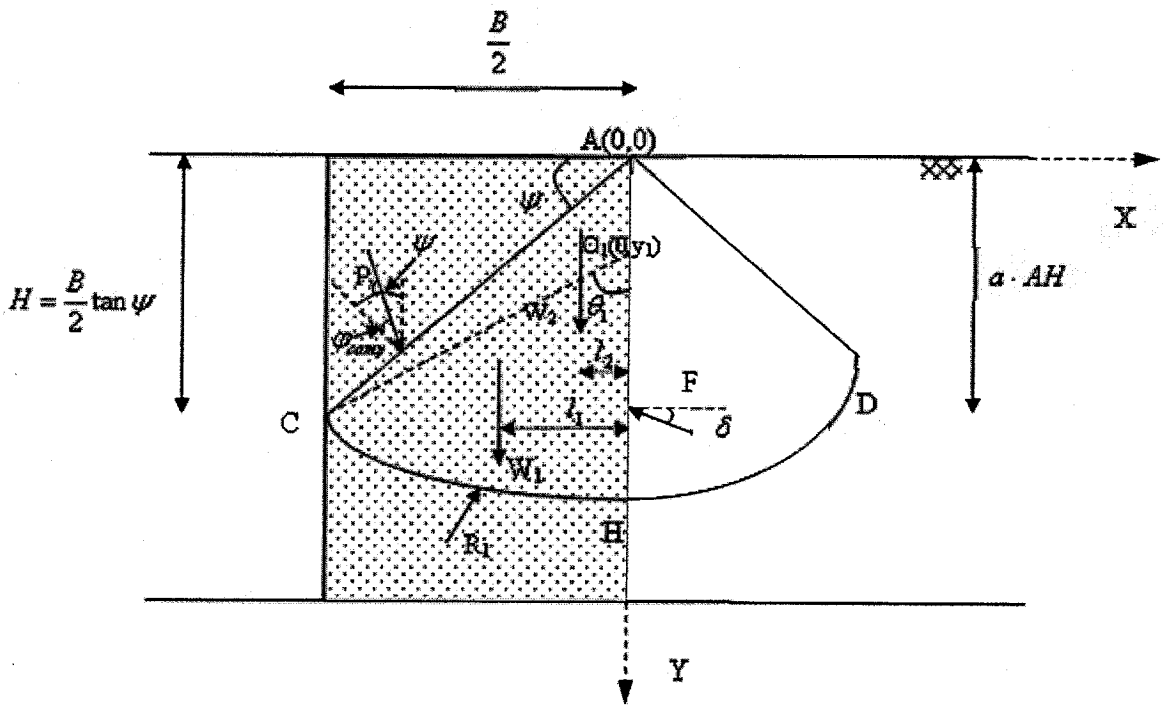

Figure 4.12 Equilibrium of forces for composite soil section ($\phi \neq 0$, $\gamma \neq 0$, $q=0$, $c=0$).

The lines O_1C and O_1H are arcs of the logspiral defined as r_o and r_1 respectively and are determined by the following equation

$$r_1 = r_o e^{\theta_1 \tan \phi_{comp}} \tag{4.37}$$

Let

$$AC = \frac{\frac{B}{2}}{\cos\psi} \tag{4.38}$$

From ΔACO_1 using the sine rules

$$\frac{\sin(90-\psi)}{O_1C} = \frac{\sin(180-\theta_1)}{AC} \tag{4.39}$$

So

$$r_o = \frac{B}{2\sin\theta_1} \tag{4.40}$$

Combining Equations 4.37 and 4.40 results

$$r_1 = \frac{B}{2\sin\theta_1} e^{\theta_1 \tan \varphi_{comp}} \tag{4.41}$$

Substituting Equations 4.40 and 4.41 into Equation 4.36 gives

$$W_1 = \gamma_{comp} \frac{B^2 (e^{2\theta_1 \tan \varphi_{comp}} - 1)}{16\sin^2\theta_1 \tan\varphi_{comp}} \tag{4.42}$$

2. Weight of the triangle ACO_1 equals to

$$W_2 = \frac{1}{2}\gamma_{comp} \frac{B}{2} y_1 \tag{4.43}$$

From ΔACO_1 using sine rules

$$\frac{\sin(180-\theta_1)}{AC} = \frac{\sin(180-90+\psi-180+\theta_1)}{AO_1} \tag{4.44}$$

Utilizing Equation 4.38 gives

$$AO_1 = y_1 = \frac{B(\tan\psi - \cot\theta_1)}{2} \tag{4.45}$$

Substituting Equations 4.45 into Equation 4.43 gives

$$W_2 = \gamma_{comp}\frac{B^2(\tan\psi - \cot\theta_1)}{8} \tag{4.46}$$

3. The frictional resisting force R_1 along the arc CH. The line of action of this force passes through the center of the logspiral.
4. P_γ acting on line AC.
5. The reaction of the force, F, applied on the soft soil section.

Taking moment about point O_1 gives

$$\Sigma M_{O1} = 0 \rightarrow W_1 l_1 + W_2 l_2 + P_\gamma[\cos(\psi - \varphi_{comp})\frac{B}{3} + \sin(\psi - \varphi_{comp})(\frac{B}{3}\tan\psi - y_1)]$$
$$= F\cos\delta(a \cdot AH - y_1) \tag{4.47}$$

The lever arm l_1 is defined by Hijab (1956) as

$$l_1 = \frac{4\tan\varphi_{comp}}{3(9\tan^2\varphi_{comp}+1)} \cdot \frac{r_1^3 - r_o^3(3\tan\varphi_{comp}\sin\theta_1 + \cos\theta_1)}{(r_1^2 - r_o^2)} \tag{4.48}$$

Combining 4.40 and 4.41 into 4.48 yields

$$l_1 = \frac{2B\tan\varphi_{comp}}{3\sin\theta_1(9\tan^2\varphi_{comp}+1)(e^{2\theta_1\tan\varphi_{comp}}-1)}[e^{3\theta_1\tan\varphi_{comp}} - (3\tan\varphi_{comp}\sin\theta_1 + \cos\theta_1)] \tag{4.49}$$

Moreover, lever arm l_2 is determined as

$$l_2 = \frac{1}{3}\cdot\frac{B}{2} = \frac{B}{6} \tag{4.50}$$

The height AH equals to

$$AH = y_1 + r_1 = \frac{B}{2\sin\theta_1}(\tan\psi\sin\theta_1 - \cos\theta_1 + e^{\theta_1 \tan\varphi_{comp}}) \tag{4.51}$$

Substituting Equations 4.42, 4.45, 4.46, 4.49, 4.50 and 4.51 into Equation 4.47 gives

$$\gamma_{comp}\frac{B^3}{24\sin^3\theta_1(9\tan^2\varphi_{comp}+1)}[e^{3\theta_1\tan\varphi_{comp}} - (3\tan\varphi_{comp}\sin\theta_1 + \cos\theta_1)] + \gamma_{comp}\frac{B^3(\tan\psi - \cot\theta_1)}{48}$$

$$+ P_\gamma[\cos(\psi - \varphi_{comp})\frac{B}{3} + \sin(\psi - \varphi_{comp})(\frac{B}{3}\tan\psi - \frac{B(\tan\psi - \cot\theta_1)}{2})]$$

$$= F\cos\delta\frac{B}{2}[(a-1)\cdot(\tan\psi - \cot\theta_1) + a\frac{e^{\theta_1\tan\varphi_{comp}}}{\sin\theta_1})] \tag{4.52}$$

or

$$F = \frac{\gamma_{comp}\frac{B^3}{24\sin^3\theta_1(9\tan^2\varphi_{comp}+1)}[e^{3\theta_1\tan\varphi_{comp}} - (3\tan\varphi_{comp}\sin\theta_1 + \cos\theta_1)] + \gamma_{comp}\frac{B^3(\tan\psi - \cot\theta_1)}{48}}{\cos\delta\frac{B}{2}[(a-1)\cdot(\tan\psi - \cot\theta_1) + a\frac{e^{\theta_1\tan\varphi_{comp}}}{\sin\theta_1})]}$$

$$\frac{+ P_\gamma[\cos(\psi - \varphi_{comp})\frac{B}{3} + \sin(\psi - \varphi_{comp})(\frac{B}{3}\tan\psi - \frac{B(\tan\psi - \cot\theta_1)}{2})]}{} \tag{4.53}$$

In order to minimize the ultimate bearing capacity, the force F should be at its minimum value. This condition can be described as $\frac{\partial F}{\partial v} = 0$ where v is related to logspiral geometry such as its center coordinates or θ_1. (Kumbhojkar (1993)) Differentiating the above equation with respect to θ_1 and equating the result to zero, the values of the critical θ_1 and F will be then estimated. Differentiating the above equation is presented in Appendix 2 which is determined utilizing Maple software.

Derivation of equilibrium equations were continued for the soft soil section. This section is subject to the following forces (Figure 4.13):

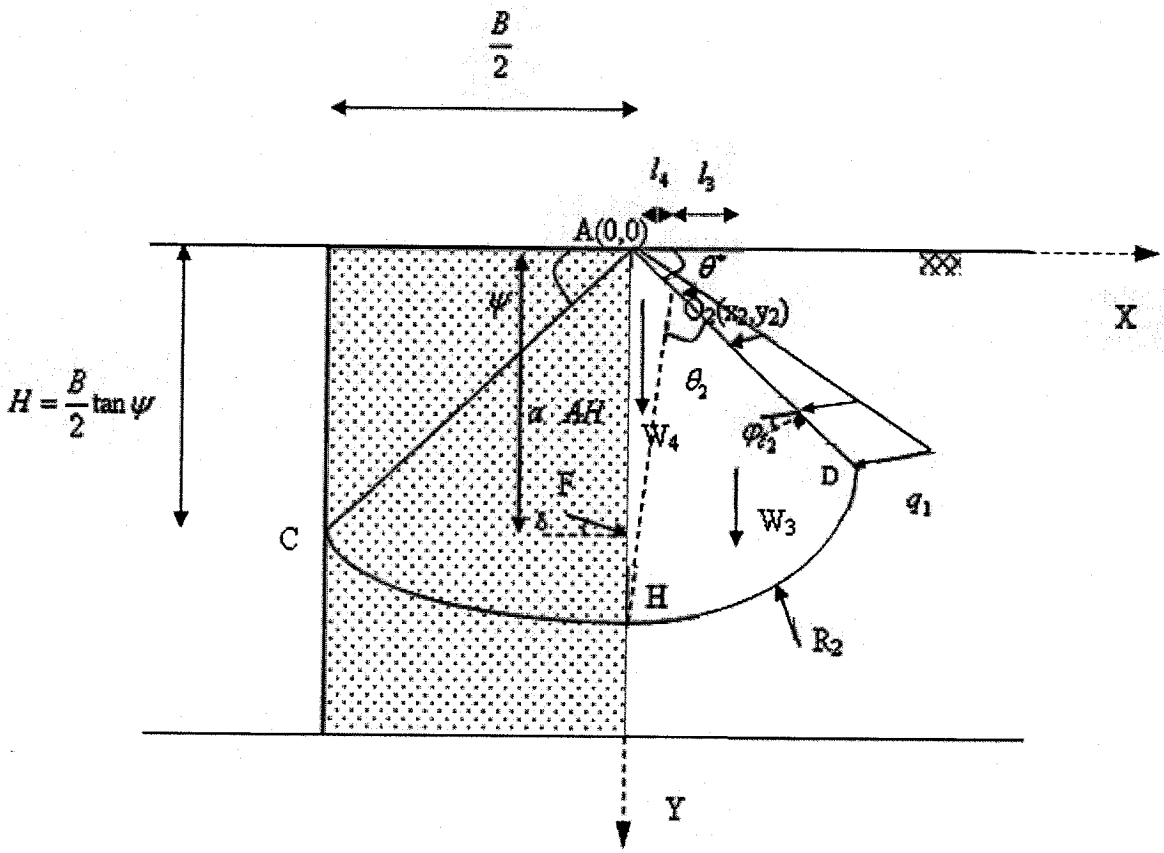

Figure 4.13 Equilibrium of forces for soft soil section ($\phi \neq 0$, $\gamma \neq 0$, $q=0$, $c=0$).

1. Weight W_3 which is equal to the weight of a sector of the logspiral block O_2HD given as

$$W_3 = \gamma_c \frac{r_3^2 - r_2^2}{4\tan\varphi_{c_2}} \tag{4.54}$$

The lines O_2H and O_2D are arcs r_2 and r_3 of a logspiral respectively defined by the equation

$$r_3 = r_2 e^{\theta_2 \tan\varphi_{c2}} \tag{4.55}$$

Using the sine rule for triangle AHO_2 gives

$$\frac{\sin(180-\theta_2)}{AH} = \frac{\sin(90-\theta^*)}{O_2H} \tag{4.56}$$

or

$$r_2 = (r_1 + y_1)\frac{\cos\theta^*}{\sin\theta_2} = (e^{\theta_1 \tan\varphi_{comp}} + \tan\psi\sin\theta_1 - \cos\theta_1)\frac{B\cos\theta^*}{2\sin\theta_2\sin\theta_1} \tag{4.57}$$

Hence combining Equations 4.55 and 4.57 gives

$$r_3 = (e^{\theta_1 \tan\varphi_{comp}} + \tan\psi\sin\theta_1 - \cos\theta_1)\frac{B\cos\theta^*}{2\sin\theta_2\sin\theta_1} e^{\theta_2 \tan\varphi_{c2}} \tag{4.58}$$

Substituting Equations 4.57 and 4.58 into Equation 4.54 results

$$W_3 = \frac{\gamma_c B^2 \cos^2\theta^*}{16\tan\varphi_{c2}\sin^2\theta_2\sin^2\theta_1}(e^{\theta_1 \tan\varphi_{comp}} + \tan\psi\sin\theta_1 - \cos\theta_1)^2(e^{2\theta_2 \tan\varphi_{c2}} - 1) \tag{4.59}$$

2. Weight of the triangle AHO_2, W_4, which is defined as

$$W_4 = \frac{\gamma_c \cdot AH \cdot x_2}{2} \tag{4.60}$$

Considering triangle AHO_2

$$x_2 = -r_2\cos(\theta^* + \theta_2) \tag{4.61}$$

Substituting Equation 4.57 into Equation 4.61 yields

$$x_2 = \frac{B}{2\sin\theta_1}(e^{\theta_1 \tan\varphi_{comp}} + \tan\psi \sin\theta_1 - \cos\theta_1)\cdot(-\cos^2\theta^* \cot\theta_2 + \sin\theta^* \cos\theta^*) \quad (4.62)$$

So

$$W_4 = \frac{\gamma_c B^2}{8\sin^2\theta_1}(\tan\psi \sin\theta_1 - \cos\theta_1 + e^{\theta_1 \tan\varphi_{comp}})^2 \cdot(-\cos^2\theta^* \cot\theta_2 + \sin\theta^* \cos\theta^*) \quad (4.63)$$

3. The frictional resisting force R_2 along the arc *HD*. The line of action of this force passes through the center of the logspiral.
4. Force due to the resultant of the stress in the passive Rankine zone *ADE* on plans *AD* which can be written as (Figure 4.13)

$$q_1 = \gamma_c AD \sin\theta^* \tan(90-\theta^*) \quad \text{(Silvestri, 2003)} \quad (4.64)$$

5. The reaction of the force, *F*.

Taking moment around point O_2 gives

$$\Sigma M_{O_2} = 0 \rightarrow \frac{q_1 \cos\varphi_c}{2} AD(\frac{2}{3}AD - AO_2) + W_3 l_3 = W_4 l_4 + F\sin\delta \cdot x_2 + F\cos\delta(a\cdot AH - y_2)$$

(4.65)

In order to drive the lever arm l_3, the distance between the center of gravity of logspiral and its center O_2 should be determined first as follows:

If the point *C* and *A* are the centroid and logspiral center respectively and *AM* and *AN* represent the arcs of the logspiral (Figure 4.14), considering the triangle *FCD* results.

$$CF = \frac{b}{\cos\theta^*} \quad (4.66)$$

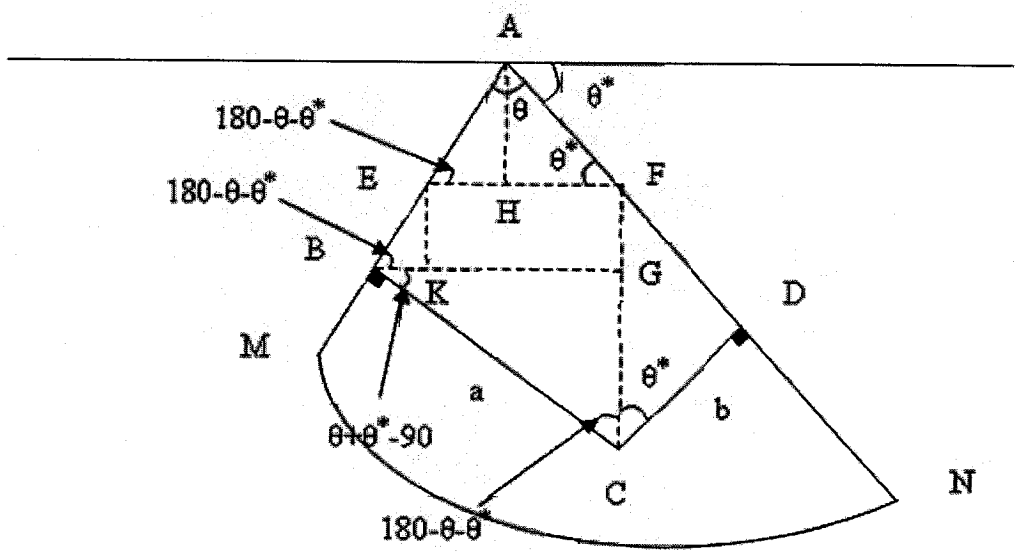

Figure 4.14 Centroid of the sector of the logspiral.

Considering the triangle BCG gives

$$BG = a\sin(\theta + \theta^*) \tag{4.67}$$

and

$$CG = -a\cos(\theta + \theta^*) \tag{4.68}$$

Given

$$FG = CF - CG \tag{4.69}$$

Substituting Equations 4.66 and 4.68 into Equation 4.69 gives

$$FG = \frac{b}{\cos\theta^*} + a\cos(\theta + \theta^*) \tag{4.70}$$

From triangle EBK using Equation 4.70

$$BK = \frac{-(\frac{b}{\cos\theta^*} + a\cos(\theta + \theta^*))}{\tan(\theta + \theta^*)} \tag{4.71}$$

From Figure 4.14

$$KG = BG - BK \tag{4.72}$$

Combining Equations 4.67, 4.71 and 4.72 yields

$$KG = EF = a\sin(\theta + \theta^*) + \frac{\frac{b}{\cos\theta^*} + a\cos(\theta + \theta^*)}{\tan(\theta + \theta^*)} \tag{4.73}$$

From the triangle AEF

$$\frac{\sin\theta}{EF} = \frac{\sin(180 - \theta - \theta^*)}{AF} \tag{4.74}$$

Substituting Equation 4.73 into 4.74 results

$$AF = \frac{[a\sin(\theta+\theta^*) + \frac{\frac{b}{\cos\theta^*} + a\cos(\theta+\theta^*)}{\tan(\theta+\theta^*)}]\sin(\theta+\theta^*)}{\sin\theta} \tag{4.75}$$

Again from the triangle AHF

$$HF = AF\cos\theta^* \tag{4.76}$$

Combining Equations 4.75 and 4.76, HF can be determined as

$$HF = \frac{a\cos\theta^* + b\cos(\theta+\theta^*)}{\sin\theta} \tag{4.77}$$

a and b are define by Hijab (1956) as

$$\frac{a}{r_o} = \frac{4}{3}\cdot\frac{\tan\varphi}{9\tan^2\varphi+1}\cdot\frac{(\frac{r_1}{r_o})^3(3\tan\varphi\sin\theta-\cos\theta)+1}{(\frac{r_1}{r_o})^2-1} \tag{4.78}$$

and

$$\frac{b}{r_o} = \frac{4}{3}\cdot\frac{\tan\varphi}{9\tan^2\varphi+1}\cdot\frac{(\frac{r_1}{r_o})^3-3\tan\varphi\sin\theta-\cos\theta}{(\frac{r_1}{r_o})^2-1} \tag{4.79}$$

Substituting a and b in the Equation 4.77, after simplification yields

$$HF = \frac{4\tan\varphi\{r_1^3(3\tan\varphi\cos\theta^*-\sin\theta^*)+r_o^3[\sin(\theta^*+\theta)-3\tan\varphi\cos(\theta^*+\theta)]\}}{3(9\tan^2\varphi+1)(r_1^2-r_o^2)} \tag{4.80}$$

Applying Equation 4.80 to the model the lever arm l_3 is determined as

$$l_3 = \frac{4\tan\varphi_{c_2}\{r_3^3(3\tan\varphi_{c_2}\cos\theta^*-\sin\theta^*)+r_2^3[\sin(\theta^*+\theta_2)-3\tan\varphi_{c_2}\cos(\theta^*+\theta_2)]\}}{3(9\tan^2\varphi_{c_2}+1)(r_3^2-r_2^2)} \tag{4.81}$$

Substituting Equations 4.57 and 4.58 into Equation 4.81 results

$$l_3 = \frac{2B\cos\theta^* \tan\varphi_{c_2}}{3(9\tan^2\varphi_{c_2}+1)(e^{2\theta_2\tan\varphi_{c2}}-1)\sin\theta_2\sin\theta_1}\{(e^{\theta_1\tan\varphi_{comp}}+\tan\psi\sin\theta_1-\cos\theta_1)$$

$$\cdot[e^{3\theta_2\tan\varphi_{c2}}(3\tan\varphi_{c_2}\cos\theta^*-\sin\theta^*)+\sin(\theta^*+\theta_2)-3\tan\varphi_{c_2}\cos(\theta^*+\theta_2)]\} \quad (4.82)$$

and the lever arm l_4 is given as

$$l_4 = \frac{2x_2}{3} \quad (4.83)$$

So

$$l_4 = \frac{B}{3\sin\theta_1}(e^{\theta_1\tan\varphi_{comp}}+\tan\psi\sin\theta_1-\cos\theta_1)\cdot(-\cos^2\theta^*\cot\theta_2+\sin\theta^*\cos\theta^*) \quad (4.84)$$

In order to solve the Equation 4.65 the values of AD, AO_2 and AH must be known.

From Figure 4.13

$$y_2 = x_2\tan\theta^* \quad (4.85)$$

Combing Equations 4.62 and 4.85 yields

$$y_2 = \frac{B}{2\sin\theta_1}(e^{\theta_1\tan\varphi_{comp}}+\tan\psi\sin\theta_1-\cos\theta_1)\cdot(-\sin\theta^*\cos\theta^*\cot\theta_2+\sin^2\theta^*) \quad (4.86)$$

Also

$$AO_2 = \frac{x_2}{\cos\theta^*} \quad (4.87)$$

By substituting Equation 4.62 into 4.87 AO_2 is determined as

$$AO_2 = \frac{B}{2\sin\theta_1}(e^{\theta_1\tan\varphi_{comp}}+\tan\psi\sin\theta_1-\cos\theta_1)\cdot(-\cos\theta^*\cot\theta_2+\sin\theta^*) \quad (4.88)$$

Given

$$AD = AO_2 + r_3 \quad (4.89)$$

Thus

$$AD=\frac{B}{2\sin\theta_1\sin\theta_2}(e^{\theta_1\tan\varphi_{comp}}+\tan\psi\sin\theta_1-\cos\theta_1)\cdot(-\cos\theta^*\cos\theta_2+\sin\theta^*\sin\theta_2+\cos\theta^*e^{\theta_2\tan\varphi_{c2}})$$

(4.90)

Substituting Equations 4.51, 4.59, 4.62, 4.63, 4.64, 4.82, 4.84, 4.86, 4.88 and 4.90 into Equation 4.65 gives

$$\frac{\gamma_c\cdot B^3\sin\theta^*\tan(90-\theta^*)\cos\varphi_c}{24\sin^3\theta_1\sin^3\theta_2}(e^{\theta_1\tan\varphi_{comp}}+\tan\psi\sin\theta_1-\cos\theta_1)^3\cdot(-\cos\theta^*\cos\theta_2+\sin\theta^*\sin\theta_2$$

$$+\cos\theta^*e^{\theta_2\tan\varphi_{c2}})^2(\frac{1}{2}\cos\theta^*\cos\theta_2-\frac{1}{2}\sin\theta_2\sin\theta^*+\cos\theta^*e^{\theta_2\tan\varphi_{c2}})$$

$$+\frac{\gamma_cB^3\cos^3\theta^*}{24\sin^3\theta_2\sin^3\theta_1(9\tan^2\varphi_c+1)}(\tan\psi\sin\theta_1-\cos\theta_1+e^{\theta_1\tan\varphi_{equ.}})^3$$

$$\cdot[e^{3\theta_2\tan\varphi_c}(3\tan\varphi_c\cos\theta^*-\sin\theta^*)+\sin(\theta^*+\theta_2)-3\tan\varphi_c\cos(\theta^*+\theta_2)]$$

$$=\frac{\gamma_cB^3}{24\sin^3\theta_1}(\tan\psi\sin\theta_1-\cos\theta_1+e^{\theta_1\tan\varphi_{comp}})^3\cdot(-\cos^2\theta^*\cot\theta_2+\sin\theta^*\cos\theta^*)^2$$

$$+F\frac{B}{4\sin\theta_1}(e^{\theta_1\tan\varphi_{comp}}+\tan\psi\sin\theta_1-\cos\theta_1)[\sin\delta(-\cos^2\theta^*\cot\theta_2+\sin\theta^*\cos\theta^*)$$

$$+\cos\delta(a+\sin\theta^*\cos\theta^*\cot\theta_2-\sin^2\theta^*)] \qquad (4.91)$$

or

$$F=\frac{\frac{\gamma_c\cdot B^3\sin\theta^*\tan(90-\theta^*)\cos\varphi_c}{24\sin^3\theta_1\sin^3\theta_2}(e^{\theta_1\tan\varphi_{comp}}+\tan\psi\sin\theta_1-\cos\theta_1)^3\cdot(-\cos\theta^*\cos\theta_2+\sin\theta^*\sin\theta_2}{\frac{B}{2\sin\theta_1}(e^{\theta_1\tan\varphi_{comp}}+\tan\psi\sin\theta_1-\cos\theta_1)}$$

$$\frac{+\cos\theta^*e^{\theta_2\tan\varphi_{c2}})^2(\frac{1}{2}\cos\theta^*\cos\theta_2-\frac{1}{2}\sin\theta_2\sin\theta^*+\cos\theta^*e^{\theta_2\tan\varphi_{c2}})}{[\sin\delta(-\cos^2\theta^*\cot\theta_2+\sin\theta^*\cos\theta^*)+\cos\delta(a+\sin\theta^*\cos\theta^*\cot\theta_2-\sin^2\theta^*)]}$$

$$+\frac{\gamma_c B^3 \cos^3\theta^*}{24\sin^3\theta_2 \sin^3\theta_1(9\tan^2\varphi_c+1)}(\tan\psi\sin\theta_1-\cos\theta_1+e^{\theta_1\tan\varphi_{comp}})^3$$

$$\cdot[e^{3\theta_2\tan\varphi_c}(3\tan\varphi_c\cos\theta^*-\sin\theta^*)+\sin(\theta^*+\theta_2)-3\tan\varphi_c\cos(\theta^*+\theta_2)]$$

$$-\frac{\gamma_c B^3}{24\sin^3\theta_1}(\tan\psi\sin\theta_1-\cos\theta_1+e^{\theta_1\tan\varphi_{comp}})^3\cdot(-\cos^2\theta^*\cot\theta_2+\sin\theta^*\cos\theta^*)^2 \quad (4.92)$$

Similar to the composite soil part the force F should be optimized with respect to θ_2. Differentiation of the above equation is presented in Appendix 2.

From Figure 4.15

$$W_w=\frac{B^2}{4}\gamma_{comp}\tan\psi \quad (4.93)$$

Considering equilibrium of the soil wedge ABC results

$$q_\gamma B=2P_\gamma\cos(\psi-\varphi_{comp})-W_w \quad (4.94)$$

Combining Equations 4.93 and 4.94 gives

$$q_\gamma=\frac{2P_\gamma}{B}\cos(\psi-\varphi_{comp})-\frac{B}{4}\gamma_{comp}\tan\psi \quad (4.95)$$

Rearranging of Equation 4.52 results

$$P_\gamma=\frac{F\cos\delta\frac{B}{2}[(a-1)\cdot(\tan\psi-\cot\theta_1)+a\frac{e^{\theta_1\tan\varphi comp}}{\sin\theta_1})]-\gamma_{comp}\frac{B^3}{24\sin^3\theta_1(9\tan^2\varphi_{comp}+1)}[e^{3\theta_1\tan\varphi comp}}{\cos(\psi-\varphi_{comp})\frac{B}{3}+\sin(\psi-\varphi_{comp})(\frac{B}{3}\tan\psi-\frac{B(\tan\psi-\cot\theta_1)}{2})}$$

$$-(3\tan\varphi_{comp}\sin\theta_1+\cos\theta_1)]-\gamma_{comp}\frac{B^3(\tan\psi-\cot\theta_1)}{48} \quad (4.96)$$

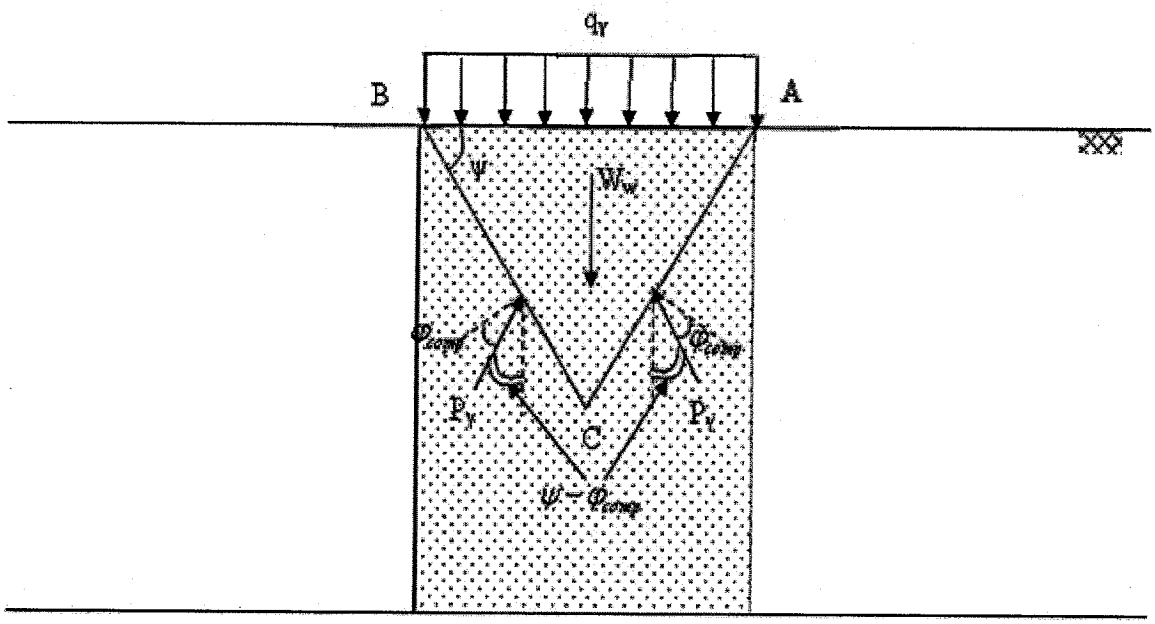

Figure 4.15 Free body diagram of the cone section.

Substituting Equation 4.96 into 4.95 gives

$$q_\gamma = \frac{1}{2}\gamma_{comp} \cdot B[2\cos(\psi - \varphi_{comp}) \frac{\frac{F}{\gamma_{comp} B^2}\cos\delta[(a-1)\cdot(\tan\psi - \cot\theta_1) + a\frac{e^{\theta_1 \tan\varphi_{comp}}}{\sin\theta_1})]}{\cos(\psi - \varphi_{comp})\frac{1}{3} + \sin(\psi - \varphi_{comp})(\frac{1}{3}\tan\psi - \frac{\tan\psi - \cot\theta_1}{2})}$$

$$- \frac{1}{12\sin^3\theta_1(9\tan^2\varphi_{comp} + 1)}[e^{3\theta_1 \tan\varphi_{comp}} - (3\tan\varphi_{comp}\sin\theta_1 + \cos\theta_1)] - \frac{(\tan\psi - \cot\theta_1)}{24} - \frac{\tan\psi}{2}] \quad (4.97)$$

where $\frac{F}{B^2}$ is calculated by rearrangement to Equation 4.92

$$\frac{F}{B^2} = \gamma_c[\frac{\frac{\sin\theta^*\tan(90-\theta^*)\cos\varphi_c}{24\sin^3\theta_1\sin^3\theta_2}(e^{\theta_1\tan\varphi_{comp}} + \tan\psi\sin\theta_1 - \cos\theta_1)^3\cdot(-\cos\theta^*\cos\theta_2 + \sin\theta^*\sin\theta_2}{\frac{1}{2\sin\theta_1}(e^{\theta_1\tan\varphi_{comp}} + \tan\psi\sin\theta_1 - \cos\theta_1)}$$

$$\frac{+\cos\theta^* e^{\theta_2\tan\varphi_{c2}})^2(\frac{1}{2}\cos\theta^*\cos\theta_2 - \frac{1}{2}\sin\theta_2\sin\theta^* + \cos\theta^* e^{\theta_2\tan\varphi_{c2}})}{[\sin\delta(-\cos^2\theta^*\cot\theta_2 + \sin\theta^*\cos\theta^*) + \cos\delta(a + \sin\theta^*\cos\theta^*\cot\theta_2 - \sin^2\theta^*)]}$$

$$+ \frac{\cos^3\theta^*}{24\sin^3\theta_2\sin^3\theta_1(9\tan^2\varphi_c + 1)}(\tan\psi\sin\theta_1 - \cos\theta_1 + e^{\theta_1\tan\varphi_{comp}})^3$$

$$\cdot[e^{3\theta_2\tan\varphi_c}(3\tan\varphi_c\cos\theta^* - \sin\theta^*) + \sin(\theta^* + \theta_2) - 3\tan\varphi_c\cos(\theta^* + \theta_2)]$$

$$- \frac{1}{24\sin^3\theta_1}(\tan\psi\sin\theta_1 - \cos\theta_1 + e^{\theta_1\tan\varphi_{comp}})^3\cdot(-\cos^2\theta^*\cot\theta_2 + \sin\theta^*\cos\theta^*)^2 \quad (4.98)$$

If Equation 4.97 is written as

$$q_\gamma = \frac{1}{2}\gamma_{comp}\cdot B\cdot N_\gamma \quad (4.99)$$

Then

$$N_\gamma = 2\cos(\psi-\varphi_{comp})\frac{\frac{F}{\gamma_{comp}B^2}\cos\delta[(a-1)\cdot(\tan\psi-\cot\theta_1)+a\frac{e^{\theta_1\tan\varphi_{comp}}}{\sin\theta_1})]}{\cos(\psi-\varphi_{comp})\frac{1}{3}+\sin(\psi-\varphi_{comp})(\frac{1}{3}\tan\psi-\frac{\tan\psi-\cot\theta_1}{2})}$$

$$-\frac{1}{12\sin^3\theta_1(9\tan^2\varphi_{comp}+1)}[e^{3\theta_1\tan\varphi_{comp}}-(3\tan\varphi_{comp}\sin\theta_1+\cos\theta_1)]-\frac{(\tan\psi-\cot\theta_1)}{24}-\frac{\tan\psi}{2} \quad (4.100)$$

Equilibrium equations were written to determine the bearing capacity due to surcharge and cohesion, q, for the composite soil and soft soil sections separately. The two equations will be combined at the end of calculation.

For the composite soil section, free body diagram in Figure 4.16 is subject to the following forces:

1. Passive force P'.
2. Cohesive force per unit area along AC.
3. Passive force F'.
4. Cohesive force per unit area along arc CH.
5. The frictional resisting force along the arc CH.
6. Cohesive force per unit area along AH.

Taking moment of all the forces around point O_1 results

$$\Sigma M_{O_1}=0\rightarrow P'[\cos(\psi-\varphi_{comp})\frac{B}{4}+\sin(\psi-\varphi_{comp})(\frac{B}{4}\tan\psi-y_1)]$$

$$+c_{comp}ACy_1\cos\psi=F'\cos\delta(m\cdot AH-y_1)+\frac{c_{comp}}{2\tan\varphi_{comp}}(r_1^2-r_o^2) \quad (4.101)$$

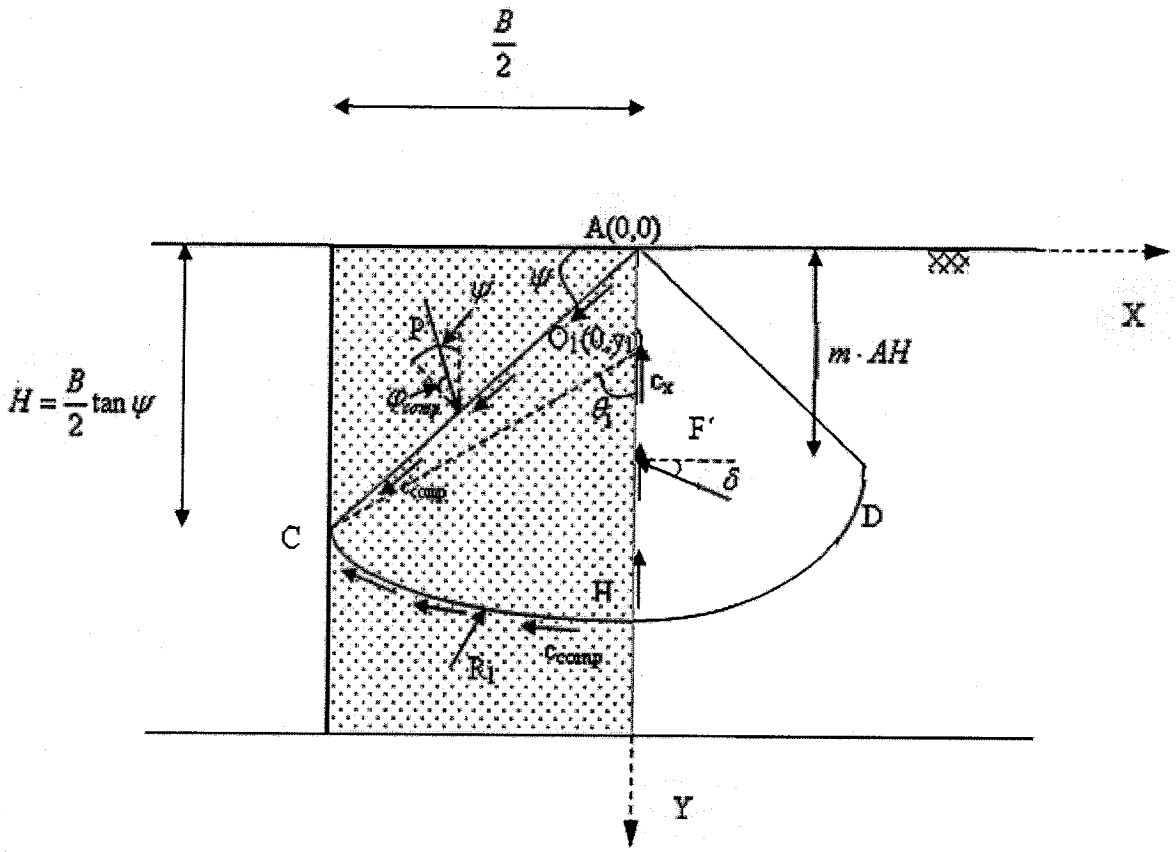

Figure 4.16 External forces acting on the composite soil section ($\phi \neq 0$, $\gamma = 0$, $q \neq 0$, $c \neq 0$).

Substituting Equations 4.38, 4.40, 4.41, 4.45 and 4.51 into 4.101 results

$$P'[\cos(\psi-\varphi_{comp})\frac{1}{4}+\frac{1}{2}\sin(\psi-\varphi_{comp})(\frac{-\tan\psi}{2}+\cot\theta_1)]+c_{comp}\frac{B(\tan\psi-\cot\theta_1)}{4}=\frac{F'\cos\delta}{2}$$

$$\cdot[m\frac{1}{\sin\theta_1}(\tan\psi\sin\theta_1-\cos\theta_1+e^{\theta_1\tan\varphi_{comp}})-(\tan\psi-\cot\theta_1)]+\frac{c_{comp}B}{8\sin^2\theta_1\tan\varphi_{comp}}(e^{2\theta_1\tan\varphi_{comp}}-1) \tag{4.102}$$

or

$$F'=\frac{P'[\cos(\psi-\varphi_{comp})\frac{1}{4}+\frac{1}{2}\sin(\psi-\varphi_{comp})(\frac{-\tan\psi}{2}+\cot\theta_1)]+c_{comp}\frac{B(\tan\psi-\cot\theta_1)}{4}}{\frac{B\cos\delta}{2}[m\frac{1}{\sin\theta_1}(\tan\psi\sin\theta_1-\cos\theta_1+e^{\theta_1\tan\varphi_{comp}})-(\tan\psi-\cot\theta_1)]}$$

$$-\frac{\frac{c_{comp}B}{8\sin^2\theta_1\tan\varphi_{comp}}(e^{2\theta_1\tan\varphi_{comp}}-1)}{} \tag{4.103}$$

This equation was minimized in order to obtain the minimum value of q' (see Appendix 2).

Considering the soft soil section, the free body of this section (Figure 4.17) is subject to the following forces:

1. Stress q_2 due to the surcharge q and cohesion effect on Rankine zone.

   Soil located above the bottom of foundation as shown in Figure 4.18 is considered as surcharge in the model $q=\gamma D_f$. (Terzaghi 1943) So q_2, the resultant of stress on AD due to the surcharge q acting on the Rankine zone wedge, is determined as

$$q_2=q\tan(45+\frac{\varphi_c}{2})+\frac{c_c}{\sin(45-\frac{\varphi_c}{2})} \tag{4.104}$$

2. Cohesive force per unit area along AH.

3. Force F'.

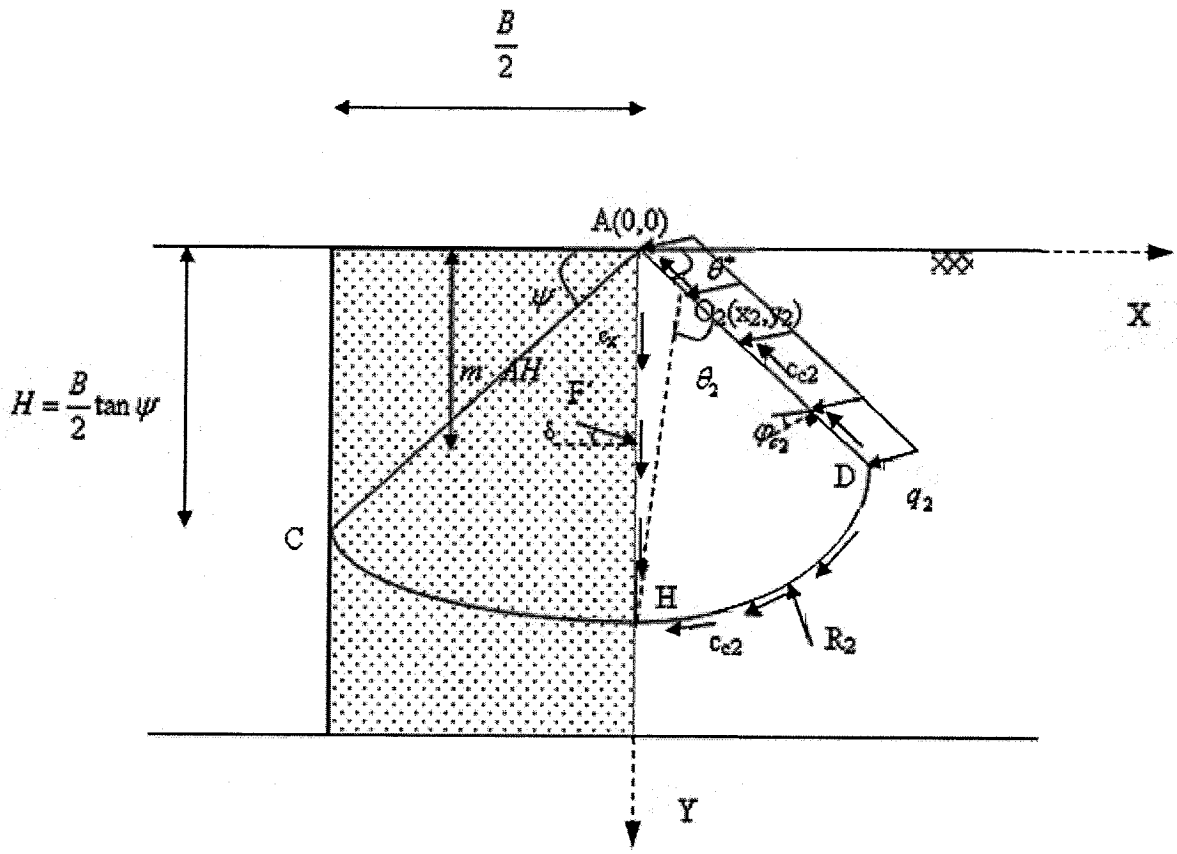

Figure 4.17 External forces acting on soft soil section ($\phi \neq 0$, $\gamma = 0$, $q \neq 0$, $c \neq 0$).

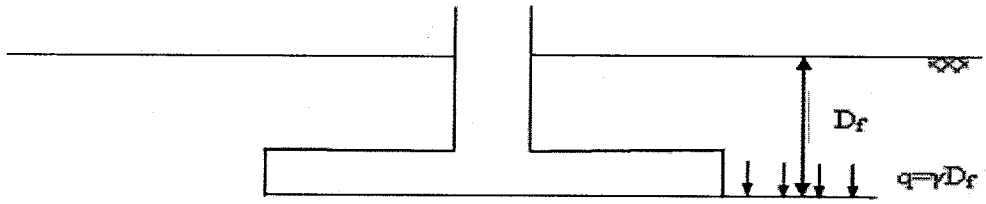

Figure 4.18 Assumed surcharge above the bottom of the foundation.

4. Cohesive force per unit area along arc *DH*.

5. The frictional resisting force R_2 along the arc *DH*.

6. Cohesive force per unit area along *AD*.

Taking moment of all the forces around point O_2 results

$$\Sigma M_{O_2} = 0 \rightarrow F'\cos\delta(m\cdot AH - y_2) + AH\cdot F'\sin\delta\cdot x_2 + c_x AH\cdot x_2 = \frac{q_2\cos\varphi_c}{2}(r_3{}^2 - AO_2{}^2)$$

$$+\frac{c_c}{2\tan\varphi_c}(r_3{}^2 - r_2{}^2) \qquad (4.105)$$

Combining Equations 4.51, 4.57, 4.58, 4.62, 4.86, 4.88, 4.104 and 4.105 gives

$$\frac{B^2\cos\varphi_c[q\cdot\tan(45+\frac{\varphi_c}{2}) + \frac{c_c}{\sin(45-\frac{\varphi_c}{2})}]}{8\sin^2\theta_1\sin^2\theta_2}(e^{\theta_1\tan\varphi_{comp}} + \tan\psi\sin\theta_1 - \cos\theta_1)^2[\cos^2\theta^* e^{2\theta_2\tan\varphi_c} - (-\cos\theta^*$$

$$\cdot\cos\theta_2 + \sin\theta^*\sin\theta_2)^2] + \frac{c_c}{2\tan\varphi_c}\cdot(e^{\theta_1\tan\varphi_{comp}} + \tan\psi\sin\theta_1 - \cos\theta_1)^2\frac{B^2\cos^2\theta^*}{4\sin^2\theta_1\sin^2\theta_2}\cdot(e^{2\theta_2\tan\varphi_c} - 1)$$

$$= \frac{B\cdot F'}{2\sin\theta_1}(\tan\psi\sin\theta_1 - \cos\theta_1 + e^{\theta_1\tan\varphi_{comp}})[\cos\delta(m + \sin\theta^*\cos\theta^*\cot\theta_2 - \sin^2\theta^*) + \sin\delta\cdot(-\cos^2\theta^*\cot\theta_2$$

$$+\sin\theta^*\cos\theta^*)] + c_x\frac{B^2}{4\sin^2\theta_1}(\tan\psi\sin\theta_1 - \cos\theta_1 + e^{\theta_1\tan\varphi_{comp}})^2(\sin\theta^*\cos\theta^* - \cos^2\theta^*\cot\theta_2) \qquad (4.106)$$

or

$$F' = \frac{\dfrac{B^2\cos\varphi_c[q\cdot\tan(45+\frac{\varphi_c}{2}) + \frac{c_c}{\sin(45-\frac{\varphi_c}{2})}]}{8\sin^2\theta_1\sin^2\theta_2}(e^{\theta_1\tan\varphi_{comp}} + \tan\psi\sin\theta_1 - \cos\theta_1)^2[\cos^2\theta^* e^{2\theta_2\tan\varphi c} - (-\cos\theta^*}{\dfrac{B}{2\sin\theta_1}(\tan\psi\sin\theta_1 - \cos\theta_1 + e^{\theta_1\tan\varphi_{comp}})}$$

$$\cdot\cos\theta_2 + \sin\theta^*\sin\theta_2)^2] + \frac{c_c}{2\tan\varphi_c}\cdot(e^{\theta_1\tan\varphi_{comp}} + \tan\psi\sin\theta_1 - \cos\theta_1)^2\frac{B^2\cos^2\theta^*}{4\sin^2\theta_1\sin^2\theta_2}\cdot(e^{2\theta_2\tan\varphi c} - 1)$$

$$[\cos\delta(m + \sin\theta^*\cos\theta^*\cot\theta_2 - \sin^2\theta^*) + \sin\delta\cdot(-\cos^2\theta^*\cot\theta_2 + \sin\theta^*\cos\theta^*)]$$

$$-c_x \frac{B^2}{4\sin^2\theta_1}(\tan\psi\sin\theta_1 - \cos\theta_1 + e^{\theta_1\tan\varphi_{comp}})^2(\sin\theta^*\cos\theta^* - \cos^2\theta^*\cot\theta_2) \tag{4.107}$$

Differentiation of above equation is presented in Appendix 2.

From Figure 4.19, the following Equation can be driven

$$q' = \frac{2P'}{B}\cos(\psi - \varphi_{comp}) + c_{comp}\tan\psi \tag{4.108}$$

Rearranging of Equation 4.102 results

$$P' = \frac{\frac{F'\cos\delta}{2}[m\frac{1}{\sin\theta_1}(\tan\psi\sin\theta_1 - \cos\theta_1 + e^{\theta_1\tan\varphi_{comp}}) - (\tan\psi - \cot\theta_1)]}{[\cos(\psi - \varphi_{comp})\frac{1}{4} + \frac{1}{2}\sin(\psi - \varphi_{comp})(\frac{-\tan\psi}{2} + \cot\theta_1)]}$$

$$+\frac{\frac{c_{comp}B}{8\sin^2\theta_1\tan\varphi_{comp}}(e^{2\theta_1\tan\varphi_{comp}} - 1) - c_{comp}\frac{B(\tan\psi - \cot\theta_1)}{4}}{} \tag{4.109}$$

From Equation 4.107 let

$$F' = A\cdot q + D\cdot c_c \tag{4.110}$$

where

$$A = \frac{\frac{B\cos\varphi_c\tan(45+\frac{\varphi_c}{2})}{8\sin^2\theta_1\sin^2\theta_2}(e^{\theta_1\tan\varphi_{equ.}} + \tan\psi\sin\theta_1 - \cos\theta_1)^2[\cos^2\theta^* e^{2\theta_2\tan\varphi c} - (-\cos\theta^*}{\frac{1}{2\sin\theta_1}(\tan\psi\sin\theta_1 - \cos\theta_1 + e^{\theta_1\tan\varphi_{comp}})}$$

$$\frac{\cdot\cos\theta_2 + \sin\theta^*\sin\theta_2)^2]}{[\cos\delta(m + \sin\theta^*\cos\theta^*\cot\theta_2 - \sin^2\theta^*) + \sin\delta\cdot(-\cos^2\theta^*\cot\theta_2 + \sin\theta^*\cos\theta^*)]}$$

and

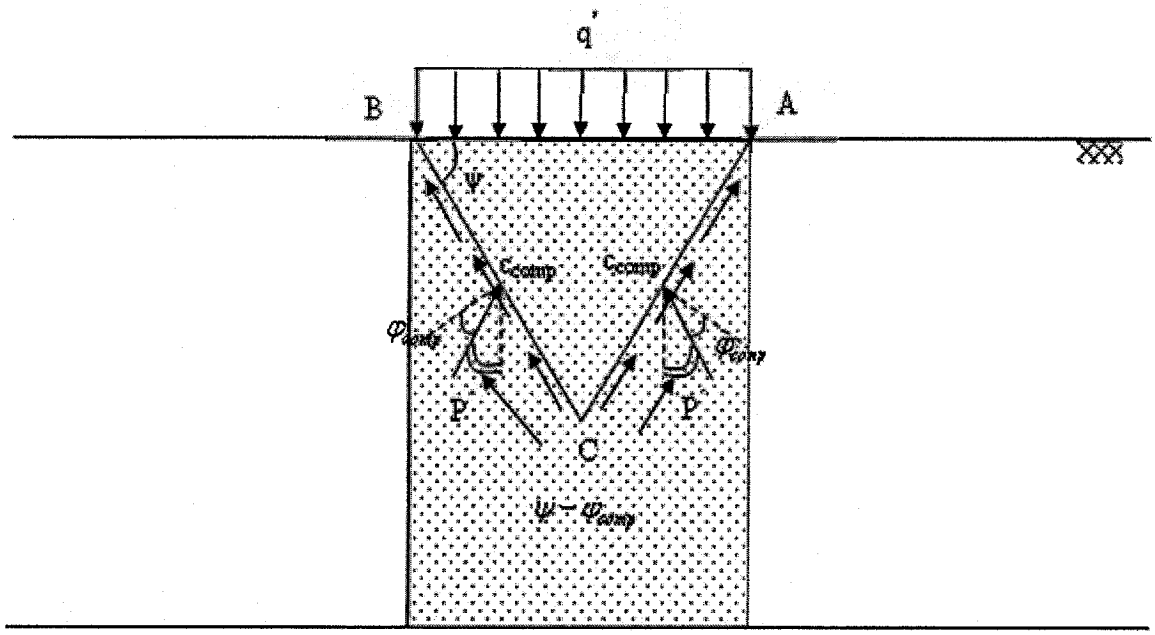

Figure 4.19 Forces acting on the triangular zone.

$$D=\frac{\dfrac{\dfrac{B\cdot\cos\varphi_c}{\sin(45-\frac{\varphi_c}{2})}}{8\sin^2\theta_1\sin^2\theta_2}(e^{\theta_1\tan\varphi_{equ.}}+\tan\psi\sin\theta_1-\cos\theta_1)^2[\cos^2\theta^* e^{2\theta_2\tan\varphi c}-(-\cos\theta^*\cdot\cos\theta_2+\sin\theta^*\sin\theta_2)^2]}{\dfrac{1}{2\sin\theta_1}(\tan\psi\sin\theta_1-\cos\theta_1+e^{\theta_1\tan\varphi_{comp}})}$$

$$+\frac{\dfrac{1}{2\tan\varphi_c}\cdot(e^{\theta_1\tan\varphi_{equ.}}+\tan\psi\sin\theta_1-\cos\theta_1)^2\dfrac{B\cos^2\theta^*}{4\sin^2\theta_1\sin^2\theta_2}\cdot(e^{2\theta_2\tan\varphi_c}-1)}{[\cos\delta(m+\sin\theta^*\cos\theta^*\cot\theta_2-\sin^2\theta^*)+\sin\delta\cdot(-\cos^2\theta^*\cot\theta_2+\sin\theta^*\cos\theta^*)]}$$

$$-\frac{c_x\cdot B}{4c_c\sin^2\theta_1}(\tan\psi\sin\theta_1-\cos\theta_1+e^{\theta_1\tan\varphi_{comp}})^2(\sin\theta^*\cos\theta^*-\cos^2\theta^*\cot\theta_2)$$

Combining Equations 4.108, 4.109 and 4.110 yields

$$q^{'}=\cos(\psi-\varphi_{comp})\frac{\dfrac{A\cdot q}{B}\cdot\cos\delta[m\dfrac{1}{\sin\theta_1}(\tan\psi\sin\theta_1-\cos\theta_1+e^{\theta_1\tan\varphi_{comp}})-(\tan\psi-\cot\theta_1)]}{[\cos(\psi-\varphi_{comp})\dfrac{1}{4}+\dfrac{1}{2}\sin(\psi-\varphi_{comp})(\dfrac{-\tan\psi}{2}+\cot\theta_1)]}$$

$$+c_{comp}\tan\psi+\cos(\psi-\varphi_{comp})\frac{\dfrac{D\cdot c_c}{B}\cdot\cos\delta[m\dfrac{1}{\sin\theta_1}(\tan\psi\sin\theta_1-\cos\theta_1+e^{\theta_1\tan\varphi_{comp}})-(\tan\psi-\cot\theta_1)]}{[\cos(\psi-\varphi_{comp})\dfrac{1}{4}+\dfrac{1}{2}\sin(\psi-\varphi_{comp})(\dfrac{-\tan\psi}{2}+\cot\theta_1)]}$$

$$+\frac{c_{comp}}{4\sin^2\theta_1\tan\varphi_{comp}}(e^{2\theta_1\tan\varphi_{comp}}-1)-c_{comp}\frac{\tan\psi-\cot\theta_1}{2} \qquad (4.111)$$

The ultimate load per unit area is given as

$$q'=qN_q+c_{comp}N_c \qquad (4.112)$$

$$N_q=\cos(\psi-\varphi_{comp})\frac{\dfrac{A}{B}\cdot\cos\delta[m\dfrac{1}{\sin\theta_1}(\tan\psi\sin\theta_1-\cos\theta_1+e^{\theta_1\tan\varphi_{comp}})-(\tan\psi-\cot\theta_1)]}{[\cos(\psi-\varphi_{comp})\dfrac{1}{4}+\dfrac{1}{2}\sin(\psi-\varphi_{comp})(\dfrac{-\tan\psi}{2}+\cot\theta_1)]} \qquad (4.113)$$

and

$$N_c = \tan\psi + \cos(\psi - \varphi_{comp}) \frac{\frac{D \cdot c_c}{B \cdot c_{comp}} \cdot \cos\delta [m \frac{1}{\sin\theta_1} (\tan\psi \sin\theta_1 - \cos\theta_1 + e^{\theta_1 \tan\varphi_{comp}}) - (\tan\psi - \cot\theta_1)]}{[\cos(\psi - \varphi_{comp}) \frac{1}{4} + \frac{1}{2} \sin(\psi - \varphi_{comp})(\frac{-\tan\psi}{2} + \cot\theta_1)]}$$

$$+ \frac{\frac{1}{4\sin^2\theta_1 \tan\varphi_{comp}} (e^{2\theta_1 \tan\varphi_{comp}} - 1) - c_{comp} \frac{\tan\psi - \cot\theta_1}{2}}{} \qquad (4.114)$$

In this investigation, the relationship between the cone angle, ψ, and angle of logspiral is developed; from Figure 4.20

$$\angle ACO_1 = 180° - (180° - 2\psi) - (90° + \varphi) = 2\psi - \varphi - 90° \qquad (4.115)$$

From triangle ACO_1

$$\psi = \theta_1 + \varphi \qquad (4.116)$$

The angle θ^* is taken as $45^\circ - \frac{\varphi}{2}$ as it represents the Rankine passive pressure zone. The value of δ was considered equal to ϕ_c as it is located on the slip line of first logspiral and c_x equal to c_{comp}. This consideration was future examined by finite element modeling of group of stone columns and the same observation was seen. In order to find the location of the line of action of the force F for the cases of q_γ and q' the location was change from 1/2 to 2/3 of the height AH. The difference of changing this length was observed to be less than 5%. Utilizing the results of the numerical model, it was noted that the length of action of F was *2/3AH* for the case q_γ and *1/2AH* for q'. These values were used in the theoretical model.

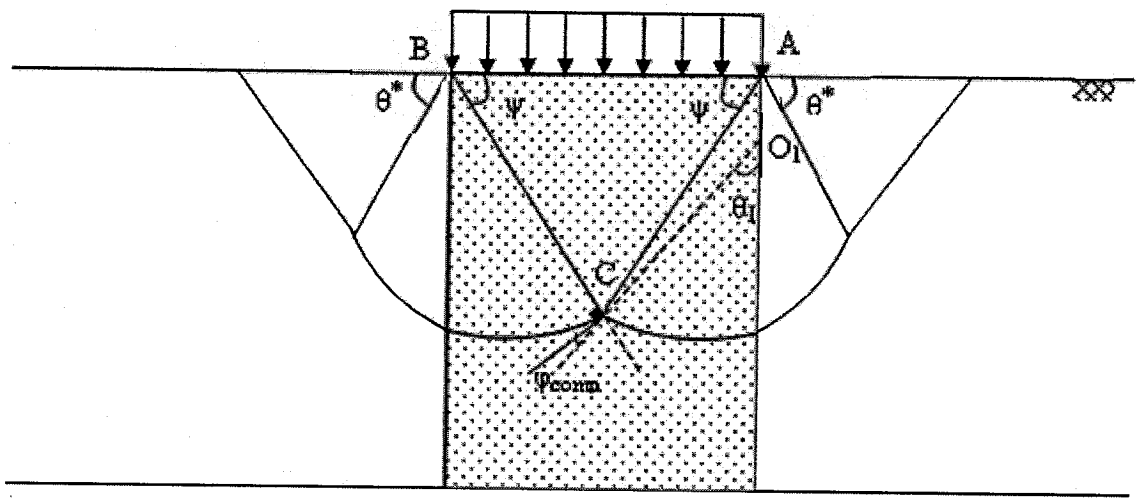

Figure 4.20 Determination of cone angle.

4.3.2 Ultimate Bearing Capacity

In order to calculate ultimate load for q_γ and q' components, the passive force F should be optimized to get the lowest value of bearing capacity according to value of the angle θ of the logspiral curve. The procedure was applied first for q_γ and then was continued to calculate q'. First, an arbitrary value of the ultimate load per unit area, q_γ was assumed. The angle of the logspiral of the composite soil part was then determined by $\frac{\partial F}{\partial \theta_1} = 0$ and by applying the Newton Raphson numerical technique. The angle of cone was calculated using the Equation 4.116. The logspiral angle for the soft soil part was also achieved using similar procedure and by $\frac{\partial F}{\partial \theta_2} = 0$. Finally, if the passive forces F from the first and second optimizations were equal then the value of q_γ was considered the desired amount otherwise the process continued by trial and error, by assuming a value of q_γ, then calculate the value of F. Agreement can be reached when, two consecutive values of F becomes equal or having a difference of less than 0.01.

Same procedure was applied for the evaluation of q' and consequently, N_γ, N_q and N_c. The ultimate bearing capacity is given by

$$q_u = q_\gamma + q' \tag{4.117}$$

In order to facilitate this procedure, the mathematical formulations were coded in a computer program which was written utilizing Visual Basic Version 6. The program G-STColumn was developed for easy application of the extensive numerical calculations of the theory. The complete list of the code is given in Appendix 3. The program predicts not only the bearing capacity q_γ and q' and the ultimate bearing capacity q_u but also the

angles of the cone and the logspirals. The program displays the final results at the end of the calculation. The wide range of input data, foundation weight and depth, friction angle, cohesion and unit weight of composite and soft soil were incorporated in the program.

4.3.3 Design Charts

Based on the results of the analytical model developed in this section, design theory is presented and design charts are introduced for the values of N_γ, N_q and N_c. These charts are presented in Figures 4.21 to 4.31. In order to use these charts, the composite values of γ, ϕ and c should be first obtained from Equations 4.25, 4.26 and 4.35. These figures are developed for $\frac{c_{comp}}{c_c} = 0.2$, 0.4, 0.6 and 0.8 and for $\frac{\gamma_{comp}}{\gamma_c} = 1$, 1.2, 1.4, 1.6, 1.8 and 2. The parameters used in the charts cover a wide range of practical cases. Interpolation should be used for intermediate value. The ultimate bearing capacity is then calculated as

$$q_u = \frac{1}{2}\gamma_{comp} B N_\gamma + q N_q + c_{comp} N_c \qquad (4.118)$$

4.3.4 Extension of the Model for Uniform Soil

The theory developed herein for soil reinforced by stone columns, can be used for unreinforced homogenous soil. In this case, it is sufficient to use the cohesion and friction angle of homogenous soil for both composite and soft soil sections. Extension of the model for uniform soil case can be used as model validation and for the determination of the cone angle based of the logspiral minimization. The values of N_γ, N_q and N_c were calculated for ϕ between 15° and 40°. The results obtained from this study were compared with the values available in the literature.

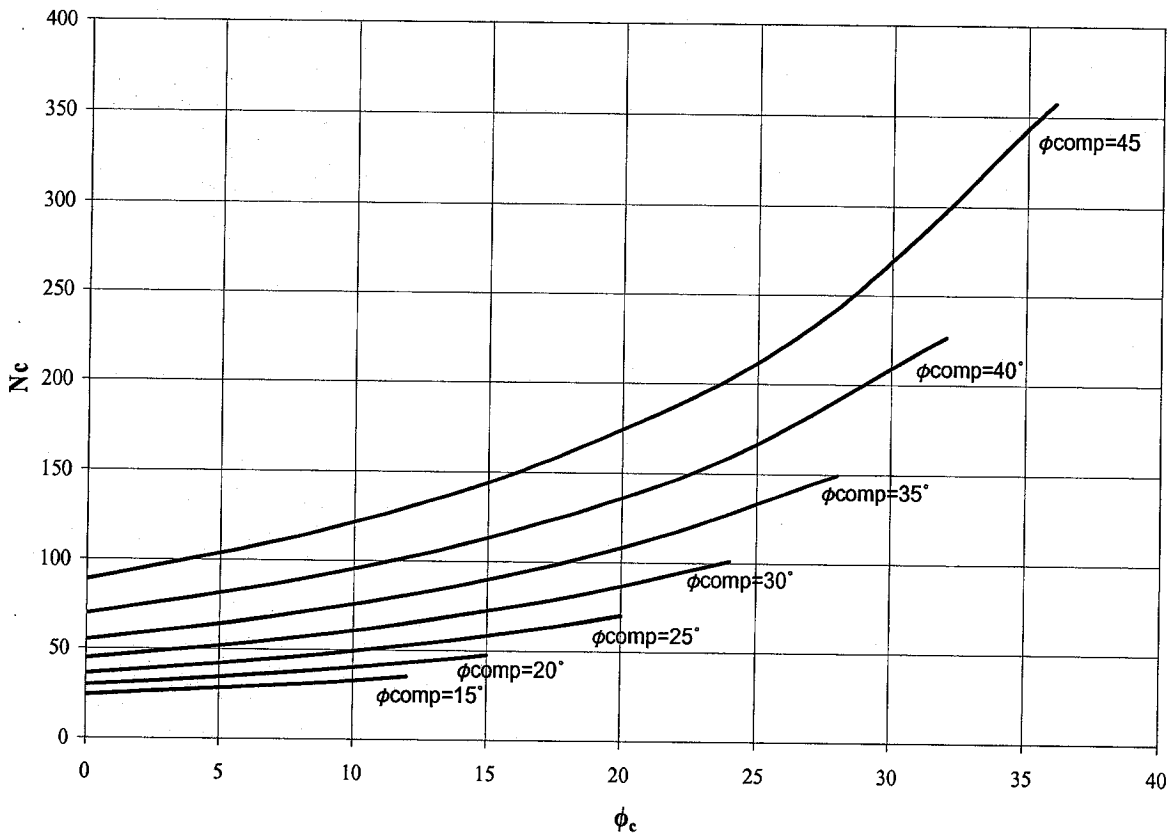

Figure 4.21 N_c vs. ϕ_{comp} - ϕ_c for $\frac{c_{comp}}{c_c}$=0.2.

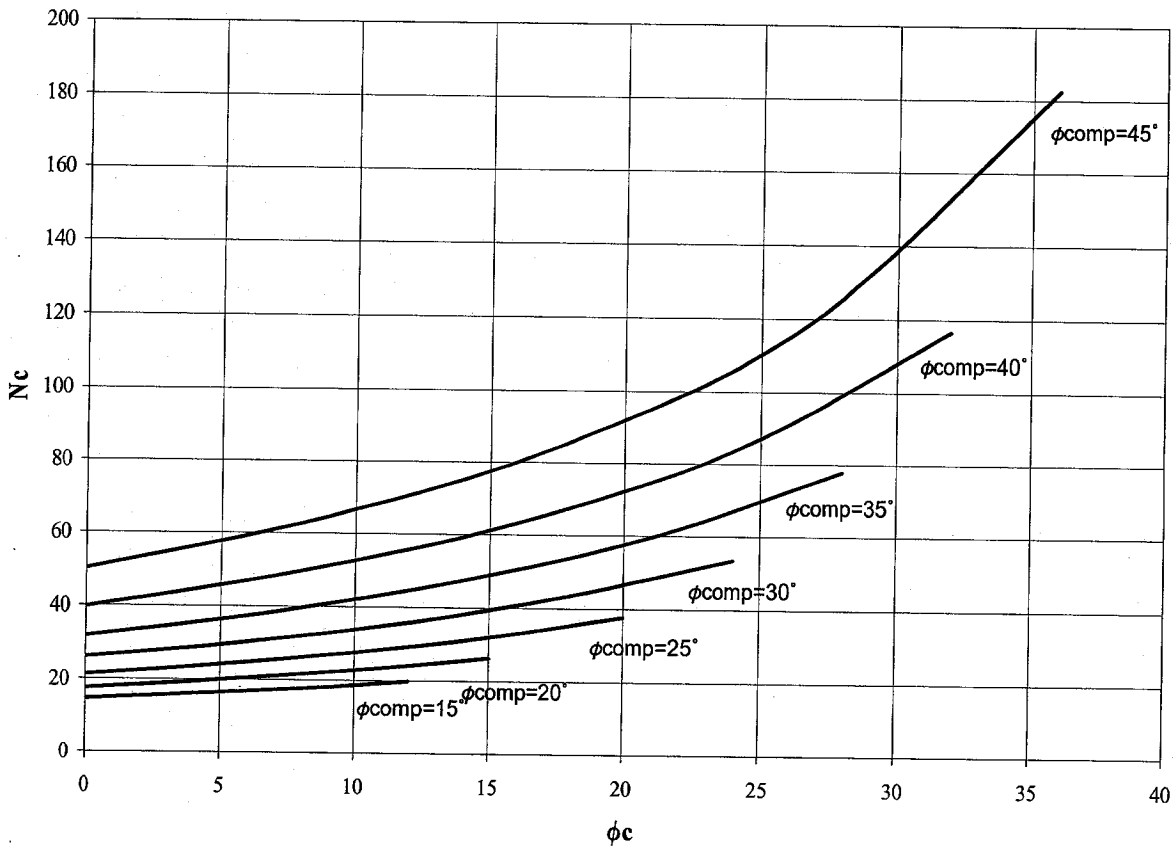

Figure 4.22 N_c vs. ϕ_{comp} - ϕ_c for $\frac{c_{comp}}{c_c}$ =0.4.

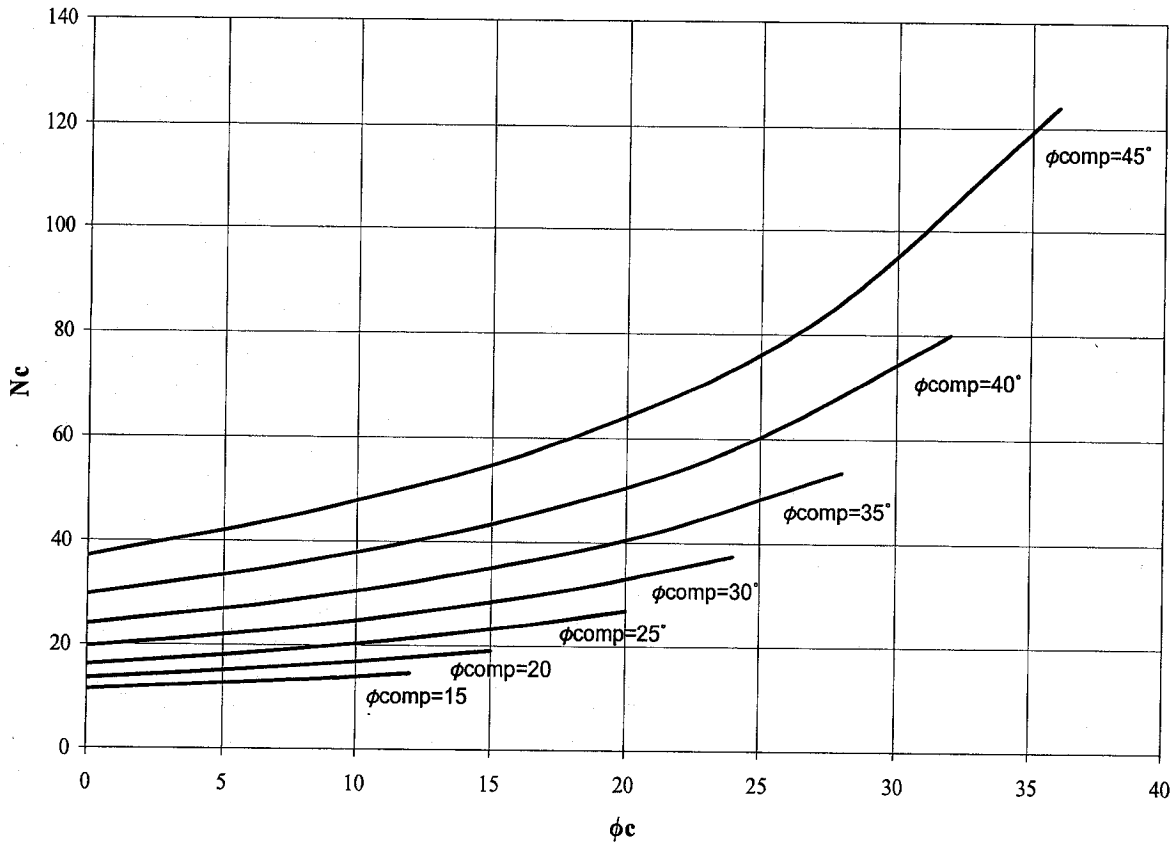

Figure 4.23 N_c vs. ϕ_{comp} - ϕ_c for $\frac{c_{comp}}{c_c}$ =0.6.

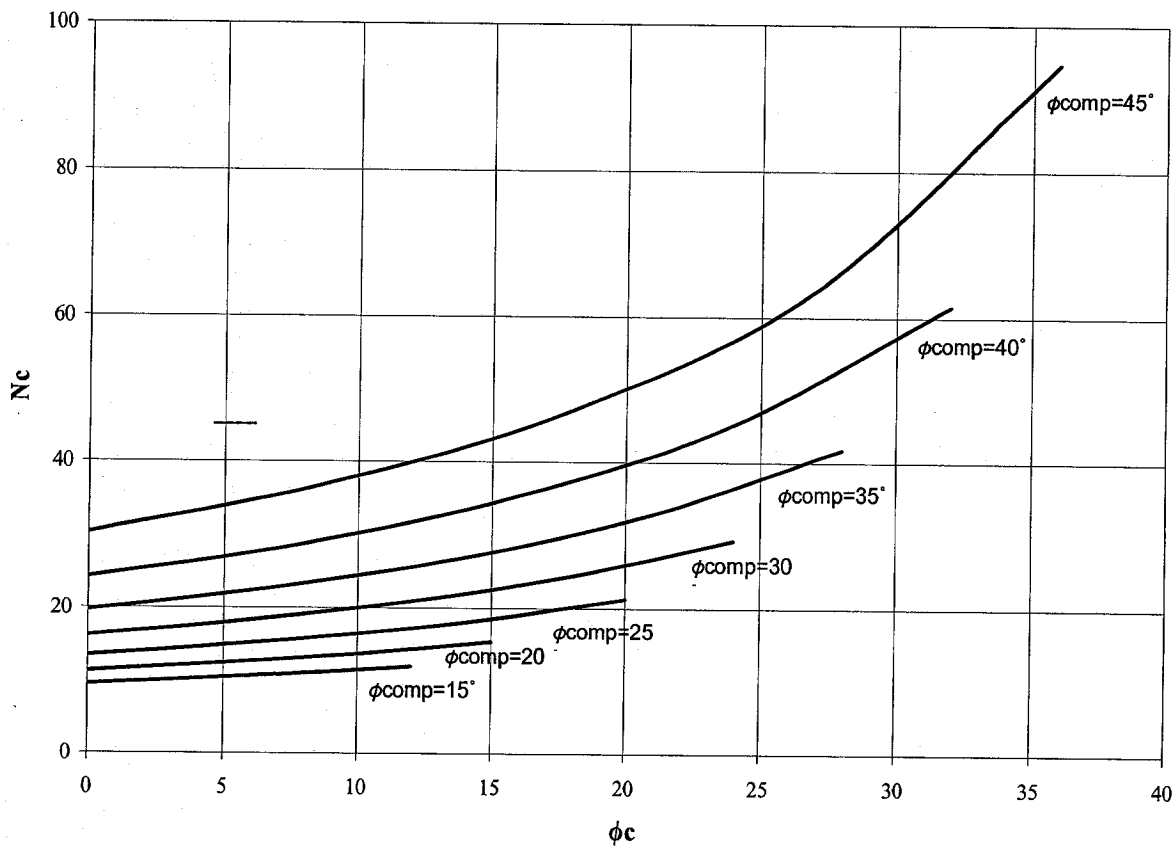

Figure 4.24 N_c vs. ϕ_{comp} - ϕ_c for $\frac{c_{comp}}{c_c}$=0.8.

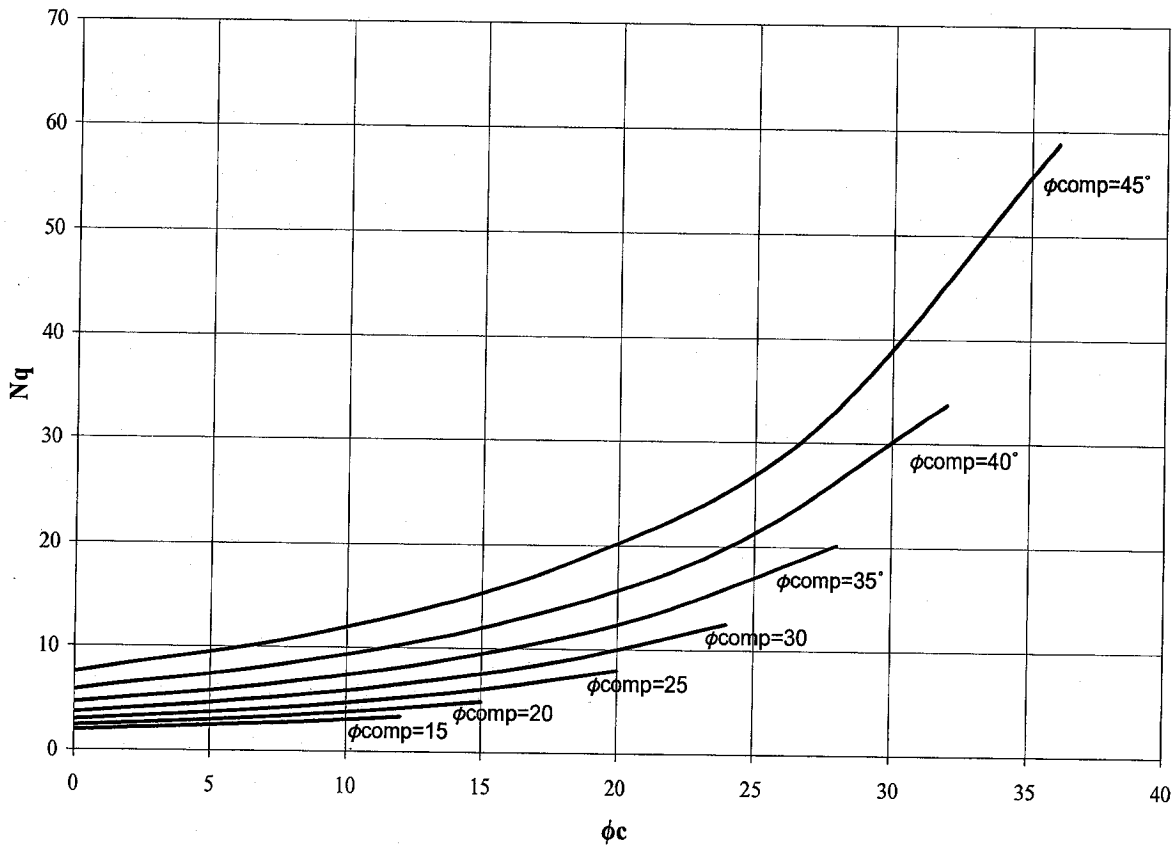

Figure 4.25 N_q vs. ϕ_{comp} - ϕ_c.

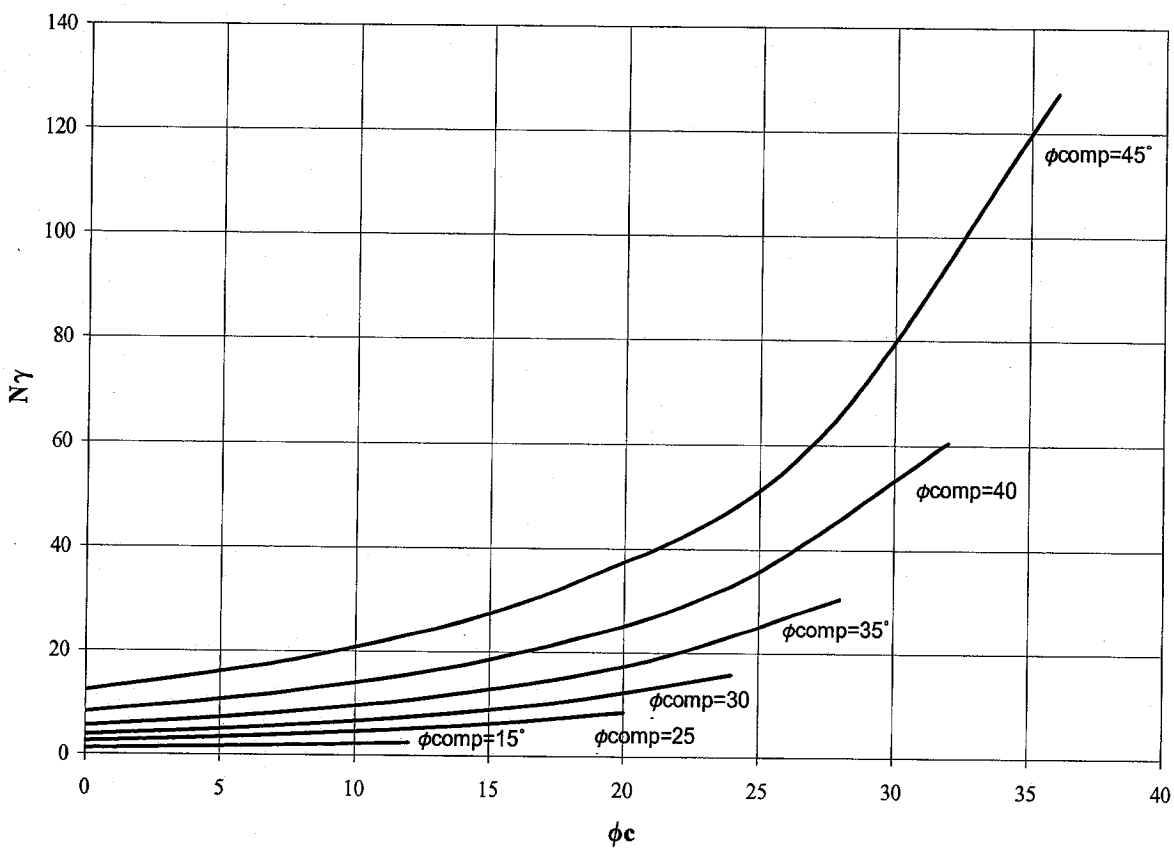

Figure 4.26 N_γ vs. ϕ_{comp} - ϕ_c for $\frac{\gamma_{comp}}{\gamma_c}$=1.

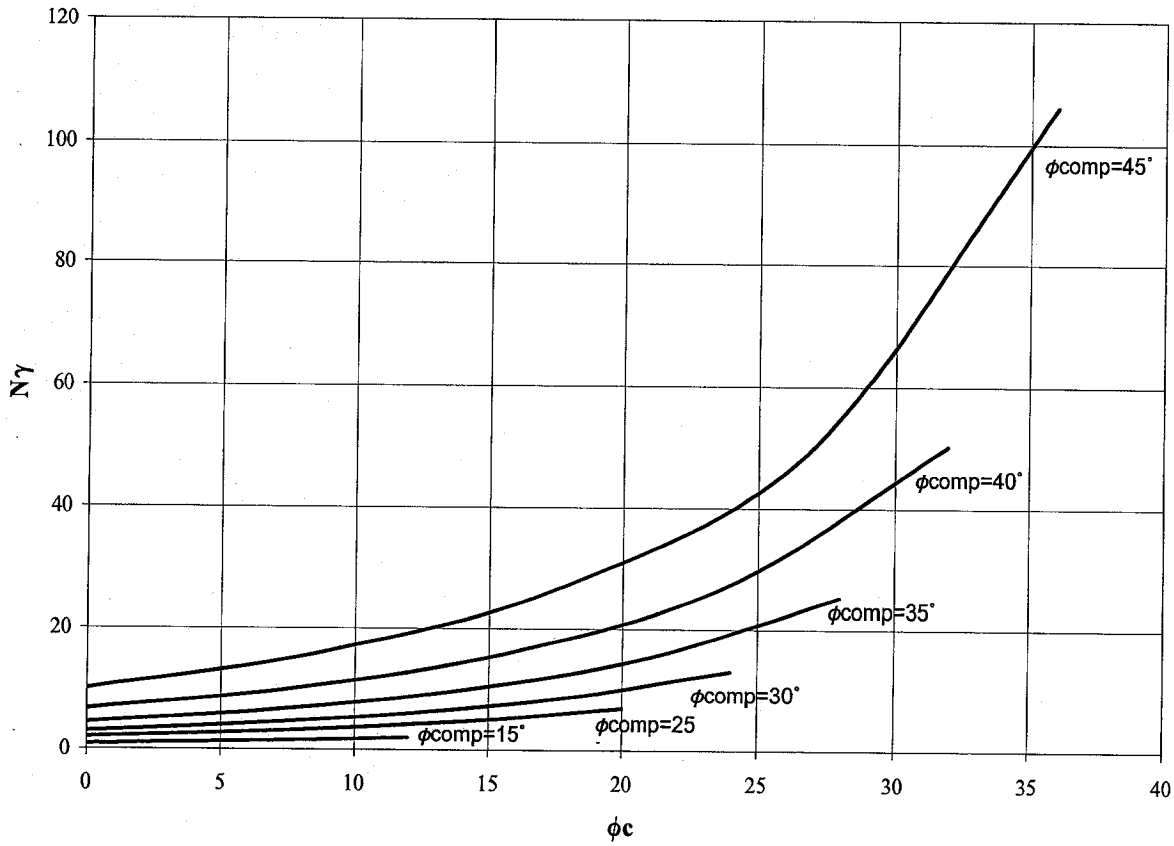

Figure 4.27 N_γ vs. ϕ_{comp} - ϕ_c for $\frac{\gamma_{comp}}{\gamma_c}$ =1.2.

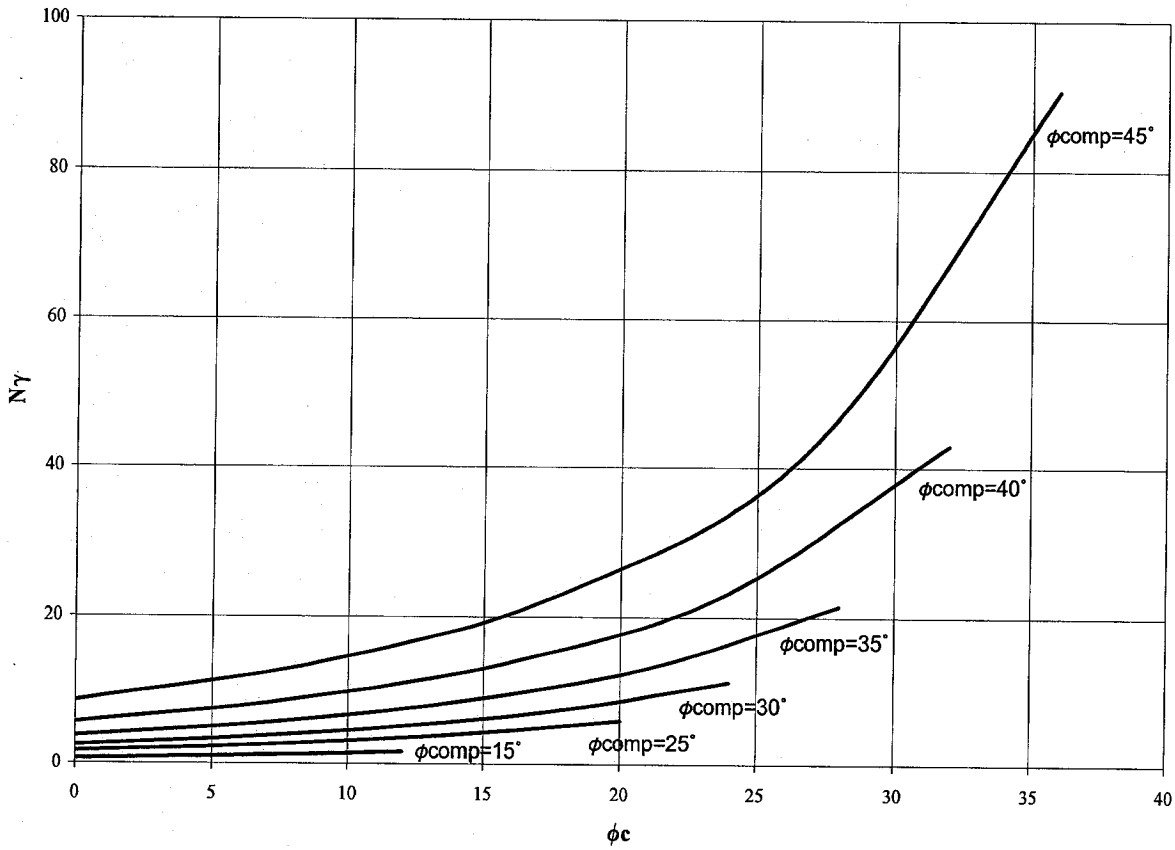

Figure 4.28 N_γ vs. ϕ_{comp} - ϕ_c for $\frac{\gamma_{comp}}{\gamma_c}$=1.4.

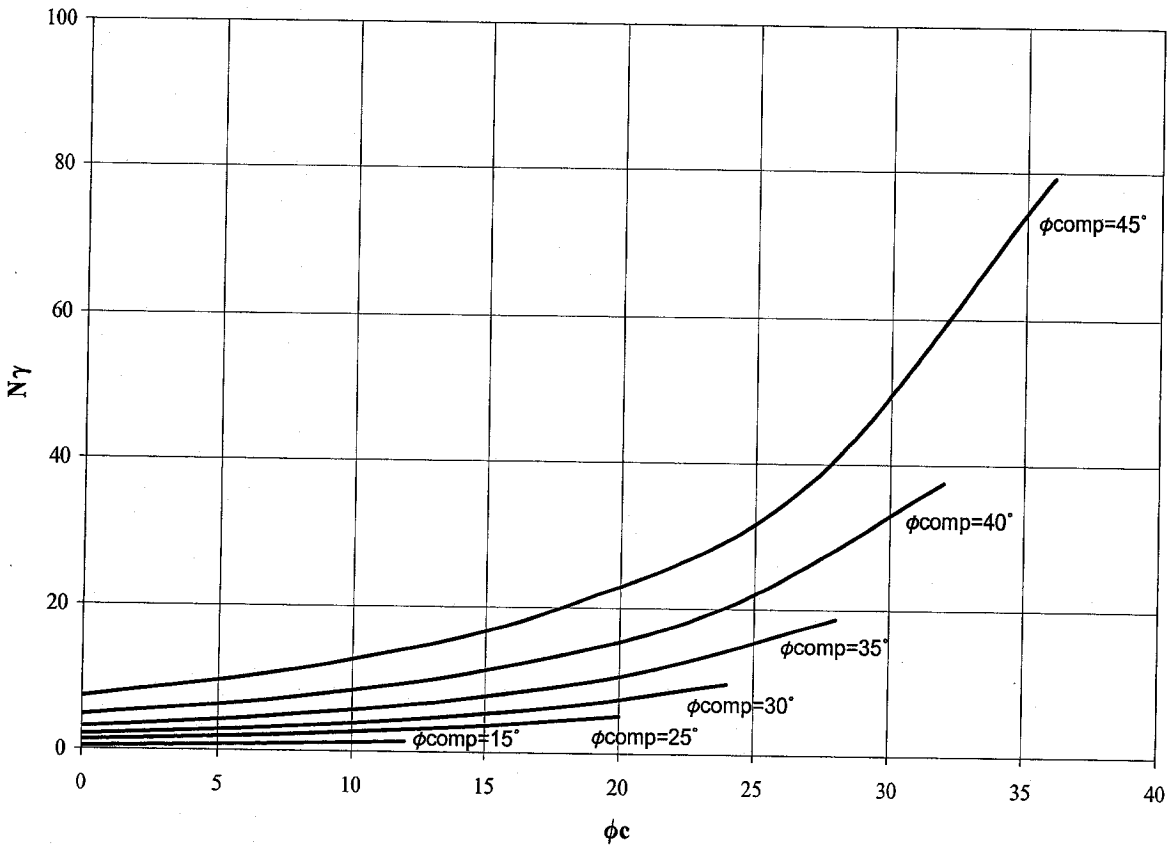

Figure 4.29 N_γ vs. ϕ_{comp} - ϕ_c for $\frac{\gamma_{comp}}{\gamma_c}$ =1.6.

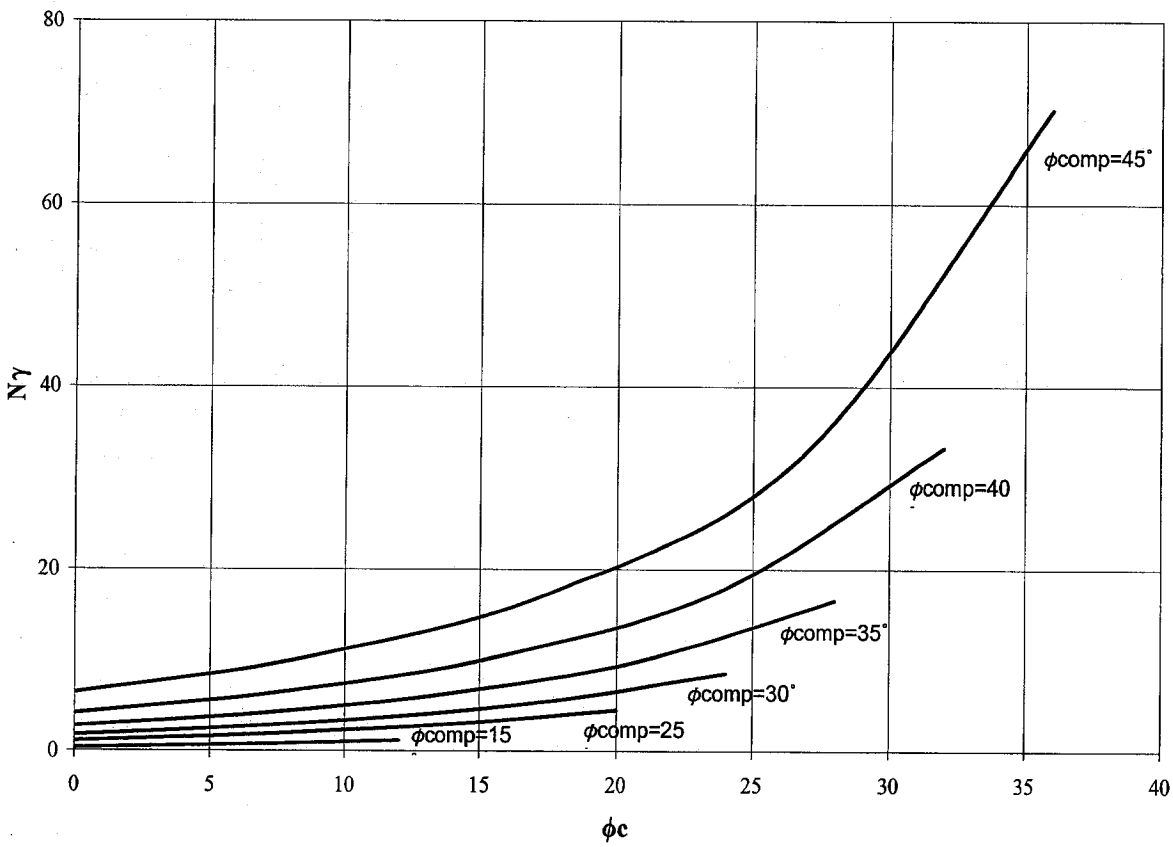

Figure 4.30 N_γ vs. ϕ_{comp} - ϕ_c for $\frac{\gamma_{comp}}{\gamma_c}$=1.8.

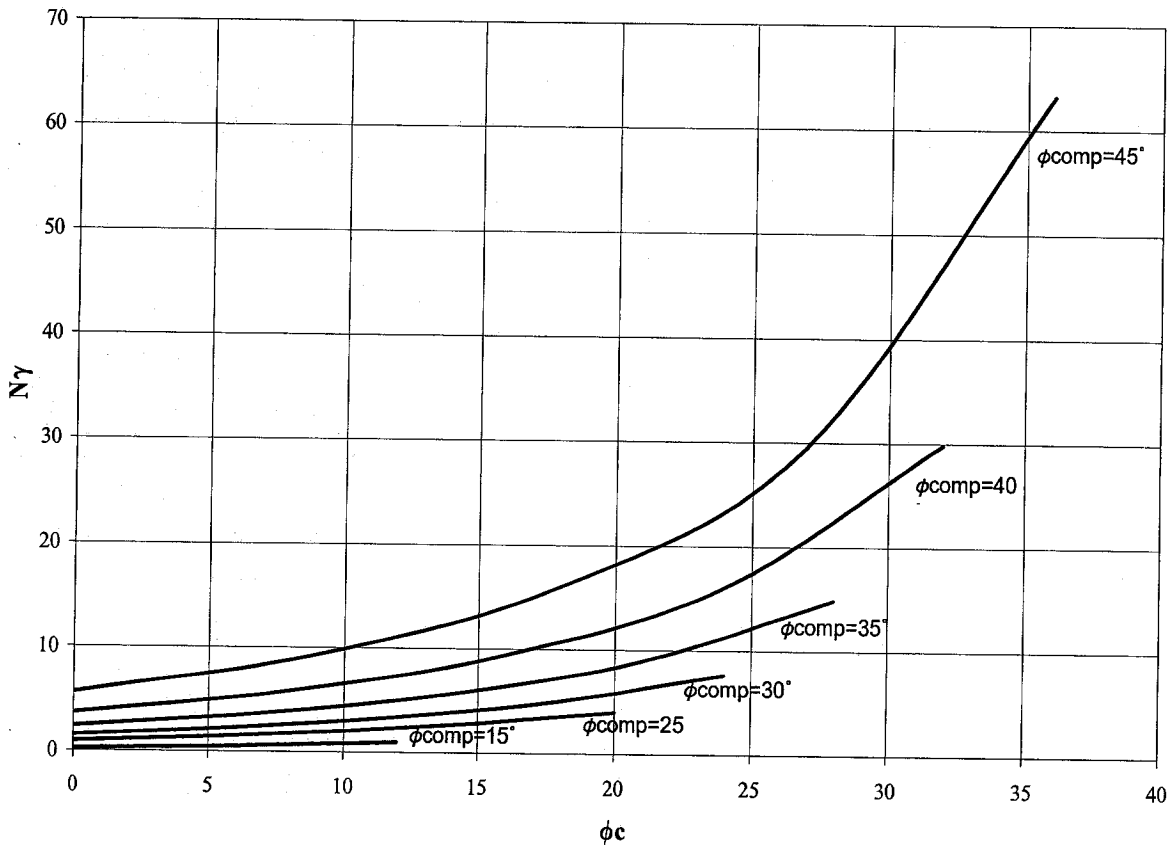

Figure 4.31 N_γ vs. ϕ_{comp} - ϕ_c for $\frac{\gamma_{comp}}{\gamma_c}$=2.

Tables 4.8 and 4.9 present the predicted values for N_c and N_q respectively. From this Table, it can be noted that close agreements were achieved. Furthermore, the proposed value of the cone angle was in good agreement with the angle $45^\circ + \frac{\varphi}{2}$ which was assumed for homogeneous soils by other researchers. This conclusion may imply that usage of $45^\circ + \frac{\varphi}{2}$ for the cone angle is reasonable for both N_c and N_q. For the case of N_γ(Table 4.10) the values calculated by the present study is higher than Vesic (1973) and Soubra (1999) and lower than Chen (1975). The value of the cone angle was determined to be slightly lower than the assumed value of $45^\circ + \frac{\varphi}{2}$.

4.3.5 Model Validation

The analytical model developed herein was validated using the available experimental data and the results of numerical model for the cases of general shear failure (Table 4.11). The numerical model was developed using the "PLAXIS" V8 program. Good agreement between the theoretical model and the two others was observed. The model was further compared with the theoretical method developed by Madhav and Vitkar (1978). Close examination of the method of Madhav and Vitkar (1978) shows that it gives higher ultimate bearing capacity comparing the proposed model and experimental and numerical results. This observation might be due to the nature of Madhav and Vitkar (1978) model which used limit analysis and is an upper bound technique.

Table 4.8 Bearing capacity factor N_c.

ϕ	This study	Vesic (1973)	Terzaghi (1943)	Soubra (1999)	Chen (1975)	ψ (this study)	ψ (45+ϕ/2)
15	10.96	10.98	12.86	10.99	10.98	52.5	52.5
16	11.62	11.63	13.68	11.65	11.63	53.0	53.0
17	12.34	12.34	14.60	12.36	12.34	53.5	53.5
18	13.08	13.10	15.12	13.13	13.11	54.0	54.0
19	13.92	13.93	16.57	13.96	13.94	54.5	54.5
20	14.82	14.83	17.69	14.86	14.84	55.0	55.0
21	15.79	15.82	18.92	15.85	15.82	55.5	55.5
22	16.88	16.88	20.27	16.92	16.89	56.0	56.0
23	18.02	18.05	21.75	18.09	18.05	56.5	56.5
24	19.30	19.32	23.36	19.37	19.33	57.0	57.0
25	20.71	20.72	25.13	20.77	20.73	57.5	57.5
26	22.24	22.25	27.09	22.32	22.26	58.0	58.0
27	23.93	23.94	29.24	24.01	23.95	58.5	58.5
28	25.80	25.80	31.61	25.88	25.81	59.0	59.0
29	27.86	27.86	34.24	27.95	27.87	59.5	59.5
30	30.11	30.14	37.16	30.24	30.15	60.0	60.0
31	32.67	32.67	40.41	32.79	32.68	60.5	60.5
32	35.46	35.49	44.04	35.62	35.50	61.0	61.0
33	38.60	38.64	48.09	38.79	38.65	61.4	61.5
34	46.13	42.16	52.64	42.34	42.18	62.0	62.0
35	46.12	46.12	57.75	46.33	46.14	62.5	62.5
36	50.55	50.59	63.53	50.82	50.50	63.0	63.0
37	55.69	55.63	70.01	55.91	55.65	63.5	63.5
38	61.36	61.35	77.50	61.68	61.37	64.0	64.0
39	67.87	67.87	85.97	68.25	67.89	64.5	64.5
40	75.31	75.31	95.66	75.77	75.34	65.0	65.0

Table 4.9 Bearing capacity factor N_q.

ϕ	This study	Vesic (1973)	Terzaghi (1943)	Silvestri (2003)	Soubra (1999)	Chen (1975)	ψ (this study)	ψ (45+ϕ/2)
15	3.96	3.94	4.45		3.95	3.94	52.5	52.5
16	4.33	4.34	4.92		4.34	4.34	53.0	53.0
17	4.79	4.77	5.45		4.78	4.77	53.5	53.5
18	5.27	5.26	6.04		5.27	5.26	54.0	54.0
19	5.79	5.80	6.70		5.81	5.80	54.5	54.5
20	6.39	6.40	7.44		6.41	6.40	55.0	55.0
21	7.06	7.07	8.26		7.08	7.07	55.5	55.5
22	7.82	7.82	9.19		7.84	7.82	56.0	56.0
23	8.65	8.66	10.23		8.68	8.66	56.5	56.5
24	9.59	9.60	11.40		9.62	9.61	57.0	57.0
25	10.64	10.66	12.72	10.91	10.69	10.66	57.5	57.5
26	11.87	11.85	14.21	12.14	11.88	11.86	58.0	58.0
27	13.19	13.20	15.90	13.36	13.23	13.20	58.5	58.5
28	14.72	14.72	17.81	15.10	14.76	14.72	59.0	59.0
29	16.44	16.44	19.98	16.87	16.49	16.45	59.5	59.5
30	18.40	18.40	22.46	18.89	18.46	18.41	60.0	60.0
31	20.63	20.63	25.28	21.20	20.70	20.64	60.5	60.5
32	23.18	23.18	28.52	23.83	23.26	23.18	61.0	61.0
33	26.06	26.09	32.23	26.84	26.19	26.10	61.4	61.5
34	29.44	29.44	36.50	30.30	29.56	29.45	62.0	62.0
35	33.27	33.30	41.44	34.29	33.44	33.31	62.5	62.5
36	37.75	37.75	47.16	38.91	37.93	37.76	63.0	63.0
37	42.95	42.92	53.80	44.25	43.13	42.93	63.5	63.5
38	48.93	48.93	61.55	50.49	49.19	48.95	64.0	64.0
39	55.95	55.96	70.61	57.77	56.28	55.97	64.5	64.5
40	64.19	64.20	81.27	66.31	64.58	64.21	65.0	65.0

Table 4.10 Bearing capacity factor N_γ

ϕ	This study	Vesic (1973)	Chen (1975)	Soubra (1999)	Frydman & Burd (1997)	ψ (this study)	ψ (45+ϕ/2)
15	2.90	2.65	2.94	1.95		51.6	52.5
16	3.39	3.06	3.42	2.32		51.7	53.0
17	3.94	3.53	3.98	2.75		51.8	53.5
18	4.51	4.07	4.61	3.25		52.0	54.0
19	5.17	4.68	5.35	3.82		52.3	54.5
20	5.95	5.39	6.20	4.49		52.6	55.0
21	6.82	6.20	7.18	5.26		52.9	55.5
22	7.83	7.13	8.32	6.15		53.3	56.0
23	9.00	8.20	9.64	7.19		53.7	56.5
24	10.37	9.44	11.18	8.40		54.1	57.0
25	11.95	10.88	12.97	9.81		54.6	57.5
26	13.78	12.54	15.05	11.46		55.0	58.0
27	15.92	14.47	17.50	13.39		55.5	58.5
28	18.43	16.72	20.36	15.67		56.0	59.0
29	21.37	19.34	23.72	18.35		56.5	59.5
30	24.85	22.40	27.67	21.51	21.70	57.0	60.0
31	28.91	25.99	32.34	25.26		57.5	60.5
32	33.76	30.22	37.86	29.71		58.0	61.0
33	39.47	35.19	44.41	35.02		58.6	61.5
34	36.33	41.06	52.20	41.37		59.1	62.0
35	54.49	48.03	61.49	49.00	54.20	59.6	62.5
36	64.33	56.31	72.62	58.21		60.7	63.0
37	76.22	66.19	85.98	69.35		60.7	63.5
38	90.61	78.03	102.10	82.91		61.3	64.0
39	108.15	92.25	121.60	99.48		61.8	64.5
40	129.63	109.41	145.30	119.84	147.00	62.1	65.0

Table 4.11 Validation of the model with (a) Experimental work (b) Finite elements modeling.

(a)

No.	Reference	C_u (kPa)	ϕ_s (°)	γ_c	γ_s	A_s (%)	B (m)	q (kPa)	q_u Measured (kPa)	q_u Theory (kPa)	q_u (Madhav & Vitkar (1978)) (kPa)
1	Mckelvey et al. (2004)	32	34	14	17.3	24	0.09	0	272	265	280
2	Mckelvey et al. (2004)	20.5	34	9.9	20.3	40	0.05	0	160	176	193.12
3	Hu (1995)	10.5	30	13.1	15.47	30	0.1	0	79	84.83	86.86
4	Hu (1995)	11.5	30	13.1	15.47	30	0.1	0	75	92.8	95.07

(b)

No.	Reference	c_c (kPa)	ϕ_c (°)	ϕ_s (°)	γ_c	γ_s	A_s %	B (m)	q (kPa)	q_u (measured) (kPa)	q_u (theory) (kPa)
1	PLAXIS	5	25	45	16.0	21	35	2.5	3.2	800	870
2	PLAXIS	5	12	45	13.0	21	35	2.5	2.6	352	334
3	PLAXIS	5	13	40	13.0	19	35	2.5	2.6	280	293
4	PLAXIS	5	15	45	14.0	21	35	2.5	2.8	420	392
5	PLAXIS	15	15	45	14.0	21	35	2.5	2.8	660	618
6	PLAXIS	5	13	40	13.0	19	30	2.62	2.6	275	261
7	PLAXIS	10	13	40	13.0	19	30	2.62	2.6	366	347
8	PLAXIS	15	13	40	13.0	19	30	2.62	2.6	458	433
9	PLAXIS	5	12	45	12.0	21	35	3	2.6	365	350
10	PLAXIS	12	12	45	12.0	21	35	3	2.6	508	491

4.4 Analytical Model for Local Shear Failure

Similar to the case of general shear failure theory, equivalent soil concept was used to model the reinforced ground and limit equilibrium technique was utilized. The composite cohesion and unit weight of the reinforced soil was considered as

$$\gamma_{comp} = A_s\gamma_s + (1 - A_s)\gamma_c \tag{4.119}$$

$$c_{comp} = A_s c_s + (1 - A_s)c_c \tag{4.120}$$

where c_s, c_c, γ_s, γ_c and A_s are cohesion and unit weight of the column material and soft soil and area ratio respectively. c_s was considered zero for granular material.

Friction angle of composite soil calculates as

$$\varphi_{comp} = \tan^{-1}[A_s\mu_s \tan\varphi_s + (1 - A_s)\mu_c \tan\varphi_c] \tag{4.121}$$

where

$$\mu_s = \frac{n}{1 + (n-1)A_s} \tag{4.122}$$

$$\mu_c = \frac{1}{1 + (n-1)A_s} \tag{4.123}$$

ϕ_s and ϕ_c represent the angle of friction of stone column material and soft soil respectively. Derivation of this equation is presented in Section 4.3. The stress ratio, n, of 3 was used in this study. (Mckelvey et al. (2004)) γ_{comp}, c_{comp} and ϕ_{comp} in Equations 4.119, 4.120 and 4.121 were used as the composite unit weight, cohesion and friction angle of the reinforced area in the proposed theoretical model.

Figures 4.32 and 4.33 illustrate the failure shape observed in the numerical model and the proposed failure pattern. Due to symmetry only half part of the problem is presented.

Figure 4.32 Rupture surface observed in the numerical model.

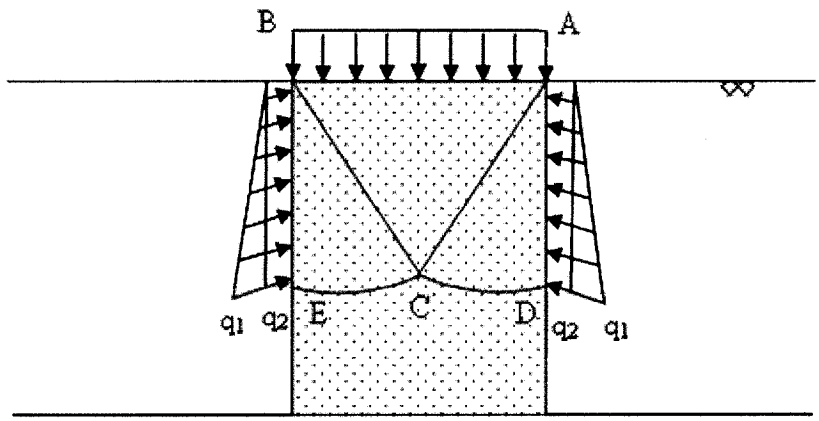

Figure 4.33 Assumed failure Mechanism.

Square arrangement of stone columns was considered in the model which can be simplified as the plane strain form.

The observed failure pattern consists of 2 zones:

3. Zone 1 represents the triangle wedge section *ABC* which is located beneath the foundation and has an angle ψ from the horizontal axis.
4. Zone 2 is a shear zone *ACD* bounded by the surface *CD* which has the logspiral shape. The curve starts at the tip of the triangle wedge and ends at point *D* located at the boundary of the reinforced area. The location of logspiral center is undetermined and will be estimated. In developing the theoretical model, due to low relative density of the soft soil, large width of the foundation and due to the large resistance of the boundary columns, failure surface does not extend to the surrounding soft soil as it ends at those columns. This observation was noted in the results of numerical model presented in Chapter 3.

4.4.1 Equilibrium Analysis

In the proposed model the ultimate bearing capacity was considered as the sum of bearing capacities due to the unit weight, cohesion and surcharge. Due to symmetry only half of the failure mechanism is considered.

Considering the bearing capacity due to unit weight, the free body of the logspiral section (Figure 4.34) is subject of the following forces:

1. Weight of the soil mass of the logspiral block *OCD*, W_1, which is calculated as

$$W_1 = \gamma_{comp} \frac{r_1^2 - r_0^2}{4 \tan \varphi_{comp}} \tag{4.124}$$

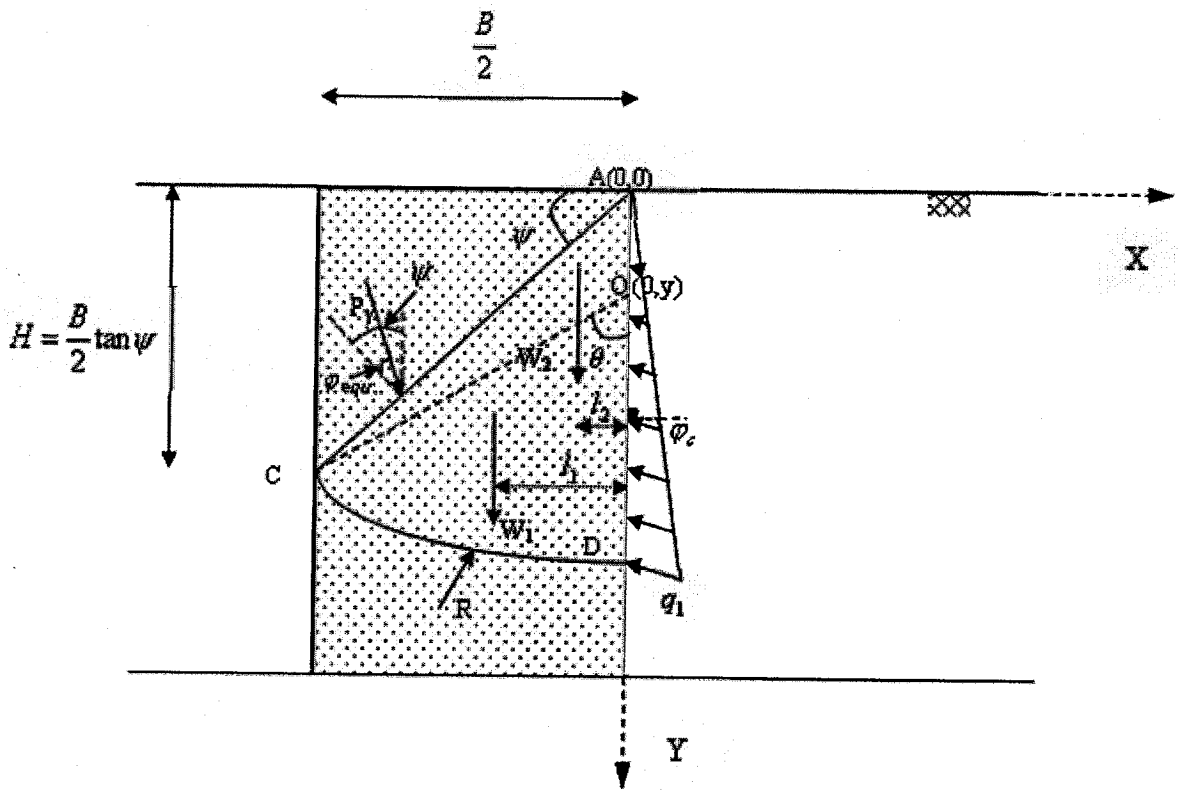

Figure 4.34 Equilibrium of forces on the logspiral section ($\phi \neq 0$, $\gamma \neq 0$, $q=0$, $c=0$).

However

$$r_o = \frac{B}{2\sin\theta} \tag{4.125}$$

and

$$r_1 = r_o e^{\theta \tan \varphi_{comp}} \tag{4.126}$$

So

$$r_1 = \frac{B}{2\sin\theta} e^{\theta \tan \varphi_{comp}} \tag{4.127}$$

Therefore

$$W_1 = \gamma_{comp} \frac{B^2 (e^{2\theta \tan \varphi_{comp}} - 1)}{16 \sin^2 \theta \tan \varphi_{comp}} \tag{4.128}$$

1. Weight of the triangle ACO given as

$$W_2 = \frac{1}{2} \gamma_{comp} \frac{B}{2} y \tag{4.129}$$

Considering Equation 4.45, the distance AO could be determined

$$AO = y = \frac{B(\tan\psi - \cot\theta)}{2} \tag{4.130}$$

Therefore

$$W_2 = \gamma_{comp} \frac{B^2 (\tan\psi - \cot\theta)}{8} \tag{4.131}$$

2. The resultant of frictional force, R, along the arc CD. The line of action of this force passes through the center of the logspiral.
3. Load P_γ due to weight of the elastic cone section and load applied to the foundation and is acting on line AC.

4. Passive force due to the resultant of the stress acting on the plan AD which can be given by the following equation.

$$q_1 = \gamma_c K_P AD \tag{4.132}$$

However

$$AD = y + r_1 = \frac{B}{2\sin\theta}(\tan\psi \sin\theta - \cos\theta + e^{\theta \tan\varphi_{comp}}) \tag{4.133}$$

So

$$q_1 = \frac{\gamma_c K_P B}{2\sin\theta}(\tan\psi \sin\theta - \cos\theta + e^{\theta \tan\varphi_{equ.}}) \tag{4.134}$$

K_P is determined using the tables of Caquot et al. (1972) for passive earth pressure coefficient. Table 4.12 presents the values of K_P with respect to ϕ.

Taking moment about point O_1 gives

$$\Sigma M_O = 0 \rightarrow W_1 l_1 + W_2 l_2 + P_\gamma[\cos(\psi - \varphi_{comp})\frac{B}{3} + \sin(\psi - \varphi_{comp})(\frac{B}{3}\tan\psi - y)]$$

$$= \frac{q_1 \cos\varphi_c}{3}[r_1^2 + \frac{y}{2(y + r_1)}(r_1^2 - y^2)] \tag{4.135}$$

The lever arm l_1 is given as (Hijab (1956))

$$l_1 = \frac{4\tan\varphi_{comp}}{3(9\tan^2\varphi_{comp} + 1)} \cdot \frac{r_1^3 - r_o^3(3\tan\varphi_{comp}\sin\theta + \cos\theta)}{(r_1^2 - r_o^2)} \tag{4.136}$$

Substituting Equations 4.125 and 4.126 into 4.136 results

$$l_1 = \frac{2B\tan\varphi_{comp}}{3\sin\theta(9\tan^2\varphi_{comp} + 1)(e^{2\theta\tan\varphi_{comp}} - 1)}[e^{3\theta\tan\varphi_{comp}} - (3\tan\varphi_{comp}\sin\theta + \cos\theta)] \tag{4.137}$$

The lever arm l_2 is determined as

$$l_2 = \frac{1}{3} \cdot \frac{B}{2} = \frac{B}{6} \tag{4.138}$$

Table 4.12 *Kp* factor.

ϕ	K_p	ϕ	K_p
10	1.66	26	4.82
11	1.77	27	5.24
12	1.88	28	5.66
13	1.98	29	6.08
14	2.09	30	6.50
15	2.20	31	7.30
16	2.38	32	8.10
17	2.56	33	8.90
18	2.74	34	9.70
19	2.92	35	10.50
20	3.10	36	12.00
21	3.36	37	13.50
22	3.62	38	15.00
23	3.88	39	16.50
24	4.14	40	18.00
25	4.40		

Combining Equations 4.127, 4.128, 4.130, 4.131, 4.134, 4.135, 4.137 and 4.138 yields

$$\gamma_{comp}\frac{B^3}{24\sin^3\theta(9\tan^2\varphi_{comp}+1)}[e^{3\theta\tan\varphi_{comp}}-(3\tan\varphi_{comp}\sin\theta+\cos\theta)]+\gamma_{comp}\frac{B^3(\tan\psi-\cot\theta)}{48}$$

$$+P_\gamma[\cos(\psi-\varphi_{comp})\frac{B}{3}+\sin(\psi-\varphi_{comp.})(\frac{B}{3}\tan\psi-\frac{B(\tan\psi-\cot\theta)}{2})]$$

$$=\frac{\gamma_c B^3 K_p\cos\varphi_c}{24\sin\theta}[\frac{e^{2\theta\tan\varphi_{comp}}}{\sin^2\theta}+\frac{\tan\psi-\cot\theta}{2}(\frac{1}{\sin\theta}e^{\theta\tan\varphi_{comp}}-\tan\psi+\cot\theta)]\cdot(\tan\psi\sin\theta$$

$$-\cos\theta+e^{\theta\tan\varphi_{comp}}) \tag{4.139}$$

or

$$P_\gamma=\frac{\frac{\gamma_c B^2 K_p\cos\varphi_c}{24\sin\theta}[\frac{e^{2\theta\tan\varphi_{comp}}}{\sin^2\theta}+\frac{\tan\psi-\cot\theta}{2}(\frac{1}{\sin\theta}e^{\theta\tan\varphi_{comp}}-\tan\psi+\cot\theta)]\cdot(\tan\psi\sin\theta}{\frac{\cos(\psi-\varphi_{comp})}{3}+\sin(\psi-\varphi_{comp})(\frac{\tan\psi}{3}-\frac{\tan\psi-\cot\theta}{2})}$$

$$\frac{-\cos\theta+e^{\theta\tan\varphi_{comp}})}{}-\frac{\gamma_{comp}\frac{B^2}{24\sin^3\theta(9\tan^2\varphi_{comp}+1)}[e^{3\theta\tan\varphi_{comp}}-(3\tan\varphi_{comp}\sin\theta+\cos\theta)]}{\frac{\cos(\psi-\varphi_{comp})}{3}+\sin(\psi-\varphi_{comp})(\frac{\tan\psi}{3}-\frac{\tan\psi-\cot\theta}{2})}$$

$$-\frac{\gamma_{comp}\frac{B^2(\tan\psi-\cot\theta)}{48}}{\frac{\cos(\psi-\varphi_{comp})}{3}+\sin(\psi-\varphi_{comp})(\frac{\tan\psi}{3}-\frac{\tan\psi-\cot\theta}{2})} \tag{4.140}$$

In order to obtain the minimum ultimate bearing capacity, the force P_γ should be minimal. This condition can be described as $\frac{\partial P_\gamma}{\partial v}=0$ were v is related to logspiral geometry such as its center coordinates or θ. Differentiating the above equation with respect to θ and equating the result to zero, the critical value of θ will be estimated (Appendix 4). The critical value of θ represents the logspiral that rupture surface actually happens. By determining the angle θ, the value of P_γ will be then calculated.

Writing the equilibrium equation for the cone section results (Figure 4.35)

$$q_\gamma B = 2P_\gamma \cos(\psi - \varphi_{comp}) - W_w \tag{4.141}$$

However

$$W_w = \frac{B^2}{4}\gamma_{comp} \tan\psi \tag{4.142}$$

So

$$q_\gamma = \frac{2P_\gamma}{B}\cos(\psi - \varphi_{comp}) - \frac{B}{4}\gamma_{comp} \tan\psi \tag{4.143}$$

Substituting Equation 4.140 into 4.143 gives

$$q_\gamma = \frac{\frac{\gamma_c B K_p \cos\varphi_c}{12\sin\theta}[\frac{e^{2\theta\tan\varphi comp}}{\sin^2\theta} + \frac{\tan\psi - \cot\theta}{2}(\frac{1}{\sin\theta}e^{\theta\tan\varphi comp} - \tan\psi + \cot\theta)]\cdot(\tan\psi\sin\theta}{\frac{1}{3} + \tan(\psi - \varphi_{comp})(\frac{\tan\psi}{3} - \frac{\tan\psi - \cot\theta}{2})}$$

$$\frac{-\cos\theta + e^{\theta\tan\varphi_{comp}})}{} - \frac{\gamma_{comp}\frac{B}{12\sin^3\theta(9\tan^2\varphi_{comp}+1)}[e^{3\theta\tan\varphi_{comp}} - (3\tan\varphi_{comp}\sin\theta + \cos\theta)]}{\frac{1}{3} + \tan(\psi - \varphi_{comp})(\frac{\tan\psi}{3} - \frac{\tan\psi - \cot\theta}{2})}$$

$$- \frac{\gamma_{comp}\frac{B(\tan\psi - \cot\theta)}{24}}{\frac{1}{3} + \tan(\psi - \varphi_{comp})(\frac{\tan\psi}{3} - \frac{\tan\psi - \cot\theta}{2})} - \frac{B}{4}\gamma_{comp}\tan\psi \tag{4.144}$$

q_γ is written in the form

$$q_\gamma = \frac{1}{2}\gamma_{comp} BN\gamma \tag{4.145}$$

where N_γ is bearing capacity factor and

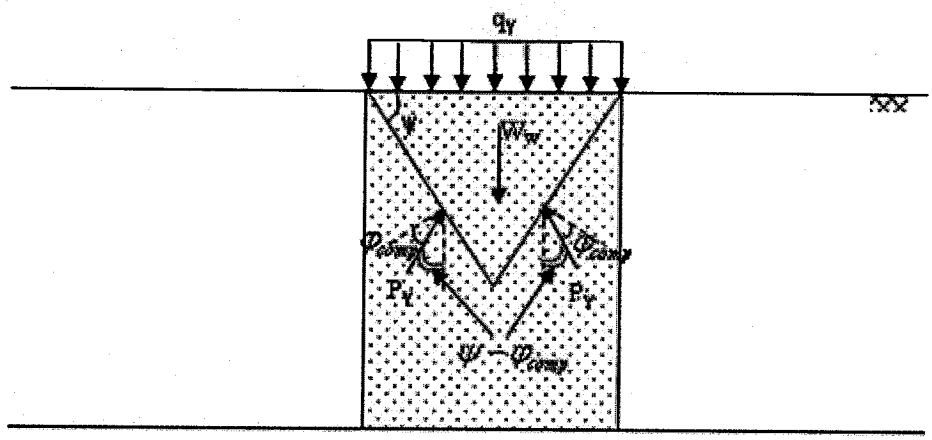

Figure 4.35 Acting forces on the cone section.

$$N_\gamma = \frac{\frac{\gamma_c K_p \cos\varphi_c}{6\gamma_{comp}\sin\theta}\left[\frac{e^{2\theta\tan\varphi_{comp}}}{\sin^2\theta}+\frac{\tan\psi-\cot\theta}{2}\left(\frac{1}{\sin\theta}e^{\theta\tan\varphi_{comp}}-\tan\psi+\cot\theta\right)\right]\cdot(\tan\psi\sin\theta}{\frac{1}{3}+\tan(\psi-\varphi_{comp})\left(\frac{\tan\psi}{3}-\frac{\tan\psi-\cot\theta}{2}\right)}$$

$$-\cos\theta+e^{\theta\tan\varphi_{comp}}) - \frac{\frac{1}{6\sin^3\theta(9\tan^2\varphi_{comp}+1)}\left[e^{3\theta\tan\varphi_{comp}}-(3\tan\varphi_{comp}\sin\theta+\cos\theta)\right]}{\frac{1}{3}+\tan(\psi-\varphi_{comp})\left(\frac{\tan\psi}{3}-\frac{\tan\psi-\cot\theta}{2}\right)}$$

$$-\frac{\frac{\tan\psi-\cot\theta}{12}}{\frac{1}{3}+\tan(\psi-\varphi_{comp})\left(\frac{\tan\psi}{3}-\frac{\tan\psi-\cot\theta}{2}\right)}-\frac{1}{2}\tan\psi \qquad (4.146)$$

For the ultimate load due to surcharge and cohesion, the free body of the composite section (Figure 4.36) is subject to the following forces:

1. Stress q_2 which is due to the surcharge q and cohesion on plan AD.

$$q_2 = K_q q + K_c c \qquad (4.147)$$

However

$$K_q = \frac{K_p}{\cos(\lambda-\beta)} \qquad (4.148)$$

In Equation 4.148, λ and β are the angle of wall with the vertical and the slope of the free surface with the horizontal surface respectively. Thus

$$\lambda = \beta = 0$$

So

$$K_q = K_p \qquad (4.149)$$

and

$$K_c = \frac{(K_q - \frac{1}{\cos\varphi_c})}{\tan\varphi_c} \tag{4.150}$$

Combining Equations 4.147, 4.149 and 4.150 gives

$$q_2 = K_P q + \frac{(K_p - \frac{1}{\cos\varphi_c})}{\tan\varphi_c} c \tag{4.151}$$

2. Passive force P'.
3. Cohesive force per unit area along AC.
4. Cohesive force per unit area along arc CD.
5. The frictional resisting force along the arc CD.
6. Cohesive force per unit area along AD.

Taking moment about point O results

$$\Sigma M_O = 0 \rightarrow P'[\cos(\psi - \varphi_{comp})\frac{B}{4} + \sin(\psi - \varphi_{comp})(\frac{B}{4}\tan\psi - y)]$$

$$+ c_{comp} ACy\cos\psi + \frac{q_2\cos\varphi_c}{2}(y^2 - r_1^{\,2}) = \frac{c_{comp}}{2\tan\varphi_{comp}}(r_1^2 - r_o^2) \tag{4.152}$$

and

$$AC = \frac{B}{2\cos\psi} \tag{4.153}$$

Substituting Equations 4.125, 4.127, 4.130, 4.151 and 4.153 into 4.152 yields

$$P'[\cos(\psi - \varphi_{comp})\frac{1}{4} + \frac{1}{2}\sin(\psi - \varphi_{comp})(\frac{-\tan\psi}{2} + \cot\theta)] + c_{comp}\frac{B(\tan\psi - \cot\theta)}{4}$$

$$+ \frac{B(K_P q + \frac{(K_p - \frac{1}{\cos\varphi_c})}{\tan\varphi_c} c_c)\cos\varphi_c}{8}[(\tan\psi - \cot\theta)^2 - \frac{e^{2\theta\tan\varphi comp}}{\sin^2\theta}] = \frac{c_{comp}B}{8\sin^2\theta\tan\varphi_{comp}}(e^{2\theta\tan\varphi_{comp}} - 1) \tag{4.154}$$

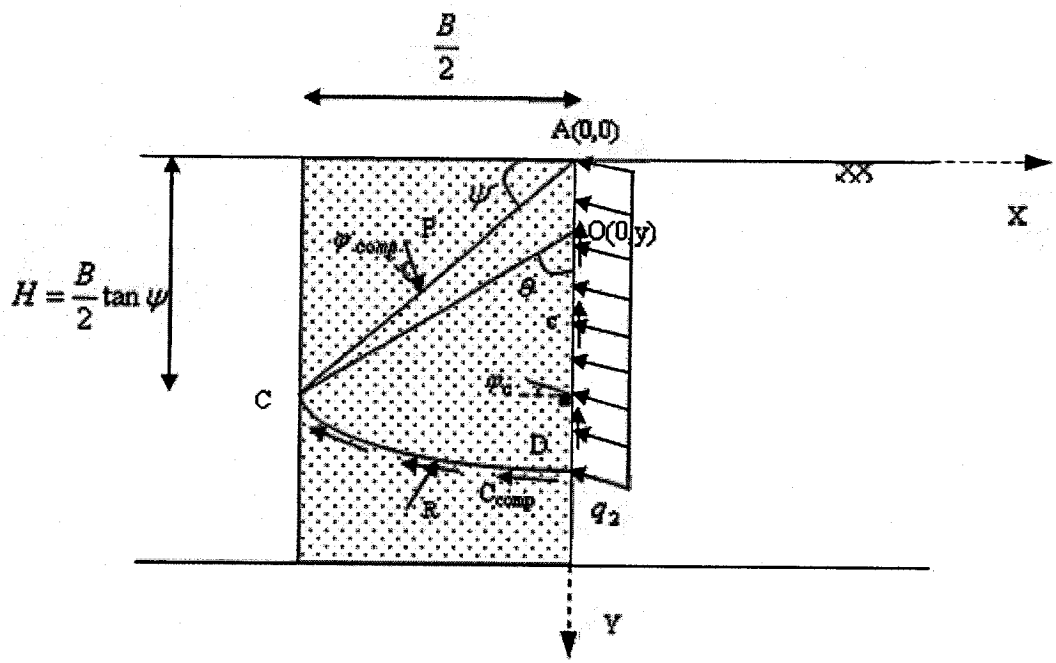

Figure 4.36 External forces acting on the logspiral section ($\phi \neq 0$, $\gamma = 0$, $q \neq 0$, $c \neq 0$).

or

$$P' = \frac{\frac{B(K_P q + \frac{(K_p - \frac{1}{\cos\varphi_c})}{\tan\varphi_c} c_c)\cos\varphi_c}{8}[\frac{e^{2\theta\tan\varphi_{comp}}}{\sin^2\theta} - (\tan\psi - \cot\theta)^2] + \frac{c_{comp}B}{4}(\frac{e^{2\theta\tan\varphi_{comp}} - 1}{2\sin^2\theta\tan\varphi_{comp}} - \tan\psi + \cot\theta)}{\cos(\psi - \varphi_{comp})\frac{1}{4} + \frac{1}{2}\sin(\psi - \varphi_{comp})(\frac{-\tan\psi}{2} + \cot\theta)} \tag{4.155}$$

Minimizing Equation 4.155 with respect to θ gives the minimum value of bearing capacity corresponding surcharge and cohesion. Appendix 4 represents the optimization of above equation.

From Figure 4.37

$$q' = \frac{2P'}{B}\cos(\psi - \varphi_{comp}) + c_{comp}\tan\psi \tag{4.156}$$

Substituting Equation 4.155 into 4.156 gives

$$q' = \frac{K_p\cos\varphi_c[\frac{e^{2\theta\tan\varphi_{comp}}}{\sin^2\theta} - (\tan\psi - \cot\theta)^2]}{1 + 2\tan(\psi - \varphi_{comp})(\frac{-\tan\psi}{2} + \cot\theta)} q$$

$$+ \frac{\frac{e^{2\theta\tan\varphi_{comp}} - 1}{2\sin^2\theta\tan\varphi_{comp}} - \tan\psi + \cot\theta + \tan\psi[\frac{1}{2} + \tan(\psi - \varphi_{comp})(\frac{-\tan\psi}{2} + \cot\theta)]}{\frac{1}{2} + \tan(\psi - \varphi_{comp})(\frac{-\tan\psi}{2} + \cot\theta)} c_{comp}$$

$$+ \frac{\frac{(K_p - \frac{1}{\cos\varphi_c})}{\tan\varphi_c}\cos\varphi_c[\frac{e^{2\theta\tan\varphi_{comp}}}{\sin^2\theta} - (\tan\psi - \cot\theta)^2]}{1 + 2\tan(\psi - \varphi_{comp})(\frac{-\tan\psi}{2} + \cot\theta)} c_c \tag{4.157}$$

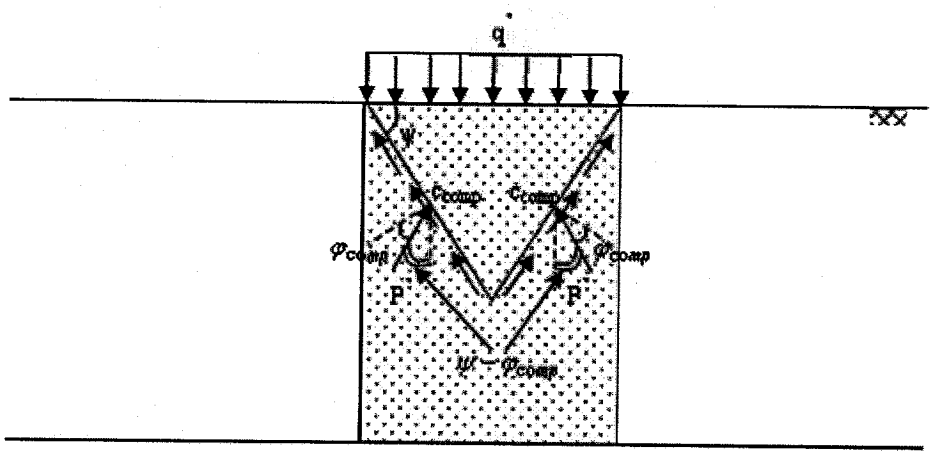

Figure 4.37 Free body diagram of the triangle wedge.

The value of q' can be expressed in the form

$$q' = qN_q + c_{comp}N_c \tag{4.158}$$

Therefore, the bearing capacity factors can be given as

$$N_q = \frac{\tan(45+\frac{\varphi_c}{2})\cos^2\varphi_c[\frac{e^{2\theta\tan\varphi_{comp}}}{\sin^2\theta} - (\tan\psi - \cot\theta)^2]}{1+2\tan(\psi-\varphi_{comp})(\frac{-\tan\psi}{2}+\cot\theta)} \tag{4.159}$$

and

$$N_c = \frac{\frac{e^{2\theta\tan\varphi_{comp}}-1}{2\sin^2\theta\tan\varphi_{comp}} - \tan\psi + \cot\theta + \tan\psi[\frac{1}{2}+\tan(\psi-\varphi_{comp})(\frac{-\tan\psi}{2}+\cot\theta)]}{\frac{1}{2}+\tan(\psi-\varphi_{comp})(\frac{-\tan\psi}{2}+\cot\theta)}$$

$$+\frac{(K_p - \frac{1}{\cos\varphi_c})}{\frac{\tan\varphi_c}{\cos\varphi_c}\cos\varphi_c[\frac{e^{2\theta\tan\varphi_{comp}}}{\sin^2\theta} - (\tan\psi-\cot\theta)^2]}{1+2\tan(\psi-\varphi_{comp})(\frac{-\tan\psi}{2}+\cot\theta)} \cdot \frac{c_c}{c_{comp}} \tag{4.160}$$

4.4.2 Ultimate Bearing Capacity

For the analytical model developed herein, the angle θ was optimized so that the critical load acting on the logspiral, P_γ (Figure 4.34) and P' (Figure 4.36) can be calculated. This was achieved by differentiating the force P and equating the result to zero, i.e. $\frac{\partial P}{\partial \theta} = 0$ and further by utilizing the Newton Raphson numerical technique. The procedure followed first by determining the contribution of the weight, cohesion and surcharge on the bearing capacity. Knowing the value of θ, the bearing capacity factors N_γ, N_q and N_c were estimated using Equations 4.146, 4.159 and 4.160. Consequently, the ultimate bearing capacity was determined by adding the contribution of all components as follows:

$$q_u = q_\gamma + q' = q_\gamma + q_q + q_c = \frac{1}{2}\gamma_{comp} B N_\gamma + q N_q + c_{comp} N_c \qquad (4.161)$$

In order to determine the ultimate bearing capacity a pre assumed cone angle is used in the literature. This consideration introduces an assumption into the model which validity of it for reinforced ground is unknown. Instead, in this investigation the angle ψ was calculated as $\theta + \varphi$ (Section 4.2). This angle was determined during the calculation and by minimization of θ.

In the boundary of composite and soft soil section the value of δ was considered equal to ϕ_c and c equal to c_{comp} as it is located on the failure surface. The location of line of action of the passive forces on vertical failure boundaries for the cases of q_1 and q_2 were considered 2/3 and 1/2 height of AD. These considerations were future examined by numerical modeling of stone columns group for local shear failure condition where similar observations were seen.

In order to facilitate the calculation, a computer program "L-STColumn" was written and the mathematical formulations were coded in the program. L-STColumn stands for Local Shear Failure of Stone Columns and was coded utilizing Visual Basic Version 6 (see Appendix 5). The parameters used in the input data are given in Table 4.13. Utilizing the input data, the program uses the trial and error procedure in order to predict the angle of logspiral at failure state and the triangular wedge angle. Moreover, the bearing capacity q_γ, q' and the ultimate bearing capacity q_u of the foundation is calculated. The computer code displays final results at the end of the calculation. In order to facilitate the theoretical model for practical usage, design charts were developed using the program for the wide rage soil and ground characteristics.

Table 4.13 Input data for L-STColumn computer program.

Angle of shearing resistance of composite soil, ϕ_{comp}	= ------- degrees
Angle of shearing resistance of soft soil, ϕ_c	= ------- degrees
Cohesion of soft soil, c_c	= ------- kPa
Unit weight of composite soil, γ_{comp}	= ------- kN/m^3
Unit weight of soft soil, γ_c	= ------- kN/m^3
Foundation weight, B	= ------- meters
Foundation surcharge, q	= ------- kPa

4.4.3 Design Charts

Design charts are presented for the values of the bearing capacity factors of N_γ, N_q and N_c. These charts are shown in Figures 4.38 to 4.48. These figures were developed for $\frac{c_{comp}}{c_c} =$ 0.2, 0.4, 0.6 and 0.8 and for $\frac{\gamma_{comp}}{\gamma_c} = 1$, 1.2, 1.4, 1.6, 1.8 and 2. Each chart was designed for different ranges of ϕ_{comp}, ϕ_c. Prior using these charts, the values of the composite parameters should be determined using Equations 4.119, 4.120 and 4.121. Utilizing the values obtained from these charts, the ultimate bearing capacity of the foundation can be predicted using Equation 4.161.

4.4.4 Model Validation

The theoretical model was validated using the available experimental results of Mckelvey et al. (2004) and Hu (1995) and the results of the present numerical model. (see Table 4.14). From this Table, good agreement can be noted.

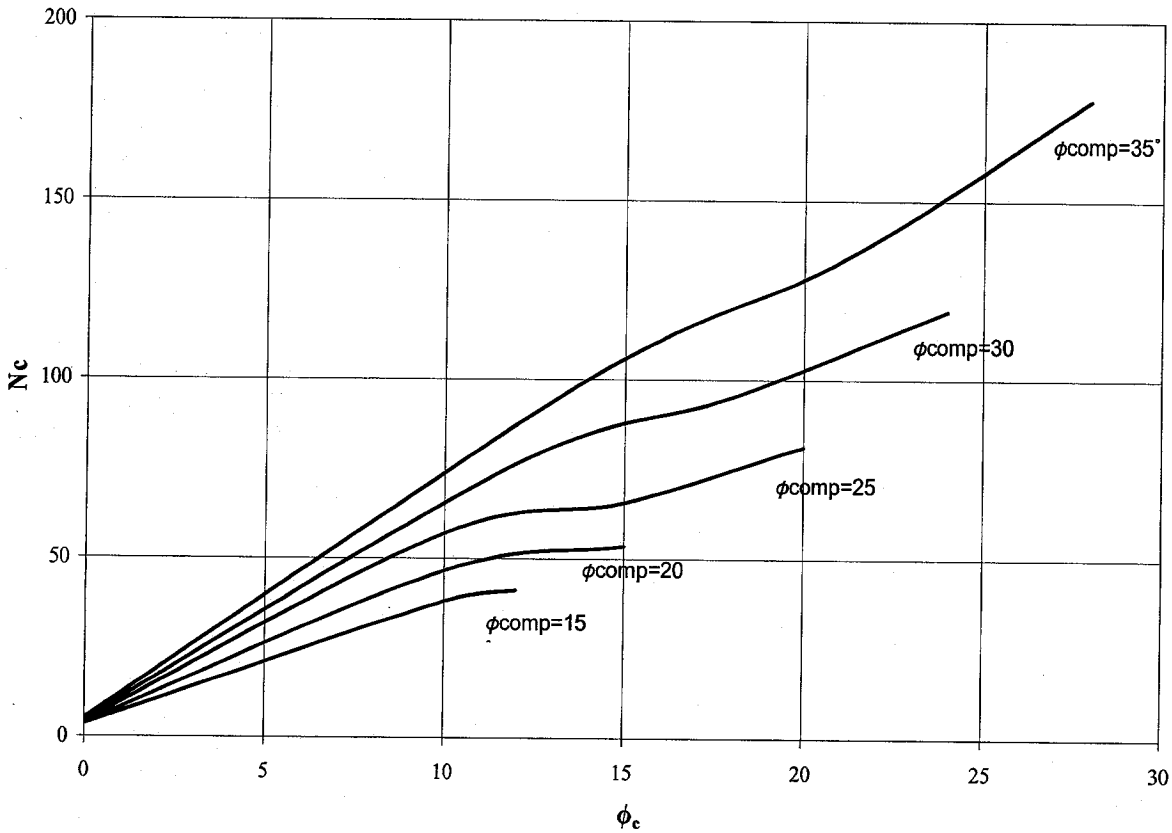

Figure 4.38 N_c vs. ϕ_{comp} - ϕ_c for $\frac{c_{comp}}{c_c}$=0.2.

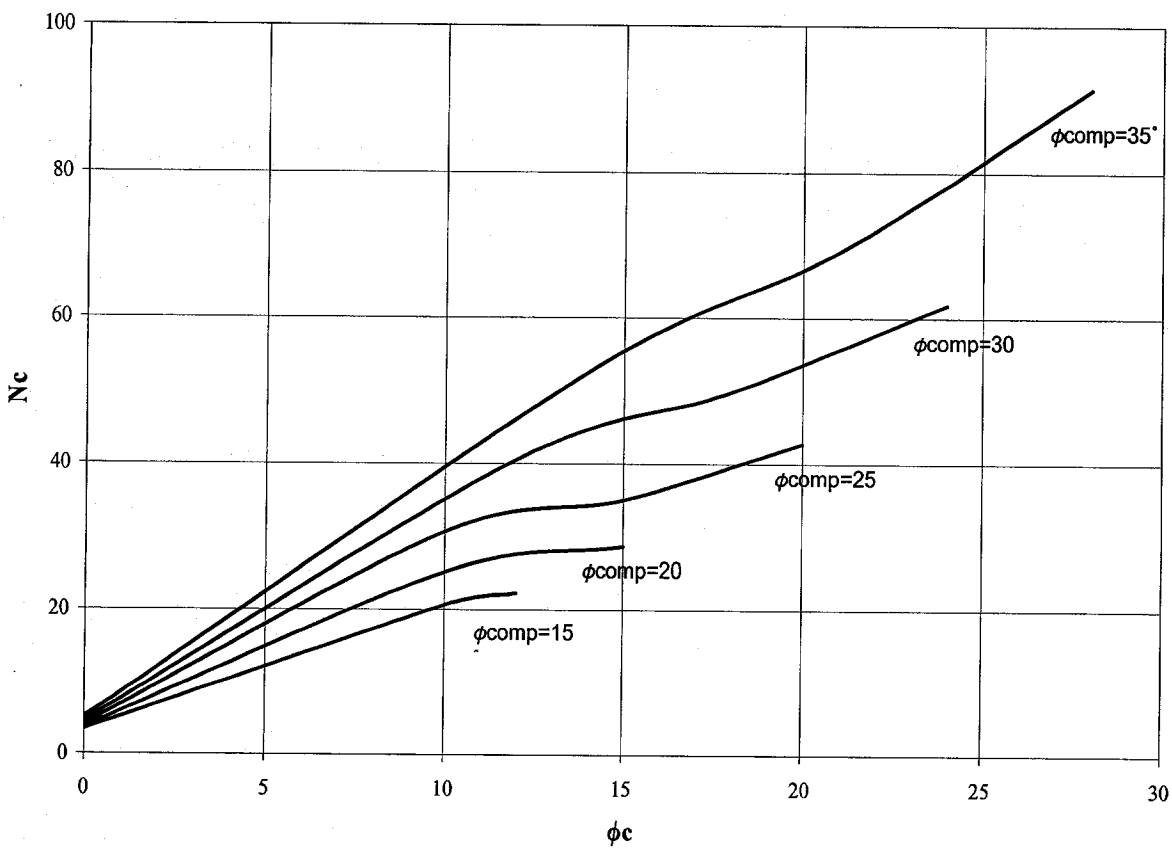

Figure 4.39 N_c vs. ϕ_{comp} - ϕ_c for $\frac{c_{comp}}{c_c}$ =0.4.

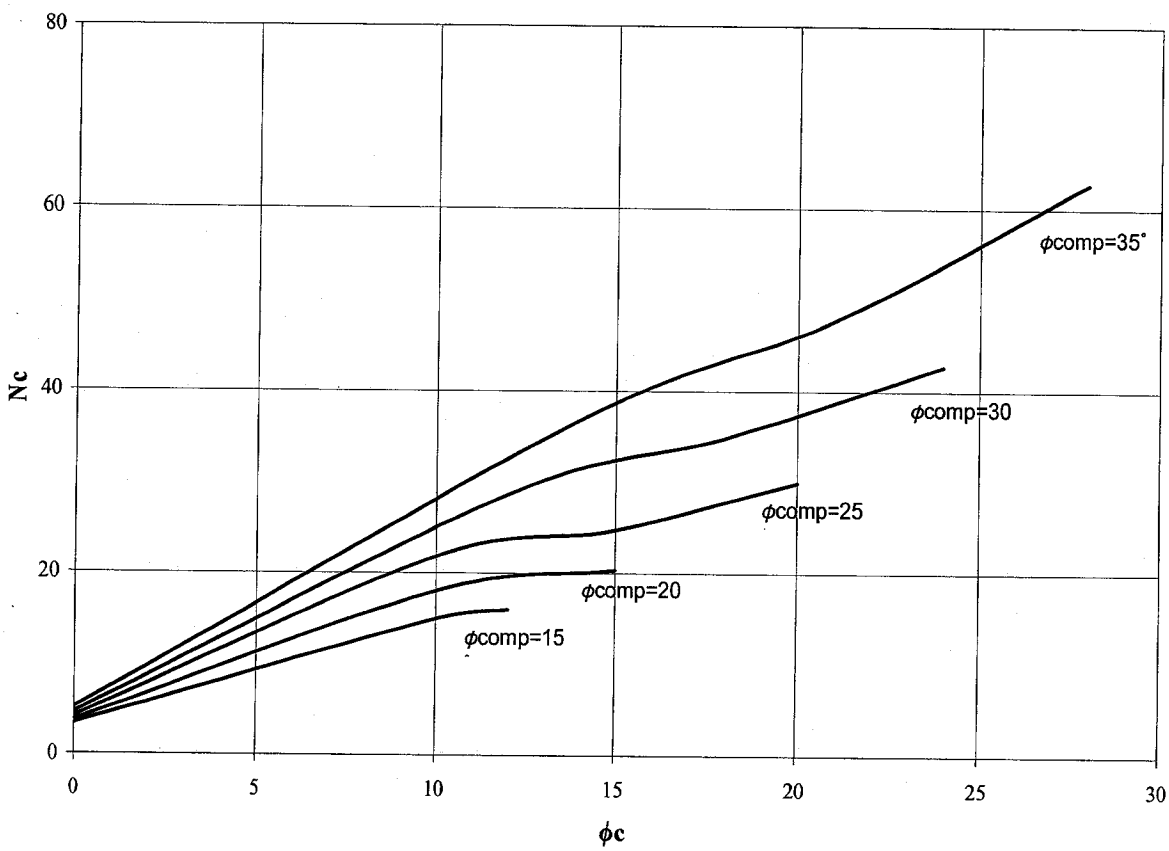

Figure 4.40 N_c vs. ϕ_{comp} - ϕ_c for $\frac{c_{comp}}{c_c}$=0.6.

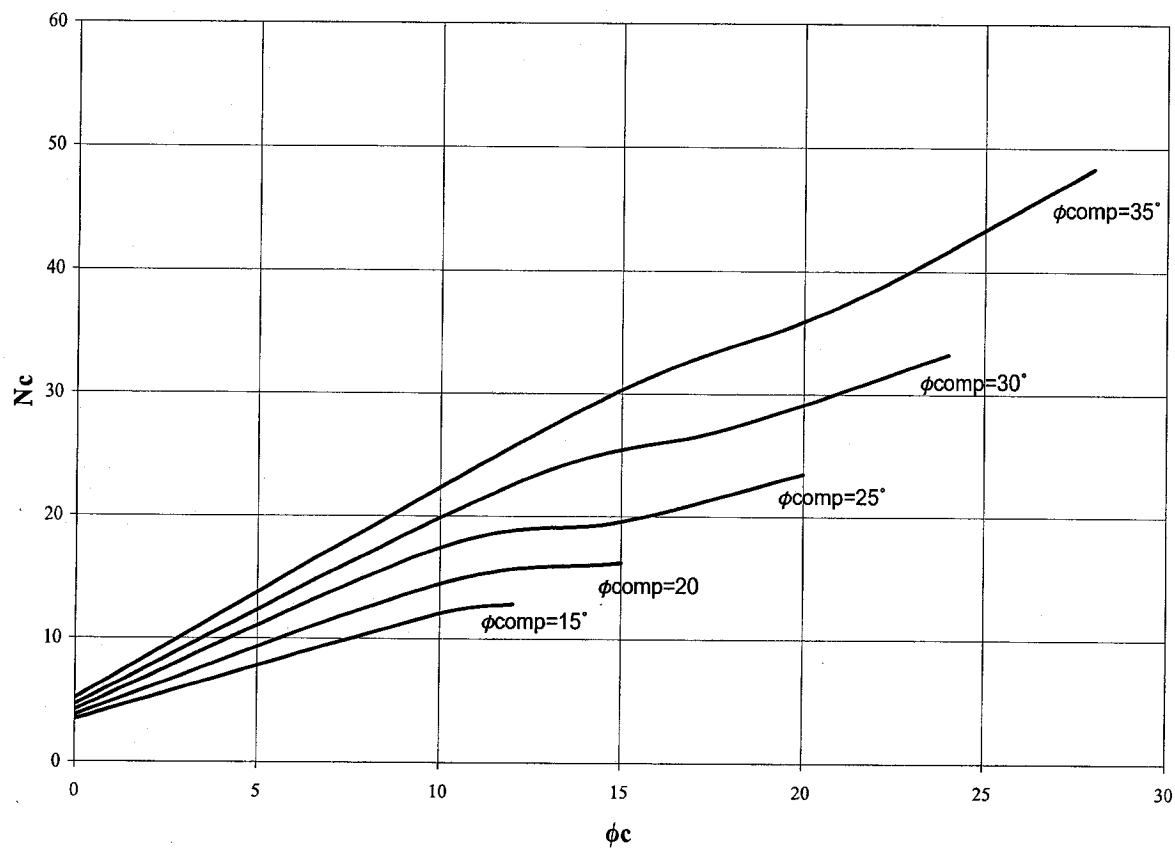

Figure 4.41 N_c vs. ϕ_{comp} - ϕ_c for $\frac{c_{comp}}{c_c}$ =0.8.

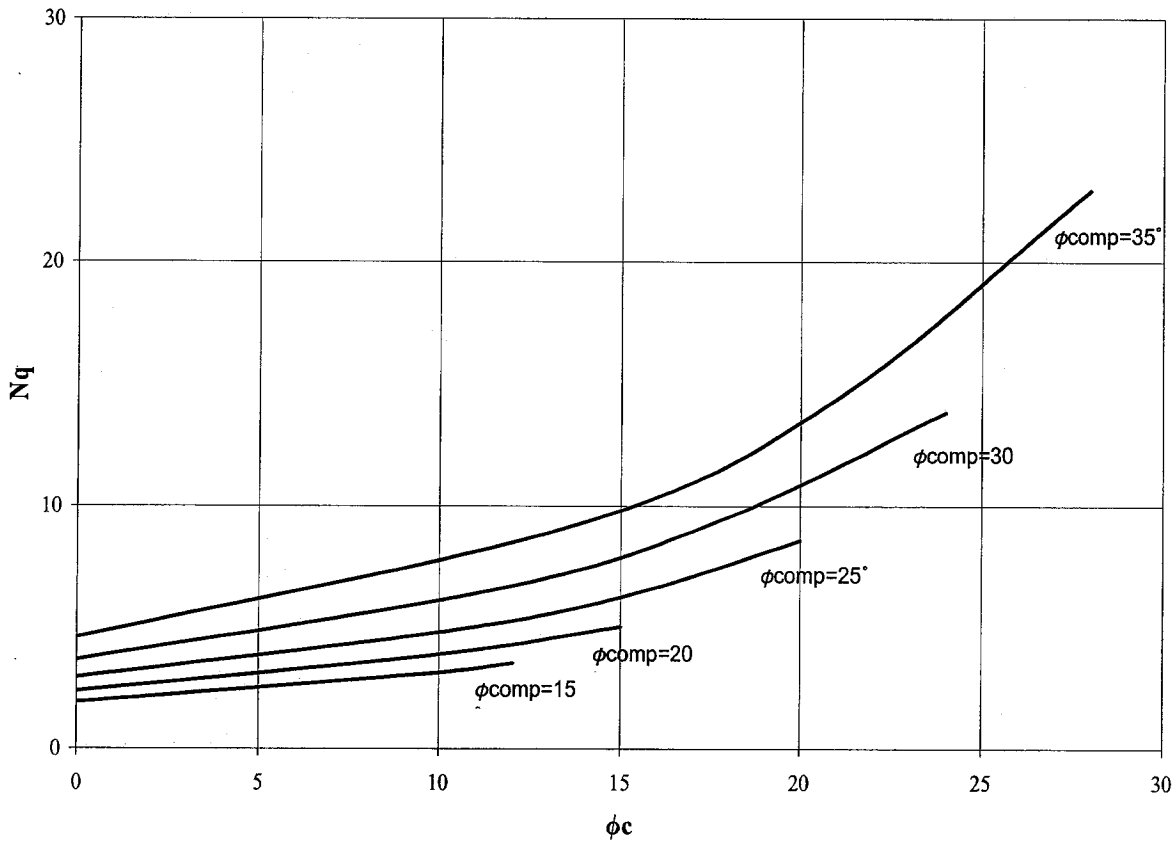

Figure 4.42 N_q vs. ϕ_{comp} - ϕ_c.

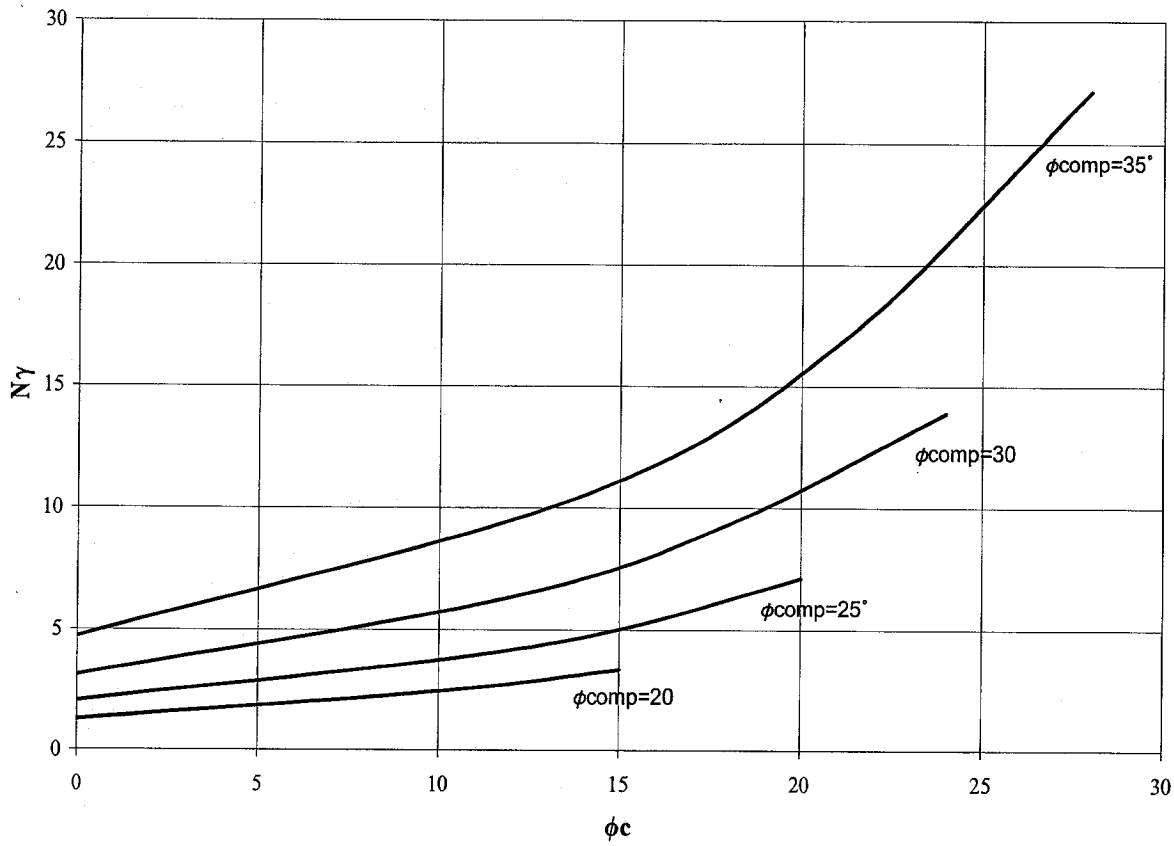

Figure 4.43 N_γ vs. ϕ_{comp} - ϕ_c for $\frac{\gamma_{comp}}{\gamma_c}$ =1.

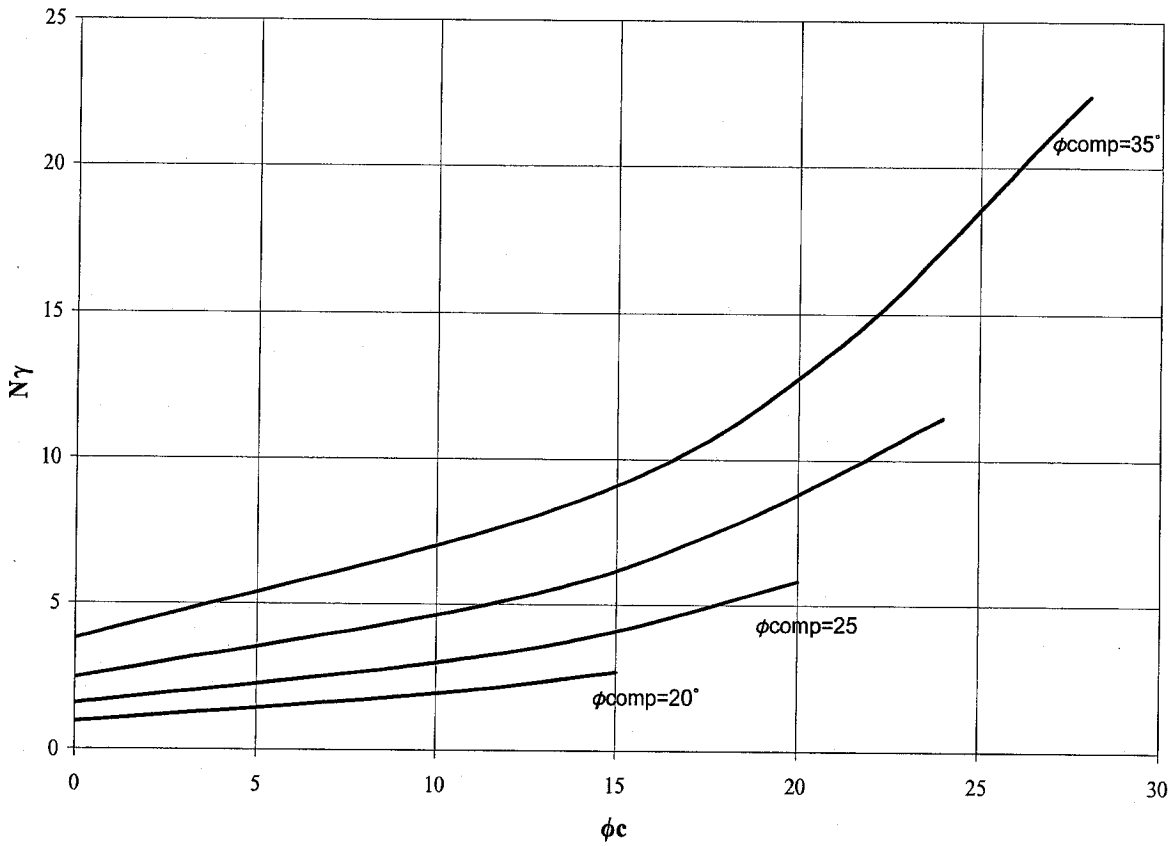

Figure 4.44 N_γ vs. ϕ_{comp} - ϕ_c for $\frac{\gamma_{comp}}{\gamma_c}$ =1.2.

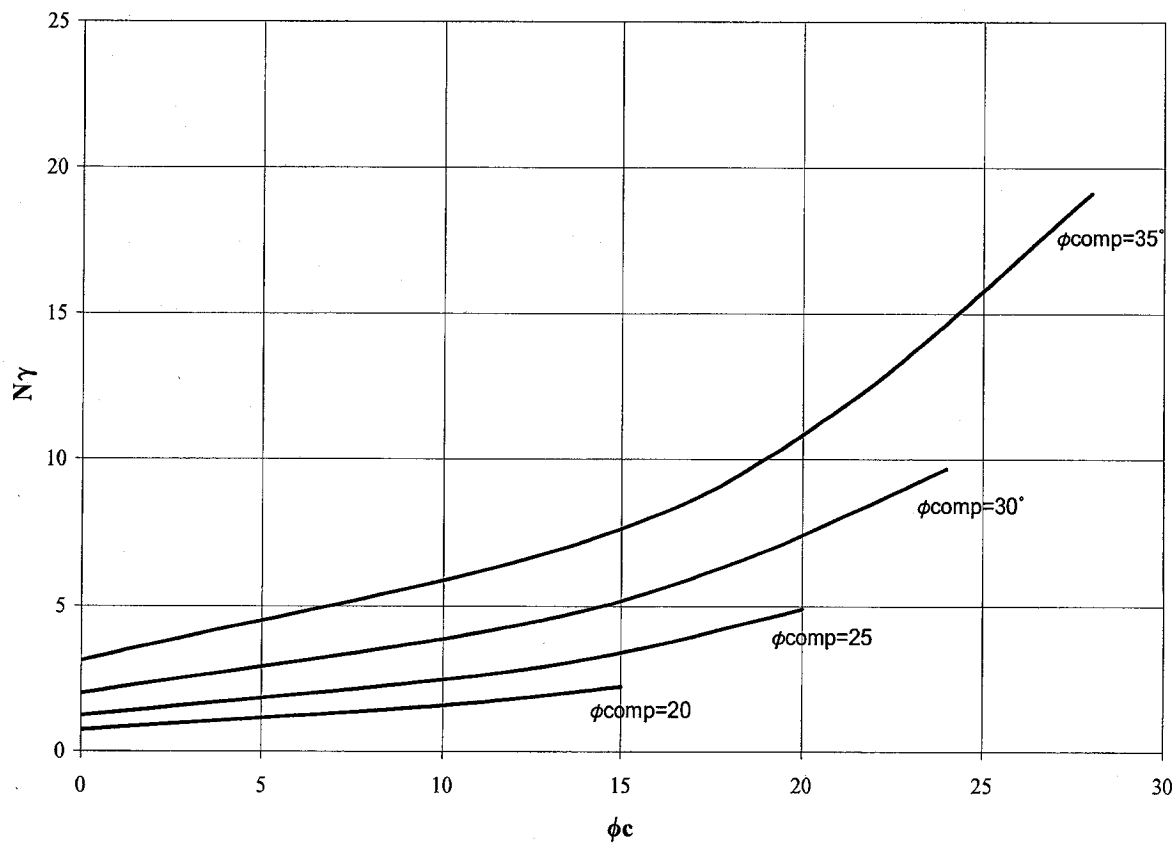

Figure 4.45 N_γ vs. ϕ_{comp} - ϕ_c for $\frac{\gamma_{comp}}{\gamma_c}$ =1.4.

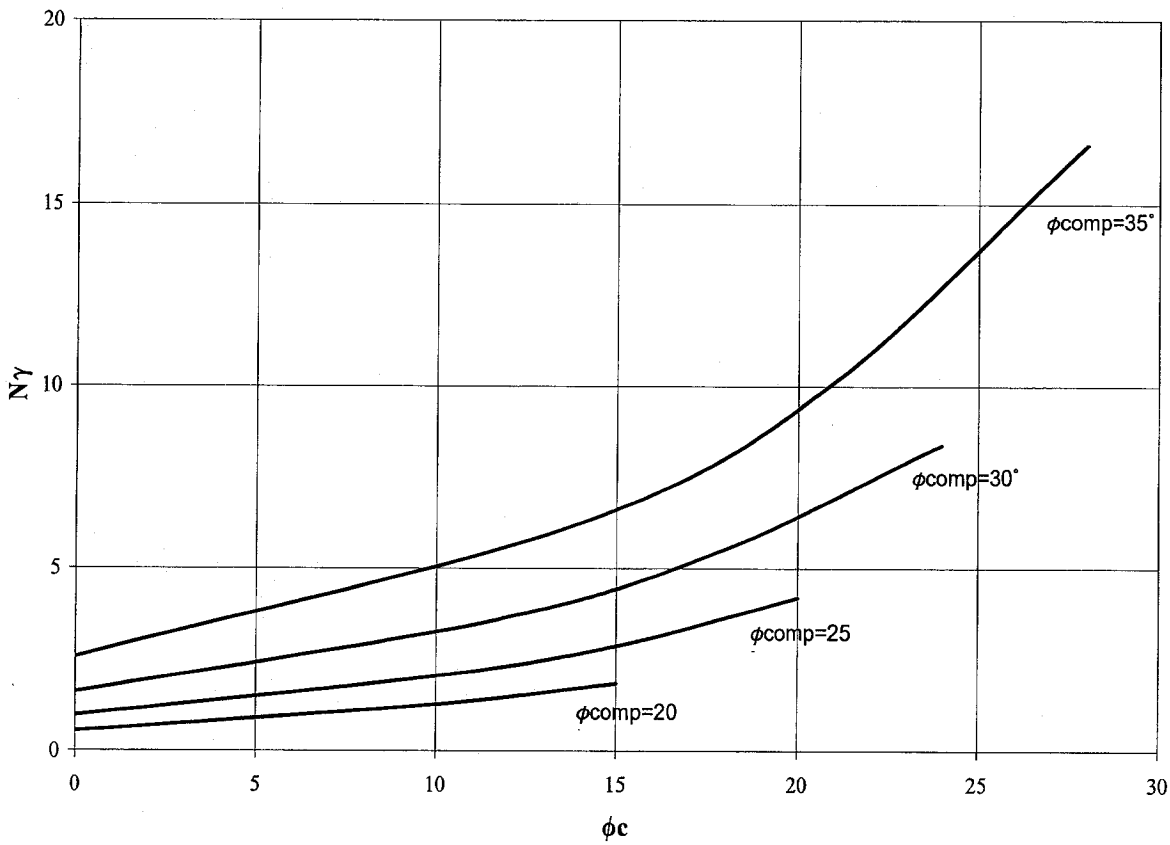

Figure 4.46 N_γ vs. ϕ_{comp} - ϕ_c for $\frac{\gamma_{comp}}{\gamma_c}$ =1.6.

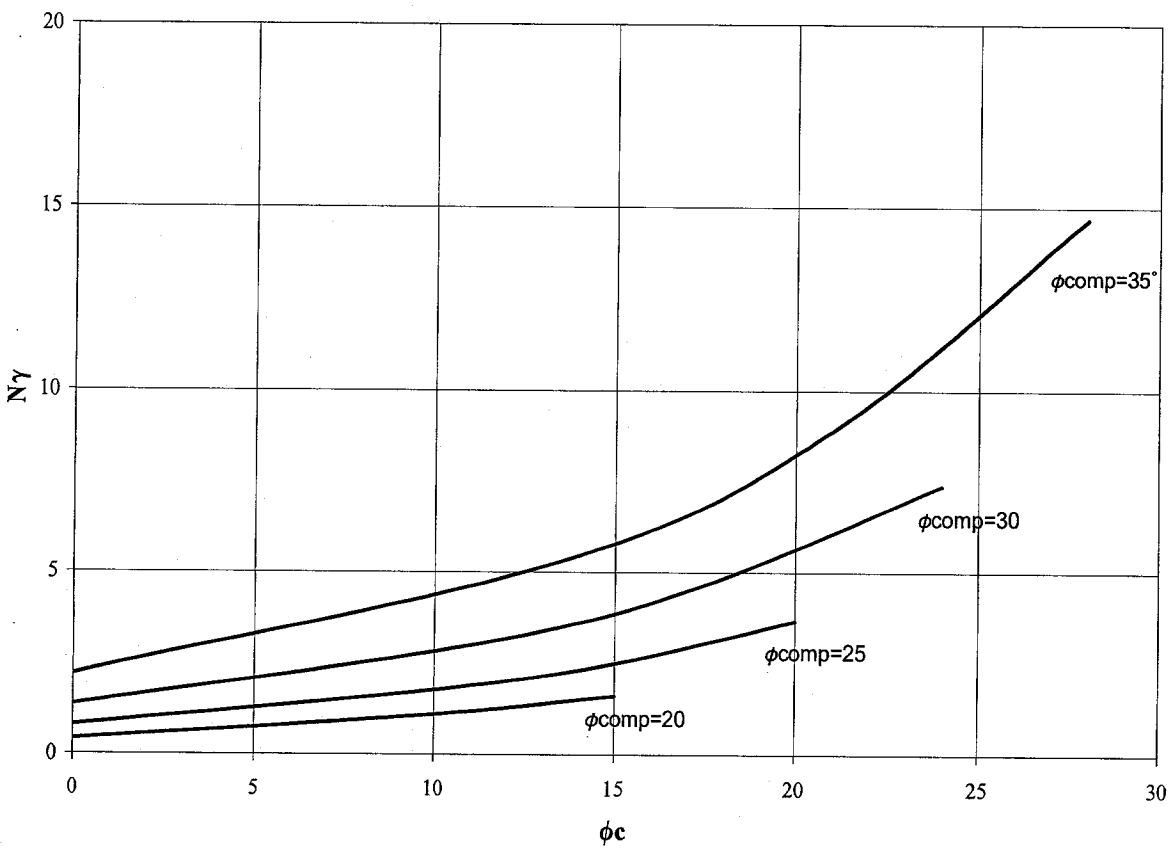

Figure 4.47 N_γ vs. ϕ_{comp} - ϕ_c for $\frac{\gamma_{comp}}{\gamma_c}$ =1.8.

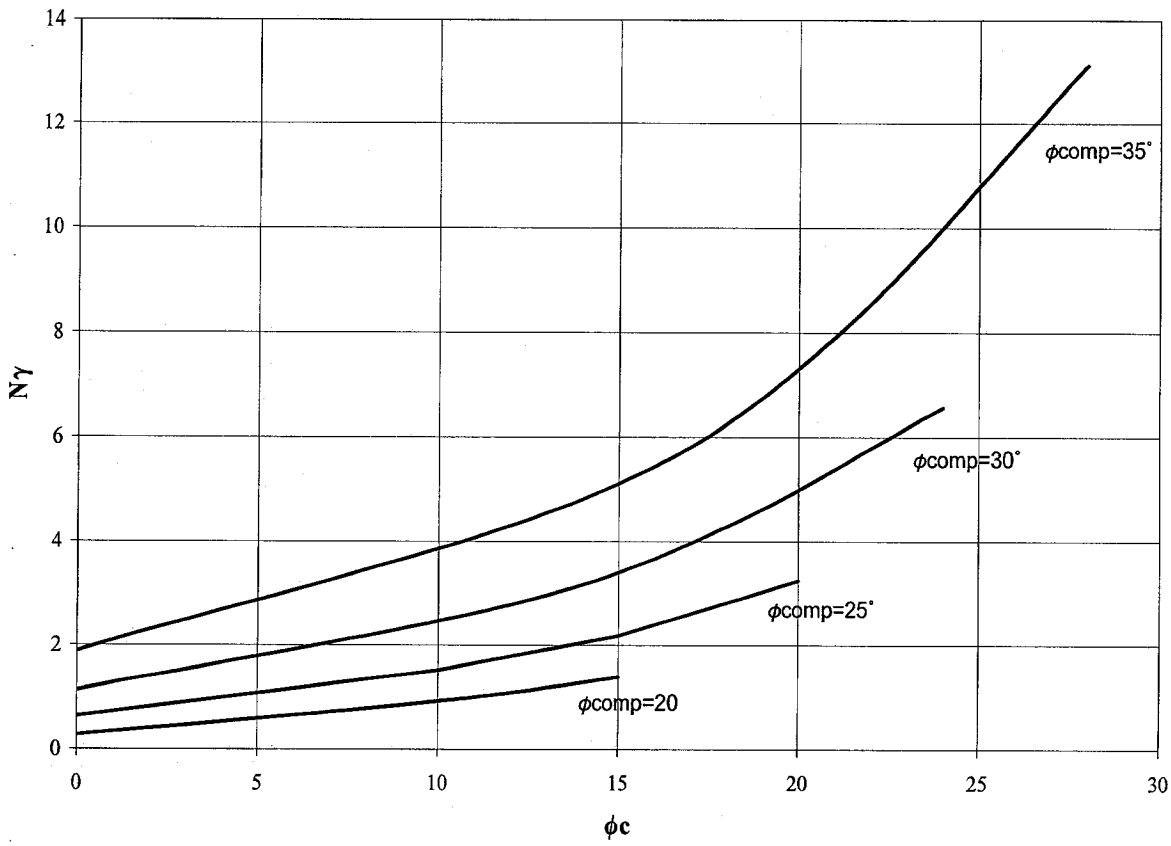

Figure 4.48 N_γ vs. ϕ_{comp} - ϕ_c for $\frac{\gamma_{comp}}{\gamma_c}$ =2.

Table 4.14 Validation of the theoretical model with (a) Experimental work (b) Finite elements modeling.

(a)

No.	Reference	C_u (kPa)	ϕ_s (°)	γ_c	γ_s	A_s (%)	B (m)	d (m)	L (m)	q (kPa)	q_u Measured (kPa)	q_u Theory (kPa)
1	Mckelvey et al. (2004)	27.2	34	8.4	19.6	23	0.1	0.025	0.25	0	86	79
2	Hu(1995)	16.5	30	13.1	15.47	24	0.1	0.011	0.15	0	77	55

(b)

No.	Reference	c_c (kPa)	ϕ_c (°)	ϕ_s (°)	γ_c	γ_s	A_s (%)	B (m)	d (m)	q (kPa)	q_u Measured (kPa)	q_u Theory (kPa)
1	PLAXIS	5	15	40	14.0	19	20	2.98	1	0	193	226
2	PLAXIS	5	13	35	13	16	30	2.62	1	2.6	190	178
3	PLAXIS	12	25	45	16	21	20	4.96	1	1.6	1210	1330
4	PLAXIS	8	10	45	12	21	30	2.62	1	18	298	329
5	PLAXIS	3	10	45	12	21	30	2.62	1	0	161	135

4.5 Analytical Model for Punching Shear Failure

In developing this model, stone column and soft soil material were treated separately. Based on the results of the present numerical model, the rupture surface was taken as a triangular wedge. The theory was developed for group of stone columns installed in square arrangement; accordingly, plane-strain condition was considered (Figure 4.49).

4.5.1 Equilibrium Analysis

If r_o is the radius of the columns and s is the distance between two columns (Figure 4.50), the area replacement ratio A_s (ratio of the area of stone columns over unreinforced soil) and the volume of the cone V of the reinforced ground, can be calculated as

$$A_s = \frac{\pi \cdot r_o^2}{s^2} \tag{4.162}$$

$$V = \frac{B^2 \tan\psi}{4} \tag{4.163}$$

Consequently, ratio of the area of remaining soft soil to the total area is then, 1-A_s.

The total load applied to the reinforced area is equal to the ultimate load of the foundation, Q_u, plus weight of the soil inside the failure cone, W. This is equal to the passive earth pressure acting on the cone or the failure surface (Figure 4.49). In the following equations subscript s and c are used to indicate stone and clay respectively.

$$Q_u + W = 2P_{ps}\cos(\psi - \varphi_s) + 2P_{pc}\cos(\psi - \phi_c) + 2C\sin\psi \tag{4.164}$$

and

$$W = \frac{A_s\gamma_s B^2 \tan\psi}{4} + \frac{(1-A_s)B^2\gamma_c \tan\psi}{4} \tag{4.165}$$

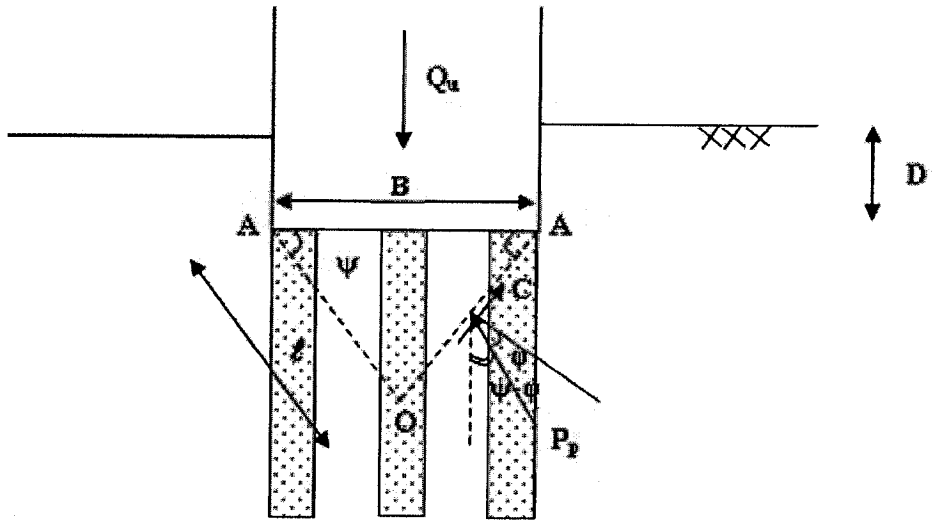

Figure 4.49 Failure of reinforced ground with stone columns under rigid foundation.

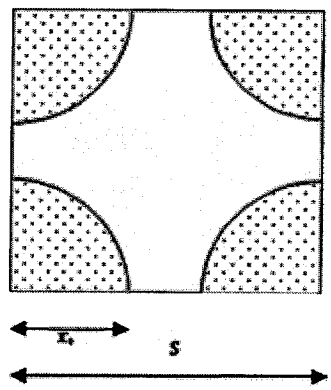

Figure 4.50 Tributary area of stone columns inside the soil.

Equations 4.164 and 4.165 are divided into two parts in order to calculate the values of the stone and soft soil materials. The passive earth pressure on each side on the cone consists of P_p and the cohesive component C. The reactions from stone and soft soil on the cone are equal to

$$P_{ps} = \frac{K_{ps}\gamma_s A_s^2 l^2}{2} + K_{qs}\gamma_s D A_s l + K_{cs} c A_s l \tag{4.166}$$

$$P_{pc} = \frac{K_{pc}\gamma_c (1-A_s)^2 l^2}{2} + K_{qc}\gamma_c D(1-A_s) l + K_{cc} c(1-A_s) l \tag{4.167}$$

C is the sum of the cohesion of clay on each side of the cone where

$$C = c(1-A_s) l \tag{4.168}$$

Q_u represents the load corresponding to uniform ultimate stress, q_u, acting on the foundation width.

$$Q_u = q_u \cdot B \tag{4.169}$$

Upon substituting Equations 4.165, 4.166, 4.167, 4.168 and 4.169 into Equation 4.164 and by rearrangements of the result yields

$$q_u = \frac{\gamma_s N_{\gamma s} B}{2} + \gamma_s D N_{qs} + c_s N_{cs} + \frac{\gamma_c N_{\gamma c} B}{2} + \gamma_c D N_{qc} + c_c N_{cc} \tag{4.170}$$

where

$$N_{\gamma s} = \frac{K_{ps} A_s^2 \cos(\psi - \varphi_s)}{2\cos^2\psi} - \frac{A_s \tan\psi}{2}$$

$$N_{qs} = \frac{K_{qs} A_s \cos(\psi - \varphi_s)}{\cos\psi}$$

$$N_{cs} = \frac{K_{cs} A_s \cos(\psi - \varphi_s)}{\cos\psi} + A_s \tan\psi$$

$$N_{\gamma c} = \frac{K_{pc}(1-A_s)^2 \cos(\psi - \varphi_c)}{2\cos^2 \psi} - \frac{(1-As)\tan\psi}{2}$$

$$N_{qc} = \frac{K_{qc}(1-A_s)\cos(\psi - \varphi_c)}{\cos\psi}$$

$$N_{cc} = \frac{K_{cc}(1-A_s)\cos(\psi - \varphi_c)}{\cos\psi} + (1-A_s)\tan\psi$$

Due to the fact that the material of the stone is cohesionless, the third part of the Equation 4.170 will be omitted.

In order to determine the cone angle, ψ, when soil under the foundation is stone only, this angle is equal to

$$\psi = \frac{\pi}{4} + \frac{\varphi_s}{2} \qquad \text{for} \quad A_s = 1 \tag{4.171}$$

For unreinforced foundation the angle ψ is equal to

$$\psi = \frac{\pi}{4} + \frac{\varphi_c}{2} \qquad \text{for} \quad A_s = 0 \tag{4.172}$$

The equivalent failure angle of reinforced ground with stone columns is located between these two angles. If a linear relationship between these two values was assumed (Wood et al., 2000) then

Referring to Figure 4.43

$$\psi = aA_s + b \tag{4.173}$$

By submitting Equations 4.171 and 4.172 into Equation 4.173, after rearrangement will yield to

$$\psi = \frac{A_s(\varphi_s - \varphi_c)}{2} + \frac{\pi}{4} + \frac{\varphi_c}{2} \tag{4.174}$$

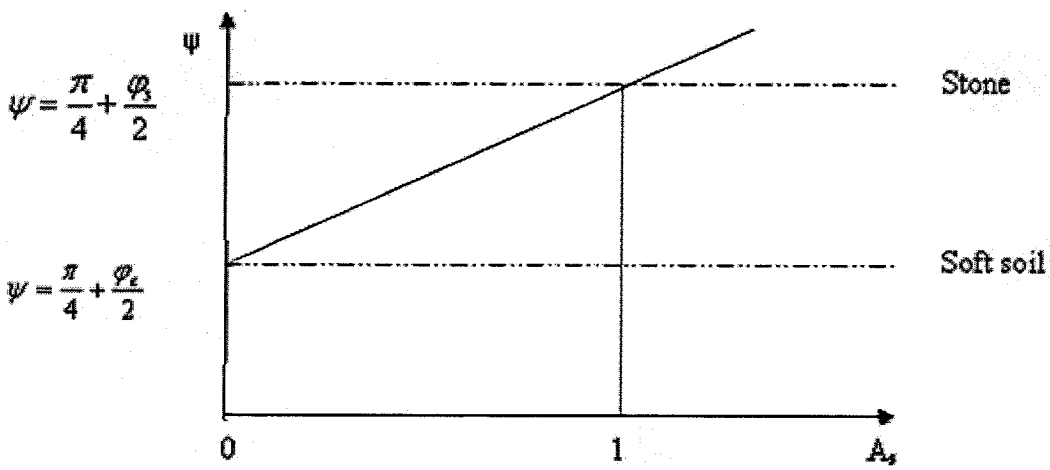

Figure 4.51 Variation of angle ψ with area replacement ratio.

In order to calculate the values of the factors N_γ, N_q and N_c, the coefficients K_γ, K_q and K_c should be determined first. Caquot et al. (1972) provide tables to calculate the active and passive earth pressure for sloped walls and for different wall friction angle, δ. Table of $\delta = -\phi$ was used for calculation of K_γ. The values of K_q and K_c were determined using following equations. (Costet and Sanglerat, 1982)

$$K_q = \frac{K_\gamma}{\cos(\beta - \lambda)} \tag{4.175}$$

$$K_c = \frac{(K_q - 1/\cos\varphi)}{\tan\varphi} \tag{4.176}$$

In Equation 4.175, the angle of β is the slope of ground surface with regard to horizontal surface, which is zero herein and λ is the angle of 90°-ψ.

4.5.2 Design Tables

The proposed theory can be used to estimate the bearing capacity of ground reinforced with stone columns for the case of punching shear failure. The stone columns should be extended beyond the reinforced area. In order to make the equations easy to use for practical purposes Table 4.15 to 4.19 are provided. Knowing the value of A_s and the angle of shearing resistance for soft soil and stone the amount of N_γ, N_q and N_c of the two materials can be easily evaluated. Substituting these values into Equation 4.170 the ultimate load of the foundation can be calculated. As N_c is zero for granular material this table is not provided. For soft soil material there is no significant change when ϕ of stone changes. Therefore, these factors can be used for all different values of friction angle for stone material.

Table 4.15 Values of N_γ for stone.

	ϕ_s	15°	20°	25°	30°	35°	40°	45°
A_s%	ϕ_c/ϕ_s							
10	**0**	0.00	0.00	0.04	0.14	0.35	0.94	2.71
10	**0.1**	0.00	0.00	0.04	0.14	0.35	0.93	2.67
10	**0.2**	0.00	0.00	0.04	0.14	0.35	0.93	2.64
10	**0.3**	0.00	0.00	0.04	0.14	0.35	0.93	2.61
10	**0.4**	0.00	0.00	0.04	0.14	0.35	0.94	2.58
10	**0.5**	0.00	0.00	0.04	0.14	0.36	0.95	2.60
10	**0.6**	0.00	0.00	0.04	0.14	0.36	0.96	2.61
10	**0.7**	0.00	0.00	0.04	0.14	0.37	0.98	2.68
10	**0.8**	0.00	0.00	0.04	0.14	0.38	1.01	2.76
10	**0.9**	0.00	0.00	0.04	0.15	0.40	1.04	2.87
10	**1**	0.00	0.00	0.04	0.15	0.42	1.09	3.03
20	**0**	0.00	0.09	0.27	0.65	1.52	3.81	10.78
20	**0.1**	0.00	0.09	0.27	0.66	1.52	3.80	10.68
20	**0.2**	0.00	0.09	0.27	0.66	1.53	3.84	10.59
20	**0.3**	0.00	0.09	0.28	0.67	1.54	3.88	10.46
20	**0.4**	0.00	0.09	0.28	0.68	1.56	3.92	10.53
20	**0.5**	0.00	0.09	0.29	0.70	1.63	3.99	10.60
20	**0.6**	0.00	0.09	0.29	0.71	1.66	4.05	10.69
20	**0.7**	0.00	0.09	0.29	0.73	1.69	4.13	11.01
20	**0.8**	0.00	0.09	0.30	0.74	1.73	4.25	11.35
20	**0.9**	0.00	0.10	0.30	0.75	1.79	4.40	11.78
20	**1**	0.00	0.10	0.31	0.77	1.85	4.56	12.38
30	**0**	0.08	0.29	0.70	1.57	3.51	8.67	24.08
30	**0.1**	0.08	0.29	0.71	1.58	3.54	8.75	23.90
30	**0.2**	0.08	0.29	0.71	1.60	3.57	8.83	23.65
30	**0.3**	0.08	0.29	0.72	1.63	3.61	8.92	23.79
30	**0.4**	0.08	0.30	0.73	1.65	3.65	9.05	23.93
30	**0.5**	0.09	0.30	0.76	1.74	3.93	9.18	24.06
30	**0.6**	0.09	0.31	0.77	1.76	3.97	9.32	24.54
30	**0.7**	0.09	0.31	0.78	1.78	4.04	9.52	25.19
30	**0.8**	0.09	0.32	0.79	1.81	4.11	9.79	25.89
30	**0.9**	0.09	0.32	0.80	1.83	4.20	10.09	26.83
30	**1**	0.09	0.32	0.81	1.86	4.32	10.41	28.03

Table 4.16 Values of N_q for stone.

	ϕ_s	15°	20°	25°	30°	35°	40°	45°
A_s%	ϕ_c/ϕ_s							
10	0	0.51	0.94	1.78	3.57	7.63	18.47	51.17
10	0.1	0.51	0.93	1.74	3.44	7.25	17.21	46.99
10	0.2	0.51	0.91	1.70	3.33	6.89	16.12	43.29
10	0.3	0.50	0.90	1.67	3.23	6.60	15.31	39.88
10	0.4	0.50	0.89	1.64	3.14	6.32	14.52	36.68
10	0.5	0.49	0.87	1.60	3.05	6.06	13.81	34.29
10	0.6	0.49	0.87	1.58	2.97	5.87	13.15	31.93
10	0.7	0.49	0.86	1.55	2.90	5.70	12.51	30.15
10	0.8	0.49	0.85	1.52	2.84	5.55	12.01	28.63
10	0.9	0.48	0.84	1.50	2.78	5.42	11.56	27.22
10	1	0.48	0.84	1.48	2.72	5.33	11.12	26.13
20	0	1.02	1.85	3.47	6.86	14.42	34.15	93.06
20	0.1	1.01	1.82	3.40	6.66	13.78	32.24	86.58
20	0.2	1.01	1.80	3.34	6.47	13.26	30.79	80.51
20	0.3	1.00	1.78	3.28	6.31	12.77	29.39	74.53
20	0.4	0.99	1.75	3.23	6.16	12.29	28.07	70.17
20	0.5	0.99	1.75	3.21	6.12	12.19	26.88	65.96
20	0.6	0.98	1.73	3.15	5.96	11.80	25.73	62.00
20	0.7	0.98	1.71	3.10	5.82	11.46	24.63	59.28
20	0.8	0.97	1.70	3.05	5.69	11.13	23.81	56.59
20	0.9	0.97	1.69	3.00	5.56	10.87	23.01	54.19
20	1	0.96	1.67	2.96	5.44	10.66	22.24	52.26
30	0	1.52	2.73	5.08	9.91	20.46	47.81	127.58
30	0.1	1.51	2.69	5.00	9.68	19.79	45.92	119.64
30	0.2	1.50	2.66	4.93	9.47	19.15	44.09	111.80
30	0.3	1.49	2.64	4.85	9.27	18.53	42.33	106.05
30	0.4	1.48	2.61	4.79	9.08	17.95	40.76	100.51
30	0.5	1.48	2.61	4.82	9.21	18.40	39.24	95.00
30	0.6	1.47	2.59	4.73	8.97	17.81	37.74	90.95
30	0.7	1.46	2.57	4.66	8.76	17.28	36.48	87.40
30	0.8	1.45	2.55	4.58	8.55	16.77	35.41	83.88
30	0.9	1.45	2.53	4.51	8.35	16.34	34.38	80.92
30	1	1.44	2.51	4.44	8.16	15.98	33.36	78.39

Table 4.17 Values of $N\gamma$ for clay.

ϕ_c	10°	15°	20°	25°
A_s%				
10	0.85	1.97	4.24	8.78
20	0.63	1.52	3.32	6.93
30	0.43	1.12	2.50	5.29

Table 4.18 Values of N_q for soft soil.

ϕ_c	10°	15°	20°	25°
A_s%				
10	2.57	4.31	7.50	13.26
20	2.28	3.82	6.63	11.73
30	1.99	3.34	5.78	10.23

Table 4.19 Values of N_c for soft soil.

ϕ_c	10°	15°	20°	25°
A_s%				
10	9.47	12.73	18.12	26.50
20	8.38	11.28	16.02	23.45
30	7.31	9.84	13.95	20.43

4.5.3 Model Validation

The proposed analytical model was validated with the numerical model developed by PLAXIS software where good agreement between the two was obtained. (See Table 4.20)

4.6 Design Procedure

In order to determine the ultimate bearing capacity of ground reinforced with group of stone columns, first the mode of failure of the ground should be identifies. Figure 3.32 should be used where general, local or punching shear failure mode will be evaluated. Next, by knowing the failure pattern analytical model corresponding to that collapse shape should be used. If general shear failure is identified Figures 4.21 to 4.31 should be utilized; whereas, Figures 4.38 to 4.48 or Tables 4.15 to 4.19 should be considered for the cases of local and punching shear failure correspondingly. In case of single stone column Equation 4.24 should be used. Figure 4.52 is developed in order to calculate the bearing capacity of stone columns for the practical purpose. Knowing soil and geometry parameters of reinforced ground, by utilizing this figure bearing capacity of the reinforced ground can easily be determined.

Table 4.20 Validation of the analytical model

No.	Reference	c_c (kPa)	ϕ_c (°)	ϕ_s (°)	γ_c	γ_s	A_s (%)	B (m)	d (m)	q (kPa)	q_u Measured (kPa)	q_u Theory (kPa)
1	PLAXIS	5	15	35	14	16	20	4.96	1	14	387	421
2	PLAXIS	5	13	35	13	16	20	4.96	1	15.6	375	438
3	PLAXIS	5	15	35	14	16	10	6.6	1	14	354	333
4	PLAXIS	8	15	40	14	19	10	6.6	1	14	497	591
5	PLAXIS	12	15	40	14	19	10	6.6	1	0	370	303

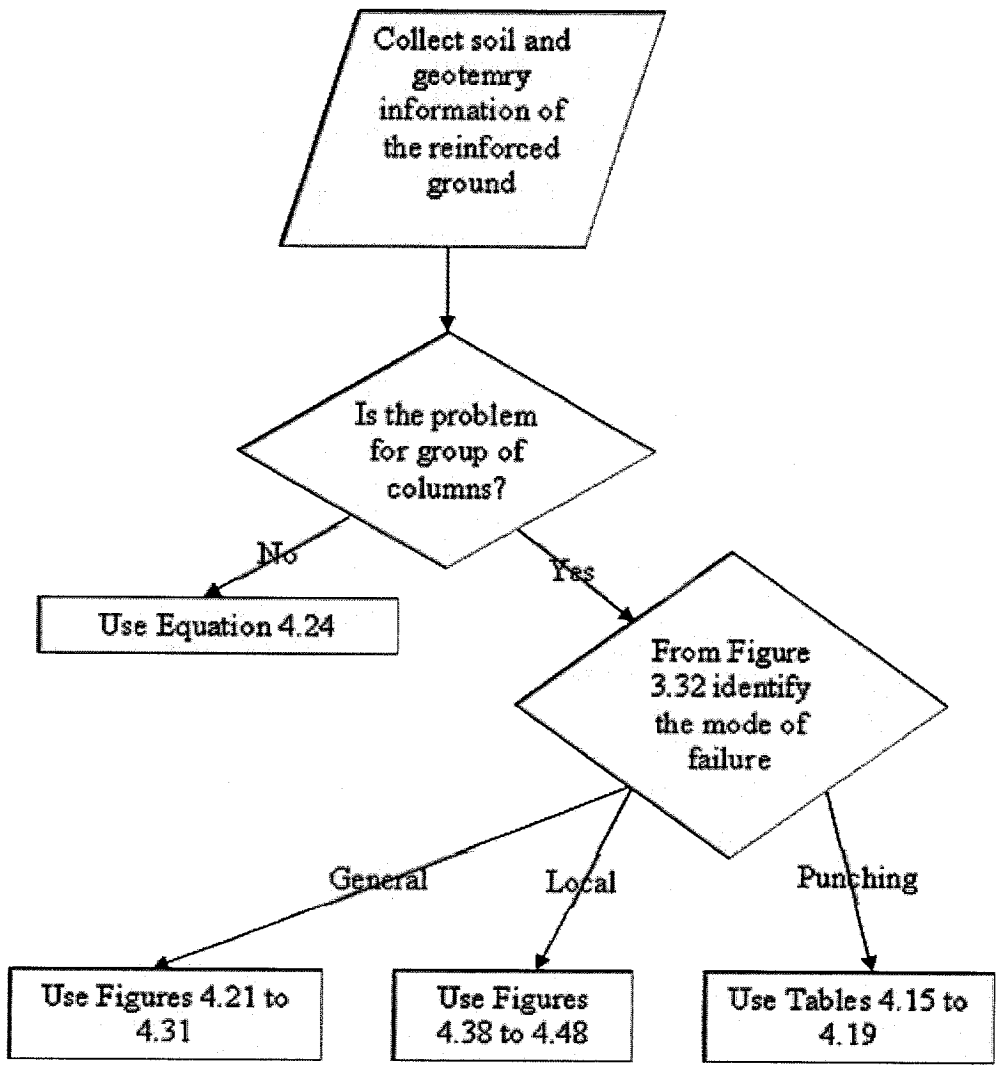

Figure 4.52 Design procedure to calculate bearing capacity of stone columns ground reinforcement technique.

CHAPTER 5

CONCLUSIONS AND RECOMMENDATIONS

5.1 General

This chapter summarizes the conclusions which are drawn from the present study. Recommendations for future research on this subject are also given.

5.2 Conclusions

1. A numerical model was developed to simulate the case of a system consisted of group of stone columns embedded in soft clay. The model is capable to produce the failure mechanism within the columns and the surrounding soil and the bearing capacity of a raft foundation supported by this system. The model was validated with available experimental work.
2. The results of present numerical model for the case of single stone columns showed that the column fails by bulging, which takes place in the upper part of the column and extend up to 4 times of column diameter. While for group of stone columns, due to columns interaction, failure may not take place by bulging but rather general, local or punching shear. The mode of failure, which will take place, depends on soil/stone/geometry conditions. Nevertheless, due to similarity, bulging shape may take place only in the center columns.

3. The results of the present numerical model were used to conduct parametric study in order to identify the parameters which govern group behavior. Furthermore, these results were used to develop charts to identify the expected mode of failure for a given soil/column/geometry conditions.
4. Design theories were developed to predict the ultimate bearing capacity of this system for the three possible modes of failure, namely general, local and punching shear. These theories were based on limit equilibrium technique, the equivalent soil concept and Mohr Coulomb failure criteria.
5. The developed theories were validated with homogeneous soil theories, the results of the present numerical model as well as soils reinforced with stone columns, where good agreements were noted.
6. The formulations of the proposed theories were coded in computer programs and presented in the form of the classical theory for bearing capacity. Design charts were developed to assist practicing engineering; first to establish the appropriate mode of failure of the given soil/column/geometry conditions, then to predict the ultimate bearing capacity of the system.
7. For single stone column an analytical model was proposed which is capable to calculate settlement and bearing capacity of reinforced ground. The model was compared with other available analytical methods and experimental work. Good agreement with the experimental research was reported.

5.3 Recommendations for Future Research

1. There are needs for laboratories and field load test results to validate further the theories developed in this thesis.
2. The research in this study is limited only for the case of raft foundations. However, for some cases like embankments, flexible foundations may be used over the reinforced ground.
3. The effect of method of installation of stone columns should be investigated.
4. Development of theoretical method for settlement of group of stone columns, after adopting the appropriate deform mode.
5. Extend the current study for layered soil.
6. Extend current study to simulate dynamic behavior on stone columns group.
7. Study the liquefaction effect on stone columns installed in sand.

REFRENCES

Aboshi, H. Ichimoto, E., Enoki, M. and Harada, K. (1979) "The composer- a method to improve characteristics of soft clays by inclusion of large diameter sand columns", Proc. Int. Conf. on Soil Reinforcement, Paris, 211-216.

Ambily, A. P. and Gandhi S. R. (2007) "Behavior of Stone Columns Based on Experimental and FEM Analysis", Jour. of Geotechnical and Geoenvironmental Engineering, ASCE, 133, No. 4, 405-415.

Ayadat, T. and Hanna, A.M. (2005) "Encapsulated stone columns as a soil improvement technique for collapsible soil", Ground Improvement, Vol. 9, No. 4, 137-147.

Bachus R.C. and Barksdale R.D. (1984) "Vertical and lateral behavior of model stone columns", Proc. Int. Conf. in In-situ Soil and Rock Reinforcement, Paris, 99-104.

Bae, W.S., Bang, W.S. and Byung, C.A. (2002) "Behavior of foundation system improved with stone columns", Proc. 12th Int. Offshore and Polar Engineering Conf., Kitakyushu, Japan, 675-678.

Balaam, N. P. (1978) "Load settlement behavior of granular piles", Ph.D. Thesis, University of Sydney.

Balaam, N.P. and Booker, J.R. (1981) "Analysis of rigid rafts supported by granular piles", Int. Jour. For Numerical and Analytical Methods in Geomechanics, 5, 379-403.

Balaam N.P. and Poulos H.G. (1983) "The behavior of foundations supported by clay stabilized by stone columns", Proc. 8th European Conf. on Soil Mechanics and Foundation Engineering, Helsinki, 199-204.

Balaam, N.P. and Booker, J.R. (1985) "Effect of stone column yield on settlement of rigid foundations in stabilized clay", Int. Jour. for Numerical and Analytical Methods in Geomechanics, Vol. 9, 331-351.

Barksdale R.D. and Bachus, R.C. (1983) "Design and construction of stone columns", Final Report SCEGIT-83-104, Federal Highway Administration, Washington.

Barksdale R.D. and Goughnour R.R. (1984) "Settlement performance of stone columns in the US", Proc. Int. Conf. on In-situ Soil and Rock Reinforcement, Paris, 105-110.

Bell, A.L. (1915) "The lateral pressure and resistance of clay and the supporting power of clay foundations.", Proc. ICE, 199-233.

Bolton, M.D. (1986) "The strength and dilatancy of sands", Geotechnique, Vol. 36, No. 1, 65-78.

Bowles, J. E. (1982) "Foundation analysis and design", McGraw Hill, 3rd ed., USA.

Brauns, J. (1978) "Initial bearing capacity of stone columns and sand piles", Symposium on Soil Reinforcing and Stabilizing Techniques, Sydney, 477-496.

Budhu, M. (2000) "Soil mechanics and foundations", John Wiley & Sons, INC., 1st ed., New York.

Canetta G. and Nova R. (1989) "Numerical modeling of a circular foundation over vibrofloated sand", Proc. 3rd Numerical models in geomechanics (NUMOG), 215-222.

Caquot, A., Kerisel, J. and Absi, E. (1972) "Tables de butée et de poussée", 2nd ed., Gauthier-Villars Éditeur, Paris.

Chen, W. F. (1975) "Limit Analysis and Soil Plasticity", Elsevier Scientific Publishing Company, New York.

Christoulas St., Bouckovalas G. and Giannaros Ch. (2000) "An experimental study on model stone columns", Soils and Foundations, Vol. 40, No. 6, 11-22.

Clark, J. I. (1998) "The settlement and bearing capacity of very large foundations on strong soils: 1996 R. M. Hardy keynote address", Canadian Geotechnical Journal. Vol. 35, 131-145.

Cooper, M.R. and Rose, A.N. (1999) "Stone column support for an embankment on deep alluvial soils", Proc. of the Institution of Civil Engineers – Geotechnical Engineering, Vol. 137, No. 1, 15-25.

Costet, J. and Sanglerat, G. (1983) "Cours Pratique de Mecanique des Sols", Dunod Edition. Paris (In French).

Das B.M. (2000) "Fundamentals of geotechnical engineering" Brooks/Cole, 1st ed., USA.

Datye K.R. (1982) "Settlement and bearing capacity of foundation system with stone columns", Proc. Symposium on Soil & Rock Improvement Techniques Including Geotextiles, Reinforced Earth and Modern Piling Methods, AIT, Bangkok, Thailand.

Dhouib, A., Wehr, J., Soyez, B. and Priebe H.J. (2004) "Méthod de Priebe: Origine, développement et applications", Proc. Int. Symposium on Ground Improvement, Paris, 131-146 (In French).

Etezad, M., Hanna, A.M. and Ayadat, T. (2005a) "Numerical Model for Group of Stone Columns" Proc. 73rd Annual Meeting of ICOLD, Tehran, Iran.

Etezad, M., Hanna, A.M., and Ayadat, T. (2005b) "Analytical model of a group of stone columns", Proc. 33rd Annual Conference of the Canadian Society for Civil Engineering, Toronto, Canada.

Etezad, M., Hanna, A.M., and Ayadat, T. (2006) "Bearing capacity of group of stone columns", Proc. VIth European Conference on Numerical Methods in Geotechnical Engineering. Graz, Austria, 781-786.

Etezad, M., Hanna, A.M. and Ayadat, T. (2007) "Modes of failure of group of stone columns under a raft foundation" Proceedings, 10th Australia New Zealand conference on Geomechanics, Brisbane, Australia.

Gerrard, C.M., Pande, G.N. and Schweiger, H.F. (1984) "Modeling behavior of soft clay reinforced with stone columns", Proc. Int. Conf. on In-situ Soil and Rock Reinforcement, Paris, 145-150.

Gibson, R.E. and Anderson, W.F. (1961) "In-situ measurements of soil properties with pressuremeter" Civ. Eng. And Pub. Works Rev., Vol. 56, No. 658, 615-618.

Goughnour, R.R. (1983) "Settlement of vertically loaded stone columns in soft ground", Proc. 8th European Conf. on Soil Mechanics and Foundation Engineering, Helsinki, 235-240.

Goughnour, R.R. and Barksdale, R.D. (1984), "Performance of a stone column supported embankment", Proc. of Int. Conf. on Case Histories in Geotechnical Eng., University of Missouri-Rolla, 2, 735-741.

Goughnour, R.R. and Bayuk, A.A. (1979a) "Analysis of stone column-soil matrix interaction under vertical load", Proc. Int. Conf. on Soil Reinforcement, Paris, 271-277.

Goughnour, R.R. and Bayuk, A.A. (1979b) "Field study of long term settlements of loads supported by stone columns in soft ground", Proc. Int. Conf. on Soil Reinforcement, Paris, 279-285.

Greenwood, D.A. (1970) "Mechanical improvement of soils below ground surface", Proc. of Ground Engineering Conf., Instn. Civ. Eng., 11-22.

Greenwood, D.A. and Kirsch, K. (1984) "Specialist ground treatment by vibratory and dynamic methods", Proc. Int. Conf. on Piling and Ground Treatment, London, 17-45.

Hu, W. (1995) "Physical modeling of group behavior of stone column foundations", Ph.D. Thesis, University of Glasgow.

Hu, W., Wood, D.M. and Stewart W. (1997) "Ground improvement using stone column foundations: results of model tests", Proc. Int. Conf. on Ground Improvement Techniques, Macau, 247-256.

Hughes, J.M.O and Withers, N.J. (1974) "Reinforcing of soft cohesive soils with stone columns", Ground Engineering, 42-49.

Hughes, J.M.O., Withers, N.J. and Greenwood, D.A. (1975) "A field trial of the reinforcing effect of a stone column in soil", Geotechnique, Vol. 25, No. 1, 31-44.

Kamon M. and D.T. Bergado (1991) "Ground improvement techniques", Proc. 9th Asian Regional Conf. on Soil Mechanics and Foundation Engineering, 2, 521-548.

Kolár, V. and Nemec, I. (1989) "Modeling of soil-structure interaction", Elsevier, New York.

Kumbhojkar, A.S. (1993). "Numerical evaluation of Terzaghi's N_γ", ASCE, Journal of Geotechnical Engineering, Vol. 119, No. 3, 598-607.

Lee, J.S. and Pande, G.N. (1994) "Analysis of stone column reinforced foundations" Departmental Research Report CR/835/94, University College of Swansea.

Lee, J.S. and Pande, G.N. (1998) "Analysis of stone-column reinforced foundations", Int. Jour. for Numerical and Analytical Methods in Geomechanics, Vol. 22, No. 12, 1001-1020.

Madhav, M.R. and Vitkar, P.P. (1978), "Strip footing on weak clay stabilized with a granular trench or pile", Canadian Geotechnical Journal, 605-609.

McKelvey, D. (2002) "The performance of vibro stone column reinforced foundations in deep soft ground", Ph.D. thesis, Queen's University of Belfast, Belfast, UK.

McKelvey, D. and Sivakumar, V. (2000) "A review of the performance of vibro stone column foundations" Proc. 3rd Int. Conf. on Ground Improvement Techniques, Singapore, 245-254.

McKelvey, D., Sivakumar, V., Bell, A. and Graham, J. (2004) "Modeling vibrated stone columns in soft clay", Proceedings of the Institution of Civil Engineers: Geotechnical Engineering, Vol.157, No. 3,137-149.

Mestat, P. and Riou, Y. (2004) "Validation des modèles numériques de sol amélioré par colonnes ", Proc. Int. Symp. on Ground Improvement, Paris, 229-243 (In French).

Mestat Ph., Magnan J.P. and Dhouib A. (2006) "Bearing capacity of group of stone columns", Proc. VIth European Conference on Numerical Methods in Geotechnical Engineering. Graz, Austria, 471-476.

Mitchell, J.K. and Katti R.K. (1981) "Soil improvement – state of the art report" 10th Int. Conf. on Soil Mechanics and Foundation Eng. Stockholm, 261-313.

Mitchell, J.K. and Huber, T.R. (1985) "Performance of a stone column foundation", Jour. of Geotechnical Engineering ASCE, Vol. 111, No. 2, 205-223.

Ohbayashi, J. Harada K. and Yamamoto M. (1999) "Resistance against liquefaction of ground improved by sand compaction pile method", Proc. 2nd Int. Conf. on Earthquake Engineering, Balkema, Rotterdam, 549-554.

Pande, G.N. and Lee, J.S. (1993) "Homogenization techniques for strain localization and interface analysis", Proc. 2th Asian-Pacific Conf. Computational Mechanics, 411-417.

Poorooshasb, H.B., Holubec, I. and Sherbourne A.N. (1966) "Yielding and flow of sand in triaxial compression, Part 1", Canadian Geotechnical Journal, Vol. 3, No. 4, 179-189.

Poorooshasb, H.B., Holubec, I. and Sherbourne A.N. (1967) "Yielding and flow of sand in triaxial compression, Part 2 and 3", Canadian Geotechnical Journal, Vol. 4, No. 4, 376-397.

Poorooshasb, H.B. and Meyerhof, G.G. (1997) "Analysis of behavior of stone columns and lime columns", Computers and Geotechnics, Vol. 20, No. 1, 47-70.

Poorooshasb, H.B., Miura, N. and Noorzad, A. (1997), "An Upper Bound Analysis of the Behavior of stone columns.", Special lecture delivered by the first author at the inauguration ceremony of the new facilities of the Institute for Lowland Technology, Saga University, Saga, Japan.

Priebe, H.J. (1976) "Abschätzung des Setzungsverhaltens eines durch Stopfverdichtung verbesserten Baugrundes", Die Bautechnik, 53, H.5, 160-162 (In German).

Priebe, H.J. (1991) "Vibro replacement – design criteria and quality control", Deep Foundation Improvements: Design, Construction and Testing, ASTM STP 1089, Philadelphia, 62-72.

Priebe, H.J. (1995) "The design of vibro replacement", Ground Engineering, Vol. 28, No. 10, 31-37.

Rao, N.S., Reddy, K.M. and Rumar, P.H. (1997) "Studies on groups of stone columns in soft clays", Geotechnical Engineering – Bangkok, Vol. 28, No. 2, 165-182.

Saha, S., Santhanu, S. and Roy, A. (2000) "Analysis of stone column in soft ground" Proc. Indian Geotech. Conf., Bombay, India, 297-300.

Schweiger, H.F. and Pande, G.N. (1986) "Numerical analysis of stone column supported foundations", Computers and Geotechnics, Vol. 2, 347-372.

Schweiger, H.F. and Pande, G.N. (1988) "Numerical analysis of road embankment constructed on soft clay stabilized with stone columns", Proc. Num. Methods in Geomechanics, Rotterdam, 1329-1333.

Schweiger, H.F. and Pande, G.N. (1989) "Modeling stone column reinforced soil – a modified voigt approach", Proc. 3rd Numerical Models in Geomechanics (NUMOG), 204-214.

Shahu, J.T., Madhav, M.R. and Hayashi, S. (2000) "Analysis of granular pile-mat system for soils with stiff crust", Geotechnical Engineering – Bangkok, Vol. 31, No. 1, 1-16.

Silvestri, V. (2003) "A limit equilibrium solution for bearing capacity of strip foundations on sand", Canadian Geotechnical Journal, Vol. 40, No. 2, 351-361.

Steuerman, S., (1939) "A new soil compaction device", Eng. News Record., Now York.

Terashi, M., Kitazume, M. and Minagawa, S. (1991) "Bearing capacity of improved ground by sand compaction piles", Deep Foundation Improvements: Design, Construction and Testing, ASTM – STP 1089, 47-61.

Thorburn, S. and MacVicar, R.S.L. (1968) "Soil stabilization employing surface and depth vibrators", The Structural Engineer, Vol. 46, No. 10, 309-316.

Vautrain, J. (1997) "Reinforced earth wall on stone columns in soil", Proc. Int. Symp. On Soft Clay, Bangkok, 613-626.

Vesic, A.S. (1972) "Expansion of cavities in infinite soil mass", Jour. Of the Soil Mechanics and Foundations div., ASCE, Vol. 98, 265-290.

The Vibroflotation Group "Vibratory ground improvement manual", Retrieved 2007, from

http://www.vibroflotation.com/vibroflotation6.htm

Wehr, W. (1999) "Schottersäulen – das verhalten von einzelnen säulen und säulengruppen", Geotechnik, Vol. 22, No. 1, 40-47, (In German).

Wood, M.D. and Hu, W. (1997) "Mechanism of load transfer deduced from failure modes of model stone column foundations", Proc. Deformation and Progressive Failure in Geomechanics, 799-804.

Wood, M.D., Hu, W. and Nash, D.F.T. (2000) "Group effects in stone column foundations: model tests", Geotechnique, Vol. 50, No. 6, 689-698.

Wong, H. Y. (1975) "Vibroflotation – its effect on weak cohesive soils", Civ. Eng., London, No. 824, 44-67.

Wright, H. and Touquet, J. L. (2004) "Calcul des colonnes ballastées sous un dallage-comparaison des résultats de différentes méthodes", Proc. Int. Symp. on Ground Improvement, Paris, 333-346 (In French).

APPENDIX 1

Soil and geometry parameters used in the numerical model for determination of mode of failure for group of stone columns are presented here.

No.	A_s %	ϕ_s	ϕ_c	$\tan(\phi_s)^*$ $\tan(\phi_c)$	B (m)	D_f (m)	d (m)	d/B	c (kN/m^2)	γ_c (kN/m^3)	$\gamma c^* D_f/c$	Failure shape
1	35	35	5	0.06	2.5	0.2	1	0.40	5	8	0.3	local
2	35	40	5	0.07	2.5	0.2	1	0.40	5	8	0.3	local
3	35	40	5	0.07	2.5	5.0	1	0.40	5	8	8.0	local
4	35	45	5	0.09	2.5	0.2	1	0.40	2	8	0.8	local
5	35	45	5	0.09	2.5	1.0	1	0.40	5	8	1.6	local
6	35	45	5	0.09	2.5	2.0	1	0.40	5	8	3.2	local
7	35	45	5	0.09	2.5	3.0	1	0.40	2	8	12.0	local
8	35	45	5	0.09	2.5	5.0	1	0.40	5	8	8.0	local
9	35	40	25	0.39	2.5	4.0	1	0.40	10	16	6.4	local
10	35	35	25	0.33	2.5	5.0	1	0.40	15	16	5.3	local
11	35	35	10	0.12	2.5	0.2	1	0.40	5	12	0.5	local
12	35	40	10	0.15	2.5	0.2	1	0.40	2	12	1.2	local
13	35	35	12	0.15	2.5	0.2	1	0.40	5	13	0.5	local
14	35	45	13	0.23	2.5	1.0	1	0.40	5	13.5	2.7	local
15	35	45	10	0.18	2.5	0.2	1	0.40	2	12	1.2	local
16	35	45	10	0.18	2.5	1.0	1	0.40	5	12	2.4	local
17	35	40	25	0.39	2.5	0.7	1	0.40	5	16	2.2	local
18	35	45	25	0.47	2.5	2.0	1	0.40	2	16	16.0	local
19	35	35	10	0.12	2.5	1.0	1	0.40	3	12	4.0	local
20	35	35	10	0.12	2.5	2.0	1	0.40	2	12	12.0	local
21	35	35	10	0.12	2.5	2.5	1	0.40	15	12	2.0	local
22	35	45	25	0.47	2.5	3.0	1	0.40	5	16	9.6	local
23	35	45	12	0.21	2.5	1.3	1	0.40	5	13	3.4	local
24	35	45	10	0.18	2.5	2.0	1	0.40	5	12	4.8	local
25	35	40	10	0.15	2.5	2.0	1	0.40	8	12	3.0	local
26	35	40	10	0.15	1.5	3.0	0.6	0.40	15	12	2.4	local
27	35	40	10	0.15	1.5	3.0	0.6	0.40	15	12	2.4	local
28	35	40	10	0.15	1.5	2.0	0.6	0.40	2	12	12.0	local
29	35	45	10	0.18	3.0	0.2	1.2	0.40	5	12	0.5	local
30	35	35	13	0.16	2.5	0.2	1	0.40	5	13.5	0.5	general
31	35	40	12	0.18	2.5	0.2	1	0.40	5	13	0.5	general
32	35	40	12	0.18	2.5	0.2	1	0.40	15	13	0.2	general
33	35	40	25	0.39	2.5	3.0	1	0.40	10	16	4.8	general
34	35	35	25	0.33	2.5	4.0	1	0.40	15	16	4.3	general

35	35	40	13	0.19	2.5	0.2	1	0.40	2	13.5	1.4	general
36	35	35	15	0.19	2.5	0.2	1	0.40	5	14	0.6	general
37	35	45	12	0.21	2.5	0.2	1	0.40	15	13	0.2	general
38	35	45	12	0.21	3.0	0.2	1.2	0.40	10	13	0.3	general
39	35	45	13	0.23	2.5	0.2	1	0.40	2	13.5	1.4	general
40	35	40	15	0.22	2.5	0.2	1	0.40	5	14	0.6	general
41	35	45	15	0.27	2.5	0.2	1	0.40	10	14	0.3	general
42	35	45	15	0.27	2.5	1.0	1	0.40	5	14	2.8	general
43	35	45	25	0.47	2.5	0.2	1	0.40	2	16	1.6	general
44	35	45	25	0.47	2.5	1.0	1	0.40	5	16	3.2	general
45	35	45	25	0.47	2.5	0.3	1	0.40	10	16	0.5	general
46	35	45	25	0.47	2.5	1.0	1	0.40	15	16	1.1	general
47	35	45	25	0.47	2.5	2.0	1	0.40	6	16	5.3	general
48	35	45	25	0.47	2.5	0.5	1	0.40	10	16	0.8	general
49	35	45	25	0.47	2.5	1.0	1	0.40	3	16	5.3	general
50	35	45	10	0.18	2.5	0.3	1	0.40	10	12	0.4	general
51	35	45	10	0.18	1.5	0.1	0.6	0.40	2	12	0.6	general
52	35	40	15	0.22	1.5	0.4	0.6	0.40	3	14	1.9	general
53	35	45	10	0.18	1.5	0.3	0.6	0.40	15	12	0.2	general
54	35	45	10	0.18	1.5	0.3	0.6	0.40	10	12	0.4	general
55	35	45	25	0.47	2.5	1.5	1	0.40	15	16	1.6	general
56	35	40	15	0.22	2.5	1.0	1	0.40	10	14	1.4	general
57	35	40	15	0.22	2.5	0.3	1	0.40	2	14	2.1	general
58	35	40	15	0.22	2.5	0.2	1	0.40	15	14	0.2	general
59	35	45	25	0.47	2.5	0.5	1	0.40	2	16	4.0	general
60	30	40	13	0.19	2.6	0.2	1	0.38	5	13.5	0.5	general
61	30	40	13	0.19	3.1	0.2	1.2	0.38	15	13.5	0.2	general
62	30	45	15	0.27	3.1	1.5	1.2	0.38	10	14	2.1	general
63	30	40	25	0.39	3.1	3.5	1.2	0.38	15	16	3.7	general
64	30	40	12	0.18	2.6	0.2	1	0.38	5	13	0.5	general
65	30	45	12	0.21	2.6	0.2	1	0.38	5	13	0.5	general
66	30	45	25	0.47	2.6	0.2	1	0.38	5	16	0.6	general
67	30	40	13	0.19	3.1	0.2	1.2	0.38	15	13.5	0.2	general
68	30	40	15	0.22	2.6	1.3	1	0.38	5	16	4.2	local
69	30	35	13	0.16	3.1	0.2	1.2	0.38	8	13.5	0.3	local
70	30	35	13	0.16	3.1	0.2	1.2	0.38	2	13.5	1.4	local
71	30	40	13	0.19	2.6	0.5	1	0.38	5	13	1.3	local
72	30	45	5	0.09	2.6	5.0	1	0.38	5	8	8.0	local
73	30	40	10	0.15	2.6	0.2	1	0.38	5	12	0.5	local
74	30	45	10	0.18	2.6	0.2	1	0.38	5	12	0.5	local
75	30	45	10	0.18	3.1	0.2	1.2	0.38	2	12	1.2	local
76	30	45	25	0.47	2.6	1.0	1	0.38	2	16	8.0	local
77	20	35	5	0.06	3.0	0.2	1	0.34	5	8	0.3	local
78	20	40	5	0.07	3.0	0.2	1	0.34	5	8	0.3	local
79	20	40	5	0.07	3.0	4.7	1	0.34	15	8	2.5	local
80	20	45	5	0.09	3.0	0.2	1	0.34	5	8	0.3	local

81	20	45	5	0.09	3.0	0.2	1	0.34	5	8	0.3	local
82	20	45	5	0.09	3.0	1.0	1	0.34	15	8	0.5	local
83	20	45	5	0.09	3.0	3.0	1	0.34	10	8	2.4	local
84	20	45	15	0.27	3.0	4.0	1	0.34	15	14	3.7	local
85	20	40	25	0.39	3.0	2.0	1	0.34	5	16	6.4	local
86	20	45	25	0.47	3.0	1.5	1	0.34	10	16	2.4	local
87	20	45	25	0.47	3.0	1.0	1	0.34	15	16	1.1	local
88	20	45	25	0.47	3.0	2.0	1	0.34	5	16	6.4	local
89	20	45	25	0.47	3.0	5.0	1	0.34	15	16	5.3	local
90	20	35	5	0.06	1.8	0.2	0.6	0.34	10	8	0.2	local
91	20	40	5	0.07	1.8	0.2	0.6	0.34	15	8	0.1	local
92	20	40	5	0.07	1.8	5.0	0.6	0.34	15	8	2.7	local
93	20	45	5	0.09	1.8	2.0	0.6	0.34	10	8	1.6	local
94	20	45	5	0.09	1.8	0.2	0.6	0.34	15	8	0.1	local
95	20	45	5	0.09	3.6	1.0	1.2	0.34	10	8	0.8	local
96	20	45	5	0.09	3.6	0.2	1.2	0.34	5	8	0.3	local
97	20	45	15	0.27	3.6	0.2	1.2	0.34	5	14	0.6	local
98	20	40	25	0.39	3.6	0.2	1.2	0.34	5	16	0.6	local
99	20	45	25	0.47	3.6	0.2	1.2	0.34	5	16	0.6	local
100	20	45	25	0.47	3.6	1.0	1.2	0.34	5	16	3.2	local
101	20	45	25	0.47	2.4	0.2	0.8	0.34	5	16	0.6	local
102	20	45	25	0.47	2.4	5.0	0.8	0.34	5	16	16.0	local
103	20	45	25	0.47	3.0	1.0	1	0.34	3	16	5.3	local
104	20	45	25	0.47	3.0	1.5	1	0.34	8	16	3.0	local
105	20	45	25	0.47	3.0	3.0	1	0.34	10	16	4.8	local
106	20	45	25	0.47	3.6	1.2	1.2	0.34	2	16	9.6	local
107	20	45	25	0.47	3.6	4.0	1.2	0.34	15	16	4.3	local
108	20	40	15	0.22	3.0	4.0	1	0.34	10	14	5.6	local
109	20	40	15	0.22	3.0	3.0	1	0.34	6	14	7.0	local
110	20	40	15	0.22	3.0	2.0	1	0.34	15	14	1.9	local
111	20	35	10	0.12	3.0	1.0	1	0.34	5	12	2.4	local
112	20	35	10	0.12	3.0	3.0	1	0.34	12	12	3.0	local
113	20	35	10	0.12	3.0	0.3	1	0.34	4	12	0.9	local
114	20	35	10	0.12	3.0	0.1	1	0.34	3	12	0.4	local
115	20	35	10	0.12	1.8	0.3	0.6	0.34	12	12	0.3	local
116	20	35	5	0.06	1.8	0.2	0.6	0.34	15	8	0.1	local
117	20	40	5	0.07	1.8	0.2	0.6	0.34	10	8	0.2	local
118	20	45	5	0.09	1.8	0.2	0.6	0.34	10	8	0.2	local
119	20	45	5	0.09	1.8	0.2	0.6	0.34	15	8	0.1	local
120	20	45	5	0.09	3.6	1.0	1.2	0.34	15	8	0.5	local
121	20	35	10	0.12	2.4	0.2	0.8	0.34	5	12	0.5	local
122	20	35	10	0.12	2.4	0.2	0.8	0.34	15	12	0.2	local
123	20	40	25	0.39	3.0	1.0	1	0.34	5	16	3.2	local
124	20	40	5	0.07	3.0	5.0	1	0.34	5	8	8.0	local
125	20	35	10	0.12	3.0	0.2	1	0.34	5	12	0.5	local
126	20	45	5	0.09	3.6	0.2	1.2	0.34	10	8	0.2	local

127	20	45	15	0.27	3.6	0.2	1.2	0.34	10	14	0.3	local
128	20	40	25	0.39	3.6	0.2	1.2	0.34	8	16	0.4	local
129	20	45	25	0.47	3.6	0.2	1.2	0.34	8	16	0.4	local
130	20	45	25	0.47	3.6	1.0	1.2	0.34	9	16	1.8	local
131	20	45	25	0.47	2.4	0.2	0.8	0.34	12	16	0.3	local
132	20	45	25	0.47	2.4	5.0	0.8	0.34	15	16	5.3	local
133	20	40	12	0.18	3.0	5.0	1	0.34	5	13	13.0	punching
134	20	40	5	0.07	1.8	5.0	0.6	0.34	8	8	5.0	punching
135	20	40	25	0.39	3.0	4.0	1	0.34	5	16	12.8	punching
136	20	45	25	0.47	3.0	3.5	1	0.34	4	16	14.0	punching
137	20	45	15	0.27	3.0	3.5	1	0.34	4	14	12.3	punching
138	20	40	5	0.07	1.8	5.0	0.6	0.34	10	8	4.0	punching
139	20	40	15	0.22	3.6	3.0	1.2	0.34	3	14	14.0	punching
140	20	45	5	0.09	3.0	0.5	1	0.34	2	13	3.3	punching
141	15	45	25	0.47	3.3	0.1	1	0.30	5	16	0.3	local
142	15	40	15	0.22	3.3	0.1	1	0.30	5	14	0.3	local
143	10	45	25	0.47	3.8	0.2	1	0.26	5	16	0.6	local
144	10	45	25	0.47	3.8	1.0	1	0.26	5	16	3.2	local
145	10	45	25	0.47	3.8	2.0	1	0.26	5	16	6.4	local
146	10	40	25	0.39	3.8	2.0	1	0.26	5	16	6.4	local
147	10	40	13	0.19	3.8	0.2	1	0.26	5	13.5	0.5	local
148	10	40	13	0.19	3.0	0.2	0.8	0.26	10	13.5	0.3	local
149	10	40	12	0.18	3.0	0.2	0.8	0.26	2	13	1.3	local
150	10	40	13	0.19	3.0	0.2	0.8	0.26	15	13.5	0.2	local
151	10	40	15	0.22	3.8	5.0	1	0.26	5	14	14.0	local
152	10	40	12	0.18	3.8	0.2	1	0.26	5	13	0.5	local
153	10	40	15	0.22	2.3	2.0	0.6	0.26	10	14	2.8	local
154	10	45	5	0.09	2.3	0.1	0.6	0.26	15	8	0.1	local
155	10	45	25	0.47	2.3	0.3	0.6	0.26	15	16	0.3	local
156	10	45	25	0.47	2.3	0.3	0.6	0.26	8	16	0.6	local
157	10	40	12	0.18	3.0	0.2	0.8	0.26	10	13	0.3	local
158	10	40	10	0.15	3.0	0.2	0.8	0.26	2	12	1.2	punching
159	10	40	10	0.15	3.0	0.2	0.8	0.26	2	12	1.2	punching
160	10	40	12	0.18	3.8	5.0	1	0.26	5	13	13.0	punching
161	10	40	25	0.39	3.8	1.0	1	0.26	2	16	8.0	punching
162	10	35	25	0.33	3.8	3.0	1	0.26	8	16	6.0	punching
163	10	40	10	0.15	3.8	0.2	1	0.26	5	12	0.5	punching
164	10	40	15	0.22	3.8	4.0	1	0.26	5	14	11.2	punching
165	10	40	15	0.22	3.8	3.0	1	0.26	5	14	8.4	punching
166	10	45	10	0.18	3.8	2.5	1	0.26	10	12	3.0	punching
167	10	40	10	0.15	3.8	0.2	1	0.26	5	12	0.5	punching
168	10	45	25	0.47	3.8	1.0	1	0.26	2	16	8.0	punching
169	10	35	10	0.12	3.8	0.1	1	0.26	5	12	0.2	punching
170	10	35	10	0.12	2.3	1.5	0.6	0.26	2	12	9.0	punching
171	10	45	5	0.09	3.8	0.2	1	0.26	5	8	0.3	punching
172	10	35	10	0.12	2.3	1.5	0.6	0.26	15	12	1.2	punching

173	35	45	5	0.09	4.0	1.5	1	0.25	13	8	0.9	local
174	35	35	25	0.33	4.0	4.5	1	0.25	6	16	12.0	local
175	35	45	5	0.09	4.0	1.0	1	0.25	15	8	0.5	local
176	35	40	12	0.18	4.0	3.0	1	0.25	6	13	6.5	local
177	35	45	13	0.23	4.0	2.0	1	0.25	5	13.5	5.4	local
178	35	45	13	0.23	4.0	5.0	1	0.25	5	13.5	13.5	local
179	35	45	15	0.27	4.0	2.0	1	0.25	15	14	1.9	local
180	35	45	15	0.27	4.0	3.0	1	0.25	5	14	8.4	local
181	35	45	25	0.47	4.0	3.0	1	0.25	15	16	3.2	local
182	35	45	25	0.47	4.0	1.0	1	0.25	5	16	3.2	local
183	35	45	25	0.47	4.0	2.0	1	0.25	5	16	6.4	local
184	35	45	25	0.47	4.0	2.5	1	0.25	15	16	2.7	local
185	35	45	25	0.47	4.0	3.0	1	0.25	5	16	9.6	local
186	35	45	25	0.47	4.0	5.0	1	0.25	6	16	13.3	local
187	35	45	25	0.47	4.0	3.0	1	0.25	5	16	9.6	local
188	35	45	25	0.47	4.0	3.0	1	0.25	15	16	3.2	local
189	35	35	10	0.12	4.0	1.0	1	0.25	10	12	1.2	local
190	35	45	5	0.09	4.0	3.0	1	0.25	5	8	4.8	punching
191	35	45	5	0.09	4.0	5.0	1	0.25	5	8	8.0	punching
192	35	45	10	0.18	4.0	5.0	1	0.25	5	12	12.0	punching
193	35	40	12	0.18	4.0	4.5	1	0.25	8	13	7.3	punching
194	35	40	5	0.07	4.0	4.0	1	0.25	5	8	6.4	punching
195	35	40	25	0.39	4.0	4.5	1	0.25	5	16	14.4	punching
196	35	40	5	0.07	4.8	3.0	1.2	0.25	15	8	1.6	punching
197	35	35	5	0.06	4.8	2.0	1.2	0.25	10	8	1.6	punching
198	35	45	5	0.09	4.0	4.0	1	0.25	8	8	4.0	punching
199	35	45	5	0.09	4.0	4.5	1	0.25	5	8	7.2	punching
200	35	40	5	0.07	4.0	3.0	1	0.25	8	8	3.0	punching
201	35	40	5	0.07	4.0	4.0	1	0.25	5	8	6.4	punching
202	35	40	5	0.07	4.8	0.2	1.2	0.25	2	8	0.8	punching
203	35	35	5	0.06	4.8	0.2	1.2	0.25	15	8	0.1	punching
204	35	40	10	0.15	4.0	0.5	1	0.25	5	12	1.2	punching
205	35	35	5	0.06	4.0	4.0	1	0.25	15	8	2.1	punching
206	35	45	12	0.21	4.0	5.0	1	0.25	5	13	13.0	punching
207	35	45	5	0.09	4.0	5.0	1	0.25	3	8	13.3	punching
208	35	35	10	0.12	4.0	5.0	1	0.25	10	12	6.0	punching
209	35	45	5	0.09	4.0	2.0	1	0.25	5	8	3.2	punching
210	30	45	5	0.09	4.2	4.5	1	0.24	5	8	7.2	local
211	30	45	10	0.18	4.2	1.0	1	0.24	15	12	0.8	local
212	30	45	10	0.18	4.2	2.0	1	0.24	5	12	4.8	local
213	30	45	10	0.18	4.2	5.0	1	0.24	5	12	12.0	local
214	30	40	12	0.18	4.2	1.0	1	0.24	10	13	1.3	local
215	30	35	15	0.19	4.2	2.0	1	0.24	15	14	1.9	local
216	30	45	12	0.21	4.2	4.0	1	0.24	15	13	3.5	local
217	30	45	15	0.27	4.2	5.0	1	0.24	10	14	7.0	local
218	30	45	15	0.27	4.2	1.0	1	0.24	5	14	2.8	local

219	30	40	25	0.39	4.2	3.0	1	0.24	5	16	9.6	local
220	30	45	25	0.47	4.2	2.0	1	0.24	15	16	2.1	local
221	30	35	13	0.16	3.4	0.2	0.8	0.24	2	13.5	1.4	local
222	30	45	25	0.47	4.2	1.0	1	0.24	8	16	2.0	local
223	30	45	25	0.47	4.2	3.0	1	0.24	5	16	9.6	local
224	30	45	25	0.47	4.2	2.0	1	0.24	12	16	2.7	local
225	30	45	25	0.47	2.5	3.0	0.6	0.24	10	16	4.8	local
226	30	45	25	0.47	2.5	3.0	0.6	0.24	2	16	24.0	local
227	30	45	25	0.47	2.5	2.0	0.6	0.24	15	16	2.1	local
228	30	35	25	0.33	2.5	4.5	0.6	0.24	8	16	9.0	local
229	30	40	15	0.22	4.2	1.0	1	0.24	15	14	0.9	local
230	30	40	10	0.15	4.2	0.2	1	0.24	5	12	0.5	local
231	30	40	10	0.15	3.4	0.2	0.8	0.24	2	12	1.2	local
232	30	40	15	0.22	2.5	3.0	0.6	0.24	15	14	2.8	local
233	30	40	10	0.15	3.4	0.2	0.8	0.24	8	12	0.3	local
234	30	40	12	0.18	3.4	0.2	0.8	0.24	15	13	0.2	local
235	30	40	12	0.18	3.4	0.2	0.8	0.24	5	13	0.5	punching
236	30	35	25	0.33	4.2	3.0	1	0.24	3	16	16.0	punching
237	30	45	15	0.27	4.2	5.0	1	0.24	7	14	10.0	punching
238	30	45	12	0.21	4.2	4.0	1	0.24	10	13	5.2	punching
239	30	45	5	0.09	4.2	4.0	1	0.24	5	8	6.4	punching
240	30	45	25	0.47	4.2	3.0	1	0.24	3	16	16.0	punching
241	30	40	15	0.22	4.2	2.0	1	0.24	2	14	14.0	punching
242	30	40	13	0.19	4.2	5.0	1	0.24	12	13.5	5.6	punching
243	30	45	5	0.09	4.2	0.2	1	0.24	5	8	0.3	punching
244	30	35	10	0.12	4.2	1.5	1	0.24	3	12	6.0	punching
245	30	35	13	0.16	4.2	0.2	1	0.24	5	13.5	0.5	punching
246	30	40	25	0.39	4.2	3.0	1	0.24	4	16	12.0	punching
247	30	35	13	0.16	3.4	3.0	0.8	0.24	10	13.5	4.1	punching
248	30	35	5	0.06	4.2	0.2	1	0.24	5	8	0.3	punching
249	30	40	5	0.07	4.2	3.0	1	0.24	5	8	4.8	punching
250	30	35	13	0.16	4.2	0.2	1	0.24	5	13.5	0.5	punching
251	30	45	5	0.09	4.2	5.0	1	0.24	6	8	6.7	punching
252	30	40	10	0.15	4.2	3.0	1	0.24	5	12	7.2	punching
253	30	45	5	0.09	4.2	5.0	1	0.24	5	8	8.0	punching
254	30	45	5	0.09	4.2	4.0	1	0.24	10	8	3.2	punching
255	30	45	25	0.47	4.2	3.0	1	0.24	3	16	16.0	punching
256	30	45	12	0.21	4.2	1.0	1	0.24	2	13	6.5	punching
257	30	40	12	0.18	4.2	0.2	1	0.24	5	13	0.5	punching
258	30	35	10	0.12	2.5	1.0	0.6	0.24	8	12	1.5	punching
259	30	45	5	0.09	4.2	1.0	1	0.24	7	8	1.1	punching
260	30	45	5	0.09	4.2	2.0	1	0.24	10	8	1.6	punching
261	30	45	5	0.09	4.2	3.0	1	0.24	12	8	2.0	punching
262	30	40	5	0.07	4.2	1.0	1	0.24	2	8	4.0	punching
263	30	40	5	0.07	4.2	1.5	1	0.24	15	8	0.8	punching
264	30	40	5	0.07	4.2	3.0	1	0.24	10	8	2.4	punching

265	20	35	25	0.33	5.0	0.2	1	0.20	5	16	0.6	local
266	20	35	25	0.33	5.0	0.5	1	0.20	5	16	1.6	local
267	20	40	25	0.39	4.0	3.0	0.8	0.2	10	16	4.8	local
268	20	45	25	0.47	5.0	2.0	1	0.2	6	16	5.3	local
269	20	45	15	0.27	4.0	0.6	0.8	0.2	8	14	1.1	local
270	20	45	15	0.27	4.0	0.2	0.8	0.20	8	14	0.4	local
271	20	40	25	0.39	5.0	0.2	1	0.20	5	16	0.6	local
272	20	45	25	0.47	5.0	0.2	1	0.20	2	16	1.6	local
273	20	40	25	0.39	4.0	0.2	0.8	0.20	10	16	0.3	local
274	20	45	25	0.47	5.0	0.1	1	0.20	10	16	0.2	local
275	20	45	25	0.47	3.0	0.2	0.6	0.20	2	16	1.6	local
276	20	35	25	0.33	5.0	0.5	1	0.20	5	16	1.6	local
277	20	45	25	0.47	3.0	4.0	0.6	0.20	8	16	8.0	punching
278	20	45	15	0.27	5.0	0.2	1	0.20	5	14	0.6	punching
279	20	35	25	0.33	5.0	5.0	1	0.20	10	16	8.0	punching
280	20	45	15	0.27	4.0	0.2	0.8	0.20	5	14	0.6	punching
281	20	45	25	0.47	3.0	3.0	0.6	0.20	5	16	9.6	punching
282	20	35	25	0.33	3.0	3.0	0.6	0.20	5	16	9.6	punching
283	20	35	15	0.19	5.0	0.2	1	0.20	5	14	0.6	punching
284	20	35	15	0.19	5.0	5.0	1	0.20	10	14	7.0	punching
285	20	35	25	0.33	5.0	2.0	1	0.20	9	16	3.6	punching
286	20	40	15	0.22	5.0	0.2	1	0.20	5	14	0.6	punching
287	20	45	15	0.27	5.0	0.2	1	0.20	5	14	0.6	punching
288	20	35	25	0.33	5.0	5.0	1	0.20	15	16	5.3	punching
289	20	45	25	0.47	5.0	0.8	1	0.20	2	16	6.4	punching
290	20	40	25	0.39	4.0	0.2	0.8	0.20	5	16	0.6	punching
291	20	40	25	0.39	5.0	0.2	1	0.20	5	16	0.6	punching
292	20	40	25	0.39	3.0	2.0	0.6	0.20	3	16	10.7	punching
293	20	40	25	0.39	3.0	4.0	0.6	0.20	10	16	6.4	punching
294	20	35	25	0.33	3.0	5.0	0.6	0.20	15	16	5.3	punching
295	20	45	5	0.09	3.0	1.0	0.6	0.20	2	8	4.0	punching
296	20	45	5	0.09	3.0	2.0	0.6	0.20	8	8	2.0	punching
297	20	45	5	0.09	3.0	1.5	0.6	0.20	10	8	1.2	punching
298	35	40	25	0.39	5.5	0.2	1	0.18	2	16	1.6	local
299	35	45	25	0.47	5.5	0.2	1	0.18	5	16	0.6	local
300	35	35	25	0.33	6.6	3.0	1.2	0.18	10	16	4.8	local
301	35	45	25	0.47	6.6	5.0	1.2	0.18	9	16	8.9	local
302	35	45	25	0.47	5.5	2.0	1	0.18	5	16	6.4	local
303	35	40	15	0.22	6.6	0.2	1.2	0.18	10	14	0.3	local
304	35	45	13	0.23	6.6	0.2	1.2	0.18	15	13.5	0.2	local
305	35	40	15	0.22	6.6	0.2	1.2	0.18	15	14	0.2	local
306	35	40	15	0.22	5.5	0.2	1	0.18	5	14	0.6	local
307	35	45	13	0.23	5.5	0.2	1	0.18	5	13.5	0.5	punching
308	35	40	5	0.07	5.5	0.2	1	0.18	5	8	0.3	punching
309	35	45	15	0.27	6.6	2.0	1.2	0.18	8	14	3.5	punching
310	35	40	25	0.39	5.5	2.0	1	0.18	2	16	16.0	punching

311	35	45	13	0.23	6.6	0.2	1.2	0.18	2	13.5	1.4	punching
312	35	45	25	0.47	5.5	3.0	1	0.18	5	16	9.6	punching
313	35	40	13	0.19	5.5	0.2	1	0.18	2	13.5	1.4	punching
314	35	40	13	0.19	6.6	0.2	1.2	0.18	2	13.5	1.4	punching
315	35	40	13	0.19	6.6	0.2	1.2	0.18	10	13.5	0.3	punching
316	35	45	5	0.09	5.5	0.2	1	0.18	5	8	0.3	punching
317	35	45	5	0.09	5.5	2.0	1	0.18	5	8	3.2	punching
318	35	45	5	0.09	5.5	3.0	1	0.18	15	8	1.6	punching
319	30	40	25	0.39	4.7	0.2	0.8	0.17	5	16	0.6	local
320	30	45	15	0.27	5.9	0.2	1	0.17	5	14	0.6	local
321	30	40	25	0.39	4.7	0.2	0.8	0.17	15	16	0.2	local
322	30	45	15	0.27	4.7	0.2	0.8	0.17	10	14	0.3	local
323	30	45	15	0.27	4.7	0.2	0.8	0.17	10	14	0.3	local
324	30	40	25	0.39	5.9	0.6	1	0.17	5	16	1.9	local
325	30	45	25	0.47	5.9	1.0	1	0.17	5	16	3.2	local
326	30	40	25	0.39	5.9	3.0	1	0.17	15	16	3.2	local
327	30	40	15	0.22	5.9	0.2	1	0.17	5	14	0.6	punching
328	30	40	25	0.39	5.9	1.0	1	0.17	2	16	8.0	punching
329	30	45	25	0.47	5.9	3.0	1	0.17	7	16	6.9	punching
330	30	35	25	0.33	5.9	3.0	1	0.17	12	16	4.0	punching
331	30	45	25	0.47	5.9	1.5	1	0.17	2	16	12.0	punching
332	30	40	15	0.22	4.7	2.0	0.8	0.17	8	14	3.5	punching
333	30	40	15	0.22	5.9	0.2	1	0.17	5	14	0.6	punching
334	30	40	15	0.22	4.7	3.0	0.8	0.17	10	14	4.2	punching
335	10	45	25	0.47	6.6	0.2	1	0.15	5	16	0.6	local
336	10	35	25	0.33	5.3	0.2	0.8	0.15	15	16	0.2	local
337	10	40	25	0.39	6.6	0.6	1	0.15	15	16	0.6	local
338	10	35	25	0.33	5.3	0.2	0.8	0.15	8	16	0.4	local
339	10	35	25	0.33	6.6	0.2	1	0.15	15	16	0.2	local
340	10	45	25	0.47	6.6	5.0	1	0.15	15	16	5.3	punching
341	10	45	25	0.47	4.0	4.0	0.6	0.15	8	16	8.0	punching
342	10	45	25	0.47	6.6	2.0	1	0.15	10	16	3.2	punching
343	10	40	10	0.15	6.6	0.2	1	0.15	5	12	0.5	punching
344	10	40	25	0.39	6.6	0.4	1	0.15	5	16	1.3	punching
345	10	40	10	0.15	5.3	3.0	0.8	0.15	10	12	3.6	punching
346	10	40	15	0.22	5.3	2.0	0.8	0.15	8	14	3.5	punching
347	10	40	10	0.15	5.3	2.5	0.8	0.15	15	12	2.0	punching
348	10	45	25	0.47	6.6	0.6	1	0.15	5	16	1.9	punching
349	10	40	15	0.22	6.6	0.2	1	0.15	5	14	0.6	punching
350	10	45	15	0.27	6.6	0.2	1	0.15	5	14	0.6	punching
351	10	45	15	0.27	5.3	0.2	0.8	0.15	2	14	1.4	punching
352	10	40	15	0.22	5.3	2.0	0.8	0.15	15	14	1.9	punching
353	10	45	15	0.27	5.3	4.0	0.8	0.15	8	14	7.0	punching
354	10	45	10	0.18	4.0	1.0	0.6	0.15	2	12	6.0	punching
355	10	35	10	0.12	6.6	0.1	1	0.15	5	12	0.2	punching

APPENDIX 2

First and second derivation of the force F and F' in the general shear failure theoretical model is presented here. These derivations were used to determine these forces using Newton Raphson numerical technique.

First derivation of Equation 4.53 respect to θ_1

$$R0 := \frac{1}{\cos(\delta) B \left((a-1)(\tan(\psi) - \cot(\theta 1)) + \frac{a\, e^{(\theta 1 \tan(\phi 1))}}{\sin(\theta 1)} \right)} \left(2 \left(\frac{\gamma 1 B^3 \left(3 \tan(\phi 1)\, e^{(3 \theta 1 \tan(\phi 1))} - 3 \tan(\phi 1) \cos(\theta 1) + \sin(\theta 1) \right)}{24 \sin(\theta 1)^3 (9 \tan(\phi 1)^2 + 1)} \right. \right.$$

$$\left. \left. - \frac{\gamma 1 B^3 \left(e^{(3 \theta 1 \tan(\phi 1))} - 3 \tan(\phi 1) \sin(\theta 1) - \cos(\theta 1) \right) \cos(\theta 1)}{8 \sin(\theta 1)^4 (9 \tan(\phi 1)^2 + 1)} + \frac{1}{48} \gamma 1 B^3 (1 + \cot(\theta 1)^2) + \frac{1}{2} P \sin(-\psi + \phi 1) B (1 + \cot(\theta 1)^2) \right) \right)$$

$$- \frac{1}{\cos(\delta) B \left((a-1)(\tan(\psi) - \cot(\theta 1)) + \frac{a\, e^{(\theta 1 \tan(\phi 1))}}{\sin(\theta 1)} \right)^2} \left(2 \left(\frac{\gamma 1 B^3 \left(e^{(3 \theta 1 \tan(\phi 1))} - 3 \tan(\phi 1) \sin(\theta 1) - \cos(\theta 1) \right)}{24 \sin(\theta 1)^3 (9 \tan(\phi 1)^2 + 1)} + \frac{1}{48} \gamma 1 B^3 (\tan(\psi) - \cot(\theta 1)) \right. \right.$$

$$\left. \left. + P \left(\frac{1}{3} \cos(-\psi + \phi 1) B - \sin(-\psi + \phi 1) \left(\frac{1}{3} B \tan(\psi) - \frac{1}{2} B (\tan(\psi) - \cot(\theta 1)) \right) \right) \right) \left((a-1)(1 + \cot(\theta 1)^2) + \frac{a \tan(\phi 1)\, e^{(\theta 1 \tan(\phi 1))}}{\sin(\theta 1)} - \frac{a\, e^{(\theta 1 \tan(\phi 1))} \cos(\theta 1)}{\sin(\theta 1)^2} \right)$$

Second derivation of Equation 4.53 respect to θ_1

$$R0 := \frac{1}{\cos(\delta)\,B\left((a-1)\left(\tan(\psi)-\cot(\theta 1)\right)+\frac{a\,e^{(\theta 1\tan(\phi 1))}}{\sin(\theta 1)}\right)}\left(2\left(\frac{\gamma 1 B^3\left(9\tan(\phi 1)^2 e^{(3\theta 1\tan(\phi 1))}+3\tan(\phi 1)\sin(\theta 1)+\cos(\theta 1)\right)}{24\sin(\theta 1)^3(9\tan(\phi 1)^2+1)}\right.\right.$$
$$-\frac{\gamma 1 B^3\left(3\tan(\phi 1)e^{(3\theta 1\tan(\phi 1))}-3\tan(\phi 1)\cos(\theta 1)+\sin(\theta 1)\right)\cos(\theta 1)}{4\sin(\theta 1)^4(9\tan(\phi 1)^2+1)}+\frac{\gamma 1 B^3\left(e^{(3\theta 1\tan(\phi 1))}-3\tan(\phi 1)\sin(\theta 1)-\cos(\theta 1)\right)}{8\sin(\theta 1)^3(9\tan(\phi 1)^2+1)}$$
$$\left.\left.+\frac{\gamma 1 B^3\left(e^{(3\theta 1\tan(\phi 1))}-3\tan(\phi 1)\sin(\theta 1)-\cos(\theta 1)\right)\cos(\theta 1)^2}{2\sin(\theta 1)^5(9\tan(\phi 1)^2+1)}+\frac{1}{24}\gamma 1 B^3\cot(\theta 1)\left(-1-\cot(\theta 1)^2\right)-P\sin(\psi-\phi 1)B\cot(\theta 1)\left(-1-\cot(\theta 1)^2\right)\right)\right)$$
$$-\frac{1}{\cos(\delta)\,B\left((a-1)\left(\tan(\psi)-\cot(\theta 1)\right)+\frac{a\,e^{(\theta 1\tan(\phi 1))}}{\sin(\theta 1)}\right)^2}\left(4\left(\frac{\gamma 1 B^3\left(3\tan(\phi 1)e^{(3\theta 1\tan(\phi 1))}-3\tan(\phi 1)\cos(\theta 1)+\sin(\theta 1)\right)}{24\sin(\theta 1)^3(9\tan(\phi 1)^2+1)}\right.\right.$$
$$\left.-\frac{\gamma 1 B^3\left(e^{(3\theta 1\tan(\phi 1))}-3\tan(\phi 1)\sin(\theta 1)-\cos(\theta 1)\right)\cos(\theta 1)}{8\sin(\theta 1)^4(9\tan(\phi 1)^2+1)}+\frac{1}{48}\gamma 1 B^3\left(1+\cot(\theta 1)^2\right)-\frac{1}{2}P\sin(\psi-\phi 1)B\left(1+\cot(\theta 1)^2\right)\right)\left((a-1)\left(1+\cot(\theta 1)^2\right)\right.$$
$$\left.\left.+\frac{a\tan(\phi 1)\,e^{(\theta 1\tan(\phi 1))}}{\sin(\theta 1)}-\frac{a\,e^{(\theta 1\tan(\phi 1))}\cos(\theta 1)}{\sin(\theta 1)^2}\right)\right)$$
$$-\frac{1}{\cos(\delta)\,B\left((a-1)\left(\tan(\psi)-\cot(\theta 1)\right)+\frac{a\,e^{(\theta 1\tan(\phi 1))}}{\sin(\theta 1)}\right)^2}\left(2\left(\frac{\gamma 1 B^3\left(e^{(3\theta 1\tan(\phi 1))}-3\tan(\phi 1)\sin(\theta 1)-\cos(\theta 1)\right)}{24\sin(\theta 1)^3(9\tan(\phi 1)^2+1)}+\frac{1}{48}\gamma 1 B^3\left(\tan(\psi)-\cot(\theta 1)\right)\right.\right.$$
$$\left.\left.+P\left(\frac{1}{3}\cos(\psi-\phi 1)B+\sin(\psi-\phi 1)\left(\frac{1}{3}B\tan(\psi)-\frac{1}{2}B\left(\tan(\psi)-\cot(\theta 1)\right)\right)\right)\right)\left(2(a-1)\cot(\theta 1)\left(-1-\cot(\theta 1)^2\right)+\frac{a\tan(\phi 1)^2 e^{(\theta 1\tan(\phi 1))}}{\sin(\theta 1)}\right.$$
$$\left.-\frac{2a\tan(\phi 1)\,e^{(\theta 1\tan(\phi 1))}\cos(\theta 1)}{\sin(\theta 1)^2}+\frac{a\,e^{(\theta 1\tan(\phi 1))}}{\sin(\theta 1)}+\frac{2a\,e^{(\theta 1\tan(\phi 1))}\cos(\theta 1)^2}{\sin(\theta 1)^3}\right)\Bigg)$$

$$+\frac{1}{\cos(\delta)\,B\left((a-1)\left(\tan(\psi)-\cot(\theta 1)\right)+\frac{a\,e^{(\theta 1\tan(\phi 1))}}{\sin(\theta 1)}\right)^3}\left(4\left(\frac{\gamma 1\,B^3\left(e^{(3\,\theta 1\tan(\phi 1))}-3\tan(\phi 1)\sin(\theta 1)-\cos(\theta 1)\right)}{24\sin(\theta 1)^3\left(9\tan(\phi 1)^2+1\right)}+\frac{1}{48}\gamma 1\,B^3\left(\tan(\psi)-\cot(\theta 1)\right)\right.\right.$$

$$\left.\left.+P\left(\frac{1}{3}\cos(\psi-\phi 1)\,B+\sin(\psi-\phi 1)\left(\frac{1}{3}B\tan(\psi)-\frac{1}{2}B\left(\tan(\psi)-\cot(\theta 1)\right)\right)\right)\right)\left(\left((a-1)\left(1+\cot(\theta 1)^2\right)+\frac{a\tan(\phi 1)\,e^{(\theta 1\tan(\phi 1))}}{\sin(\theta 1)}-\frac{a\,e^{(\theta 1\tan(\phi 1))}\cos(\theta 1)}{\sin(\theta 1)^2}\right)^2\right)$$

First derivation of Equation 4.92 respect to θ_2

$$RI:=\frac{1}{B\left(e^{(\theta 1\tan(\phi 1))}+\tan(\psi)\sin(\theta 1)-\cos(\theta 1)\right)\left(\sin(\delta)\left(\sin(\theta 3)\cos(\theta 3)-\cos(\theta 3)^2\cot(\theta 2)\right)+\cos(\delta)\left(a+\sin(\theta 3)\cos(\theta 3)\cot(\theta 2)-\sin(\theta 3)^2\right)\right)}\left(2\left(\right.\right.$$

$$\frac{1}{12\sin(\theta 1)^3\sin(\theta 2)^3}\left(\gamma 2\,B^3\left(e^{(\theta 1\tan(\phi 1))}+\tan(\psi)\sin(\theta 1)-\cos(\theta 1)\right)^3\cos(\phi 2)\sin(\theta 3)\cot(\theta 3)\left(-\cos(\theta 3)\cos(\theta 2)+\sin(\theta 3)\sin(\theta 2)+\cos(\theta 3)\,e^{(\theta 2\tan(\phi 2))}\right)\right.$$

$$\left.\left.\left(\frac{1}{2}\cos(\theta 3)\cos(\theta 2)-\frac{1}{2}\sin(\theta 3)\sin(\theta 2)+\cos(\theta 3)\,e^{(\theta 2\tan(\phi 2))}\right)\left(\cos(\theta 3)\sin(\theta 2)+\sin(\theta 3)\cos(\theta 2)+\cos(\theta 3)\tan(\phi 2)\,e^{(\theta 2\tan(\phi 2))}\right)\right)$$

$$+\frac{1}{24\sin(\theta 1)^3\sin(\theta 2)^3}\left(\gamma 2\,B^3\left(e^{(\theta 1\tan(\phi 1))}+\tan(\psi)\sin(\theta 1)-\cos(\theta 1)\right)^3\cos(\phi 2)\sin(\theta 3)\cot(\theta 3)\right.$$

$$\left.\left(-\cos(\theta 3)\cos(\theta 2)+\sin(\theta 3)\sin(\theta 2)+\cos(\theta 3)\,e^{(\theta 2\tan(\phi 2))}\right)^2\left(-\frac{1}{2}\cos(\theta 3)\sin(\theta 2)-\frac{1}{2}\sin(\theta 3)\cos(\theta 2)+\cos(\theta 3)\tan(\phi 2)\,e^{(\theta 2\tan(\phi 2))}\right)\right)$$

$$-\frac{1}{8\sin(\theta 1)^3\sin(\theta 2)^4}\left(\gamma 2\,B^3\left(e^{(\theta 1\tan(\phi 1))}+\tan(\psi)\sin(\theta 1)-\cos(\theta 1)\right)^3\cos(\phi 2)\sin(\theta 3)\cot(\theta 3)\right.$$

$$\left.\left(-\cos(\theta 3)\cos(\theta 2)+\sin(\theta 3)\sin(\theta 2)+\cos(\theta 3)\,e^{(\theta 2\tan(\phi 2))}\right)^2\left(\frac{1}{2}\cos(\theta 3)\cos(\theta 2)-\frac{1}{2}\sin(\theta 3)\sin(\theta 2)+\cos(\theta 3)\,e^{(\theta 2\tan(\phi 2))}\right)\cos(\theta 2)\right)$$

$$+$$

$$\frac{\gamma 2\,B^3\cos(\theta 3)^3\left(e^{(\theta 1\tan(\phi 1))}+\tan(\psi)\sin(\theta 1)-\cos(\theta 1)\right)^3\left(3\tan(\phi 2)\,e^{(3\,\theta 2\tan(\phi 2))}\left(3\tan(\phi 2)\cos(\theta 3)-\sin(\theta 3)\right)+\cos(\theta 3+\theta 2)+3\tan(\phi 2)\sin(\theta 3+\theta 2)\right)}{24\sin(\theta 1)^3\sin(\theta 2)^3\left(9\tan(\phi 2)^2+1\right)}$$

$$-\frac{\gamma 2 B^3 \cos(\theta 3)^3 \left(e^{(\theta 1 \tan(\phi 1))} + \tan(\psi)\sin(\theta 1) - \cos(\theta 1)\right)^3 \left(e^{(3\,\theta 2 \tan(\phi 2))} (3\tan(\phi 2)\cos(\theta 3) - \sin(\theta 3)) + \sin(\theta 3 + \theta 2) - 3\tan(\phi 2)\cos(\theta 3 + \theta 2)\right)\cos(\theta 2)}{8\sin(\theta 1)^3 \sin(\theta 2)^4 (9\tan(\phi 2)^2 + 1)}$$

$$+\frac{\gamma 2 B^3 \left(e^{(\theta 1 \tan(\phi 1))} + \tan(\psi)\sin(\theta 1) - \cos(\theta 1)\right)^3 (\sin(\theta 3)\cos(\theta 3) - \cos(\theta 3)^2 \cot(\theta 2))\cos(\theta 3)^2 (-1 - \cot(\theta 2)^2)}{12\sin(\theta 1)^3}\Bigg)\sin(\theta 1)\Bigg)$$

$$-\frac{1}{B\left(e^{(\theta 1 \tan(\phi 1))} + \tan(\psi)\sin(\theta 1) - \cos(\theta 1)\right)(\sin(\delta)(\sin(\theta 3)\cos(\theta 3) - \cos(\theta 3)^2\cot(\theta 2)) + \cos(\delta)(a + \sin(\theta 3)\cos(\theta 3)\cot(\theta 2) - \sin(\theta 3)^2))^2}\Bigg(2\Bigg($$

$$\frac{1}{24\sin(\theta 1)^3 \sin(\theta 2)^3}\Bigg(\gamma 2 B^3 \left(e^{(\theta 1 \tan(\phi 1))} + \tan(\psi)\sin(\theta 1) - \cos(\theta 1)\right)^3 \cos(\phi 2)\sin(\theta 3)\cot(\theta 3)$$

$$\left(-\cos(\theta 3)\cos(\theta 2) + \sin(\theta 3)\sin(\theta 2) + \cos(\theta 3)\, e^{(\theta 2 \tan(\phi 2))}\right)^2 \left(\frac{1}{2}\cos(\theta 3)\cos(\theta 2) - \frac{1}{2}\sin(\theta 3)\sin(\theta 2) + \cos(\theta 3)\, e^{(\theta 2 \tan(\phi 2))}\right)\Bigg)$$

$$+\frac{\gamma 2 B^3 \cos(\theta 3)^3 \left(e^{(\theta 1 \tan(\phi 1))} + \tan(\psi)\sin(\theta 1) - \cos(\theta 1)\right)^3 \left(e^{(3\,\theta 2 \tan(\phi 2))} (3\tan(\phi 2)\cos(\theta 3) - \sin(\theta 3)) + \sin(\theta 3 + \theta 2) - 3\tan(\phi 2)\cos(\theta 3 + \theta 2)\right)}{24\sin(\theta 1)^3 \sin(\theta 2)^3 (9\tan(\phi 2)^2 + 1)}$$

$$-\frac{\gamma 2 B^3 \left(e^{(\theta 1 \tan(\phi 1))} + \tan(\psi)\sin(\theta 1) - \cos(\theta 1)\right)^3 (\sin(\theta 3)\cos(\theta 3) - \cos(\theta 3)^2 \cot(\theta 2))^2}{24\sin(\theta 1)^3}\Bigg)\sin(\theta 1)(-\sin(\delta)\cos(\theta 3)^2(-1 - \cot(\theta 2)^2)$$

$$+\cos(\delta)\sin(\theta 3)\cos(\theta 3)(-1 - \cot(\theta 2)^2))\Bigg)$$

Second derivation of Equation 4.92 respect to θ_2

$$R1 := \frac{1}{B\left(e^{(\theta 1 \tan(\phi 1))} + \tan(\psi)\sin(\theta 1) - \cos(\theta 1)\right)(\sin(\delta)(\sin(\theta 3)\cos(\theta 3) - \cos(\theta 3)^2\cot(\theta 2)) + \cos(\delta)(a + \sin(\theta 3)\cos(\theta 3)\cot(\theta 2) - \sin(\theta 3)^2))^2}\Bigg(2\Bigg($$

$$\frac{1}{12\sin(\theta 1)^3 \sin(\theta 2)^3}\Bigg(\gamma 2 B^3 \left(e^{(\theta 1 \tan(\phi 1))} + \tan(\psi)\sin(\theta 1) - \cos(\theta 1)\right)^3 \cos(\phi 2)\sin(\theta 3)\cot(\theta 3)$$

$$\left(\cos(\theta3)\sin(\theta2)+\sin(\theta3)\cos(\theta2)+\cos(\theta3)\tan(\phi2)\,e^{(\theta2\tan(\phi2))}\right)^2\left(\frac{1}{2}\cos(\theta3)\cos(\theta2)-\frac{1}{2}\sin(\theta3)\sin(\theta2)+\cos(\theta3)\,e^{(\theta2\tan(\phi2))}\right)\Bigg)$$

$$+\frac{1}{6\sin(\theta1)^3\sin(\theta2)^3}\left(\gamma2B^3\left(e^{(\theta1\tan(\phi1))}+\tan(\psi)\sin(\theta1)-\cos(\theta1)\right)^3\cos(\phi2)\sin(\theta3)\cot(\theta3)\left(-\cos(\theta3)\cos(\theta2)+\sin(\theta3)\sin(\theta2)+\cos(\theta3)\,e^{(\theta2\tan(\phi2))}\right)\right.$$

$$\left.\left(-\frac{1}{2}\cos(\theta3)\sin(\theta2)-\frac{1}{2}\sin(\theta3)\cos(\theta2)+\cos(\theta3)\tan(\phi2)\,e^{(\theta2\tan(\phi2))}\right)\left(\cos(\theta3)\sin(\theta2)+\sin(\theta3)\cos(\theta2)+\cos(\theta3)\tan(\phi2)\,e^{(\theta2\tan(\phi2))}\right)\right)$$

$$+\frac{1}{12\sin(\theta1)^3\sin(\theta2)^3}\left(\gamma2B^3\left(e^{(\theta1\tan(\phi1))}+\tan(\psi)\sin(\theta1)-\cos(\theta1)\right)^3\cos(\phi2)\sin(\theta3)\cot(\theta3)\left(-\cos(\theta3)\cos(\theta2)+\sin(\theta3)\sin(\theta2)\right.\right.$$

$$\left.\left.+\cos(\theta3)\,e^{(\theta2\tan(\phi2))}\right)\left(\frac{1}{2}\cos(\theta3)\cos(\theta2)-\frac{1}{2}\sin(\theta3)\sin(\theta2)+\cos(\theta3)\,e^{(\theta2\tan(\phi2))}\right)\left(\cos(\theta3)\cos(\theta2)-\sin(\theta3)\sin(\theta2)+\cos(\theta3)\tan(\phi2)^2\,e^{(\theta2\tan(\phi2))}\right)\right)$$

$$-\frac{1}{2\sin(\theta1)^3\sin(\theta2)^4}\left(\gamma2B^3\left(e^{(\theta1\tan(\phi1))}+\tan(\psi)\sin(\theta1)-\cos(\theta1)\right)^3\cos(\phi2)\sin(\theta3)\cot(\theta3)\left(-\cos(\theta3)\cos(\theta2)+\sin(\theta3)\sin(\theta2)+\cos(\theta3)\,e^{(\theta2\tan(\phi2))}\right)\right.$$

$$\left.\left(\frac{1}{2}\cos(\theta3)\cos(\theta2)-\frac{1}{2}\sin(\theta3)\sin(\theta2)+\cos(\theta3)\,e^{(\theta2\tan(\phi2))}\right)\left(\cos(\theta3)\sin(\theta2)+\sin(\theta3)\cos(\theta2)+\cos(\theta3)\tan(\phi2)\,e^{(\theta2\tan(\phi2))}\right)\cos(\theta2)\right)$$

$$+\frac{1}{24\sin(\theta1)^3\sin(\theta2)^3}\left(\gamma2B^3\left(e^{(\theta1\tan(\phi1))}+\tan(\psi)\sin(\theta1)-\cos(\theta1)\right)^3\cos(\phi2)\sin(\theta3)\cot(\theta3)\right.$$

$$\left.\left(-\cos(\theta3)\cos(\theta2)+\sin(\theta3)\sin(\theta2)+\cos(\theta3)\,e^{(\theta2\tan(\phi2))}\right)^2\left(-\frac{1}{2}\cos(\theta3)\cos(\theta2)+\frac{1}{2}\sin(\theta3)\sin(\theta2)+\cos(\theta3)\tan(\phi2)^2\,e^{(\theta2\tan(\phi2))}\right)\right)$$

$$-\frac{1}{4\sin(\theta1)^3\sin(\theta2)^4}\left(\gamma2B^3\left(e^{(\theta1\tan(\phi1))}+\tan(\psi)\sin(\theta1)-\cos(\theta1)\right)^3\cos(\phi2)\sin(\theta3)\cot(\theta3)\right.$$

$$\left.\left(-\cos(\theta3)\cos(\theta2)+\sin(\theta3)\sin(\theta2)+\cos(\theta3)\,e^{(\theta2\tan(\phi2))}\right)^2\left(-\frac{1}{2}\cos(\theta3)\sin(\theta2)-\frac{1}{2}\sin(\theta3)\cos(\theta2)+\cos(\theta3)\tan(\phi2)\,e^{(\theta2\tan(\phi2))}\right)\cos(\theta2)\right)$$

$$+\frac{1}{8\sin(\theta1)^3\sin(\theta2)^3}\left(\gamma2B^3\left(e^{(\theta1\tan(\phi1))}+\tan(\psi)\sin(\theta1)-\cos(\theta1)\right)^3\cos(\phi2)\sin(\theta3)\cot(\theta3)\right.$$

$$\left.\left(-\cos(\theta3)\cos(\theta2)+\sin(\theta3)\sin(\theta2)+\cos(\theta3)\,e^{(\theta2\tan(\phi2))}\right)^2\left(\frac{1}{2}\cos(\theta3)\cos(\theta2)-\frac{1}{2}\sin(\theta3)\sin(\theta2)+\cos(\theta3)\,e^{(\theta2\tan(\phi2))}\right)\right)$$

$$+\frac{1}{2\sin(\theta 1)^3\sin(\theta 2)^5}\left(\gamma 2 B^3\left(e^{(\theta 1\tan(\phi 1))}+\tan(\psi)\sin(\theta 1)-\cos(\theta 1)\right)^3\cos(\phi 2)\sin(\theta 3)\cot(\theta 3)\right.$$

$$\left.\left(-\cos(\theta 3)\cos(\theta 2)+\sin(\theta 3)\sin(\theta 2)+\cos(\theta 3)e^{(\theta 2\tan(\phi 2))}\right)^2\left(\frac{1}{2}\cos(\theta 3)\cos(\theta 2)-\frac{1}{2}\sin(\theta 3)\sin(\theta 2)+\cos(\theta 3)e^{(\theta 2\tan(\phi 2))}\right)\cos(\theta 2)^2\right)$$

$$+\frac{\gamma 2 B^3\cos(\theta 3)^3\left(e^{(\theta 1\tan(\phi 1))}+\tan(\psi)\sin(\theta 1)-\cos(\theta 1)\right)^3\left(9\tan(\phi 2)^2 e^{(3\,\theta 2\tan(\phi 2))}(3\tan(\phi 2)\cos(\theta 3)-\sin(\theta 3))-\sin(\theta 3+\theta 2)+3\tan(\phi 2)\cos(\theta 3+\theta 2)\right)}{24\sin(\theta 1)^3\sin(\theta 2)^3(9\tan(\phi 2)^2+1)}$$

$$-\frac{1}{4\sin(\theta 1)^3\sin(\theta 2)^4(9\tan(\phi 2)^2+1)}\left(\gamma 2 B^3\cos(\theta 3)^3\left(e^{(\theta 1\tan(\phi 1))}+\tan(\psi)\sin(\theta 1)-\cos(\theta 1)\right)^3\left(3\tan(\phi 2)e^{(3\,\theta 2\tan(\phi 2))}(3\tan(\phi 2)\cos(\theta 3)-\sin(\theta 3))\right.\right.$$

$$\left.\left.+\cos(\theta 3+\theta 2)+3\tan(\phi 2)\sin(\theta 3+\theta 2)\right)\cos(\theta 2)\right)$$

$$+\frac{\gamma 2 B^3\cos(\theta 3)^3\left(e^{(\theta 1\tan(\phi 1))}+\tan(\psi)\sin(\theta 1)-\cos(\theta 1)\right)^3\left(e^{(3\,\theta 2\tan(\phi 2))}(3\tan(\phi 2)\cos(\theta 3)-\sin(\theta 3))+\sin(\theta 3+\theta 2)-3\tan(\phi 2)\cos(\theta 3+\theta 2)\right)}{8\sin(\theta 1)^3\sin(\theta 2)^3(9\tan(\phi 2)^2+1)}$$

$$+\frac{\gamma 2 B^3\cos(\theta 3)^3\left(e^{(\theta 1\tan(\phi 1))}+\tan(\psi)\sin(\theta 1)-\cos(\theta 1)\right)^3\left(e^{(3\,\theta 2\tan(\phi 2))}(3\tan(\phi 2)\cos(\theta 3)-\sin(\theta 3))+\sin(\theta 3+\theta 2)-3\tan(\phi 2)\cos(\theta 3+\theta 2)\right)\cos(\theta 2)^2}{2\sin(\theta 1)^3\sin(\theta 2)^5(9\tan(\phi 2)^2+1)}$$

$$-\frac{\gamma 2 B^3\left(e^{(\theta 1\tan(\phi 1))}+\tan(\psi)\sin(\theta 1)-\cos(\theta 1)\right)^3\cos(\theta 3)^4(-1-\cot(\theta 2)^2)^2}{12\sin(\theta 1)^3}$$

$$-\frac{\gamma 2 B^3\left(e^{(\theta 1\tan(\phi 1))}+\tan(\psi)\sin(\theta 1)-\cos(\theta 1)\right)^3(\sin(\theta 3)\cos(\theta 3)-\cos(\theta 3)^2\cot(\theta 2))\cos(\theta 3)^2\cot(\theta 2)(-1-\cot(\theta 2)^2)}{6\sin(\theta 1)^3}\sin(\theta 1)$$

$$-\frac{1}{B\left(e^{(\theta 1\tan(\phi 1))}+\tan(\psi)\sin(\theta 1)-\cos(\theta 1)\right)(\sin(\delta)(\sin(\theta 3)\cos(\theta 3)-\cos(\theta 3)^2\cot(\theta 2))+\cos(\delta)(a+\sin(\theta 3)\cos(\theta 3)\cot(\theta 2)-\sin(\theta 3)^2))^2}\left(4\left(\right.\right.$$

$$\frac{1}{12\sin(\theta 1)^3\sin(\theta 2)^3}\left(\gamma 2 B^3\left(e^{(\theta 1\tan(\phi 1))}+\tan(\psi)\sin(\theta 1)-\cos(\theta 1)\right)^3\cos(\phi 2)\sin(\theta 3)\cot(\theta 3)\left(-\cos(\theta 3)\cos(\theta 2)+\sin(\theta 3)\sin(\theta 2)+\cos(\theta 3)e^{(\theta 2\tan(\phi 2))}\right)\right.$$

$$\left.\left.\left(\frac{1}{2}\cos(\theta 3)\cos(\theta 2)-\frac{1}{2}\sin(\theta 3)\sin(\theta 2)+\cos(\theta 3)e^{(\theta 2\tan(\phi 2))}\right)\left(\cos(\theta 3)\sin(\theta 2)+\sin(\theta 3)\cos(\theta 2)+\cos(\theta 3)\tan(\phi 2)e^{(\theta 2\tan(\phi 2))}\right)\right)\right.$$

$$+\frac{1}{24\sin(\theta 1)^3\sin(\theta 2)^3}\left(\gamma 2B^3\left(e^{(\theta 1\tan(\phi 1))}+\tan(\psi)\sin(\theta 1)-\cos(\theta 1)\right)^3\cos(\phi 2)\sin(\theta 3)\cot(\theta 3)\right.$$

$$\left.\left(-\cos(\theta 3)\cos(\theta 2)+\sin(\theta 3)\sin(\theta 2)+\cos(\theta 3)e^{(\theta 2\tan(\phi 2))}\right)^2\left(-\frac{1}{2}\cos(\theta 3)\sin(\theta 2)-\frac{1}{2}\sin(\theta 3)\cos(\theta 2)+\cos(\theta 3)\tan(\phi 2)e^{(\theta 2\tan(\phi 2))}\right)\right)$$

$$-\frac{1}{8\sin(\theta 1)^3\sin(\theta 2)^4}\left(\gamma 2B^3\left(e^{(\theta 1\tan(\phi 1))}+\tan(\psi)\sin(\theta 1)-\cos(\theta 1)\right)^3\cos(\phi 2)\sin(\theta 3)\cot(\theta 3)\right.$$

$$\left.\left(-\cos(\theta 3)\cos(\theta 2)+\sin(\theta 3)\sin(\theta 2)+\cos(\theta 3)e^{(\theta 2\tan(\phi 2))}\right)^2\left(\frac{1}{2}\cos(\theta 3)\cos(\theta 2)-\frac{1}{2}\sin(\theta 3)\sin(\theta 2)+\cos(\theta 3)e^{(\theta 2\tan(\phi 2))}\right)\cos(\theta 2)\right)$$

$$+\frac{\gamma 2B^3\cos(\theta 3)^3\left(e^{(\theta 1\tan(\phi 1))}+\tan(\psi)\sin(\theta 1)-\cos(\theta 1)\right)^3\left(3\tan(\phi 2)e^{(3\theta 2\tan(\phi 2))}(3\tan(\phi 2)\cos(\theta 3)-\sin(\theta 3))+\cos(\theta 3+\theta 2)+3\tan(\phi 2)\sin(\theta 3+\theta 2)\right)}{24\sin(\theta 1)^3\sin(\theta 2)^3(9\tan(\phi 2)^2+1)}$$

$$-\frac{\gamma 2B^3\cos(\theta 3)^3\left(e^{(\theta 1\tan(\phi 1))}+\tan(\psi)\sin(\theta 1)-\cos(\theta 1)\right)^3\left(e^{(3\theta 2\tan(\phi 2))}(3\tan(\phi 2)\cos(\theta 3)-\sin(\theta 3))+\sin(\theta 3+\theta 2)-3\tan(\phi 2)\cos(\theta 3+\theta 2)\right)\cos(\theta 2)}{8\sin(\theta 1)^3\sin(\theta 2)^4(9\tan(\phi 2)^2+1)}$$

$$+\frac{\gamma 2B^3\left(e^{(\theta 1\tan(\phi 1))}+\tan(\psi)\sin(\theta 1)-\cos(\theta 1)\right)^3(\sin(\theta 3)\cos(\theta 3)-\cos(\theta 3)^2\cot(\theta 2))\cos(\theta 3)^2(-1-\cot(\theta 2)^2)}{12\sin(\theta 1)^3}\sin(\theta 1)(-\sin(\delta)\cos(\theta 3)^2(-1-\cot(\theta 2)^2)$$

$$+\cos(\delta)\sin(\theta 3)\cos(\theta 3)(-1-\cot(\theta 2)^2))\Bigg)$$

$$-\frac{1}{B\left(e^{(\theta 1\tan(\phi 1))}+\tan(\psi)\sin(\theta 1)-\cos(\theta 1)\right)(\sin(\delta)(\sin(\theta 3)\cos(\theta 3)-\cos(\theta 3)^2\cot(\theta 2))+\cos(\delta)(a+\sin(\theta 3)\cos(\theta 3)\cot(\theta 2)-\sin(\theta 3)^2))^2}\left(2\left(\right.\right.$$

$$\frac{1}{24\sin(\theta 1)^3\sin(\theta 2)^3}\left(\gamma 2B^3\left(e^{(\theta 1\tan(\phi 1))}+\tan(\psi)\sin(\theta 1)-\cos(\theta 1)\right)^3\cos(\phi 2)\sin(\theta 3)\cot(\theta 3)\right.$$

$$\left.\left(-\cos(\theta 3)\cos(\theta 2)+\sin(\theta 3)\sin(\theta 2)+\cos(\theta 3)e^{(\theta 2\tan(\phi 2))}\right)^2\left(\frac{1}{2}\cos(\theta 3)\cos(\theta 2)-\frac{1}{2}\sin(\theta 3)\sin(\theta 2)+\cos(\theta 3)e^{(\theta 2\tan(\phi 2))}\right)\right)$$

$$+\frac{\gamma 2B^3\cos(\theta 3)^3\left(e^{(\theta 1\tan(\phi 1))}+\tan(\psi)\sin(\theta 1)-\cos(\theta 1)\right)^3\left(e^{(3\theta 2\tan(\phi 2))}(3\tan(\phi 2)\cos(\theta 3)-\sin(\theta 3))+\sin(\theta 3+\theta 2)-3\tan(\phi 2)\cos(\theta 3+\theta 2)\right)}{24\sin(\theta 1)^3\sin(\theta 2)^3(9\tan(\phi 2)^2+1)}$$

$$
-\frac{\gamma 2 B^3 \left(e^{(\theta 1 \tan(\phi 1))} + \tan(\psi)\sin(\theta 1) - \cos(\theta 1) \right)^3 \left(\sin(\theta 3)\cos(\theta 3) - \cos(\theta 3)^2 \cot(\theta 2) \right)^2}{24 \sin(\theta 1)^3} \Bigg) \sin(\theta 1) \left(2\sin(\delta)\cos(\theta 3)^2 \cot(\theta 2)\left(-1 - \cot(\theta 2)^2\right) \right.
$$

$$
\left. - 2\cos(\delta)\sin(\theta 3)\cos(\theta 3)\cot(\theta 2)\left(-1 - \cot(\theta 2)^2\right) \right)
$$

$$
+ \frac{1}{B\left(e^{(\theta 1 \tan(\phi 1))} + \tan(\psi)\sin(\theta 1) - \cos(\theta 1) \right) \left(\sin(\delta)\left(\sin(\theta 3)\cos(\theta 3) - \cos(\theta 3)^2 \cot(\theta 2) \right) + \cos(\delta)\left(a + \sin(\theta 3)\cos(\theta 3)\cot(\theta 2) - \sin(\theta 3)^2 \right) \right)^3} \Bigg(4 \Bigg(
$$

$$
\frac{1}{24 \sin(\theta 1)^3 \sin(\theta 2)^3} \Bigg(\gamma 2 B^3 \left(e^{(\theta 1 \tan(\phi 1))} + \tan(\psi)\sin(\theta 1) - \cos(\theta 1) \right)^3 \cos(\phi 2)\sin(\theta 3)\cot(\theta 3)
$$

$$
\left(-\cos(\theta 3)\cos(\theta 2) + \sin(\theta 3)\sin(\theta 2) + \cos(\theta 3)\, e^{(\theta 2 \tan(\phi 2))} \right)^2 \left(\frac{1}{2}\cos(\theta 3)\cos(\theta 2) - \frac{1}{2}\sin(\theta 3)\sin(\theta 2) + \cos(\theta 3)\, e^{(\theta 2 \tan(\phi 2))} \right) \Bigg)
$$

$$
+ \frac{\gamma 2 B^3 \cos(\theta 3)^3 \left(e^{(\theta 1 \tan(\phi 1))} + \tan(\psi)\sin(\theta 1) - \cos(\theta 1) \right)^3 \left(e^{(3\,\theta 2 \tan(\phi 2))} \left(3\tan(\phi 2)\cos(\theta 3) - \sin(\theta 3) \right) + \sin(\theta 3 + \theta 2) - 3\tan(\phi 2)\cos(\theta 3 + \theta 2) \right)}{24 \sin(\theta 1)^3 \sin(\theta 2)^3 \left(9\tan(\phi 2)^2 + 1 \right)}
$$

$$
- \frac{\gamma 2 B^3 \left(e^{(\theta 1 \tan(\phi 1))} + \tan(\psi)\sin(\theta 1) - \cos(\theta 1) \right)^3 \left(\sin(\theta 3)\cos(\theta 3) - \cos(\theta 3)^2 \cot(\theta 2) \right)^2}{24 \sin(\theta 1)^3} \Bigg) \sin(\theta 1)
$$

$$
\left(-\sin(\delta)\cos(\theta 3)^2 \left(-1 - \cot(\theta 2)^2 \right) + \cos(\delta)\sin(\theta 3)\cos(\theta 3)\left(-1 - \cot(\theta 2)^2 \right) \right)^2 \Bigg)
$$

First derivation of Equation 4.103 respect to θ_1

$$R2 := \frac{2\left(-\frac{1}{2}P\sin(-\psi+\phi1)\left(-1-\cot(\theta1)^2\right)+\frac{1}{4}cIB\left(1+\cot(\theta1)^2\right)-\frac{cIBe^{(2\,\theta1\tan(\phi1))}}{4\sin(\theta1)^2}+\frac{cIB\left(e^{(2\,\theta1\tan(\phi1))}-1\right)\cos(\theta1)}{4\sin(\theta1)^3\tan(\phi1)}\right)}{B\cos(\delta)\left(\frac{m\left(e^{(\theta1\tan(\phi1))}+\tan(\psi)\sin(\theta1)-\cos(\theta1)\right)}{\sin(\theta1)}-\tan(\psi)+\cot(\theta1)\right)}$$

$$-\frac{1}{B\cos(\delta)\left(\frac{m\left(e^{(\theta1\tan(\phi1))}+\tan(\psi)\sin(\theta1)-\cos(\theta1)\right)}{\sin(\theta1)}-\tan(\psi)+\cot(\theta1)\right)^2}\left(2\left(P\left(\frac{1}{4}\cos(-\psi+\phi1)-\frac{1}{2}\sin(-\psi+\phi1)\left(-\frac{1}{2}\tan(\psi)+\cot(\theta1)\right)\right)\right.\right.$$

$$\left.+\frac{1}{4}cIB\left(\tan(\psi)-\cot(\theta1)\right)-\frac{cIB\left(e^{(2\,\theta1\tan(\phi1))}-1\right)}{8\sin(\theta1)^2\tan(\phi1)}\right)\left(\frac{m\left(\tan(\phi1)\,e^{(\theta1\tan(\phi1))}+\tan(\psi)\cos(\theta1)+\sin(\theta1)\right)}{\sin(\theta1)}\right.$$

$$\left.\left.-\frac{m\left(e^{(\theta1\tan(\phi1))}+\tan(\psi)\sin(\theta1)-\cos(\theta1)\right)\cos(\theta1)}{\sin(\theta1)^2}-1-\cot(\theta1)^2\right)\right)$$

Second derivation of Equation 4.103 respect to θ_1

$$R2 := \frac{1}{B\cos(\delta)\left(\frac{m\left(e^{(\theta1\tan(\phi1))}+\tan(\psi)\sin(\theta1)-\cos(\theta1)\right)}{\sin(\theta1)}-\tan(\psi)+\cot(\theta1)\right)}\left(2\left(-P\sin(\psi-\phi1)\cot(\theta1)\left(-1-\cot(\theta1)^2\right)+\frac{1}{2}cIB\cot(\theta1)\left(-1-\cot(\theta1)^2\right)\right.\right.$$

$$\left.\left.-\frac{cIB\tan(\phi1)\,e^{(2\,\theta1\tan(\phi1))}}{2\sin(\theta1)^2}+\frac{cIBe^{(2\,\theta1\tan(\phi1))}\cos(\theta1)}{\sin(\theta1)^3}-\frac{cIB\left(e^{(2\,\theta1\tan(\phi1))}-1\right)}{4\sin(\theta1)^2\tan(\phi1)}-\frac{3cIB\left(e^{(2\,\theta1\tan(\phi1))}-1\right)\cos(\theta1)^2}{4\sin(\theta1)^4\tan(\phi1)}\right)\right)$$

$$-\frac{1}{B\cos(\delta)\left(\frac{m\left(e^{(\theta1\tan(\phi1))}+\tan(\psi)\sin(\theta1)-\cos(\theta1)\right)}{\sin(\theta1)}-\tan(\psi)+\cot(\theta1)\right)^2}\left(4\left(\frac{1}{2}P\sin(\psi-\phi1)\left(-1-\cot(\theta1)^2\right)+\frac{1}{4}cIB\left(1+\cot(\theta1)^2\right)\right.\right.$$

$$\left.\left.-\frac{cIBe^{(2\,\theta1\tan(\phi1))}}{4\sin(\theta1)^2}+\frac{cIB\left(e^{(2\,\theta1\tan(\phi1))}-1\right)\cos(\theta1)}{4\sin(\theta1)^3\tan(\phi1)}\right)\left(\frac{m\left(\tan(\phi1)\,e^{(\theta1\tan(\phi1))}+\tan(\psi)\cos(\theta1)+\sin(\theta1)\right)}{\sin(\theta1)}\right.\right.$$

$$-\frac{m\left(e^{(\theta 1\tan(\phi 1))}+\tan(\psi)\sin(\theta 1)-\cos(\theta 1)\right)\cos(\theta 1)}{\sin(\theta 1)^2}-1-\cot(\theta 1)^2\Bigg)\Bigg)$$

$$-\frac{1}{B\cos(\delta)\left(\frac{m\left(e^{(\theta 1\tan(\phi 1))}+\tan(\psi)\sin(\theta 1)-\cos(\theta 1)\right)}{\sin(\theta 1)}-\tan(\psi)+\cot(\theta 1)\right)^2}\left(2\left(P\left(\frac{1}{4}\cos(\psi-\phi 1)+\frac{1}{2}\sin(\psi-\phi 1)\left(-\frac{1}{2}\tan(\psi)+\cot(\theta 1)\right)\right)\right.\right.$$

$$\left.+\frac{1}{4}cIB(\tan(\psi)-\cot(\theta 1))-\frac{cIB\left(e^{(2\theta 1\tan(\phi 1))}-1\right)}{8\sin(\theta 1)^2\tan(\phi 1)}\right)\left(\frac{m\left(\tan(\phi 1)^2 e^{(\theta 1\tan(\phi 1))}-\tan(\psi)\sin(\theta 1)+\cos(\theta 1)\right)}{\sin(\theta 1)}\right.$$

$$-\frac{2m\left(\tan(\phi 1)e^{(\theta 1\tan(\phi 1))}+\tan(\psi)\cos(\theta 1)+\sin(\theta 1)\right)\cos(\theta 1)}{\sin(\theta 1)^2}+\frac{m\left(e^{(\theta 1\tan(\phi 1))}+\tan(\psi)\sin(\theta 1)-\cos(\theta 1)\right)}{\sin(\theta 1)}$$

$$\left.\left.+\frac{2m\left(e^{(\theta 1\tan(\phi 1))}+\tan(\psi)\sin(\theta 1)-\cos(\theta 1)\right)\cos(\theta 1)^2}{\sin(\theta 1)^3}-2\cot(\theta 1)(-1-\cot(\theta 1)^2)\right)\right)$$

$$+\frac{1}{B\cos(\delta)\left(\frac{m\left(e^{(\theta 1\tan(\phi 1))}+\tan(\psi)\sin(\theta 1)-\cos(\theta 1)\right)}{\sin(\theta 1)}-\tan(\psi)+\cot(\theta 1)\right)^3}\left(4\left(P\left(\frac{1}{4}\cos(\psi-\phi 1)+\frac{1}{2}\sin(\psi-\phi 1)\left(-\frac{1}{2}\tan(\psi)+\cot(\theta 1)\right)\right)\right.\right.$$

$$\left.+\frac{1}{4}cIB(\tan(\psi)-\cot(\theta 1))-\frac{cIB\left(e^{(2\theta 1\tan(\phi 1))}-1\right)}{8\sin(\theta 1)^2\tan(\phi 1)}\right)$$

$$\left.\left(\frac{m\left(\tan(\phi 1)e^{(\theta 1\tan(\phi 1))}+\tan(\psi)\cos(\theta 1)+\sin(\theta 1)\right)}{\sin(\theta 1)}-\frac{m\left(e^{(\theta 1\tan(\phi 1))}+\tan(\psi)\sin(\theta 1)-\cos(\theta 1)\right)\cos(\theta 1)}{\sin(\theta 1)^2}-1-\cot(\theta 1)^2\right)^2\right)$$

First derivation of Equation 4.107 respect to θ_2

$$R3 := \frac{1}{B\left(e^{(\theta 1 \tan(\phi 1))} + \tan(\psi)\sin(\theta 1) - \cos(\theta 1)\right)^2 (\sin(\delta)(\sin(\theta 3)\cos(\theta 3) - \cos(\theta 3)^2\cot(\theta 2)) + \cos(\delta)(m + \sin(\theta 3)\cos(\theta 3)\cot(\theta 2) - \sin(\theta 3)^2))}$$

$$\left(2 \left(-\frac{1}{4\sin(\theta 1)^2\sin(\theta 2)^3} \left(B^2\cos(\phi 2)\left(q\tan\left(\frac{1}{4}\pi + \frac{1}{2}\phi 2\right) + \frac{c2}{\cos\left(\frac{1}{4}\pi + \frac{1}{2}\phi 2\right)}\right)\left(e^{(\theta 1\tan(\phi 1))} + \tan(\psi)\sin(\theta 1) - \cos(\theta 1)\right)^2 \left(\cos(\theta 3)^2 e^{(2\theta 2\tan(\phi 2))} - (-\cos(\theta 3)\cos(\theta 2) + \sin(\theta 3)\sin(\theta 2))^2\right)\cos(\theta 2)\right) \right.\right.$$

$$+ \frac{1}{8\sin(\theta 1)^2\sin(\theta 2)^2} \left(B^2\cos(\phi 2)\left(q\tan\left(\frac{1}{4}\pi + \frac{1}{2}\phi 2\right) + \frac{c2}{\cos\left(\frac{1}{4}\pi + \frac{1}{2}\phi 2\right)}\right)\left(e^{(\theta 1\tan(\phi 1))} + \tan(\psi)\sin(\theta 1) - \cos(\theta 1)\right)^2 \left(2\cos(\theta 3)^2\tan(\phi 2)\right.\right.$$

$$\left.\left. e^{(2\theta 2\tan(\phi 2))} - 2(-\cos(\theta 3)\cos(\theta 2) + \sin(\theta 3)\sin(\theta 2))(\cos(\theta 3)\sin(\theta 2) + \sin(\theta 3)\cos(\theta 2))\right)\right)$$

$$- \frac{c2\left(e^{(\theta 1\tan(\phi 1))} + \tan(\psi)\sin(\theta 1) - \cos(\theta 1)\right)^2 B^2\cos(\theta 3)^2\left(e^{(2\theta 2\tan(\phi 2))} - 1\right)\cos(\theta 2)}{4\tan(\phi 2)\sin(\theta 1)^2\sin(\theta 2)^3}$$

$$+ \frac{c2\left(e^{(\theta 1\tan(\phi 1))} + \tan(\psi)\sin(\theta 1) - \cos(\theta 1)\right)^2 B^2\cos(\theta 3)^2 e^{(2\theta 2\tan(\phi 2))}}{4\sin(\theta 1)^2\sin(\theta 2)^2} + \frac{cxB^2\left(e^{(\theta 1\tan(\phi 1))} + \tan(\psi)\sin(\theta 1) - \cos(\theta 1)\right)^2\cos(\theta 3)^2(-1 - \cot(\theta 2)^2)}{4\sin(\theta 1)^2} \Bigg) \sin$$

$$(\theta 1) \Bigg)$$

$$-\frac{1}{B\left(e^{(\theta 1\tan(\phi 1))}+\tan(\psi)\sin(\theta 1)-\cos(\theta 1)\right)^2(\sin(\delta)(\sin(\theta 3)\cos(\theta 3)-\cos(\theta 3)^2\cot(\theta 2))+\cos(\delta)(m+\sin(\theta 3)\cos(\theta 3)\cot(\theta 2)-\sin(\theta 3)^2))^2}\left(2\left(\right.\right.$$

$$\left.\frac{1}{8\sin(\theta 1)^2\sin(\theta 2)^2}\left(B^2\cos(\phi 2)\left(q\tan\left(\frac{1}{4}\pi+\frac{1}{2}\phi 2\right)+\frac{c2}{\cos\left(\frac{1}{4}\pi+\frac{1}{2}\phi 2\right)}\right)\left(e^{(\theta 1\tan(\phi 1))}+\tan(\psi)\sin(\theta 1)-\cos(\theta 1)\right)^2\left(\cos(\theta 3)^2e^{(2\theta 2\tan(\phi 2))}\right.\right.\right.$$

$$\left.\left.\left.-(-\cos(\theta 3)\cos(\theta 2)+\sin(\theta 3)\sin(\theta 2))^2\right)\right)+\frac{c2\left(e^{(\theta 1\tan(\phi 1))}+\tan(\psi)\sin(\theta 1)-\cos(\theta 1)\right)^2B^2\cos(\theta 3)^2\left(e^{(2\theta 2\tan(\phi 2))}-1\right)}{8\tan(\phi 2)\sin(\theta 1)^2\sin(\theta 2)^2}\right.$$

$$\left.-\frac{cxB^2\left(e^{(\theta 1\tan(\phi 1))}+\tan(\psi)\sin(\theta 1)-\cos(\theta 1)\right)^2(\sin(\theta 3)\cos(\theta 3)-\cos(\theta 3)^2\cot(\theta 2))}{4\sin(\theta 1)^2}\right)\sin(\theta 1)(-\sin(\delta)\cos(\theta 3)^2(-1-\cot(\theta 2)^2)$$

$$\left.+\cos(\delta)\sin(\theta 3)\cos(\theta 3)(-1-\cot(\theta 2)^2))\right)$$

Second derivation of Equation 4.107 respect to θ_2

$$R3:=\frac{1}{B\left(e^{(\theta 1\tan(\phi 1))}+\tan(\psi)\sin(\theta 1)-\cos(\theta 1)\right)^2(\sin(\delta)(\sin(\theta 3)\cos(\theta 3)-\cos(\theta 3)^2\cot(\theta 2))+\cos(\delta)(m+\sin(\theta 3)\cos(\theta 3)\cot(\theta 2)-\sin(\theta 3)^2))^2}\left(2\left(\right.\right.$$

$$\left.-\frac{1}{2\sin(\theta 1)^2\sin(\theta 2)^3}\left(B^2\cos(\phi 2)\left(q\tan\left(\frac{1}{4}\pi+\frac{1}{2}\phi 2\right)+\frac{c2}{\cos\left(\frac{1}{4}\pi+\frac{1}{2}\phi 2\right)}\right)\left(e^{(\theta 1\tan(\phi 1))}+\tan(\psi)\sin(\theta 1)-\cos(\theta 1)\right)^2\left(2\cos(\theta 3)^2\tan(\phi 2)e^{(2\theta 2\tan(\phi 2))}\right.\right.\right.$$

$$\left.\left.\left.-2(-\cos(\theta 3)\cos(\theta 2)+\sin(\theta 3)\sin(\theta 2))(\cos(\theta 3)\sin(\theta 2)+\sin(\theta 3)\cos(\theta 2))\right)\cos(\theta 2)\right)\right)$$

$$+\frac{1}{4\sin(\theta 1)^2\sin(\theta 2)^2}\left(B^2\cos(\phi 2)\left(q\tan\left(\frac{1}{4}\pi+\frac{1}{2}\phi 2\right)+\frac{c2}{\cos\left(\frac{1}{4}\pi+\frac{1}{2}\phi 2\right)}\right)\left(e^{(\theta 1\tan(\phi 1))}+\tan(\psi)\sin(\theta 1)-\cos(\theta 1)\right)^2\left(\cos(\theta 3)^2 e^{(2\theta 2\tan(\phi 2))}\right.\right.$$

$$\left.\left.-(-\cos(\theta 3)\cos(\theta 2)+\sin(\theta 3)\sin(\theta 2))^2\right)\right)$$

$$+\frac{1}{4\sin(\theta 1)^2\sin(\theta 2)^4}\left(3B^2\cos(\phi 2)\left(q\tan\left(\frac{1}{4}\pi+\frac{1}{2}\phi 2\right)+\frac{c2}{\cos\left(\frac{1}{4}\pi+\frac{1}{2}\phi 2\right)}\right)\left(e^{(\theta 1\tan(\phi 1))}+\tan(\psi)\sin(\theta 1)-\cos(\theta 1)\right)^2\left(\cos(\theta 3)^2 e^{(2\theta 2\tan(\phi 2))}\right.\right.$$

$$\left.\left.-(-\cos(\theta 3)\cos(\theta 2)+\sin(\theta 3)\sin(\theta 2))^2\right)\cos(\theta 2)^2\right)$$

$$+\frac{1}{8\sin(\theta 1)^2\sin(\theta 2)^2}\left(B^2\cos(\phi 2)\left(q\tan\left(\frac{1}{4}\pi+\frac{1}{2}\phi 2\right)+\frac{c2}{\cos\left(\frac{1}{4}\pi+\frac{1}{2}\phi 2\right)}\right)\left(e^{(\theta 1\tan(\phi 1))}+\tan(\psi)\sin(\theta 1)-\cos(\theta 1)\right)^2\left(4\cos(\theta 3)^2\tan(\phi 2)^2\right.\right.$$

$$\left.\left.e^{(2\theta 2\tan(\phi 2))}-2(\cos(\theta 3)\sin(\theta 2)+\sin(\theta 3)\cos(\theta 2))^2-2(-\cos(\theta 3)\cos(\theta 2)+\sin(\theta 3)\sin(\theta 2))(\cos(\theta 3)\cos(\theta 2)-\sin(\theta 3)\sin(\theta 2))\right)\right)$$

$$-\frac{c2\left(e^{(\theta 1\tan(\phi 1))}+\tan(\psi)\sin(\theta 1)-\cos(\theta 1)\right)^2B^2\cos(\theta 3)^2e^{(2\theta 2\tan(\phi 2))}\cos(\theta 2)}{\sin(\theta 1)^2\sin(\theta 2)^3}$$

$$+\frac{c2\left(e^{(\theta 1\tan(\phi 1))}+\tan(\psi)\sin(\theta 1)-\cos(\theta 1)\right)^2B^2\cos(\theta 3)^2\left(e^{(2\theta 2\tan(\phi 2))}-1\right)}{4\tan(\phi 2)\sin(\theta 1)^2\sin(\theta 2)^2}$$

$$+\frac{3c2\left(e^{(\theta 1\tan(\phi 1))}+\tan(\psi)\sin(\theta 1)-\cos(\theta 1)\right)^2B^2\cos(\theta 3)^2\left(e^{(2\theta 2\tan(\phi 2))}-1\right)\cos(\theta 2)^2}{4\tan(\phi 2)\sin(\theta 1)^2\sin(\theta 2)^4}$$

$$+\frac{c2\left(e^{(\theta 1\tan(\phi 1))}+\tan(\psi)\sin(\theta 1)-\cos(\theta 1)\right)^2B^2\cos(\theta 3)^2\tan(\phi 2)e^{(2\theta 2\tan(\phi 2))}}{2\sin(\theta 1)^2\sin(\theta 2)^2}$$

$$-\frac{cx B^2\left(e^{(\theta 1\tan(\phi 1))}+\tan(\psi)\sin(\theta 1)-\cos(\theta 1)\right)^2\cos(\theta 3)^2\cot(\theta 2)\left(-1-\cot(\theta 2)^2\right)}{2\sin(\theta 1)^2}\Bigg)\sin(\theta 1)\Bigg)$$

$$-\frac{1}{B\left(e^{(\theta 1\tan(\phi 1))}+\tan(\psi)\sin(\theta 1)-\cos(\theta 1)\right)^2\left(\sin(\delta)\left(\sin(\theta 3)\cos(\theta 3)-\cos(\theta 3)^2\cot(\theta 2)\right)+\cos(\delta)\left(m+\sin(\theta 3)\cos(\theta 3)\cot(\theta 2)-\sin(\theta 3)^2\right)\right)^2}\Bigg(4\Bigg($$

$$-\frac{1}{4\sin(\theta 1)^2\sin(\theta 2)^3}\Bigg(B^2\cos(\phi 2)\left(q\tan\left(\frac{1}{4}\pi+\frac{1}{2}\phi 2\right)+\frac{c2}{\cos\left(\frac{1}{4}\pi+\frac{1}{2}\phi 2\right)}\right)\left(e^{(\theta 1\tan(\phi 1))}+\tan(\psi)\sin(\theta 1)-\cos(\theta 1)\right)^2\Bigg(\cos(\theta 3)^2e^{(2\theta 2\tan(\phi 2))}$$

$$-\left(-\cos(\theta 3)\cos(\theta 2)+\sin(\theta 3)\sin(\theta 2)\right)^2\Bigg)\cos(\theta 2)\Bigg)$$

$$+\frac{1}{8\sin(\theta 1)^2\sin(\theta 2)^2}\Bigg(B^2\cos(\phi 2)\left(q\tan\left(\frac{1}{4}\pi+\frac{1}{2}\phi 2\right)+\frac{c2}{\cos\left(\frac{1}{4}\pi+\frac{1}{2}\phi 2\right)}\right)\left(e^{(\theta 1\tan(\phi 1))}+\tan(\psi)\sin(\theta 1)-\cos(\theta 1)\right)^2\Bigg(2\cos(\theta 3)^2\tan(\phi 2)$$

$$e^{(2\theta 2\tan(\phi 2))}-2\left(-\cos(\theta 3)\cos(\theta 2)+\sin(\theta 3)\sin(\theta 2)\right)\left(\cos(\theta 3)\sin(\theta 2)+\sin(\theta 3)\cos(\theta 2)\right)\Bigg)\Bigg)$$

$$-\frac{c2\left(e^{(\theta 1\tan(\phi 1))}+\tan(\psi)\sin(\theta 1)-\cos(\theta 1)\right)^2B^2\cos(\theta 3)^2\left(e^{(2\theta 2\tan(\phi 2))}-1\right)\cos(\theta 2)}{4\tan(\phi 2)\sin(\theta 1)^2\sin(\theta 2)^3}$$

$$+\frac{c2\left(e^{(\theta 1\tan(\phi 1))}+\tan(\psi)\sin(\theta 1)-\cos(\theta 1)\right)^2B^2\cos(\theta 3)^2e^{(2\theta 2\tan(\phi 2))}}{4\sin(\theta 1)^2\sin(\theta 2)^2}+\frac{cxB^2\left(e^{(\theta 1\tan(\phi 1))}+\tan(\psi)\sin(\theta 1)-\cos(\theta 1)\right)^2\cos(\theta 3)^2\left(-1-\cot(\theta 2)^2\right)}{4\sin(\theta 1)^2}\Bigg)\sin$$

$$(\theta 1)\left(-\sin(\delta)\cos(\theta 3)^2\left(-1-\cot(\theta 2)^2\right)+\cos(\delta)\sin(\theta 3)\cos(\theta 3)\left(-1-\cot(\theta 2)^2\right)\right)\Bigg)$$

$$-\frac{1}{B\left(e^{(\theta 1\tan(\phi 1))}+\tan(\psi)\sin(\theta 1)-\cos(\theta 1)\right)^2(\sin(\delta)(\sin(\theta 3)\cos(\theta 3)-\cos(\theta 3)^2\cot(\theta 2))+\cos(\delta)(m+\sin(\theta 3)\cos(\theta 3)\cot(\theta 2)-\sin(\theta 3)^2))^2}\left(2\left(\frac{1}{8\sin(\theta 1)^2\sin(\theta 2)^2}\left(B^2\cos(\phi 2)\left(q\tan\left(\frac{1}{4}\pi+\frac{1}{2}\phi 2\right)+\frac{c2}{\cos\left(\frac{1}{4}\pi+\frac{1}{2}\phi 2\right)}\right)\left(e^{(\theta 1\tan(\phi 1))}+\tan(\psi)\sin(\theta 1)-\cos(\theta 1)\right)^2\left(\cos(\theta 3)^2e^{(2\theta 2\tan(\phi 2))}-(-\cos(\theta 3)\cos(\theta 2)+\sin(\theta 3)\sin(\theta 2))^2\right)\right)+\frac{c2\left(e^{(\theta 1\tan(\phi 1))}+\tan(\psi)\sin(\theta 1)-\cos(\theta 1)\right)^2B^2\cos(\theta 3)^2\left(e^{(2\theta 2\tan(\phi 2))}-1\right)}{8\tan(\phi 2)\sin(\theta 1)^2\sin(\theta 2)^2}\right)\sin(\theta 1)(2\sin(\delta)\cos(\theta 3)^2\cot(\theta 2)(-1-\cot(\theta 2)^2)-\frac{cxB^2\left(e^{(\theta 1\tan(\phi 1))}+\tan(\psi)\sin(\theta 1)-\cos(\theta 1)\right)^2(\sin(\theta 3)\cos(\theta 3)-\cos(\theta 3)^2\cot(\theta 2))}{4\sin(\theta 1)^2}\right)-2\cos(\delta)\sin(\theta 3)\cos(\theta 3)\cot(\theta 2)(-1-\cot(\theta 2)^2))\Bigg)$$

$$+\frac{1}{B\left(e^{(\theta 1\tan(\phi 1))}+\tan(\psi)\sin(\theta 1)-\cos(\theta 1)\right)^2(\sin(\delta)(\sin(\theta 3)\cos(\theta 3)-\cos(\theta 3)^2\cot(\theta 2))+\cos(\delta)(m+\sin(\theta 3)\cos(\theta 3)\cot(\theta 2)-\sin(\theta 3)^2))^3}\left(4\left(\frac{1}{8\sin(\theta 1)^2\sin(\theta 2)^2}\left(B^2\cos(\phi 2)\left(q\tan\left(\frac{1}{4}\pi+\frac{1}{2}\phi 2\right)+\frac{c2}{\cos\left(\frac{1}{4}\pi+\frac{1}{2}\phi 2\right)}\right)\left(e^{(\theta 1\tan(\phi 1))}+\tan(\psi)\sin(\theta 1)-\cos(\theta 1)\right)^2\left(\cos(\theta 3)^2e^{(2\theta 2\tan(\phi 2))}-(-\cos(\theta 3)\cos(\theta 2)+\sin(\theta 3)\sin(\theta 2))^2\right)\right)+\frac{c2\left(e^{(\theta 1\tan(\phi 1))}+\tan(\psi)\sin(\theta 1)-\cos(\theta 1)\right)^2B^2\cos(\theta 3)^2\left(e^{(2\theta 2\tan(\phi 2))}-1\right)}{8\tan(\phi 2)\sin(\theta 1)^2\sin(\theta 2)^2}\right)$$

$$-\frac{cxB^2\left(e^{(\theta 1 \tan(\phi 1))}+\tan(\psi)\sin(\theta 1)-\cos(\theta 1)\right)^2(\sin(\theta 3)\cos(\theta 3)-\cos(\theta 3)^2\cot(\theta 2))}{4\sin(\theta 1)^2}\sin(\theta 1)$$

$$(-\sin(\delta)\cos(\theta 3)^2(-1-\cot(\theta 2)^2)+\cos(\delta)\sin(\theta 3)\cos(\theta 3)(-1-\cot(\theta 2)^2))^2$$

APPENDIX 3

Program code for general shear failure theoretical model is given here.

Program List G-STColumn


```
Private Sub Command1_Click()
Dim theta11, theta12, theta1, gamma1, phi1, psi, delta, thetatemp, cg0, cg1, cg2 As
Double
Dim cg21, cg22, P As Double
Dim numb, i, X As Integer
numb = 1
numbb = 1
a = 2 / 3
m = 1 / 2

gamma1 = 1
phi1 = 30 * 3.141592 / 180
psi = 65 * 3.141592 / 180
B = 1
P = 50

gamma2 = 1
phi2 = 24 * 3.141592 / 180
theta3 = (45 - 24 / 2) * 3.141592 / 180


delta = phi2
theta1temp = 30 * 3.141592 / 180
theta2temp = 10 * 3.141592 / 180

kjj = 0.01

F1gamma = 1
F2gamma = 2

  Do
If F1gamma > F2gamma Then

X = -1
Else
```

```
X = 1
numb = numb + 1
End If
If numb = 10 Then kjj = 0.01

P = P + X * kjj / numb

Do

theta1 = theta1temp

psi = theta1 + phi1

cg0 = 8# * (-gamma1 * (B) ^ 3 * (Sin(theta1)) ^ -4 / (9# * (Tan(phi1)) ^ 2 + 1#) *
(Exp(3# * theta1 * Tan(phi1)) - 3# * Tan(phi1) * Sin(theta1) - Cos(theta1)) * Cos(theta1)
/ 8# + gamma1 * (B) ^ 3 * (Sin(theta1)) ^ -3 / (9# * (Tan(phi1)) ^ 2 + 1#) * (3# *
Tan(phi1) * Exp(3# * theta1 * Tan(phi1)) - 3# * Tan(phi1) * Cos(theta1) + Sin(theta1)) /
24# + gamma1 * (B) ^ 3 * (1# + (1# / Tan(theta1)) ^ 2) / 48# + P * Sin(-psi + phi1) * B *
(1# + (1# / Tan(theta1)) ^ 2) / 2#) / Cos(delta) * (B) ^ -2 / (Tan(psi) * Sin(theta1) -
Cos(theta1) + Exp(theta1 * Tan(phi1))) * Sin(theta1) / ((a - 1) * (Tan(psi) - 1# /
Tan(theta1)) + a * Exp(theta1 * Tan(phi1)) / Sin(theta1))
cg1 = -8# * (gamma1 * (B) ^ 3 * (Sin(theta1)) ^ -3 / (9# * (Tan(phi1)) ^ 2 + 1#) *
(Exp(3# * theta1 * Tan(phi1)) - 3# * Tan(phi1) * Sin(theta1) - Cos(theta1)) / 24# +
gamma1 * (B) ^ 3 * (Tan(psi) - 1# / Tan(theta1)) / 48# + P * (Cos(-psi + phi1) * B / 3# -
Sin(-psi + phi1) * (B * Tan(psi) / 3# - B * (Tan(psi) - 1# / Tan(theta1)) / 2#))) /
Cos(delta) * (B) ^ -2 * (Tan(psi) * Sin(theta1) - Cos(theta1) + Exp(theta1 * Tan(phi1))) ^
-2 * Sin(theta1) / ((a - 1) * (Tan(psi) - 1# / Tan(theta1)) + a * Exp(theta1 * Tan(phi1)) /
Sin(theta1)) * (Tan(psi) * Cos(theta1) + Sin(theta1) + Tan(phi1) * Exp(theta1 *
Tan(phi1)))
cg2 = 8# * (gamma1 * (B) ^ 3 * (Sin(theta1)) ^ -3 / (9# * (Tan(phi1)) ^ 2 + 1#) * (Exp(3#
* theta1 * Tan(phi1)) - 3# * Tan(phi1) * Sin(theta1) - Cos(theta1)) / 24# + gamma1 * (B)
^ 3 * (Tan(psi) - 1# / Tan(theta1)) / 48# + P * (Cos(-psi + phi1) * B / 3# - Sin(-psi + phi1)
* (B * Tan(psi) / 3# - B * (Tan(psi) - 1# / Tan(theta1)) / 2#))) / Cos(delta) * (B) ^ -2 /
(Tan(psi) * Sin(theta1) - Cos(theta1) + Exp(theta1 * Tan(phi1))) * Cos(theta1) / ((a - 1) *
(Tan(psi) - 1# / Tan(theta1)) + a * Exp(theta1 * Tan(phi1)) / Sin(theta1))
cg22 = -8# * (gamma1 * (B) ^ 3 * (Sin(theta1)) ^ -3 / (9# * (Tan(phi1)) ^ 2 + 1#) *
(Exp(3# * theta1 * Tan(phi1)) - 3# * Tan(phi1) * Sin(theta1) - Cos(theta1)) / 24# +
gamma1 * (B) ^ 3 * (Tan(psi) - 1# / Tan(theta1)) / 48# + P * (Cos(-psi + phi1) * B / 3# -
Sin(-psi + phi1) * (B * Tan(psi) / 3# - B * (Tan(psi) - 1# / Tan(theta1)) / 2#))) /
Cos(delta) * (B) ^ -2 / (Tan(psi) * Sin(theta1) - Cos(theta1) + Exp(theta1 * Tan(phi1))) *
Sin(theta1) * ((a - 1) * (Tan(psi) - 1# / Tan(theta1)) + a * Exp(theta1 * Tan(phi1)) /
Sin(theta1)) ^ -2 * ((a - 1) * (1# + (1# / Tan(theta1)) ^ 2) + a * Tan(phi1) * Exp(theta1 *
Tan(phi1)) / Sin(theta1) - a * Exp(theta1 * Tan(phi1)) * (Sin(theta1)) ^ -2 * Cos(theta1))

cg3 = cg0 + cg1 + cg2 + cg22
```

```
aaa1 = 8 * (gamma1 * (B) ^ 3 * (Sin(theta1)) ^ -5 / (9# * (Tan(phi1)) ^ 2 + 1) * (Exp(3 *
theta1 * Tan(phi1)) - 3 * Tan(phi1) * Sin(theta1) - Cos(theta1)) * (Cos(theta1)) ^ 2 / 2 -
gamma1 * (B) ^ 3 * (Sin(theta1)) ^ -4 / (9 * (Tan(phi1)) ^ 2 + 1) * (3 * Tan(phi1) *
Exp(3 * theta1 * Tan(phi1)) - 3 * Tan(phi1) * Cos(theta1) + Sin(theta1)) * Cos(theta1) / 4
+ gamma1 * (B) ^ 3 * (Sin(theta1)) ^ -3 / (9 * (Tan(phi1)) ^ 2 + 1) * (Exp(3 * theta1 *
Tan(phi1)) - 3 * Tan(phi1) * Sin(theta1) - Cos(theta1)) / 8 + gamma1 * (B) ^ 3 *
(Sin(theta1)) ^ -3 / (9 * (Tan(phi1)) ^ 2 + 1) * (9 * (Tan(phi1)) ^ 2 * Exp(3 * theta1 *
Tan(phi1)) + 3 * Tan(phi1) * Sin(theta1) + Cos(theta1)) / 24 + gamma1 * (B) ^ 3 * 1 /
Tan(theta1) * (-1 - (1 / Tan(theta1)) ^ 2) / 24 + P * Sin(-psi + phi1) * B * 1 / Tan(theta1)
* (-1 - (1 / Tan(theta1)) ^ 2)) / Cos(delta) * (B) ^ -2 / (Tan(psi) * Sin(theta1) -
Cos(theta1) + Exp(theta1 * Tan(phi1))) * Sin(theta1) / ((a - 1) * (Tan(psi) - 1# /
Tan(theta1)) + a * Exp(theta1 * Tan(phi1)) / Sin(theta1))
aaa2 = -16# * (-gamma1 * (B) ^ 3 * (Sin(theta1)) ^ -4 / (9# * (Tan(phi1)) ^ 2 + 1#) *
(Exp(3# * theta1 * Tan(phi1)) - 3# * Tan(phi1) * Sin(theta1) - Cos(theta1)) * Cos(theta1)
/ 8# + gamma1 * (B) ^ 3 * (Sin(theta1)) ^ -3 / (9# * (Tan(phi1)) ^ 2 + 1#) * (3# *
Tan(phi1) * Exp(3# * theta1 * Tan(phi1)) - 3# * Tan(phi1) * Cos(theta1) + Sin(theta1)) /
24# + gamma1 * (B) ^ 3 * (1# + (1# / Tan(theta1)) ^ 2) / 48# + P * Sin(-psi + phi1) * B *
(1# + (1# / Tan(theta1)) ^ 2) / 2#) / Cos(delta) * (B) ^ -2 * (Tan(psi) * Sin(theta1) -
Cos(theta1) + Exp(theta1 * Tan(phi1))) ^ -2 * Sin(theta1) / ((a - 1) * (Tan(psi) - 1# /
Tan(theta1)) + a * Exp(theta1 * Tan(phi1)) / Sin(theta1)) * (Tan(psi) * Cos(theta1) +
Sin(theta1) + Tan(phi1) * Exp(theta1 * Tan(phi1)))
aaa3 = 16# * (-gamma1 * (B) ^ 3 * (Sin(theta1)) ^ -4 / (9# * (Tan(phi1)) ^ 2 + 1#) *
(Exp(3# * theta1 * Tan(phi1)) - 3# * Tan(phi1) * Sin(theta1) - Cos(theta1)) * Cos(theta1)
/ 8# + gamma1 * (B) ^ 3 * (Sin(theta1)) ^ -3 / (9# * (Tan(phi1)) ^ 2 + 1#) * (3# *
Tan(phi1) * Exp(3# * theta1 * Tan(phi1)) - 3# * Tan(phi1) * Cos(theta1) + Sin(theta1)) /
24# + gamma1 * (B) ^ 3 * (1# + (1# / Tan(theta1)) ^ 2) / 48# + P * Sin(-psi + phi1) * B *
(1# + (1# / Tan(theta1)) ^ 2) / 2#) / Cos(delta) * (B) ^ -2 / (Tan(psi) * Sin(theta1) -
Cos(theta1) + Exp(theta1 * Tan(phi1))) * Cos(theta1) / ((a - 1) * (Tan(psi) - 1# /
Tan(theta1)) + a * Exp(theta1 * Tan(phi1)) / Sin(theta1))
aaa4 = -16# * (-gamma1 * (B) ^ 3 * (Sin(theta1)) ^ -4 / (9# * (Tan(phi1)) ^ 2 + 1#) *
(Exp(3# * theta1 * Tan(phi1)) - 3# * Tan(phi1) * Sin(theta1) - Cos(theta1)) * Cos(theta1)
/ 8# + gamma1 * (B) ^ 3 * (Sin(theta1)) ^ -3 / (9# * (Tan(phi1)) ^ 2 + 1#) * (3# *
Tan(phi1) * Exp(3# * theta1 * Tan(phi1)) - 3# * Tan(phi1) * Cos(theta1) + Sin(theta1)) /
24# + gamma1 * (B) ^ 3 * (1# + (1# / Tan(theta1)) ^ 2) / 48# + P * Sin(-psi + phi1) * B *
(1# + (1# / Tan(theta1)) ^ 2) / 2#) / Cos(delta) * (B) ^ -2 / (Tan(psi) * Sin(theta1) -
Cos(theta1) + Exp(theta1 * Tan(phi1))) * Sin(theta1) * ((a - 1) * (Tan(psi) - 1# /
Tan(theta1)) + a * Exp(theta1 * Tan(phi1)) / Sin(theta1)) ^ -2 * ((a - 1) * (1# + (1# /
Tan(theta1)) ^ 2) + a * Tan(phi1) * Exp(theta1 * Tan(phi1)) / Sin(theta1) - a * Exp(theta1
* Tan(phi1)) * (Sin(theta1)) ^ -2 * Cos(theta1))
aaa5 = 16# * (gamma1 * (B) ^ 3 * (Sin(theta1)) ^ -3 / (9# * (Tan(phi1)) ^ 2 + 1#) *
(Exp(3# * theta1 * Tan(phi1)) - 3# * Tan(phi1) * Sin(theta1) - Cos(theta1)) / 24# +
gamma1 * (B) ^ 3 * (Tan(psi) - 1# / Tan(theta1)) / 48# + P * (Cos(-psi + phi1) * B / 3# -
Sin(-psi + phi1) * (B * Tan(psi) / 3# - B * (Tan(psi) - 1# / Tan(theta1)) / 2#))) /
Cos(delta) * (B) ^ -2 * (Tan(psi) * Sin(theta1) - Cos(theta1) + Exp(theta1 * Tan(phi1))) ^
-3 * Sin(theta1) / ((a - 1) * (Tan(psi) - 1# / Tan(theta1)) + a * Exp(theta1 * Tan(phi1)) /
```

```
Sin(theta1)) * (Tan(psi) * Cos(theta1) + Sin(theta1) + Tan(phi1) * Exp(theta1 *
Tan(phi1))) ^ 2
aaa6 = -16# * (gamma1 * (B) ^ 3 * (Sin(theta1)) ^ -3 / (9# * (Tan(phi1)) ^ 2 + 1#) *
(Exp(3# * theta1 * Tan(phi1)) - 3# * Tan(phi1) * Sin(theta1) - Cos(theta1)) / 24# +
gamma1 * (B) ^ 3 * (Tan(psi) - 1# / Tan(theta1)) / 48# + P * (Cos(-psi + phi1) * B / 3# -
Sin(-psi + phi1) * (B * Tan(psi) / 3# - B * (Tan(psi) - 1# / Tan(theta1)) / 2#))) /
Cos(delta) * (B) ^ -2 * (Tan(psi) * Sin(theta1) - Cos(theta1) + Exp(theta1 * Tan(phi1))) ^
-2 * Cos(theta1) / ((a - 1) * (Tan(psi) - 1# / Tan(theta1)) + a * Exp(theta1 * Tan(phi1)) /
Sin(theta1)) * (Tan(psi) * Cos(theta1) + Sin(theta1) + Tan(phi1) * Exp(theta1 *
Tan(phi1)))
aaa7 = 16# * (gamma1 * (B) ^ 3 * (Sin(theta1)) ^ -3 / (9# * (Tan(phi1)) ^ 2 + 1#) *
(Exp(3# * theta1 * Tan(phi1)) - 3# * Tan(phi1) * Sin(theta1) - Cos(theta1)) / 24# +
gamma1 * (B) ^ 3 * (Tan(psi) - 1# / Tan(theta1)) / 48# + P * (Cos(-psi + phi1) * B / 3# -
Sin(-psi + phi1) * (B * Tan(psi) / 3# - B * (Tan(psi) - 1# / Tan(theta1)) / 2#))) /
Cos(delta) * (B) ^ -2 * (Tan(psi) * Sin(theta1) - Cos(theta1) + Exp(theta1 * Tan(phi1))) ^
-2 * Sin(theta1) * ((a - 1) * (Tan(psi) - 1# / Tan(theta1)) + a * Exp(theta1 * Tan(phi1)) /
Sin(theta1)) ^ -2 * (Tan(psi) * Cos(theta1) + Sin(theta1) + Tan(phi1) * Exp(theta1 *
Tan(phi1))) * ((a - 1) * (1# + (1# / Tan(theta1)) ^ 2) + a * Tan(phi1) * Exp(theta1 *
Tan(phi1)) / Sin(theta1) - a * Exp(theta1 * Tan(phi1)) * (Sin(theta1)) ^ -2 * Cos(theta1))
aaa8 = -8# * (gamma1 * (B) ^ 3 * (Sin(theta1)) ^ -3 / (9# * (Tan(phi1)) ^ 2 + 1#) *
(Exp(3# * theta1 * Tan(phi1)) - 3# * Tan(phi1) * Sin(theta1) - Cos(theta1)) / 24# +
gamma1 * (B) ^ 3 * (Tan(psi) - 1# / Tan(theta1)) / 48# + P * (Cos(-psi + phi1) * B / 3# -
Sin(-psi + phi1) * (B * Tan(psi) / 3# - B * (Tan(psi) - 1# / Tan(theta1)) / 2#))) /
Cos(delta) * (B) ^ -2 * (Tan(psi) * Sin(theta1) - Cos(theta1) + Exp(theta1 * Tan(phi1))) ^
-2 * Sin(theta1) / ((a - 1) * (Tan(psi) - 1# / Tan(theta1)) + a * Exp(theta1 * Tan(phi1)) /
Sin(theta1)) * (-Tan(psi) * Sin(theta1) + Cos(theta1) + (Tan(phi1)) ^ 2 * Exp(theta1 *
Tan(phi1)))
aaa9 = -8# * (gamma1 * (B) ^ 3 * (Sin(theta1)) ^ -3 / (9# * (Tan(phi1)) ^ 2 + 1#) *
(Exp(3# * theta1 * Tan(phi1)) - 3# * Tan(phi1) * Sin(theta1) - Cos(theta1)) / 24# +
gamma1 * (B) ^ 3 * (Tan(psi) - 1# / Tan(theta1)) / 48# + P * (Cos(-psi + phi1) * B / 3# -
Sin(-psi + phi1) * (B * Tan(psi) / 3# - B * (Tan(psi) - 1# / Tan(theta1)) / 2#))) /
Cos(delta) * (B) ^ -2 / (Tan(psi) * Sin(theta1) - Cos(theta1) + Exp(theta1 * Tan(phi1))) *
Sin(theta1) / ((a - 1) * (Tan(psi) - 1# / Tan(theta1)) + a * Exp(theta1 * Tan(phi1)) /
Sin(theta1))
aaa10 = -16# * (gamma1 * (B) ^ 3 * (Sin(theta1)) ^ -3 / (9# * (Tan(phi1)) ^ 2 + 1#) *
(Exp(3# * theta1 * Tan(phi1)) - 3# * Tan(phi1) * Sin(theta1) - Cos(theta1)) / 24# +
gamma1 * (B) ^ 3 * (Tan(psi) - 1# / Tan(theta1)) / 48# + P * (Cos(-psi + phi1) * B / 3# -
Sin(-psi + phi1) * (B * Tan(psi) / 3# - B * (Tan(psi) - 1# / Tan(theta1)) / 2#))) /
Cos(delta) * (B) ^ -2 / (Tan(psi) * Sin(theta1) - Cos(theta1) + Exp(theta1 * Tan(phi1))) *
Cos(theta1) * ((a - 1) * (Tan(psi) - 1# / Tan(theta1)) + a * Exp(theta1 * Tan(phi1)) /
Sin(theta1)) ^ -2 * ((a - 1) * (1# + (1# / Tan(theta1)) ^ 2) + a * Tan(phi1) * Exp(theta1 *
Tan(phi1)) / Sin(theta1) - a * Exp(theta1 * Tan(phi1)) * (Sin(theta1)) ^ -2 * Cos(theta1))
aaa11 = 16# * (gamma1 * (B) ^ 3 * (Sin(theta1)) ^ -3 / (9# * (Tan(phi1)) ^ 2 + 1#) *
(Exp(3# * theta1 * Tan(phi1)) - 3# * Tan(phi1) * Sin(theta1) - Cos(theta1)) / 24# +
gamma1 * (B) ^ 3 * (Tan(psi) - 1# / Tan(theta1)) / 48# + P * (Cos(-psi + phi1) * B / 3# -
Sin(-psi + phi1) * (B * Tan(psi) / 3# - B * (Tan(psi) - 1# / Tan(theta1)) / 2#))) /
```

```
Cos(delta) * (B) ^ -2 / (Tan(psi) * Sin(theta1) - Cos(theta1) + Exp(theta1 * Tan(phi1))) *
Sin(theta1) * ((a - 1) * (Tan(psi) - 1# / Tan(theta1)) + a * Exp(theta1 * Tan(phi1)) /
Sin(theta1)) ^ -3 * ((a - 1) * (1# + (1# / Tan(theta1)) ^ 2) + a * Tan(phi1) * Exp(theta1 *
Tan(phi1)) / Sin(theta1) - a * Exp(theta1 * Tan(phi1)) * (Sin(theta1)) ^ -2 * Cos(theta1))
^ 2
aaa12 = -8# * (gamma1 * (B) ^ 3 * (Sin(theta1)) ^ -3 / (9# * (Tan(phi1)) ^ 2 + 1#) *
(Exp(3# * theta1 * Tan(phi1)) - 3# * Tan(phi1) * Sin(theta1) - Cos(theta1)) / 24# +
gamma1 * (B) ^ 3 * (Tan(psi) - 1# / Tan(theta1)) / 48# + P * (Cos(-psi + phi1) * B / 3# -
Sin(-psi + phi1) * (B * Tan(psi) / 3# - B * (Tan(psi) - 1# / Tan(theta1)) / 2#))) /
Cos(delta) * (B) ^ -2 / (Tan(psi) * Sin(theta1) - Cos(theta1) + Exp(theta1 * Tan(phi1))) *
Sin(theta1) * ((a - 1) * (Tan(psi) - 1# / Tan(theta1)) + a * Exp(theta1 * Tan(phi1)) /
Sin(theta1)) ^ -2 * (2# * (a - 1) * 1# / Tan(theta1) * (-1# - (1# / Tan(theta1)) ^ 2) + a *
(Tan(phi1)) ^ 2 * Exp(theta1 * Tan(phi1)) / Sin(theta1) - 2# * a * Tan(phi1) * Exp(theta1
* Tan(phi1)) * (Sin(theta1)) ^ -2 * Cos(theta1) + 2# * a * Exp(theta1 * Tan(phi1)) *
(Sin(theta1)) ^ -3 * (Cos(theta1)) ^ 2 + a * Exp(theta1 * Tan(phi1)) / Sin(theta1))

aaa13 = aaa1 + aaa2 + aaa3 + aaa4 + aaa5 + aaa6 + aaa7 + aaa8 + aaa9 + aaa10 + aaa11 +
aaa12

If aaa13 = 0 Then

  Text1.Text = "Failure"
  Stop
End If
  theta11 = theta1temp
  theta12 = theta11 - cg3 / aaa13
  theta1temp = theta12

Loop Until Abs(theta12 - theta11) <= 0.00000001
theta1 = theta12

Text1.Text = theta1 / 3.141592 * 180

'  ngamma for theta2
theta21 = 10 * 3.141592 / 180
theta22 = 100 * 3.141592 / 180

Do
theta23 = (theta21 + theta22) / 2
 For i = 1 To 3

  If i = 1 Then
  theta2 = theta21
  ElseIf i = 2 Then
  theta2 = theta22
  Else
```

```
        theta2 = theta23
    End If

m1 = -gamma2 * (B) ^ 3 * (Sin(theta1)) ^ -3 * (Sin(theta2)) ^ -4 * (Tan(psi) * Sin(theta1)
- Cos(theta1) + Exp(theta1 * Tan(phi1))) ^ 3 * Cos(phi2) * Cos(45 * 3.141592 / 180 +
phi2 / 2#) * Tan(45 * 3.141592 / 180 + phi2 / 2#) * (-Cos(theta3) * Cos(theta2) +
Sin(theta3) * Sin(theta2) + Cos(theta3) * Exp(theta2 * Tan(phi2))) ^ 2 * (Cos(theta3) *
Cos(theta2) / 2# - Sin(theta3) * Sin(theta2) / 2# + Cos(theta3) * Exp(theta2 * Tan(phi2)))
* Cos(theta2) / 8# + gamma2 * (B) ^ 3 * (Sin(theta1)) ^ -3 * (Sin(theta2)) ^ -3 *
(Tan(psi) * Sin(theta1) - Cos(theta1) + Exp(theta1 * Tan(phi1))) ^ 3 * Cos(phi2) *
Cos(45 * 3.141592 / 180 + phi2 / 2#) * Tan(45 * 3.141592 / 180 + phi2 / 2#) * (-
Cos(theta3) * Cos(theta2) + Sin(theta3) * Sin(theta2) + Cos(theta3) * Exp(theta2 *
Tan(phi2))) * (Cos(theta3) * Cos(theta2) / 2# - Sin(theta3) * Sin(theta2) / 2# +
Cos(theta3) * Exp(theta2 * Tan(phi2))) * (Cos(theta3) * Sin(theta2) + Sin(theta3) *
Cos(theta2) + Cos(theta3) * Tan(phi2) * Exp(theta2 * Tan(phi2))) / 12#
m2 = gamma2 * (B) ^ 3 * (Sin(theta1)) ^ -3 * (Sin(theta2)) ^ -3 * (Tan(psi) * Sin(theta1)
- Cos(theta1) + Exp(theta1 * Tan(phi1))) ^ 3 * Cos(phi2) * Cos(45 * 3.141592 / 180 +
phi2 / 2#) * Tan(45 * 3.141592 / 180 + phi2 / 2#) * (-Cos(theta3) * Cos(theta2) +
Sin(theta3) * Sin(theta2) + Cos(theta3) * Exp(theta2 * Tan(phi2))) ^ 2 * (-Cos(theta3) *
Sin(theta2) / 2# - Sin(theta3) * Cos(theta2) / 2# + Cos(theta3) * Tan(phi2) * Exp(theta2 *
Tan(phi2))) / 24# - gamma2 * (B) ^ 3 * (Cos(theta3)) ^ 3 * (Sin(theta1)) ^ -3 *
(Sin(theta2)) ^ -4 / (9# * (Tan(phi2)) ^ 2 + 1#) * (Tan(psi) * Sin(theta1) - Cos(theta1) +
Exp(theta1 * Tan(phi1))) ^ 3 * (Exp(3# * theta2 * Tan(phi2)) * (3# * Tan(phi2) *
Cos(theta3) - Sin(theta3)) + Sin(theta3 + theta2) - 3# * Tan(phi2) * Cos(theta3 + theta2))
* Cos(theta2) / 8#
m3 = gamma2 * (B) ^ 3 * (Cos(theta3)) ^ 3 * (Sin(theta1)) ^ -3 * (Sin(theta2)) ^ -3 / (9#
* (Tan(phi2)) ^ 2 + 1#) * (Tan(psi) * Sin(theta1) - Cos(theta1) + Exp(theta1 *
Tan(phi1))) ^ 3 * (3# * Tan(phi2) * Exp(3# * theta2 * Tan(phi2)) * (3# * Tan(phi2) *
Cos(theta3) - Sin(theta3)) + Cos(theta3 + theta2) + 3# * Tan(phi2) * Sin(theta3 + theta2))
/ 24# + gamma2 * (B) ^ 3 * (Sin(theta1)) ^ -3 * (Tan(psi) * Sin(theta1) - Cos(theta1) +
Exp(theta1 * Tan(phi1))) ^ 3 * (-(Cos(theta3)) ^ 2 * 1# / Tan(theta2) + Sin(theta3) *
Cos(theta3)) * (Cos(theta3)) ^ 2 * (-1# - (1# / Tan(theta2)) ^ 2) / 12#
m4 = 8# * (B) ^ -2 * (Sin(theta1)) ^ 2 * (Tan(psi) * Sin(theta1) - Cos(theta1) +
Exp(theta1 * Tan(phi1))) ^ -2 / (Sin(delta) * (-(Cos(theta3)) ^ 2 * 1# / Tan(theta2) +
Sin(theta3) * Cos(theta3)) + Cos(delta) * (a + Sin(theta3) * Cos(theta3) * 1# /
Tan(theta2) - (Sin(theta3)) ^ 2))

m5 = (m1 + m2 + m3) * m4

m6 = gamma2 * (B) ^ 3 * (Sin(theta1)) ^ -3 * (Sin(theta2)) ^ -3 * (Tan(psi) * Sin(theta1)
- Cos(theta1) + Exp(theta1 * Tan(phi1))) ^ 3 * Cos(phi2) * Cos(45 * 3.141592 / 180 +
phi2 / 2#) * Tan(45 * 3.141592 / 180 + phi2 / 2#) * (-Cos(theta3) * Cos(theta2) +
Sin(theta3) * Sin(theta2) + Cos(theta3) * Exp(theta2 * Tan(phi2))) ^ 2 * (Cos(theta3) *
Cos(theta2) / 2# - Sin(theta3) * Sin(theta2) / 2# + Cos(theta3) * Exp(theta2 * Tan(phi2)))
/ 24#
```

```
m7 = gamma2 * (B) ^ 3 * (Cos(theta3)) ^ 3 * (Sin(theta1)) ^ -3 * (Sin(theta2)) ^ -3 / (9#
* (Tan(phi2)) ^ 2 + 1#) * (Tan(psi) * Sin(theta1) - Cos(theta1) + Exp(theta1 *
Tan(phi1))) ^ 3 * (Exp(3# * theta2 * Tan(phi2)) * (3# * Tan(phi2) * Cos(theta3) -
Sin(theta3)) + Sin(theta3 + theta2) - 3# * Tan(phi2) * Cos(theta3 + theta2)) / 24# -
gamma2 * (B) ^ 3 * (Sin(theta1)) ^ -3 * (Tan(psi) * Sin(theta1) - Cos(theta1) +
Exp(theta1 * Tan(phi1))) ^ 3 * (-(Cos(theta3)) ^ 2 * 1# / Tan(theta2) + Sin(theta3) *
Cos(theta3)) ^ 2 / 24#
m8 = -8# * (B) ^ -2 * (Sin(theta1)) ^ 2 * (Tan(psi) * Sin(theta1) - Cos(theta1) +
Exp(theta1 * Tan(phi1))) ^ -2 * (Sin(delta) * (-(Cos(theta3)) ^ 2 * 1# / Tan(theta2) +
Sin(theta3) * Cos(theta3)) + Cos(delta) * (a + Sin(theta3) * Cos(theta3) * 1# /
Tan(theta2) - (Sin(theta3)) ^ 2)) ^ -2 * (-Sin(delta) * (Cos(theta3)) ^ 2 * (-1# - (1# /
Tan(theta2)) ^ 2) + Cos(delta) * Sin(theta3) * Cos(theta3) * (-1# - (1# / Tan(theta2)) ^ 2))

m9 = (m6 + m7) * m8

mm = m5 + m9

  If i = 1 Then
  cg21 = mm
  ElseIf i = 2 Then
  cg22 = mm
  Else
  cg23 = mm
  End If

 Next i

If ((cg21 * cg23) > 0) Then
  theta21 = theta23
Else
  theta22 = theta23
End If

    Loop Until (Abs(theta21 - theta22) < 0.0000000001)
theta2 = theta22

Text2.Text = theta2 / 3.141592 * 180

'   P calculation ngamma for theta1

F1gamma = 8# * (gamma1 * (B) ^ 3 * (Sin(theta1)) ^ -3 / (9# * (Tan(phi1)) ^ 2 + 1#) *
(Exp(3# * theta1 * Tan(phi1)) - 3# * Tan(phi1) * Sin(theta1) - Cos(theta1)) / 24# +
gamma1 * (B) ^ 3 * (Tan(psi) - 1# / Tan(theta1)) / 48# + P * (Cos(-psi + phi1) * B / 3# -
Sin(-psi + phi1) * (B * Tan(psi) / 3# - B * (Tan(psi) - 1# / Tan(theta1)) / 2#))) /
Cos(delta) * (B) ^ -2 / (Tan(psi) * Sin(theta1) - Cos(theta1) + Exp(theta1 * Tan(phi1))) *
```

```
Sin(theta1) / ((a - 1) * (Tan(psi) - 1# / Tan(theta1)) + a * Exp(theta1 * Tan(phi1)) /
Sin(theta1))

'   P calculation ngamma for theta2

j1 = gamma2 * (B) ^ 3 * (Sin(theta1)) ^ -3 * (Sin(theta2)) ^ -3 * (Tan(psi) * Sin(theta1) -
Cos(theta1) + Exp(theta1 * Tan(phi1))) ^ 3 * Cos(phi2) * Cos(45 * 3.141592 / 180 +
phi2 / 2#) * Tan(45 * 3.141592 / 180 + phi2 / 2#) * (-Cos(theta3) * Cos(theta2) +
Sin(theta3) * Sin(theta2) + Cos(theta3) * Exp(theta2 * Tan(phi2))) ^ 2 * (Cos(theta3) *
Cos(theta2) / 2# - Sin(theta3) * Sin(theta2) / 2# + Cos(theta3) * Exp(theta2 * Tan(phi2)))
/ 24# + gamma2 * (B) ^ 3 * (Cos(theta3)) ^ 3 * (Sin(theta1)) ^ -3 * (Sin(theta2)) ^ -3 /
(9# * (Tan(phi2)) ^ 2 + 1#) * (Tan(psi) * Sin(theta1) - Cos(theta1) + Exp(theta1 *
Tan(phi1))) ^ 3 * (Exp(3# * theta2 * Tan(phi2)) * (3# * Tan(phi2) * Cos(theta3) -
Sin(theta3)) + Sin(theta3 + theta2) - 3# * Tan(phi2) * Cos(theta3 + theta2)) / 24# -
gamma2 * (B) ^ 3 * (Sin(theta1)) ^ -3 * (Tan(psi) * Sin(theta1) - Cos(theta1) +
Exp(theta1 * Tan(phi1))) ^ 3 * (-(Cos(theta3)) ^ 2 * 1# / Tan(theta2) + Sin(theta3) *
Cos(theta3)) ^ 2 / 24#
j2 = 8# * (B) ^ -2 * (Sin(theta1)) ^ 2 * (Tan(psi) * Sin(theta1) - Cos(theta1) + Exp(theta1
* Tan(phi1))) ^ -2 / (Sin(delta) * (-(Cos(theta3)) ^ 2 * 1# / Tan(theta2) + Sin(theta3) *
Cos(theta3)) + Cos(delta) * (a + Sin(theta3) * Cos(theta3) * 1# / Tan(theta2) -
(Sin(theta3)) ^ 2))



F2gamma = j1 * j2

Loop Until Abs(F1gamma - F2gamma) <= 0.01
q1 = 2 * P / B * Cos(psi - phi1) - B / 4 * gamma1 * Tan(psi)

Text8.Text = P

Text3.Text = q1
Text10.Text = psi / 3.141592 * 180

kjj = 1
P = 20
numb = 1
F1nc = 1
F2nc = 2
        Do
If F1nc > F2nc Then

X = -1
Else
X = 1
numb = numb + 1
```

```
End If

If numb = 10 Then kjj = 0.1

P = P + X * kjj / numb


'    nc and nq for theta1

c1 = 0
theta1temp = 10 * 3.141592 / 180
theta2temp = 20 * 3.141592 / 180
q = 20
c2 = 0
cx = c1

Do

theta1 = theta1temp

psi = theta1 + phi1

n1 = 4# * (P * Sin(psi - phi1) * (-1# - (1# / Tan(theta1)) ^ 2) / 2# + c1 * B * (1# + (1# /
Tan(theta1)) ^ 2) / 4# + c1 * B * (Sin(theta1)) ^ -3 / Tan(phi1) * (Exp(2# * theta1 *
Tan(phi1)) - 1#) * Cos(theta1) / 4# - c1 * B * (Sin(theta1)) ^ -2 * Exp(2# * theta1 *
Tan(phi1)) / 4#) / m * (B) ^ -1 / Cos(delta) * (Sin(theta1)) ^ 2 / (Exp(2# * theta1 *
Tan(phi1)) - (Tan(psi) * Sin(theta1) - Cos(theta1)) ^ 2) + 8# * (P * (Cos(psi - phi1) / 4# +
Sin(psi - phi1) * (-Tan(psi) / 2# + 1# / Tan(theta1)) / 2#) + c1 * B * (Tan(psi) - 1# /
Tan(theta1)) / 4# - c1 * B * (Sin(theta1)) ^ -2 / Tan(phi1) * (Exp(2# * theta1 * Tan(phi1))
- 1#) / 8#) / m * (B) ^ -1 / Cos(delta) * Sin(theta1) / (Exp(2# * theta1 * Tan(phi1)) -
(Tan(psi) * Sin(theta1) - Cos(theta1)) ^ 2) * Cos(theta1)
n2 = -4# * (P * (Cos(psi - phi1) / 4# + Sin(psi - phi1) * (-Tan(psi) / 2# + 1# / Tan(theta1))
/ 2#) + c1 * B * (Tan(psi) - 1# / Tan(theta1)) / 4# - c1 * B * (Sin(theta1)) ^ -2 / Tan(phi1)
* (Exp(2# * theta1 * Tan(phi1)) - 1#) / 8#) / m * (B) ^ -1 / Cos(delta) * (Sin(theta1)) ^ 2
* (Exp(2# * theta1 * Tan(phi1)) - (Tan(psi) * Sin(theta1) - Cos(theta1)) ^ 2) ^ -2 * (2# *
Tan(phi1) * Exp(2# * theta1 * Tan(phi1)) - 2# * (Tan(psi) * Sin(theta1) - Cos(theta1)) *
(Tan(psi) * Cos(theta1) + Sin(theta1)))

nn = n1 + n2


ccc1 = 4# * (-P * Sin(psi - phi1) * 1# / Tan(theta1) * (-1# - (1# / Tan(theta1)) ^ 2) + c1 *
B * 1# / Tan(theta1) * (-1# - (1# / Tan(theta1)) ^ 2) / 2# - 3# / 4# * c1 * B * (Sin(theta1))
^ -4 / Tan(phi1) * (Exp(2# * theta1 * Tan(phi1)) - 1#) * (Cos(theta1)) ^ 2 + c1 * B *
(Sin(theta1)) ^ -3 * Exp(2# * theta1 * Tan(phi1)) * Cos(theta1) - c1 * B * (Sin(theta1)) ^
-2 / Tan(phi1) * (Exp(2# * theta1 * Tan(phi1)) - 1#) / 4# - c1 * B * (Sin(theta1)) ^ -2 *
```

```
Tan(phi1) * Exp(2# * theta1 * Tan(phi1)) / 2#) / m * (B) ^ -1 / Cos(delta) * (Sin(theta1))
^ 2 / (Exp(2# * theta1 * Tan(phi1)) - (Tan(psi) * Sin(theta1) - Cos(theta1)) ^ 2)
ccc2 = 16# * (P * Sin(psi - phi1) * (-1# - (1# / Tan(theta1)) ^ 2) / 2# + c1 * B * (1# + (1#
/ Tan(theta1)) ^ 2) / 4# + c1 * B * (Sin(theta1)) ^ -3 / Tan(phi1) * (Exp(2# * theta1 *
Tan(phi1)) - 1#) * Cos(theta1) / 4# - c1 * B * (Sin(theta1)) ^ -2 * Exp(2# * theta1 *
Tan(phi1)) / 4#) / m * (B) ^ -1 / Cos(delta) * Sin(theta1) / (Exp(2# * theta1 * Tan(phi1)) -
(Tan(psi) * Sin(theta1) - Cos(theta1)) ^ 2) * Cos(theta1)
ccc3 = -8# * (P * Sin(psi - phi1) * (-1# - (1# / Tan(theta1)) ^ 2) / 2# + c1 * B * (1# + (1#
/ Tan(theta1)) ^ 2) / 4# + c1 * B * (Sin(theta1)) ^ -3 / Tan(phi1) * (Exp(2# * theta1 *
Tan(phi1)) - 1#) * Cos(theta1) / 4# - c1 * B * (Sin(theta1)) ^ -2 * Exp(2# * theta1 *
Tan(phi1)) / 4#) / m * (B) ^ -1 / Cos(delta) * (Sin(theta1)) ^ 2 * (Exp(2# * theta1 *
Tan(phi1)) - (Tan(psi) * Sin(theta1) - Cos(theta1)) ^ 2) ^ -2 * (2# * Tan(phi1) * Exp(2# *
theta1 * Tan(phi1)) - 2# * (Tan(psi) * Sin(theta1) - Cos(theta1)) * (Tan(psi) * Cos(theta1)
+ Sin(theta1)))
ccc4 = 8# * (P * (Cos(psi - phi1) / 4# + Sin(psi - phi1) * (-Tan(psi) / 2# + 1# /
Tan(theta1)) / 2#) + c1 * B * (Tan(psi) - 1# / Tan(theta1)) / 4# - c1 * B * (Sin(theta1)) ^ -
2 / Tan(phi1) * (Exp(2# * theta1 * Tan(phi1)) - 1#) / 8#) / m * (B) ^ -1 / Cos(delta) *
(Cos(theta1)) ^ 2 / (Exp(2# * theta1 * Tan(phi1)) - (Tan(psi) * Sin(theta1) - Cos(theta1))
^ 2)
ccc5 = -16# * (P * (Cos(psi - phi1) / 4# + Sin(psi - phi1) * (-Tan(psi) / 2# + 1# /
Tan(theta1)) / 2#) + c1 * B * (Tan(psi) - 1# / Tan(theta1)) / 4# - c1 * B * (Sin(theta1)) ^ -
2 / Tan(phi1) * (Exp(2# * theta1 * Tan(phi1)) - 1#) / 8#) / m * (B) ^ -1 / Cos(delta) *
Sin(theta1) * (Exp(2# * theta1 * Tan(phi1)) - (Tan(psi) * Sin(theta1) - Cos(theta1)) ^ 2) ^
-2 * Cos(theta1) * (2# * Tan(phi1) * Exp(2# * theta1 * Tan(phi1)) - 2# * (Tan(psi) *
Sin(theta1) - Cos(theta1)) * (Tan(psi) * Cos(theta1) + Sin(theta1))) - 8# * (P * (Cos(psi -
phi1) / 4# + Sin(psi - phi1) * (-Tan(psi) / 2# + 1# / Tan(theta1)) / 2#) + c1 * B * (Tan(psi)
- 1# / Tan(theta1)) / 4# - c1 * B * (Sin(theta1)) ^ -2 / Tan(phi1) * (Exp(2# * theta1 *
Tan(phi1)) - 1#) / 8#) / m * (B) ^ -1 / Cos(delta) * (Sin(theta1)) ^ 2 / (Exp(2# * theta1 *
Tan(phi1)) - (Tan(psi) * Sin(theta1) - Cos(theta1)) ^ 2)
ccc6 = 8# * (P * (Cos(psi - phi1) / 4# + Sin(psi - phi1) * (-Tan(psi) / 2# + 1# /
Tan(theta1)) / 2#) + c1 * B * (Tan(psi) - 1# / Tan(theta1)) / 4# - c1 * B * (Sin(theta1)) ^ -
2 / Tan(phi1) * (Exp(2# * theta1 * Tan(phi1)) - 1#) / 8#) / m * (B) ^ -1 / Cos(delta) *
(Sin(theta1)) ^ 2 * (Exp(2# * theta1 * Tan(phi1)) - (Tan(psi) * Sin(theta1) - Cos(theta1))
^ 2) ^ -3 * (2# * Tan(phi1) * Exp(2# * theta1 * Tan(phi1)) - 2# * (Tan(psi) * Sin(theta1) -
Cos(theta1)) * (Tan(psi) * Cos(theta1) + Sin(theta1))) ^ 2
ccc7 = -4# * (P * (Cos(psi - phi1) / 4# + Sin(psi - phi1) * (-Tan(psi) / 2# + 1# /
Tan(theta1)) / 2#) + c1 * B * (Tan(psi) - 1# / Tan(theta1)) / 4# - c1 * B * (Sin(theta1)) ^ -
2 / Tan(phi1) * (Exp(2# * theta1 * Tan(phi1)) - 1#) / 8#) / m * (B) ^ -1 / Cos(delta) *
(Sin(theta1)) ^ 2 * (Exp(2# * theta1 * Tan(phi1)) - (Tan(psi) * Sin(theta1) - Cos(theta1))
^ 2) ^ -2 * (4# * (Tan(phi1)) ^ 2 * Exp(2# * theta1 * Tan(phi1)) - 2# * (Tan(psi) *
Cos(theta1) + Sin(theta1)) ^ 2 - 2# * (Tan(psi) * Sin(theta1) - Cos(theta1)) * (-Tan(psi) *
Sin(theta1) + Cos(theta1)))

ccc8 = ccc1 + ccc2 + ccc3 + ccc4 + ccc5 + ccc6 + ccc7

If ccc8 = 0 Then
```

```
    Text1.Text = "Failure"
    Stop
  End If
    theta11 = theta1temp
    theta12 = theta11 - nn / ccc8
    theta1temp = theta12


Loop Until Abs(theta12 - theta11) <= 0.001

theta1 = theta12

Text6.Text = theta1 / 3.141592 * 180

'    nc and nq for theta2

theta1temp = 30 * 3.141592 / 180
theta2temp = 40 * 3.141592 / 180

Do

theta2 = theta2temp


s1 = -B * B * Cos(phi2) * (q * Tan(45 * 3.141592 / 180 + phi2 / 2#) + c2) * (Sin(theta1))
^ -2 * (Sin(theta2)) ^ -3 * (Exp(theta1 * Tan(phi1)) + Tan(psi) * Sin(theta1) -
Cos(theta1)) ^ 2 * ((Cos(theta3)) ^ 2 * Exp(2# * theta2 * Tan(phi2)) - (-Cos(theta3) *
Cos(theta2) + Sin(theta3) * Sin(theta2)) ^ 2) * Cos(theta2) / 4# + B * B * Cos(phi2) * (q
* Tan(45 * 3.141592 / 180 + phi2 / 2#) + c2) * (Sin(theta1)) ^ -2 * (Sin(theta2)) ^ -2 *
(Exp(theta1 * Tan(phi1)) + Tan(psi) * Sin(theta1) - Cos(theta1)) ^ 2 * (2# * (Cos(theta3))
^ 2 * Tan(phi2) * Exp(2# * theta2 * Tan(phi2)) - 2# * (-Cos(theta3) * Cos(theta2) +
Sin(theta3) * Sin(theta2)) * (Cos(theta3) * Sin(theta2) + Sin(theta3) * Cos(theta2))) / 8#
s2 = -c2 / Tan(phi2) * (Exp(theta1 * Tan(phi1)) + Tan(psi) * Sin(theta1) - Cos(theta1)) ^
2 * B * B * (Cos(theta3)) ^ 2 * (Sin(theta1)) ^ -2 * (Sin(theta2)) ^ -3 * (Exp(2# * theta2 *
Tan(phi2)) - 1#) * Cos(theta2) / 4# + c2 * (Exp(theta1 * Tan(phi1)) + Tan(psi) *
Sin(theta1) - Cos(theta1)) ^ 2 * B * B * (Cos(theta3)) ^ 2 * (Sin(theta1)) ^ -2 *
(Sin(theta2)) ^ -2 * Exp(2# * theta2 * Tan(phi2)) / 4# + cx * B * B * (Sin(theta1)) ^ -2 *
(Exp(theta1 * Tan(phi1)) + Tan(psi) * Sin(theta1) - Cos(theta1)) ^ 2 * (Cos(theta3)) ^ 2 *
(-1# - (1# / Tan(theta2)) ^ 2) / 4#
s3 = 4# * (B) ^ -2 * (Sin(theta1)) ^ 2 * (Exp(theta1 * Tan(phi1)) + Tan(psi) * Sin(theta1)
- Cos(theta1)) ^ -2 / (Sin(delta) * (-(Cos(theta3)) ^ 2 * 1# / Tan(theta2) + Sin(theta3) *
Cos(theta3)) + Cos(delta) * (m + Sin(theta3) * Cos(theta3) * 1# / Tan(theta2) -
(Sin(theta3)) ^ 2))

s4 = (s1 + s2) * s3
```

```
s5 = B * B * Cos(phi2) * (q * Tan(45 * 3.141592 / 180 + phi2 / 2#) + c2) * (Sin(theta1))
^ -2 * (Sin(theta2)) ^ -2 * (Exp(theta1 * Tan(phi1)) + Tan(psi) * Sin(theta1) -
Cos(theta1)) ^ 2 * ((Cos(theta3)) ^ 2 * Exp(2# * theta2 * Tan(phi2)) - (-Cos(theta3) *
Cos(theta2) + Sin(theta3) * Sin(theta2)) ^ 2) / 8# + c2 / Tan(phi2) * (Exp(theta1 *
Tan(phi1)) + Tan(psi) * Sin(theta1) - Cos(theta1)) ^ 2 * B * B * (Cos(theta3)) ^ 2 *
(Sin(theta1)) ^ -2 * (Sin(theta2)) ^ -2 * (Exp(2# * theta2 * Tan(phi2)) - 1#) / 8# - cx * B
* B * (Sin(theta1)) ^ -2 * (Exp(theta1 * Tan(phi1)) + Tan(psi) * Sin(theta1) -
Cos(theta1)) ^ 2 * (-(Cos(theta3)) ^ 2 * 1# / Tan(theta2) + Sin(theta3) * Cos(theta3)) / 4#
s6 = -4# * (B) ^ -2 * (Sin(theta1)) ^ 2 * (Exp(theta1 * Tan(phi1)) + Tan(psi) * Sin(theta1)
- Cos(theta1)) ^ -2 * (Sin(delta) * (-(Cos(theta3)) ^ 2 * 1# / Tan(theta2) + Sin(theta3) *
Cos(theta3)) + Cos(delta) * (m + Sin(theta3) * Cos(theta3) * 1# / Tan(theta2) -
(Sin(theta3)) ^ 2)) ^ -2 * (-Sin(delta) * (Cos(theta3)) ^ 2 * (-1# - (1# / Tan(theta2)) ^ 2) +
Cos(delta) * Sin(theta3) * Cos(theta3) * (-1# - (1# / Tan(theta2)) ^ 2))

s7 = s5 * s6

ss = s4 + s7


ddd1 = 3# / 4# * B * B * Cos(phi2) * (q * Tan(45 * 3.141592 / 180 + phi2 / 2#) + c2) *
(Sin(theta1)) ^ -2 * (Sin(theta2)) ^ -4 * (Exp(theta1 * Tan(phi1)) + Tan(psi) * Sin(theta1)
- Cos(theta1)) ^ 2 * ((Cos(theta3)) ^ 2 * Exp(2# * theta2 * Tan(phi2)) - (-Cos(theta3) *
Cos(theta2) + Sin(theta3) * Sin(theta2)) ^ 2) * (Cos(theta2)) ^ 2 - B * B * Cos(phi2) * (q
* Tan(45 * 3.141592 / 180 + phi2 / 2#) + c2) * (Sin(theta1)) ^ -2 * (Sin(theta2)) ^ -3 *
(Exp(theta1 * Tan(phi1)) + Tan(psi) * Sin(theta1) - Cos(theta1)) ^ 2 * (2# * (Cos(theta3))
^ 2 * Tan(phi2) * Exp(2# * theta2 * Tan(phi2)) - 2# * (-Cos(theta3) * Cos(theta2) +
Sin(theta3) * Sin(theta2)) * (Cos(theta3) * Sin(theta2) + Sin(theta3) * Cos(theta2))) *
Cos(theta2) / 2#
ddd2 = B * B * Cos(phi2) * (q * Tan(45 * 3.141592 / 180 + phi2 / 2#) + c2) *
(Sin(theta1)) ^ -2 * (Sin(theta2)) ^ -2 * (Exp(theta1 * Tan(phi1)) + Tan(psi) * Sin(theta1)
- Cos(theta1)) ^ 2 * ((Cos(theta3)) ^ 2 * Exp(2# * theta2 * Tan(phi2)) - (-Cos(theta3) *
Cos(theta2) + Sin(theta3) * Sin(theta2)) ^ 2) / 4# + B * B * Cos(phi2) * (q * Tan(45 *
3.141592 / 180 + phi2 / 2#) + c2) * (Sin(theta1)) ^ -2 * (Sin(theta2)) ^ -2 * (Exp(theta1 *
Tan(phi1)) + Tan(psi) * Sin(theta1) - Cos(theta1)) ^ 2 * (4# * (Cos(theta3)) ^ 2 *
(Tan(phi2)) ^ 2 * Exp(2# * theta2 * Tan(phi2)) - 2# * (Cos(theta3) * Sin(theta2) +
Sin(theta3) * Cos(theta2)) ^ 2 - 2# * (-Cos(theta3) * Cos(theta2) + Sin(theta3) *
Sin(theta2)) * (Cos(theta3) * Cos(theta2) - Sin(theta3) * Sin(theta2))) / 8#
ddd3 = 3# / 4# * c2 / Tan(phi2) * (Exp(theta1 * Tan(phi1)) + Tan(psi) * Sin(theta1) -
Cos(theta1)) ^ 2 * B * B * (Cos(theta3)) ^ 2 * (Sin(theta1)) ^ -2 * (Sin(theta2)) ^ -4 *
(Exp(2# * theta2 * Tan(phi2)) - 1#) * (Cos(theta2)) ^ 2 - c2 * (Exp(theta1 * Tan(phi1)) +
Tan(psi) * Sin(theta1) - Cos(theta1)) ^ 2 * B * B * (Cos(theta3)) ^ 2 * (Sin(theta1)) ^ -2 *
(Sin(theta2)) ^ -3 * Exp(2# * theta2 * Tan(phi2)) * Cos(theta2) + c2 / Tan(phi2) *
(Exp(theta1 * Tan(phi1)) + Tan(psi) * Sin(theta1) - Cos(theta1)) ^ 2 * B * B *
```

(Cos(theta3)) ^ 2 * (Sin(theta1)) ^ -2 * (Sin(theta2)) ^ -2 * (Exp(2# * theta2 * Tan(phi2)) - 1#) / 4#
ddd4 = c2 * (Exp(theta1 * Tan(phi1)) + Tan(psi) * Sin(theta1) - Cos(theta1)) ^ 2 * B * B * (Cos(theta3)) ^ 2 * (Sin(theta1)) ^ -2 * (Sin(theta2)) ^ -2 * Tan(phi2) * Exp(2# * theta2 * Tan(phi2)) / 2# - cx * B * B * (Sin(theta1)) ^ -2 * (Exp(theta1 * Tan(phi1)) + Tan(psi) * Sin(theta1) - Cos(theta1)) ^ 2 * (Cos(theta3)) ^ 2 * 1# / Tan(theta2) * (-1# - (1# / Tan(theta2)) ^ 2) / 2#
ddd5 = 4# * (B) ^ -2 * (Sin(theta1)) ^ 2 * (Exp(theta1 * Tan(phi1)) + Tan(psi) * Sin(theta1) - Cos(theta1)) ^ -2 / (Sin(delta) * (-(Cos(theta3)) ^ 2 * 1# / Tan(theta2) + Sin(theta3) * Cos(theta3)) + Cos(delta) * (m + Sin(theta3) * Cos(theta3) * 1# / Tan(theta2) - (Sin(theta3)) ^ 2))

ddd6 = (ddd1 + ddd2 + ddd3 + ddd4) * ddd5

ddd7 = -B * B * Cos(phi2) * (q * Tan(45 * 3.141592 / 180 + phi2 / 2#) + c2) * (Sin(theta1)) ^ -2 * (Sin(theta2)) ^ -3 * (Exp(theta1 * Tan(phi1)) + Tan(psi) * Sin(theta1) - Cos(theta1)) ^ 2 * ((Cos(theta3)) ^ 2 * Exp(2# * theta2 * Tan(phi2)) - (-Cos(theta3) * Cos(theta2) + Sin(theta3) * Sin(theta2)) ^ 2) * Cos(theta2) / 4# + B * B * Cos(phi2) * (q * Tan(45 * 3.141592 / 180 + phi2 / 2#) + c2) * (Sin(theta1)) ^ -2 * (Sin(theta2)) ^ -2 * (Exp(theta1 * Tan(phi1)) + Tan(psi) * Sin(theta1) - Cos(theta1)) ^ 2 * (2# * (Cos(theta3)) ^ 2 * Tan(phi2) * Exp(2# * theta2 * Tan(phi2)) - 2# * (-Cos(theta3) * Cos(theta2) + Sin(theta3) * Sin(theta2)) * (Cos(theta3) * Sin(theta2) + Sin(theta3) * Cos(theta2))) / 8# - c2 / Tan(phi2) * (Exp(theta1 * Tan(phi1)) + Tan(psi) * Sin(theta1) - Cos(theta1)) ^ 2 * B * B * (Cos(theta3)) ^ 2 * (Sin(theta1)) ^ -2 * (Sin(theta2)) ^ -3 * (Exp(2# * theta2 * Tan(phi2)) - 1#) * Cos(theta2) / 4#
ddd8 = c2 * (Exp(theta1 * Tan(phi1)) + Tan(psi) * Sin(theta1) - Cos(theta1)) ^ 2 * B * B * (Cos(theta3)) ^ 2 * (Sin(theta1)) ^ -2 * (Sin(theta2)) ^ -2 * Exp(2# * theta2 * Tan(phi2)) / 4# + cx * B * B * (Sin(theta1)) ^ -2 * (Exp(theta1 * Tan(phi1)) + Tan(psi) * Sin(theta1) - Cos(theta1)) ^ 2 * (Cos(theta3)) ^ 2 * (-1# - (1# / Tan(theta2)) ^ 2) / 4#
ddd9 = -8# * (B) ^ -2 * (Sin(theta1)) ^ 2 * (Exp(theta1 * Tan(phi1)) + Tan(psi) * Sin(theta1) - Cos(theta1)) ^ -2 * (Sin(delta) * (-(Cos(theta3)) ^ 2 * 1# / Tan(theta2) + Sin(theta3) * Cos(theta3)) + Cos(delta) * (m + Sin(theta3) * Cos(theta3) * 1# / Tan(theta2) - (Sin(theta3)) ^ 2)) ^ -2 * (-Sin(delta) * (Cos(theta3)) ^ 2 * (-1# - (1# / Tan(theta2)) ^ 2) + Cos(delta) * Sin(theta3) * Cos(theta3) * (-1# - (1# / Tan(theta2)) ^ 2))

ddd10 = (ddd7 + ddd8) * ddd9

ddd11 = 8# * (B * B * Cos(phi2) * (q * Tan(45 * 3.141592 / 180 + phi2 / 2#) + c2) * (Sin(theta1)) ^ -2 * (Sin(theta2)) ^ -2 * (Exp(theta1 * Tan(phi1)) + Tan(psi) * Sin(theta1) - Cos(theta1)) ^ 2 * ((Cos(theta3)) ^ 2 * Exp(2# * theta2 * Tan(phi2)) - (-Cos(theta3) * Cos(theta2) + Sin(theta3) * Sin(theta2)) ^ 2) / 8# + c2 / Tan(phi2) * (Exp(theta1 * Tan(phi1)) + Tan(psi) * Sin(theta1) - Cos(theta1)) ^ 2 * B * B * (Cos(theta3)) ^ 2 * (Sin(theta1)) ^ -2 * (Sin(theta2)) ^ -2 * (Exp(2# * theta2 * Tan(phi2)) - 1#) / 8# - cx * B * B * (Sin(theta1)) ^ -2 * (Exp(theta1 * Tan(phi1)) + Tan(psi) * Sin(theta1) - Cos(theta1)) ^ 2 * (-(Cos(theta3)) ^ 2 * 1# / Tan(theta2) + Sin(theta3) * Cos(theta3)) / 4#)

```
ddd12 = (B) ^ -2 * (Sin(theta1)) ^ 2 * (Exp(theta1 * Tan(phi1)) + Tan(psi) * Sin(theta1) -
Cos(theta1)) ^ -2 * (Sin(delta) * (-(Cos(theta3)) ^ 2 * 1# / Tan(theta2) + Sin(theta3) *
Cos(theta3)) + Cos(delta) * (m + Sin(theta3) * Cos(theta3) * 1# / Tan(theta2) -
(Sin(theta3)) ^ 2)) ^ -3 * (-Sin(delta) * (Cos(theta3)) ^ 2 * (-1# - (1# / Tan(theta2)) ^ 2) +
Cos(delta) * Sin(theta3) * Cos(theta3) * (-1# - (1# / Tan(theta2)) ^ 2)) ^ 2

ddd13 = ddd11 * ddd12

ddd14 = -4# * (B * B * Cos(phi2) * (q * Tan(45 * 3.141592 / 180 + phi2 / 2#) + c2) *
(Sin(theta1)) ^ -2 * (Sin(theta2)) ^ -2 * (Exp(theta1 * Tan(phi1)) + Tan(psi) * Sin(theta1)
- Cos(theta1)) ^ 2 * ((Cos(theta3)) ^ 2 * Exp(2# * theta2 * Tan(phi2)) - (-Cos(theta3) *
Cos(theta2) + Sin(theta3) * Sin(theta2)) ^ 2) / 8# + c2 / Tan(phi2) * (Exp(theta1 *
Tan(phi1)) + Tan(psi) * Sin(theta1) - Cos(theta1)) ^ 2 * B * B * (Cos(theta3)) ^ 2 *
(Sin(theta1)) ^ -2 * (Sin(theta2)) ^ -2 * (Exp(2# * theta2 * Tan(phi2)) - 1#) / 8# - cx * B
* B * (Sin(theta1)) ^ -2 * (Exp(theta1 * Tan(phi1)) + Tan(psi) * Sin(theta1) -
Cos(theta1)) ^ 2 * (-(Cos(theta3)) ^ 2 * 1# / Tan(theta2) + Sin(theta3) * Cos(theta3)) / 4#)
ddd15 = (B) ^ -2 * (Sin(theta1)) ^ 2 * (Exp(theta1 * Tan(phi1)) + Tan(psi) * Sin(theta1) -
Cos(theta1)) ^ -2 * (Sin(delta) * (-(Cos(theta3)) ^ 2 * 1# / Tan(theta2) + Sin(theta3) *
Cos(theta3)) + Cos(delta) * (m + Sin(theta3) * Cos(theta3) * 1# / Tan(theta2) -
(Sin(theta3)) ^ 2)) ^ -2 * (2# * Sin(delta) * (Cos(theta3)) ^ 2 * 1# / Tan(theta2) * (-1# -
(1# / Tan(theta2)) ^ 2) - 2# * Cos(delta) * Sin(theta3) * Cos(theta3) * 1# / Tan(theta2) *
(-1# - (1# / Tan(theta2)) ^ 2))

ddd16 = ddd14 * ddd15


ddd19 = ddd6 + ddd10 + ddd13 + ddd16

If ddd19 = 0 Then

   Text1.Text = "Failure"
   Stop
End If
   theta21 = theta2temp
   theta22 = theta21 - ss / ddd19
   theta2temp = theta22

Loop Until Abs(theta22 - theta21) <= 0.00000001
theta2 = theta22

Text7.Text = theta2 / 3.141592 * 180

'   P calculation nc and nq for theta1

F1nc = 4# * (P * (Cos(psi - phi1) / 4# + Sin(psi - phi1) * (-Tan(psi) / 2# + 1# /
Tan(theta1)) / 2#) + c1 * B * (Tan(psi) - 1# / Tan(theta1)) / 4# - c1 * B * (Sin(theta1)) ^ -
```

```
2 / Tan(phi1) * (Exp(2# * theta1 * Tan(phi1)) - 1#) / 8#) / m * (B) ^ -1 / Cos(delta) *
(Sin(theta1)) ^ 2 / (Exp(2# * theta1 * Tan(phi1)) - (Tan(psi) * Sin(theta1) - Cos(theta1)) ^
2)

'   P calculation nc and nq for theta2

k1 = B * B * Cos(phi2) * (q * Tan(45 * 3.141592 / 180 + phi2 / 2#) + c2) * (Sin(theta1))
^ -2 * (Sin(theta2)) ^ -2 * (Exp(theta1 * Tan(phi1)) + Tan(psi) * Sin(theta1) -
Cos(theta1)) ^ 2 * ((Cos(theta3)) ^ 2 * Exp(2# * theta2 * Tan(phi2)) - (-Cos(theta3) *
Cos(theta2) + Sin(theta3) * Sin(theta2)) ^ 2) / 8# + c2 / Tan(phi2) * (Exp(theta1 *
Tan(phi1)) + Tan(psi) * Sin(theta1) - Cos(theta1)) ^ 2 * B * B * (Cos(theta3)) ^ 2 *
(Sin(theta1)) ^ -2 * (Sin(theta2)) ^ -2 * (Exp(2# * theta2 * Tan(phi2)) - 1#) / 8# - cx * B
* B * (Sin(theta1)) ^ -2 * (Exp(theta1 * Tan(phi1)) + Tan(psi) * Sin(theta1) -
Cos(theta1)) ^ 2 * (-(Cos(theta3)) ^ 2 * 1# / Tan(theta2) + Sin(theta3) * Cos(theta3)) / 4#
k2 = 4# * (Sin(theta1)) ^ 2 * (B) ^ -2 * (Exp(theta1 * Tan(phi1)) + Tan(psi) * Sin(theta1)
- Cos(theta1)) ^ -2 / (Sin(delta) * (-(Cos(theta3)) ^ 2 * 1# / Tan(theta2) + Sin(theta3) *
Cos(theta3)) + Cos(delta) * (m + Sin(theta3) * Cos(theta3) * 1# / Tan(theta2) -
(Sin(theta3)) ^ 2))

F2nc = k1 * k2


        Loop Until Abs(F1nc - F2nc) <= 0.01
q2 = 2 * P / B * Cos(psi - phi1) + c1 * Tan(psi)

qu = q1 + q2
Text3.Text = q1
Text4.Text = q2
Text5.Text = qu
Text9.Text = P
Text11.Text = psi / 3.141592 * 180

Stop
End Sub
```

APPENDIX 4

First and second derivation of the forces P_γ, P' in the local shear failure analytical model is presented here. These derivations were used to determine these forces using Newton Raphson numerical technique.

First derivation of Equation 4.140 respect to θ

$$
\begin{aligned}
R0 := & \frac{1}{\frac{1}{3}\cos(\psi-\phi 1)+\sin(\psi-\phi 1)\left(-\frac{1}{6}\tan(\psi)+\frac{1}{2}\cot(\theta)\right)}\left(\frac{1}{24\sin(\theta)}\left(\gamma 2 B^2\cos(\phi 2)\left(\frac{2\tan(\phi 1)\,e^{(2\theta\tan(\phi 1))}}{\sin(\theta)^2}-\frac{2\,e^{(2\theta\tan(\phi 1))}\cos(\theta)}{\sin(\theta)^3}\right.\right.\right.\\
& \left.\left.\left.+\frac{1}{2}(1+\cot(\theta)^2)\left(\frac{e^{(\theta\tan(\phi 1))}}{\sin(\theta)}-\tan(\psi)+\cot(\theta)\right)+\frac{1}{2}(\tan(\psi)-\cot(\theta))\left(\frac{\tan(\phi 1)\,e^{(\theta\tan(\phi 1))}}{\sin(\theta)}-\frac{e^{(\theta\tan(\phi 1))}\cos(\theta)}{\sin(\theta)^2}-1-\cot(\theta)^2\right)\right)\left(\tan(\psi)\sin(\theta)-\cos(\theta)\right.\right.\right.\\
& \left.\left.\left.+e^{(\theta\tan(\phi 1))}\right)KP\right)\\
& +\frac{\gamma 2 B^2\cos(\phi 2)\left(\frac{e^{(2\theta\tan(\phi 1))}}{\sin(\theta)^2}+\frac{1}{2}(\tan(\psi)-\cot(\theta))\left(\frac{e^{(\theta\tan(\phi 1))}}{\sin(\theta)}-\tan(\psi)+\cot(\theta)\right)\right)\left(\tan(\psi)\cos(\theta)+\sin(\theta)+\tan(\phi 1)\,e^{(\theta\tan(\phi 1))}\right)KP}{24\sin(\theta)}\\
& -\frac{\gamma 2 B^2\cos(\phi 2)\left(\frac{e^{(2\theta\tan(\phi 1))}}{\sin(\theta)^2}+\frac{1}{2}(\tan(\psi)-\cot(\theta))\left(\frac{e^{(\theta\tan(\phi 1))}}{\sin(\theta)}-\tan(\psi)+\cot(\theta)\right)\right)\left(\tan(\psi)\sin(\theta)-\cos(\theta)+e^{(\theta\tan(\phi 1))}\right)KP\cos(\theta)}{24\sin(\theta)^2}\\
& -\frac{\gamma 1 B^2\left(3\tan(\phi 1)\,e^{(3\theta\tan(\phi 1))}-3\tan(\phi 1)\cos(\theta)+\sin(\theta)\right)}{24\sin(\theta)^3(9\tan(\phi 1)^2+1)}+\frac{\gamma 1 B^2\left(e^{(3\theta\tan(\phi 1))}-3\tan(\phi 1)\sin(\theta)-\cos(\theta)\right)\cos(\theta)}{8\sin(\theta)^4(9\tan(\phi 1)^2+1)}-\frac{1}{48}\gamma 1 B^2(1+\cot(\theta)^2)\Bigg)
\end{aligned}
$$

$$-\frac{1}{\left(\frac{1}{3}\cos(\psi-\phi1)+\sin(\psi-\phi1)\left(-\frac{1}{6}\tan(\psi)+\frac{1}{2}\cot(\theta)\right)\right)^2}\left(\left(\gamma2\,B^2\cos(\phi2)\left(\frac{e^{(2\,\theta\tan(\phi1))}}{\sin(\theta)^2}+\frac{1}{2}(\tan(\psi)-\cot(\theta))\left(\frac{e^{(\theta\tan(\phi1))}}{\sin(\theta)}-\tan(\psi)+\cot(\theta)\right)\right)\left(\tan(\psi)\sin(\theta)-\cos(\theta)+e^{(\theta\tan(\phi1))}\right)KP\right)\right.$$
$$\left.-\frac{\gamma1\,B^2\left(e^{(3\,\theta\tan(\phi1))}-3\tan(\phi1)\sin(\theta)-\cos(\theta)\right)}{24\sin(\theta)^3(9\tan(\phi1)^2+1)}-\frac{1}{48}\gamma1\,B^2(\tan(\psi)-\cot(\theta))\right)\sin(\psi-\phi1)\left(-\frac{1}{2}-\frac{1}{2}\cot(\theta)^2\right)\Bigg)$$

Second derivation of Equation 4.140 respect to θ

$$RI:=\frac{1}{\frac{1}{3}\cos(\psi-\phi1)+\sin(\psi-\phi1)\left(-\frac{1}{6}\tan(\psi)+\frac{1}{2}\cot(\theta)\right)}\left(\frac{1}{24\sin(\theta)}\left(\gamma2\,B^2\cos(\phi2)\left(\frac{4\tan(\phi1)^2e^{(2\,\theta\tan(\phi1))}}{\sin(\theta)^2}-\frac{8\tan(\phi1)e^{(2\,\theta\tan(\phi1))}\cos(\theta)}{\sin(\theta)^3}\right.\right.\right.$$
$$+\frac{6e^{(2\,\theta\tan(\phi1))}\cos(\theta)^2}{\sin(\theta)^4}+\frac{2e^{(2\,\theta\tan(\phi1))}}{\sin(\theta)^2}+\cot(\theta)(-1-\cot(\theta)^2)\left(\frac{e^{(\theta\tan(\phi1))}}{\sin(\theta)}-\tan(\psi)+\cot(\theta)\right)$$
$$+(1+\cot(\theta)^2)\left(\frac{\tan(\phi1)e^{(\theta\tan(\phi1))}}{\sin(\theta)}-\frac{e^{(\theta\tan(\phi1))}\cos(\theta)}{\sin(\theta)^2}-1-\cot(\theta)^2\right)$$
$$\left.\left.+\frac{1}{2}(\tan(\psi)-\cot(\theta))\left(\frac{\tan(\phi1)^2e^{(\theta\tan(\phi1))}}{\sin(\theta)}-\frac{2\tan(\phi1)e^{(\theta\tan(\phi1))}\cos(\theta)}{\sin(\theta)^2}+\frac{2e^{(\theta\tan(\phi1))}\cos(\theta)^2}{\sin(\theta)^3}+\frac{e^{(\theta\tan(\phi1))}}{\sin(\theta)}-2\cot(\theta)(-1-\cot(\theta)^2)\right)\right)\left(\tan(\psi)\sin(\theta)\right.\right.$$
$$\left.\left.-\cos(\theta)+e^{(\theta\tan(\phi1))}\right)KP\right)\Bigg)$$

$$+\frac{1}{12\sin(\theta)}\left(\gamma 2 B^2\cos(\phi 2)\left(\frac{2\tan(\phi 1)\,e^{(2\theta\tan(\phi 1))}}{\sin(\theta)^2}-\frac{2\,e^{(2\theta\tan(\phi 1))}\cos(\theta)}{\sin(\theta)^3}+\frac{1}{2}(1+\cot(\theta)^2)\left(\frac{e^{(\theta\tan(\phi 1))}}{\sin(\theta)}-\tan(\psi)+\cot(\theta)\right)\right.\right.$$
$$\left.\left.+\frac{1}{2}(\tan(\psi)-\cot(\theta))\left(\frac{\tan(\phi 1)\,e^{(\theta\tan(\phi 1))}}{\sin(\theta)}-\frac{e^{(\theta\tan(\phi 1))}\cos(\theta)}{\sin(\theta)^2}-1-\cot(\theta)^2\right)\right)\left(\tan(\psi)\cos(\theta)+\sin(\theta)+\tan(\phi 1)\,e^{(\theta\tan(\phi 1))}\right)KP\right)$$
$$-\frac{1}{12\sin(\theta)^2}\left(\gamma 2 B^2\cos(\phi 2)\left(\frac{2\tan(\phi 1)\,e^{(2\theta\tan(\phi 1))}}{\sin(\theta)^2}-\frac{2\,e^{(2\theta\tan(\phi 1))}\cos(\theta)}{\sin(\theta)^3}+\frac{1}{2}(1+\cot(\theta)^2)\left(\frac{e^{(\theta\tan(\phi 1))}}{\sin(\theta)}-\tan(\psi)+\cot(\theta)\right)\right.\right.$$
$$\left.\left.+\frac{1}{2}(\tan(\psi)-\cot(\theta))\left(\frac{\tan(\phi 1)\,e^{(\theta\tan(\phi 1))}}{\sin(\theta)}-\frac{e^{(\theta\tan(\phi 1))}\cos(\theta)}{\sin(\theta)^2}-1-\cot(\theta)^2\right)\right)\left(\tan(\psi)\sin(\theta)-\cos(\theta)+e^{(\theta\tan(\phi 1))}\right)KP\cos(\theta)\right)$$
$$+\frac{\gamma 2 B^2\cos(\phi 2)\left(\frac{e^{(2\theta\tan(\phi 1))}}{\sin(\theta)^2}+\frac{1}{2}(\tan(\psi)-\cot(\theta))\left(\frac{e^{(\theta\tan(\phi 1))}}{\sin(\theta)}-\tan(\psi)+\cot(\theta)\right)\right)\left(-\tan(\psi)\sin(\theta)+\cos(\theta)+\tan(\phi 1)^2\,e^{(\theta\tan(\phi 1))}\right)KP}{24\sin(\theta)}$$
$$-\frac{\gamma 2 B^2\cos(\phi 2)\left(\frac{e^{(2\theta\tan(\phi 1))}}{\sin(\theta)^2}+\frac{1}{2}(\tan(\psi)-\cot(\theta))\left(\frac{e^{(\theta\tan(\phi 1))}}{\sin(\theta)}-\tan(\psi)+\cot(\theta)\right)\right)\left(\tan(\psi)\cos(\theta)+\sin(\theta)+\tan(\phi 1)\,e^{(\theta\tan(\phi 1))}\right)KP\cos(\theta)}{12\sin(\theta)^2}$$
$$+\frac{\gamma 2 B^2\cos(\phi 2)\left(\frac{e^{(2\theta\tan(\phi 1))}}{\sin(\theta)^2}+\frac{1}{2}(\tan(\psi)-\cot(\theta))\left(\frac{e^{(\theta\tan(\phi 1))}}{\sin(\theta)}-\tan(\psi)+\cot(\theta)\right)\right)\left(\tan(\psi)\sin(\theta)-\cos(\theta)+e^{(\theta\tan(\phi 1))}\right)KP\cos(\theta)^2}{12\sin(\theta)^3}$$
$$+\frac{\gamma 2 B^2\cos(\phi 2)\left(\frac{e^{(2\theta\tan(\phi 1))}}{\sin(\theta)^2}+\frac{1}{2}(\tan(\psi)-\cot(\theta))\left(\frac{e^{(\theta\tan(\phi 1))}}{\sin(\theta)}-\tan(\psi)+\cot(\theta)\right)\right)\left(\tan(\psi)\sin(\theta)-\cos(\theta)+e^{(\theta\tan(\phi 1))}\right)KP}{24\sin(\theta)}$$
$$-\frac{\gamma 1 B^2\left(9\tan(\phi 1)^2\,e^{(3\theta\tan(\phi 1))}+3\tan(\phi 1)\sin(\theta)+\cos(\theta)\right)}{24\sin(\theta)^3(9\tan(\phi 1)^2+1)}+\frac{\gamma 1 B^2\left(3\tan(\phi 1)\,e^{(3\theta\tan(\phi 1))}-3\tan(\phi 1)\cos(\theta)+\sin(\theta)\right)\cos(\theta)}{4\sin(\theta)^4(9\tan(\phi 1)^2+1)}$$
$$\left.-\frac{\gamma 1 B^2\left(e^{(3\theta\tan(\phi 1))}-3\tan(\phi 1)\sin(\theta)-\cos(\theta)\right)\cos(\theta)^2}{2\sin(\theta)^5(9\tan(\phi 1)^2+1)}-\frac{\gamma 1 B^2\left(e^{(3\theta\tan(\phi 1))}-3\tan(\phi 1)\sin(\theta)-\cos(\theta)\right)}{8\sin(\theta)^3(9\tan(\phi 1)^2+1)}-\frac{1}{24}\gamma 1 B^2\cot(\theta)(-1-\cot(\theta)^2)\right)$$

$$-\frac{1}{\left(\frac{1}{3}\cos(\psi-\phi1)+\sin(\psi-\phi1)\left(-\frac{1}{6}\tan(\psi)+\frac{1}{2}\cot(\theta)\right)\right)^2}\left(2\left(\frac{1}{24\sin(\theta)}\left(\gamma2B^2\cos(\phi2)\left(\frac{2\tan(\phi1)\,e^{(2\theta\tan(\phi1))}}{\sin(\theta)^2}-\frac{2e^{(2\theta\tan(\phi1))}\cos(\theta)}{\sin(\theta)^3}\right.\right.\right.\right.$$
$$\left.\left.\left.\left.+\frac{1}{2}(1+\cot(\theta)^2)\left(\frac{e^{(\theta\tan(\phi1))}}{\sin(\theta)}-\tan(\psi)+\cot(\theta)\right)+\frac{1}{2}(\tan(\psi)-\cot(\theta))\left(\frac{\tan(\phi1)\,e^{(\theta\tan(\phi1))}}{\sin(\theta)}-\frac{e^{(\theta\tan(\phi1))}\cos(\theta)}{\sin(\theta)^2}-1-\cot(\theta)^2\right)\right)\right)\right)\left(\tan(\psi)\sin(\theta)-\cos(\theta)\right.$$
$$\left.+e^{(\theta\tan(\phi1))}\right)KP\Bigg)$$
$$+\frac{\gamma2B^2\cos(\phi2)\left(\frac{e^{(2\theta\tan(\phi1))}}{\sin(\theta)^2}+\frac{1}{2}(\tan(\psi)-\cot(\theta))\left(\frac{e^{(\theta\tan(\phi1))}}{\sin(\theta)}-\tan(\psi)+\cot(\theta)\right)\right)\left(\tan(\psi)\cos(\theta)+\sin(\theta)+\tan(\phi1)\,e^{(\theta\tan(\phi1))}\right)KP}{24\sin(\theta)}$$
$$-\frac{\gamma2B^2\cos(\phi2)\left(\frac{e^{(2\theta\tan(\phi1))}}{\sin(\theta)^2}+\frac{1}{2}(\tan(\psi)-\cot(\theta))\left(\frac{e^{(\theta\tan(\phi1))}}{\sin(\theta)}-\tan(\psi)+\cot(\theta)\right)\right)\left(\tan(\psi)\sin(\theta)-\cos(\theta)+e^{(\theta\tan(\phi1))}\right)KP\cos(\theta)}{24\sin(\theta)^2}$$
$$-\frac{\gamma1B^2\left(3\tan(\phi1)\,e^{(3\theta\tan(\phi1))}-3\tan(\phi1)\cos(\theta)+\sin(\theta)\right)}{24\sin(\theta)^3(9\tan(\phi1)^2+1)}+\frac{\gamma1B^2\left(e^{(3\theta\tan(\phi1))}-3\tan(\phi1)\sin(\theta)-\cos(\theta)\right)\cos(\theta)}{8\sin(\theta)^4(9\tan(\phi1)^2+1)}-\frac{1}{48}\gamma1B^2(1+\cot(\theta)^2)\Bigg)\sin(\psi-\phi1$$
$$)\left(-\frac{1}{2}-\frac{1}{2}\cot(\theta)^2\right)\Bigg)$$
$$+\frac{1}{\left(\frac{1}{3}\cos(\psi-\phi1)+\sin(\psi-\phi1)\left(-\frac{1}{6}\tan(\psi)+\frac{1}{2}\cot(\theta)\right)\right)^3}\left(2\left(\right.\right.$$

$$\frac{\gamma 2 B^2 \cos(\phi 2)\left(\frac{e^{(2\,\theta\tan(\phi 1))}}{\sin(\theta)^2}+\frac{1}{2}(\tan(\psi)-\cot(\theta))\left(\frac{e^{(\theta\tan(\phi 1))}}{\sin(\theta)}-\tan(\psi)+\cot(\theta)\right)\right)\left(\tan(\psi)\sin(\theta)-\cos(\theta)+e^{(\theta\tan(\phi 1))}\right) KP}{24\sin(\theta)}$$

$$-\frac{\gamma 1 B^2\left(e^{(3\,\theta\tan(\phi 1))}-3\tan(\phi 1)\sin(\theta)-\cos(\theta)\right)}{24\sin(\theta)^3(9\tan(\phi 1)^2+1)}-\frac{1}{48}\gamma 1 B^2(\tan(\psi)-\cot(\theta))\Bigg)\sin(\psi-\phi 1)^2\left(-\frac{1}{2}-\frac{1}{2}\cot(\theta)^2\right)^2\Bigg)$$

$$+\frac{1}{\left(\frac{1}{3}\cos(\psi-\phi 1)+\sin(\psi-\phi 1)\left(-\frac{1}{6}\tan(\psi)+\frac{1}{2}\cot(\theta)\right)\right)^2}\Bigg(\Bigg($$

$$\frac{\gamma 2 B^2 \cos(\phi 2)\left(\frac{e^{(2\,\theta\tan(\phi 1))}}{\sin(\theta)^2}+\frac{1}{2}(\tan(\psi)-\cot(\theta))\left(\frac{e^{(\theta\tan(\phi 1))}}{\sin(\theta)}-\tan(\psi)+\cot(\theta)\right)\right)\left(\tan(\psi)\sin(\theta)-\cos(\theta)+e^{(\theta\tan(\phi 1))}\right) KP}{24\sin(\theta)}$$

$$-\frac{\gamma 1 B^2\left(e^{(3\,\theta\tan(\phi 1))}-3\tan(\phi 1)\sin(\theta)-\cos(\theta)\right)}{24\sin(\theta)^3(9\tan(\phi 1)^2+1)}-\frac{1}{48}\gamma 1 B^2(\tan(\psi)-\cot(\theta))\Bigg)\sin(\psi-\phi 1)\cot(\theta)(-1-\cot(\theta)^2)\Bigg)$$

First derivation of Equation 4.155 respect to θ

$$R2 := \frac{1}{\frac{1}{4}\cos(\psi - \phi 1) + \frac{1}{2}\sin(\psi - \phi 1)\left(-\frac{1}{2}\tan(\psi) + \cot(\theta)\right)}\left(\frac{1}{8}B\left(KP\,q + \frac{\left(KP - \frac{1}{\cos(\phi 2)}\right)c2}{\tan(\phi 2)}\right)\cos(\phi 2)\left(\frac{2\tan(\phi 1)\,e^{(2\,\theta\tan(\phi 1))}}{\sin(\theta)^2} - \frac{2\,e^{(2\,\theta\tan(\phi 1))}\cos(\theta)}{\sin(\theta)^3}\right.\right.$$

$$\left.\left. - 2\,(\tan(\psi) - \cot(\theta))\,(1 + \cot(\theta)^2)\right) + \frac{1}{4}c1\,B\left(-1 - \cot(\theta)^2 - \frac{\left(e^{(2\,\theta\tan(\phi 1))} - 1\right)\cos(\theta)}{\sin(\theta)^3\tan(\phi 1)} + \frac{e^{(2\,\theta\tan(\phi 1))}}{\sin(\theta)^2}\right)\right)$$

$$- \frac{1}{2\left(\frac{1}{4}\cos(\psi - \phi 1) + \frac{1}{2}\sin(\psi - \phi 1)\left(-\frac{1}{2}\tan(\psi) + \cot(\theta)\right)\right)^2}\left(\left(\frac{1}{8}B\left(KP\,q + \frac{\left(KP - \frac{1}{\cos(\phi 2)}\right)c2}{\tan(\phi 2)}\right)\cos(\phi 2)\left(\frac{e^{(2\,\theta\tan(\phi 1))}}{\sin(\theta)^2} - (\tan(\psi) - \cot(\theta))^2\right)\right.\right.$$

$$\left.\left. + \frac{1}{4}c1\,B\left(-\tan(\psi) + \cot(\theta) + \frac{e^{(2\,\theta\tan(\phi 1))} - 1}{2\sin(\theta)^2\tan(\phi 1)}\right)\right)\sin(\psi - \phi 1)\,(-1 - \cot(\theta)^2)\right)$$

Second derivation of Equation 4.155 respect to θ

$$R3 := \frac{1}{\frac{1}{4}\cos(\psi - \phi 1) + \frac{1}{2}\sin(\psi - \phi 1)\left(-\frac{1}{2}\tan(\psi) + \cot(\theta)\right)}\left(\frac{1}{8}B\left(KP\,q + \frac{\left(KP - \frac{1}{\cos(\phi 2)}\right)c2}{\tan(\phi 2)}\right)\cos(\phi 2)\left(\frac{4\tan(\phi 1)^2\,e^{(2\,\theta\tan(\phi 1))}}{\sin(\theta)^2} - \frac{8\tan(\phi 1)\,e^{(2\,\theta\tan(\phi 1))}\cos(\theta)}{\sin(\theta)^3}\right.\right.$$

$$\left.\left. + \frac{6\,e^{(2\,\theta\tan(\phi 1))}\cos(\theta)^2}{\sin(\theta)^4} + \frac{2\,e^{(2\,\theta\tan(\phi 1))}}{\sin(\theta)^2} - 2\,(1 + \cot(\theta)^2)^2 - 4\,(\tan(\psi) - \cot(\theta))\cot(\theta)\,(-1 - \cot(\theta)^2)\right)\right.$$

$$\left. + \frac{1}{4}c1\,B\left(-2\cot(\theta)\,(-1 - \cot(\theta)^2) + \frac{3\left(e^{(2\,\theta\tan(\phi 1))} - 1\right)\cos(\theta)^2}{\sin(\theta)^4\tan(\phi 1)} - \frac{4\,e^{(2\,\theta\tan(\phi 1))}\cos(\theta)}{\sin(\theta)^3} + \frac{e^{(2\,\theta\tan(\phi 1))} - 1}{\sin(\theta)^2\tan(\phi 1)} + \frac{2\tan(\phi 1)\,e^{(2\,\theta\tan(\phi 1))}}{\sin(\theta)^2}\right)\right)$$

$$- \frac{1}{\left(\frac{1}{4}\cos(\psi - \phi 1) + \frac{1}{2}\sin(\psi - \phi 1)\left(-\frac{1}{2}\tan(\psi) + \cot(\theta)\right)\right)^2}\left(\left(\frac{1}{8}B\left(KP\,q + \frac{\left(KP - \frac{1}{\cos(\phi 2)}\right)c2}{\tan(\phi 2)}\right)\cos(\phi 2)\left(\frac{2\tan(\phi 1)\,e^{(2\,\theta\tan(\phi 1))}}{\sin(\theta)^2} - \frac{2\,e^{(2\,\theta\tan(\phi 1))}\cos(\theta)}{\sin(\theta)^3}\right)\right.\right.$$

$$-2\left(\tan(\psi)-\cot(\theta)\right)\left(1+\cot(\theta)^2\right)\Bigg)+\frac{1}{4}c1B\left(-1-\cot(\theta)^2-\frac{\left(e^{(2\,\theta\tan(\phi1))}-1\right)\cos(\theta)}{\sin(\theta)^3\tan(\phi1)}+\frac{e^{(2\,\theta\tan(\phi1))}}{\sin(\theta)^2}\right)\Bigg)\sin(\psi-\phi1)\left(-1-\cot(\theta)^2\right)\Bigg)$$

$$+\frac{1}{2\left(\frac{1}{4}\cos(\psi-\phi1)+\frac{1}{2}\sin(\psi-\phi1)\left(-\frac{1}{2}\tan(\psi)+\cot(\theta)\right)\right)^3}\Bigg(\Bigg(\frac{1}{8}B\left(KP\,q+\frac{\left(KP-\frac{1}{\cos(\phi2)}\right)c2}{\tan(\phi2)}\right)\cos(\phi2)\left(\frac{e^{(2\,\theta\tan(\phi1))}}{\sin(\theta)^2}-\left(\tan(\psi)-\cot(\theta)\right)^2\right)$$

$$+\frac{1}{4}c1B\left(-\tan(\psi)+\cot(\theta)+\frac{e^{(2\,\theta\tan(\phi1))}-1}{2\sin(\theta)^2\tan(\phi1)}\right)\Bigg)\sin(\psi-\phi1)^2\left(-1-\cot(\theta)^2\right)^2\Bigg)$$

$$+\frac{1}{\left(\frac{1}{4}\cos(\psi-\phi1)+\frac{1}{2}\sin(\psi-\phi1)\left(-\frac{1}{2}\tan(\psi)+\cot(\theta)\right)\right)^2}\Bigg(\Bigg(\frac{1}{8}B\left(KP\,q+\frac{\left(KP-\frac{1}{\cos(\phi2)}\right)c2}{\tan(\phi2)}\right)\cos(\phi2)\left(\frac{e^{(2\,\theta\tan(\phi1))}}{\sin(\theta)^2}-\left(\tan(\psi)-\cot(\theta)\right)^2\right)$$

$$+\frac{1}{4}c1B\left(-\tan(\psi)+\cot(\theta)+\frac{e^{(2\,\theta\tan(\phi1))}-1}{2\sin(\theta)^2\tan(\phi1)}\right)\Bigg)\sin(\psi-\phi1)\cot(\theta)\left(-1-\cot(\theta)^2\right)\Bigg)$$

APPENDIX 5

Program code for local shear failure theoretical model is given here.

Program List L-STColumn


```
Private Sub Command1_Click()
Dim theta11, theta12, theta1, gamma1, phi1, psi, thetatemp, cg0, cg1, cg2 As Double
Dim cg21, cg22, P As Double
Dim numb, i As Integer

pi = 3.141592
gamma1 = 14
phi1 = 25 * 3.141592 / 180
B = 2

gamma2 = 12
phi2 = 10 * 3.141592 / 180
KP = 1.66

theta1temp = 10 * 3.141592 / 180

Do

theta = theta1temp
psi = theta + phi1

cg1 = gamma2 * B * B * Cos(phi2) * (2# * Tan(phi1) * Exp(2# * theta * Tan(phi1)) *
(Sin(theta)) ^ -2 - 2# * Exp(2# * theta * Tan(phi1)) * (Sin(theta)) ^ -3 * Cos(theta) + (1#
+ (1# / Tan(theta)) ^ 2) * (Exp(theta * Tan(phi1)) / Sin(theta) - Tan(psi) + 1# /
Tan(theta)) / 2# + (Tan(psi) - 1# / Tan(theta)) * (Tan(phi1) * Exp(theta * Tan(phi1)) /
Sin(theta) - Exp(theta * Tan(phi1)) * (Sin(theta)) ^ -2 * Cos(theta) - 1# - (1# / Tan(theta))
^ 2) / 2#) * (Tan(psi) * Sin(theta) - Cos(theta) + Exp(theta * Tan(phi1))) * KP / Sin(theta)
/ 24# + gamma2 * B * B * Cos(phi2) * (Exp(2# * theta * Tan(phi1)) * (Sin(theta)) ^ -2 +
(Tan(psi) - 1# / Tan(theta)) * (Exp(theta * Tan(phi1)) / Sin(theta) - Tan(psi) + 1# /
Tan(theta)) / 2#) * (Tan(psi) * Cos(theta) + Sin(theta) + Tan(phi1) * Exp(theta *
Tan(phi1))) * KP / Sin(theta) / 24#
cg2 = -gamma2 * B * B * Cos(phi2) * (Exp(2# * theta * Tan(phi1)) * (Sin(theta)) ^ -2 +
(Tan(psi) - 1# / Tan(theta)) * (Exp(theta * Tan(phi1)) / Sin(theta) - Tan(psi) + 1# /
Tan(theta)) / 2#) * (Tan(psi) * Sin(theta) - Cos(theta) + Exp(theta * Tan(phi1))) * KP *
```

(Sin(theta)) ^ -2 * Cos(theta) / 24# - gamma1 * B * B * (3# * Tan(phi1) * Exp(3# * theta * Tan(phi1)) - 3# * Tan(phi1) * Cos(theta) + Sin(theta)) * (Sin(theta)) ^ -3 / (9# * (Tan(phi1)) ^ 2 + 1#) / 24# + gamma1 * B * B * (Exp(3# * theta * Tan(phi1)) - 3# * Tan(phi1) * Sin(theta) - Cos(theta)) * (Sin(theta)) ^ -4 / (9# * (Tan(phi1)) ^ 2 + 1#) * Cos(theta) / 8# - gamma1 * B * B * (1# + (1# / Tan(theta)) ^ 2) / 48#
cg3 = 1 / (Cos(psi - phi1) / 3# + Sin(psi - phi1) * (-Tan(psi) / 6# + 1# / Tan(theta) / 2#))

cg4 = (cg1 + cg2) * cg3

cg5 = -(gamma2 * B * B * Cos(phi2) * (Exp(2# * theta * Tan(phi1)) * (Sin(theta)) ^ -2 + (Tan(psi) - 1# / Tan(theta)) * (Exp(theta * Tan(phi1)) / Sin(theta) - Tan(psi) + 1# / Tan(theta)) / 2#) * (Tan(psi) * Sin(theta) - Cos(theta) + Exp(theta * Tan(phi1))) * KP / Sin(theta) / 24# - gamma1 * B * B * (Exp(3# * theta * Tan(phi1)) - 3# * Tan(phi1) * Sin(theta) - Cos(theta)) * (Sin(theta)) ^ -3 / (9# * (Tan(phi1)) ^ 2 + 1#) / 24# - gamma1 * B * B * (Tan(psi) - 1# / Tan(theta)) / 48#) * (Cos(psi - phi1) / 3# + Sin(psi - phi1) * (-Tan(psi) / 6# + 1# / Tan(theta) / 2#)) ^ -2 * Sin(psi - phi1) * (-1# / 2# - (1# / Tan(theta)) ^ 2 / 2#)

cg7 = cg4 + cg5

aa1 = gamma2 * B * B * Cos(phi2) * (4 * (Tan(phi1)) ^ 2 * Exp(2 * theta * Tan(phi1)) * (Sin(theta)) ^ -2 - 8 * Tan(phi1) * Exp(2# * theta * Tan(phi1)) * (Sin(theta)) ^ -3 * Cos(theta) + 6# * Exp(2# * theta * Tan(phi1)) * (Sin(theta)) ^ -4 * (Cos(theta)) ^ 2 + 2# * Exp(2# * theta * Tan(phi1)) * (Sin(theta)) ^ -2 + 1# / Tan(theta) * (-1# - (1# / Tan(theta)) ^ 2) * (Exp(theta * Tan(phi1)) / Sin(theta) - Tan(psi) + 1# / Tan(theta)) + (1# + (1# / Tan(theta)) ^ 2) * (Tan(phi1) * Exp(theta * Tan(phi1)) / Sin(theta) - Exp(theta * Tan(phi1)) * (Sin(theta)) ^ -2 * Cos(theta) - 1# - (1# / Tan(theta)) ^ 2) + (Tan(psi) - 1# / Tan(theta)) * ((Tan(phi1)) ^ 2 * Exp(theta * Tan(phi1)) / Sin(theta) - 2# * Tan(phi1) * Exp(theta * Tan(phi1)) * (Sin(theta)) ^ -2 * Cos(theta) + 2# * Exp(theta * Tan(phi1)) * (Sin(theta)) ^ -3 * (Cos(theta)) ^ 2 + Exp(theta * Tan(phi1)) / Sin(theta) - 2# * 1# / Tan(theta) * (-1# - (1# / Tan(theta)) ^ 2)) / 2#) * (Tan(psi) * Sin(theta) - Cos(theta) + Exp(theta * Tan(phi1))) * KP / Sin(theta) / 24#
aa2 = gamma2 * B * B * Cos(phi2) * (2# * Tan(phi1) * Exp(2# * theta * Tan(phi1)) * (Sin(theta)) ^ -2 - 2# * Exp(2# * theta * Tan(phi1)) * (Sin(theta)) ^ -3 * Cos(theta) + (1# + (1# / Tan(theta)) ^ 2) * (Exp(theta * Tan(phi1)) / Sin(theta) - Tan(psi) + 1# / Tan(theta)) / 2# + (Tan(psi) - 1# / Tan(theta)) * (Tan(phi1) * Exp(theta * Tan(phi1)) / Sin(theta) - Exp(theta * Tan(phi1)) * (Sin(theta)) ^ -2 * Cos(theta) - 1# - (1# / Tan(theta)) ^ 2) / 2#) * (Tan(psi) * Cos(theta) + Sin(theta) + Tan(phi1) * Exp(theta * Tan(phi1))) * KP / Sin(theta) / 12#
aa3 = -gamma2 * B * B * Cos(phi2) * (2# * Tan(phi1) * Exp(2# * theta * Tan(phi1)) * (Sin(theta)) ^ -2 - 2# * Exp(2# * theta * Tan(phi1)) * (Sin(theta)) ^ -3 * Cos(theta) + (1# + (1# / Tan(theta)) ^ 2) * (Exp(theta * Tan(phi1)) / Sin(theta) - Tan(psi) + 1# / Tan(theta)) / 2# + (Tan(psi) - 1# / Tan(theta)) * (Tan(phi1) * Exp(theta * Tan(phi1)) / Sin(theta) - Exp(theta * Tan(phi1)) * (Sin(theta)) ^ -2 * Cos(theta) - 1# - (1# / Tan(theta)) ^ 2) / 2#) * (Tan(psi) * Sin(theta) - Cos(theta) + Exp(theta * Tan(phi1))) * KP * (Sin(theta)) ^ -2 * Cos(theta) / 12# + gamma2 * B * B * Cos(phi2) * (Exp(2# * theta *

Tan(phi1)) * (Sin(theta)) ^ -2 + (Tan(psi) - 1# / Tan(theta)) * (Exp(theta * Tan(phi1)) / Sin(theta) - Tan(psi) + 1# / Tan(theta)) / 2#) * (-Tan(psi) * Sin(theta) + Cos(theta) + (Tan(phi1)) ^ 2 * Exp(theta * Tan(phi1))) * KP / Sin(theta) / 24#
aa4 = -gamma2 * B * B * Cos(phi2) * (Exp(2# * theta * Tan(phi1)) * (Sin(theta)) ^ -2 + (Tan(psi) - 1# / Tan(theta)) * (Exp(theta * Tan(phi1)) / Sin(theta) - Tan(psi) + 1# / Tan(theta)) / 2#) * (Tan(psi) * Cos(theta) + Sin(theta) + Tan(phi1) * Exp(theta * Tan(phi1))) * KP * (Sin(theta)) ^ -2 * Cos(theta) / 12# + gamma2 * B * B * Cos(phi2) * (Exp(2# * theta * Tan(phi1)) * (Sin(theta)) ^ -2 + (Tan(psi) - 1# / Tan(theta)) * (Exp(theta * Tan(phi1)) / Sin(theta) - Tan(psi) + 1# / Tan(theta)) / 2#) * (Tan(psi) * Sin(theta) - Cos(theta) + Exp(theta * Tan(phi1))) * KP * (Sin(theta)) ^ -3 * (Cos(theta)) ^ 2 / 12# + gamma2 * B * B * Cos(phi2) * (Exp(2# * theta * Tan(phi1)) * (Sin(theta)) ^ -2 + (Tan(psi) - 1# / Tan(theta)) * (Exp(theta * Tan(phi1)) / Sin(theta) - Tan(psi) + 1# / Tan(theta)) / 2#) * (Tan(psi) * Sin(theta) - Cos(theta) + Exp(theta * Tan(phi1))) * KP / Sin(theta) / 24#
aa5 = -gamma1 * B * B * (9# * (Tan(phi1)) ^ 2 * Exp(3# * theta * Tan(phi1)) + 3# * Tan(phi1) * Sin(theta) + Cos(theta)) * (Sin(theta)) ^ -3 / (9# * (Tan(phi1)) ^ 2 + 1#) / 24# + gamma1 * B * B * (3# * Tan(phi1) * Exp(3# * theta * Tan(phi1)) - 3# * Tan(phi1) * Cos(theta) + Sin(theta)) * (Sin(theta)) ^ -4 / (9# * (Tan(phi1)) ^ 2 + 1#) * Cos(theta) / 4# - gamma1 * B * B * (Exp(3# * theta * Tan(phi1)) - 3# * Tan(phi1) * Sin(theta) - Cos(theta)) * (Sin(theta)) ^ -5 / (9# * (Tan(phi1)) ^ 2 + 1#) * (Cos(theta)) ^ 2 / 2# - gamma1 * B * B * (Exp(3# * theta * Tan(phi1)) - 3# * Tan(phi1) * Sin(theta) - Cos(theta)) * (Sin(theta)) ^ -3 / (9# * (Tan(phi1)) ^ 2 + 1#) / 8# - gamma1 * B * B * 1# / Tan(theta) * (-1# - (1# / Tan(theta)) ^ 2) / 24#
aa6 = 1 / (Cos(psi - phi1) / 3# + Sin(psi - phi1) * (-Tan(psi) / 6# + 1# / Tan(theta) / 2#))

aa7 = (aa1 + aa2 + aa3 + aa4 + aa5) * aa6

aa8 = gamma2 * B * B * Cos(phi2) * (2# * Tan(phi1) * Exp(2# * theta * Tan(phi1)) * (Sin(theta)) ^ -2 - 2# * Exp(2# * theta * Tan(phi1)) * (Sin(theta)) ^ -3 * Cos(theta) + (1# + (1# / Tan(theta)) ^ 2) * (Exp(theta * Tan(phi1)) / Sin(theta) - Tan(psi) + 1# / Tan(theta)) / 2# + (Tan(psi) - 1# / Tan(theta)) * (Tan(phi1) * Exp(theta * Tan(phi1)) / Sin(theta) - Exp(theta * Tan(phi1)) * (Sin(theta)) ^ -2 * Cos(theta) - 1# - (1# / Tan(theta)) ^ 2) / 2#) * (Tan(psi) * Sin(theta) - Cos(theta) + Exp(theta * Tan(phi1))) * KP / Sin(theta) / 24# + gamma2 * B * B * Cos(phi2) * (Exp(2# * theta * Tan(phi1)) * (Sin(theta)) ^ -2 + (Tan(psi) - 1# / Tan(theta)) * (Exp(theta * Tan(phi1)) / Sin(theta) - Tan(psi) + 1# / Tan(theta)) / 2#) * (Tan(psi) * Cos(theta) + Sin(theta) + Tan(phi1) * Exp(theta * Tan(phi1))) * KP / Sin(theta) / 24#
aa9 = -gamma2 * B * B * Cos(phi2) * (Exp(2# * theta * Tan(phi1)) * (Sin(theta)) ^ -2 + (Tan(psi) - 1# / Tan(theta)) * (Exp(theta * Tan(phi1)) / Sin(theta) - Tan(psi) + 1# / Tan(theta)) / 2#) * (Tan(psi) * Sin(theta) - Cos(theta) + Exp(theta * Tan(phi1))) * KP * (Sin(theta)) ^ -2 * Cos(theta) / 24# - gamma1 * B * B * (3# * Tan(phi1) * Exp(3# * theta * Tan(phi1)) - 3# * Tan(phi1) * Cos(theta) + Sin(theta)) * (Sin(theta)) ^ -3 / (9# * (Tan(phi1)) ^ 2 + 1#) / 24# + gamma1 * B * B * (Exp(3# * theta * Tan(phi1)) - 3# * Tan(phi1) * Sin(theta) - Cos(theta)) * (Sin(theta)) ^ -4 / (9# * (Tan(phi1)) ^ 2 + 1#) * Cos(theta) / 8# - gamma1 * B * B * (1# + (1# / Tan(theta)) ^ 2) / 48#

```
aa10 = -2# * (Cos(psi - phi1) / 3# + Sin(psi - phi1) * (-Tan(psi) / 6# + 1# / Tan(theta) / 2#)) ^ -2 * Sin(psi - phi1) * (-1# / 2# - (1# / Tan(theta)) ^ 2 / 2#)

aa11 = (aa8 + aa9) * aa10

aa12 = 2# * (gamma2 * B * B * Cos(phi2) * (Exp(2# * theta * Tan(phi1)) * (Sin(theta)) ^ -2 + (Tan(psi) - 1# / Tan(theta)) * (Exp(theta * Tan(phi1)) / Sin(theta) - Tan(psi) + 1# / Tan(theta)) / 2#) * (Tan(psi) * Sin(theta) - Cos(theta) + Exp(theta * Tan(phi1))) * KP / Sin(theta) / 24# - gamma1 * B * B * (Exp(3# * theta * Tan(phi1)) - 3# * Tan(phi1) * Sin(theta) - Cos(theta)) * (Sin(theta)) ^ -3 / (9# * (Tan(phi1)) ^ 2 + 1#) / 24# - gamma1 * B * B * (Tan(psi) - 1# / Tan(theta)) / 48#) * (Cos(psi - phi1) / 3# + Sin(psi - phi1) * (-Tan(psi) / 6# + 1# / Tan(theta) / 2#)) ^ -3 * (Sin(psi - phi1)) ^ 2 * (-1# / 2# - (1# / Tan(theta)) ^ 2 / 2#) ^ 2
aa13 = (gamma2 * B * B * Cos(phi2) * (Exp(2# * theta * Tan(phi1)) * (Sin(theta)) ^ -2 + (Tan(psi) - 1# / Tan(theta)) * (Exp(theta * Tan(phi1)) / Sin(theta) - Tan(psi) + 1# / Tan(theta)) / 2#) * (Tan(psi) * Sin(theta) - Cos(theta) + Exp(theta * Tan(phi1))) * KP / Sin(theta) / 24# - gamma1 * B * B * (Exp(3# * theta * Tan(phi1)) - 3# * Tan(phi1) * Sin(theta) - Cos(theta)) * (Sin(theta)) ^ -3 / (9# * (Tan(phi1)) ^ 2 + 1#) / 24# - gamma1 * B * B * (Tan(psi) - 1# / Tan(theta)) / 48#) * (Cos(psi - phi1) / 3# + Sin(psi - phi1) * (-Tan(psi) / 6# + 1# / Tan(theta) / 2#)) ^ -2 * Sin(psi - phi1) * 1# / Tan(theta) * (-1# - (1# / Tan(theta)) ^ 2)

aa15 = aa7 + aa11 + aa12 + aa13

If aa15 = 0 Then

   Text1.Text = "Failure"
   Stop
End If
   theta11 = theta1temp
   theta12 = theta11 - cg7 / aa15
   theta1temp = theta12

Loop Until Abs(theta12 - theta11) <= 0.00000001
theta = theta12
Text1.Text = theta

'  Py calculation  for theta

P1 = (gamma2 * B * B * Cos(phi2) * (Exp(2# * theta * Tan(phi1)) * (Sin(theta)) ^ -2 + (Tan(psi) - 1# / Tan(theta)) * (Exp(theta * Tan(phi1)) / Sin(theta) - Tan(psi) + 1# / Tan(theta)) / 2#) * (Tan(psi) * Sin(theta) - Cos(theta) + Exp(theta * Tan(phi1))) * KP / Sin(theta) / 24# - gamma1 * B * B * (Exp(3# * theta * Tan(phi1)) - 3# * Tan(phi1) * Sin(theta) - Cos(theta)) * (Sin(theta)) ^ -3 / (9# * (Tan(phi1)) ^ 2 + 1#) / 24# - gamma1 * B * B * (Tan(psi) - 1# / Tan(theta)) / 48#) / (Cos(psi - phi1) / 3# + Sin(psi - phi1) * (-Tan(psi) / 6# + 1# / Tan(theta) / 2#))
```

```
q1 = 2 * P1 / B * Cos(psi - phi1) - B / 4 * gamma1 * Tan(psi)
Text3.Text = P1

theta1temp = 10 * 3.141592 / 180
q = 0
c1 = 3.5
c2 = 5

Do

theta = theta1temp

psi = theta + phi1

bb1 = (B * (KP * q + (KP - 1# / Cos(phi2)) / Tan(phi2) * c2) * Cos(phi2) * (2# *
Tan(phi1) * Exp(2# * theta * Tan(phi1)) * (Sin(theta)) ^ -2 - 2# * Exp(2# * theta *
Tan(phi1)) * (Sin(theta)) ^ -3 * Cos(theta) - 2# * (Tan(psi) - 1# / Tan(theta)) * (1# + (1# /
Tan(theta)) ^ 2)) / 8# + c1 * B * (-1# - (1# / Tan(theta)) ^ 2 - (Sin(theta)) ^ -3 / Tan(phi1)
* (Exp(2# * theta * Tan(phi1)) - 1#) * Cos(theta) + Exp(2# * theta * Tan(phi1)) *
(Sin(theta)) ^ -2) / 4#) / (Cos(psi - phi1) / 4# + Sin(psi - phi1) * (-Tan(psi) / 2# + 1# /
Tan(theta)) / 2#) - (B * (KP * q + (KP - 1# / Cos(phi2)) / Tan(phi2) * c2) * Cos(phi2) *
(Exp(2# * theta * Tan(phi1)) * (Sin(theta)) ^ -2 - (Tan(psi) - 1# / Tan(theta)) ^ 2) / 8# +
c1 * B * (-Tan(psi) + 1# / Tan(theta) + (Sin(theta)) ^ -2 / Tan(phi1) * (Exp(2# * theta *
Tan(phi1)) - 1#) / 2#) / 4#) * (Cos(psi - phi1) / 4# + Sin(psi - phi1) * (-Tan(psi) / 2# + 1#
/ Tan(theta)) / 2#) ^ -2 * Sin(psi - phi1) * (-1# - (1# / Tan(theta)) ^ 2) / 2#

cc1 = (B * (KP * q + (KP - 1# / Cos(phi2)) / Tan(phi2) * c2) * Cos(phi2) * (4# *
(Tan(phi1)) ^ 2 * Exp(2# * theta * Tan(phi1)) * (Sin(theta)) ^ -2 - 8# * Tan(phi1) *
Exp(2# * theta * Tan(phi1)) * (Sin(theta)) ^ -3 * Cos(theta) + 6# * Exp(2# * theta *
Tan(phi1)) * (Sin(theta)) ^ -4 * (Cos(theta)) ^ 2 + 2# * Exp(2# * theta * Tan(phi1)) *
(Sin(theta)) ^ -2 - 2# * (1# + (1# / Tan(theta)) ^ 2) ^ 2 - 4# * (Tan(psi) - 1# / Tan(theta)) *
1# / Tan(theta) * (-1# - (1# / Tan(theta)) ^ 2)) / 8# + c1 * B * (-2# * 1# / Tan(theta) * (-1#
- (1# / Tan(theta)) ^ 2) + 3# * (Sin(theta)) ^ -4 / Tan(phi1) * (Exp(2# * theta * Tan(phi1))
- 1#) * (Cos(theta)) ^ 2 - 4# * Exp(2# * theta * Tan(phi1)) * (Sin(theta)) ^ -3 * Cos(theta)
+ (Sin(theta)) ^ -2 / Tan(phi1) * (Exp(2# * theta * Tan(phi1)) - 1#) + 2# * Tan(phi1) *
Exp(2# * theta * Tan(phi1)) * (Sin(theta)) ^ -2) / 4#) / (Cos(psi - phi1) / 4# + Sin(psi -
phi1) * (-Tan(psi) / 2# + 1# / Tan(theta)) / 2#)
cc2 = -(B * (KP * q + (KP - 1 / Cos(phi2)) / Tan(phi2) * c2) * Cos(phi2) * (2 * Tan(phi1)
* Exp(2 * theta * Tan(phi1)) * (Sin(theta)) ^ -2 - 2 * Exp(2 * theta * Tan(phi1)) *
(Sin(theta)) ^ -3 * Cos(theta) - 2 * (Tan(psi) - 1 / Tan(theta)) * (1 + (1 / Tan(theta)) ^ 2)) /
8 + c1 * B * (-1 - (1 / Tan(theta)) ^ 2 - (Sin(theta)) ^ -3 / Tan(phi1) * (Exp(2 * theta *
Tan(phi1)) - 1) * Cos(theta) + Exp(2 * theta * Tan(phi1)) * (Sin(theta)) ^ -2) / 4) *
(Cos(psi - phi1) / 4 + Sin(psi - phi1) * (-Tan(psi) / 2 + 1 / Tan(theta)) / 2) ^ -2 * Sin(psi -
phi1) * (-1 - (1 / Tan(theta)) ^ 2) + (B * (KP * q + (KP - 1 / Cos(phi2)) / Tan(phi2) * c2)
* Cos(phi2) * (Exp(2 * theta * Tan(phi1)) * (Sin(theta)) ^ -2 - (Tan(psi) - 1 / Tan(theta))
```

```
^ 2) / 8 + c1 * B * (-Tan(psi) + 1 / Tan(theta) + (Sin(theta)) ^ -2 / Tan(phi1) * (Exp(2 *
theta * Tan(phi1)) - 1) / 2) / 4) * (Cos(psi - phi1) / 4 + Sin(psi - phi1) * (-Tan(psi) / 2 + 1
/ Tan(theta)) / 2) ^ -3 * (Sin(psi - phi1)) ^ 2 * (-1# - (1# / Tan(theta)) ^ 2) ^ 2 / 2#
cc3 = (B * (KP * q + (KP - 1# / Cos(phi2)) / Tan(phi2) * c2) * Cos(phi2) * (Exp(2# *
theta * Tan(phi1)) * (Sin(theta)) ^ -2 - (Tan(psi) - 1# / Tan(theta)) ^ 2) / 8# + c1 * B * (-
Tan(psi) + 1# / Tan(theta) + (Sin(theta)) ^ -2 / Tan(phi1) * (Exp(2# * theta * Tan(phi1)) -
1#) / 2#) / 4#) * (Cos(psi - phi1) / 4# + Sin(psi - phi1) * (-Tan(psi) / 2# + 1# / Tan(theta))
/ 2#) ^ -2 * Sin(psi - phi1) * 1# / Tan(theta) * (-1# - (1# / Tan(theta)) ^ 2)

cc5 = cc1 + cc2 + cc3

If cc5 = 0 Then

   Text1.Text = "Failure"
   Stop
 End If
    theta11 = theta1temp
    theta12 = theta11 - bb1 / cc5
    theta1temp = theta12

Loop Until Abs(theta12 - theta11) <= 0.00000001

theta = theta12
Text2.Text = theta

'   P' calculation  for theta

P2 = (B * (KP * q + (KP - 1# / Cos(phi2)) / Tan(phi2) * c2) * Cos(phi2) * (Exp(2# *
theta * Tan(phi1)) * (Sin(theta)) ^ -2 - (Tan(psi) - 1# / Tan(theta)) ^ 2) / 8# + c1 * B * (-
Tan(psi) + 1# / Tan(theta) + (Sin(theta)) ^ -2 / Tan(phi1) * (Exp(2# * theta * Tan(phi1)) -
1#) / 2#) / 4#) / (Cos(psi - phi1) / 4# + Sin(psi - phi1) * (-Tan(psi) / 2# + 1# / Tan(theta)) /
2#)

Text4.Text = P2

'   Bearing capacity calculation

q2 = 2 * P2 / B * Cos(psi - phi1) + c1 * Tan(psi)
q = q1 + q2

Text5.Text = q1
Text6.Text = q2
Text7.Text = q

End Sub
```

APPENDIX 6

Program code for bulging failure theoretical model is presented here.

Program List B-STColumn

© Mohammad Etezad Borojerdi

```
Private Sub Command1_Click()

Dim gammas, phisf, phisc, udl, l, a, b, v, epf, mbar, EE1, numb0, E, m, nf, nc As Double
Dim c1, c2, k0, dres, n0, d1, Acal, Bcal, Ccal, Afcal, Bfcal, Cfcal, depres As Double
Dim kjj0, P, Y, numb0, dep3, dep1c, dep1, d1temp As Double

gammas = 20

phisf = 41 * 3.14 / 180

phisc = 36 * 3.14 / 180

udl = 200

l = 5

a = 1 / 2

b = 3.16 / 2

v = 0.2

epf = 0.05

mbar = -0.44

EE1 = 1000

numb0 = 1

E = (1 - v - 2 * v ^ 2) / (1 - v) * EE1

m = 2 / (mbar - 1)
```

```
nf = (1 + Sin(phisf)) / (1 - Sin(phisf))

nc = (1 + Sin(phisc)) / (1 - Sin(phisc))

c1 = v / (1 - v)

c2 = E * ((1 + v) * a ^ 2 + (1 - v) * b ^ 2) / ((1 - v ^ 2) * (b ^ 2 - a ^ 2))

k0 = 1 - Sin(phisf)

dres = k0 * gammas * 1

n0 = 1 / k0

d1 = 0.1 * udl

Acal = 1
Ccal = (1 - nf) / epf ^ 2
Bcal = -2 * Ccal * epf

Afcal = nc
Cfcal = (nc - nf) * epf ^ 2
Bfcal = -2 * Cfcal / epf

depres = (-Bcal + Sqr(Bcal ^ 2 - 4 * (Acal - n0) * Ccal)) / (2 * Ccal)

kjj0 = 100

Do

 If d1temp < d1 Then

Y = -1

 numb0 = numb0 + 1

 Else

Y = 1

 End If
If numb0 = 50 Then kjj0 = 5
If numb0 = 70 Then kjj0 = 1
```

```
If numb0 = 100 Then kjj0 = 0.1
If numb0 = 50000 Then Stop

d1 = d1 + Y * kjj0 / numb0


P = (b ^ 2 * udl - a ^ 2 * d1) / (b ^ 2 - a ^ 2)


dep3 = (1 - 2 * v ^ 2 - v) * P / ((1 - v) * E) / (m - 2 * v * a ^ 2 / ((1 - v) * (b ^ 2 - a ^ 2)))


dep1c = ((1 - 2 * v ^ 2 - v) * P / ((1 - v) * E) + 2 * v * a ^ 2 * dep3 / ((1 - v) * (b ^ 2 - a ^
2)))

dep1 = dep1c

 If (dep1 + depres) < epf Then

d1temp = (dres + c1 * P - c2 * dep3) * (Acal + Bcal * (depres + m * dep3) + Ccal *
(depres + m * dep3) ^ 2) - gammas * 1

    Else

d1temp = (dres + c1 * P - c2 * dep3) * (Afcal + Bfcal * (depres + m * dep3) ^ (-1) +
Cfcal * (depres + m * dep3) ^ (-2)) - gammas * 1


  End If


Loop Until Abs(d1temp - d1) <= 0.001

Text1.Text = P
Text2.Text = d1
Text3.Text = dep3
Text4.Text = dep1 * 1


End Sub
```